Universidad de La Laguna

Escuela de Doctorado y Estudios de Posgrado

TÍTULO DE LA TESIS DOCTORAL

Multipartite entanglement in harmonic oscillators subjected to dissipative quantum dynamics

---

AUTOR/A

ANTONIO ALEJANDRO	VALIDO	FLORES

DIRECTOR/A

DANIEL	ALONSO	RAMIREZ

CODIRECTOR/A

DEPARTAMENTO O INSTITUTO UNIVERSITARIO

FECHA DE LECTURA

18/05/15

Multipartite entanglement in harmonic oscillators subjected to dissipative quantum dynamics

Antonio Alejandro Valido Flores

PhD THESIS
Departamento de Física
Universidad de La Laguna
La Laguna, April 2015

Supervisor
Daniel Alonso Ramírez

Daniel Alonso Ramírez, profesor titular de Física Aplicada adscrito al Departamento de Física de la Universidad de La Laguna,

CERTIFICA:

Que D. **Antonio Alejandro Valido Flores** ha realizado bajo mi dirección y supervisión los trabajos conducentes a su Tesis Doctoral titulada:

Multipartite entanglement in harmonic oscillators subjected to dissipative quantum dynamics

Examinada la presente memoria, me declaro conforme con su contenido y considero que cumple los requisitos académicos y científicos para optar al título de Doctor en Física y, por consiguiente, ser sometida al juicio del tribunal que proponga la Comisión de Doctorado de la Universidad de La Laguna.

Y para que así conste donde convenga y surta los efectos oportunos, expido el presente certificado en La Laguna, a 13 de abril de 2015.

Fdo.: Daniel Alonso Ramírez

Multipartite entanglement in harmonic oscillators subjected to dissipative quantum dynamics

Antonio Alejandro Valido Flores

PhD THESIS
Departamento de Física
Universidad de La Laguna
La Laguna, April 2015

Supervisor
Daniel Alonso Ramírez

Preface

This PhD thesis addresses the dynamics of multipartite entanglement in the mechanical degrees of freedom of experimentally accessible quantum systems when dissipation is unavoidable. It was carried out between September 2010 and March 2015 at Universidad de La Laguna, under supervision of Prof. Daniel Alonso Ramírez, and thanks to the financial support of the Canary Island Agency of Research (ACIISSI) through a PhD research fellowship. The research programme is part of the national project FIS2010-19998, funded by the former Spanish Ministry of Sciences. A considerable part of this thesis was done during several academic visits (over 9 months) to the quantum theory groups led by Dr. Sigmund Kohler at Instituto de Ciencias Materiales de Madrid (ICMM), and Dr. Florian Mintert at Imperial College London. Additional financial support from ACIISI and Vicerectorado de Investigación de la Universidad de La Laguna for those visits was obtained. The printing of this thesis was financially supported by ACIISSI (85% co-founded by European Social Fund) through Universidad de La Laguna ("se agradece la financiación concedida a la ULL por la Agencia Canaria de Investigación, Innovación y Sociedad de la Información, cofinanciada en un 85% por el Fondo Social Europeo").

By means of the present I submit this thesis for its consideration "as thesis as a compedium" at Universidad de La Laguna. The present thesis is based in the work collected on the papers [A1]-[A4] which are listed below, and of which I am the main responsible of the conceptual development, calculations, writing, composition and illustration.

Publications included in the compendium

[A1] "*Hierarchies of multipartite entanglement for continuous-variable states*", Antonio A. Valido, Federico Levi, and Florian Mintert, Phys. Rev. A 90, 052321 (2014).

[A2] "*Gaussian entanglement induced by an extended thermal environment*", Antonio A. Valido, Daniel Alonso, and Sigmund Kohler, Phys. Rev. A 88, 042303 (2013).

[A3] "*Gaussian tripartite entanglement out of equilibrium*", Antonio A. Valido, Luis A. Correa, and Daniel Alonso, Phys. Rev. A 88, 012309 (2013).

[A4] "*Quantum correlations and energy currents across finite harmonic chains*", Antonio A. Valido, Antonia Ruiz, and Daniel Alonso, arXiv:1503.09051 (2015).

Other publications

[A5] "*Asymptotic discord and entanglement of nonresonant harmonic oscillators under weak and strong dissipation*", Luis A. Correa, Antonio A. Valido and Daniel Alonso, Phys. Rev. A 86, 012110 (2012).

$|$**Acknow.**$\rangle + |$**Agrad.**$\rangle$

En primer lugar, quiero expresar mi agradecimiento a Daniel por la confianza depositada, por darme la oportunidad y animarme a hacer la tesis. Esta no habría sido posible sin su sabiduría, dedicación y esfuerzo como director de la misma, y por lo que me siento muy agradecido.

Thanks to Instituto de Ciencias Materiales de Madrid, Freiburg Institute for Advanced Studies, and Imperial College London for their warm hospitality. Specially, I am very grateful to Dr. Sigmund Kohler and Dr. Florian Mintert for giving me the chance to work with them, and for stimulating and inspiring discussions. Undoubtedly, our fruitful collaborations have considerably contributed to the success of this thesis.

Merecidos agradecimientos son para mi colega y amigo Luis A. Correa. Muchas gracias por tu inestimable compañerismo y ayuda desde que empezáramos la licenciatura. Ojalá algún día pueda pagarte el valioso conocimiento que me has enseñado como profesional de la ciencia.

Quiero agradecer especialmente a los profesores José Pascual y Toñi por su continuo apoyo y preocupación en la consecusión de esta tesis. También quiero dar las gracias a el profesor Santiago, por acceder a tutelar mi beca de doctorado y su plena disposición durante el desarrollo de la misma.

También estoy muy agradecido a otros compañeros y amigos fuera y dentro del ámbito de la Física, a los cuales me siento afortunado de haber conocido. Como son demasiados para mencionarlos aquí, me van a permitir que les dedique un sentido agradecimiento general.

No puedo dejar pasar la ocasión sin agradecer el incombustible apoyo e inmenso cariño de mis padres, Juan y Gloria, y mi hermano Borja. Juan y Gloria han sabido transmitirme su incansable fuerza de voluntad y han incentivado mi curiosidad por la física desde pequeño. También quiero aprovechar la oportunidad para agradecer muy especialmente a mi familia "villera", Domingo, Teresa y Álvaro, por haberme acogido en su casa y quererme como uno más de la familia. Por último, y no por ello menos importante, quiero expresar que en muchísima medida el éxito de esta tesis se lo debo al sol que nutre de energía mi mundo, a mi novia Cora. No habría logrado terminar este proyecto sin tu apoyo, paciencia y amor. Cora, te lo agradezco con todo mi amor.

To the memory of Domingo Hernández Hernández

Dedicado a la memoria de Domingo Hernández Hernández

Abstract

A meaningful description of the *low-energy* dynamics of multipartite entanglement is provided for harmonic oscillator systems in general dissipative scenarios. Without doing any central approximation, this mainly relies on a set of reasonable physical statements on the environment and system-environment interaction consistent with a linear analysis of the open-system dynamics.

We first investigate the inseparability properties of arbitrary entangled states, which generally entails an optimization procedure of certain functional defined in the infinite-dimensional Hilbert space of continuous-variable systems. Using a Gaussian-like assumption analogous to that used in the derivation of Gaussian entanglement of formation, we derive a computational-efficient form of such functional which considerable simplifies the optimization task. This consists on a hierarchy of separability criteria that permit in a unified way to characterize k-partite entanglement of broad classes of Gaussian and non-Gaussian states. The strength of the criteria is proven by showing that they satisfactorily reproduce previous results from the theory of entanglement, like PPT criterion applied to arbitrary two-mode and pure three-mode Gaussian states.

The separability criteria allow to monitor the transient evolution of multipartite entanglement under the environmental influence, this permitted to show that non-Gaussian entanglement may be as robust against harmful dissipative effects and thermal noise as Gaussian one. We devote special attention to the *stationary* properties of tripartite entanglement when the system oscillators are in contact with either a common environment or independent environments at initial different temperatures. For the former dissipative scheme, it is shown that the environment mediates an effective many-party interaction with a spatial long-range feature between system oscillators, which is able to generate tripartite entanglement whereas two-mode entanglement is degraded. Regarding the second scheme, it is illustrated that thermal non-equilibrium conditions result in a rich variety of quantum correlations, however a temperature gradient eventually destroys the entanglement shared by the system oscillators as a consequence of the growth of thermal noise. Finally, the stationary entanglement and energy current across a finite harmonic chain are studied in detail by doing an extensive numerical analysis of both phenomena for a broad range of the parameters (*i.e.*, temperatures, oscillator frequencies, and oscillator coupling strengths). Our numerical findings are discussed in terms of the derived energy current expressions, these show an explicit dependence on the two-time correlation functions (between oscillator operators) which carry quantum correlations.

Outline

This thesis is divided into four chapters. The first one sets the stage of the discussion throughout the present dissertation, it includes a comprehensive introduction to the theory of entanglement and the physical statements in which the open-systems dynamics treatment grounds. Chapter 2 contains the core of the research carried out during this thesis. That is the separability criterion proposed in Ref.[**A1**], and a summary of the main results and conceptual developments collected in Refs. [**A2**], [**A3**], and [**A4**]. Chapter 3 contains the conclusions drawn from the performed investigation, and it includes a brief discussion of future perspectives. Finally, the compedium of publications can be found in Chapter 4.

Contents

Preface **v**

Acknowledgments **vii**

Abstract **x**

Outline **xii**

1 Introduction **1**
1.1 Continuous variable systems 4
1.2 Quantum entanglement 7
1.2.1 The concept of (in)separability 9
1.2.2 Multipartite entanglement 19
1.2.3 k-separability and k-partite entanglement 20
1.2.4 SLOCC classification and others 24
1.3 Modelling open quantum systems 27
1.3.1 Microscopic approach to dissipative harmonic oscillators 29
1.3.2 Generalized Langevin equation 35
1.3.3 Time-independent Fokker-Planck equation 44

2 Entanglement dynamics **49**
2.1 Separability criteria for CV multipartite entanglement 50
2.1.1 A Gaussian-like assumption 52
2.2 Entanglement dynamics in dissipative scenarios 57
2.2.1 Transient Entanglement 58
2.2.2 Stationary three-mode Gaussian entanglement 63

3 Conclusion and prospects **75**

4 Compendium **79**

Article 1 **81**

Article 2 **95**

Article 3 **109**

Article 4 **119**

A Microscopic model **151**

Bibliography **155**

Chapter 1

Introduction

The best possible knowledge of a whole
does not necessarily include the best possible knowledge of all its parts.
-Erwin Schrödinger (Extracted from [215])

Schrödinger in 1935 recognized a quantum phenomenon which is considered to be the most radical departure of quantum mechanics from the classical way of thought [215]. Such phenomenon was originally coined as quantum *entanglement*, and manifests itself as non-local correlations between observables of composite quantum systems that by no means can be simulated classically. Shortly before, the Einsten-Podolsky-Rosen "Gedankenexperiment" deeply shook up the Physics Community by showing that entanglement could make the predictions of quantum mechanics incompatible with the intuitive idea of *local realism* [73]. From that moment, entanglement became a central issue on several heated debates concerning the foundations of quantum mechanics during the subsequent century. It was after the seminal contribution of Bell in 1964, where he translated the Einsten-Podolsky-Rosen ideas into a set of measurable inequalities [30], that entanglement could be experimentally tested. More than fifty years later, the profound consequences raised form Bell's inequalities still lack of a complete understating within the Physics Community [214].

Only recently the way entanglement was perceived changed drastically thanks to the birth of the quantum information theory [37; 66; 21]. The initial research in the field rapidly revealed that entanglement is a key ingredient for the success of many potential applications like quantum computation [176], teleportation [163], or quantum cryptography. As a consequence, entanglement is nowadays viewed as an important resource in the raising quantum technology [69]. Despite the conceptual difficulty associated with the phenomenon, this vision has lead in the last few years to a formidable increase of general knowledge about entanglement [242]. Impressive enough, the latter has come along with a remarkable progress in the preparation and manipulation of small quantum systems (see Nobel lectures from Haroche [119] and Wineland [254]) like radiation fields into cavities [160], trapped atomic ions [174], or more recently, cold atoms in optical lattices [38].

A continuous and fruitful collaboration between theoreticians and experimentalists have permitted that the creation and control of entanglement would be currently accessible to several laboratories around the world [149; 152; 117]. However, the lack of experimentally friendly criteria for detecting this quantum correlation still limits the range of entanglement assessment to systems with a relatively small number of constituents. Indeed, there are few tools which permit us to theoretically characterize entanglement in general multipartite systems.

Unfortunately, the presence of such valuable capital is threatened by environmental effects, such as *dissipation* and *noise*, as soon as the number of constituents of the experimental setup starts to grow [170]. Entanglement is microscopically conceived as a manifestation of coherent superposition of many-particle eigenstates of composite quantum systems, and thus, it is very susceptible to decoherence mechanisms arisen from the *uncontrolled* interaction with the environmental degrees of freedom. These mechanisms can play such an important role in the fate of entanglement as to cause its complete disappearance on a finite time [260], unlike the populations and coherences defined in the density operator which typically decay asymptotically. Then, before a satisfactory quantum technology can be developed, it is necessary to focus the theoretical efforts on the scaling properties of entanglement as well as its robustness against environmental coupling with increasing system size [44; 90].

Indeed, the dynamics of entanglement has been the subject of an intensive investigation in the crossover of open quantum systems and quantum information theory, which has considerable contributed to our current understanding of entanglement under noisy and dissipative effects, see [25] for a comprehensive overview. For instance, it was shown that it is possible to construct entangled states which are immune to decoherence when the whole system suffers from the same source of noise [156], this is widely known as decoherence-free subspaces. Furthermore, though environmental effects are generally detrimental for entanglement, two particles may become entangled by the interaction with the same reservoir in certain limits [40; 198; 256]. Remarkably enough, it was proved that one may precisely drive quantum systems on preferred states, like large-particle entangled states [148], through the dissipation produced by the interaction with engineering artificial *reservoirs* [65; 147]. On the other hand, investigations on multipartite systems suggest that the larger the system the faster the decay of entanglement due to the environmental influence over each of its parties [49; 24; 23]. These are just a few results on the extensively amount of work developed on this research topic, however, a complete comprehension of entanglement in multicomponent systems influenced by environmental effects is still out of reach, for instance, there is no yet an equation of motion that governs the entanglement dynamics in general dissipative scenarios (see [146; 235]).

Yet very little is known about the dynamics of entanglement supported by the *mechanical* degrees of freedom on multi-particle or nanoscopic systems, for instance nanomechanical oscillators under realistic conditions of dissipation and noise [26]. The fact that the observation of quantum behaviour in this kind of setups entails the ability of cooling the mechanical motion to extremely low temperatures makes the analysis of entanglement challenging for theoreticians as well as experimentalists. On one hand, the

potential for doing general statements of the most aforementioned theoretical investigation relies upon the assumption that the system follows a *memoryless* quantum evolution, known as Markovian, which holds only approximately on mechanical systems at relatively high temperatures (e.g. see the damped harmonic oscillator [105; 161]). In addition, as the interest is foremost in the mechanical motion, dissipation that is generally difficult to deal with is a non-negligible source of decoherence. Surprisingly, on the other hand, an accurate degree of control over nano-mechanical oscillators has been recently achieved [108; 179; 42], which hopefully will open the door of the largely unexplored quantum world in macroscopic systems (where superconducting materials remain as an exception). Novel experimental investigation on mechanical setups, like cold atoms in optical lattices [21], are revealing that they apparently satisfy a basic prerequisite to materialize the ideas of quantum information theory: that the experimental efforts required to manipulate the system scale (non-exponentially) with the number of its constituents. Thankfully, theoretical studies also benefit from employing mechanical systems, since their quantum properties at low temperatures may be fairly well captured by a paradigmatic model based on harmonic oscillators.

Being aware of the importance of entanglement in quantum theory, whose reliable description needs an accurate characterization of the unavoidable environmental influence, and motivated by the fundamental role played by harmonic oscillators in quantum mechanics, we aim to (theoretically) explore the creation, manipulation and detection of multipartite entanglement in harmonic oscillators subjected to dissipative quantum dynamics. The endeavour that constitutes this investigation is far from being simple. First, a precise characterization of multipartite entanglement in systems under general conditions (*i.e.* in mixed states) is still an open problem in the quantum information theory. For instance, there are several easy-handling estimators of entanglement in mechanical setups but whose range of applicability is usually limited to specific forms of the system state (e.g. Gaussian states). For this reason it is of particular interest to work out new tools which may provide insightful information about multipartite entanglement in general scenarios of (non-Gaussian) states. Second, though there has been an important progress in the treatment of the open-system dynamics beyond the Markovian approximation [251; 43; 245; 209], during its analysis it is easy to meet with difficulties (e.g. the problem usually becomes numerically intractable) which can ultimately make the characterization of entanglement inaccessible. In an attempt to face with this circumstance it proves convenient to consider some simple and general statements about the environment and its interaction with the system, in order to give a practical as well as physically meaningful description of the dissipative quantum dynamics of mechanical degrees of freedom. To be more precise, the main objective of the present dissertation is twofold: we study and elaborate simple tools to characterize multipartite entanglement in either Gaussian and non-Gaussian states, and secondly, we analyze the dissipative dynamics of entanglement in harmonic oscillators for a broad class of physical situations.

To start with, we give a brief introduction to the formalism based on the so-called Wigner function to describe harmonic oscillator systems. Afterwards the introduction divides into two main parts. The first deals with the definition and characterization of en-

tanglement in harmonic oscillators, while the second part contains the formalism employed to solve the open-system dynamics.

1.1 Continuous variable systems

Nowadays some of the most promising experimental setups to perform ideas from quantum information theory include the modes of a radiation field in a set of optical or microwave cavities [41], the center-of-mass motion of nanomechanical oscillators [26] or ultracold atoms arranged in optical lattices [38]. The principal characteristic that share all these setups is that their mechanical degrees of freedom can be described in a general way as harmonic oscillators with great degree of accuracy. For instance, the single-site potential over an atom in optical lattices is approximately harmonic with typical frequencies ω_0 of $2\pi \times 100$ kHz (see Ref.[21]), while nanomechanical oscillators with masses around pico-gramme (*i.e.*, 10^{-15}kg) start to develop quantum properties near its ground state, where the amplitude of their non-linear oscillations is relatively small at temperatures around 0.1 K [179]. Furthermore, it is a ubiquitous situation in other fields of physics, like condensed matter [18], that the mechanical degrees of freedom of systems which differ in microscopic details can be described with the same language (*i.e.*, harmonic oscillators). Since we are mainly interested in the low-energy dynamics of the foregoing systems, where we expect quantum effects to be dominant, such description is well justified in the present dissertation. As a consequence, it is important to realize that the conclusions drawn from this treatment will relate to *universal* aspects of quantum entanglement. With the word universal we refer to the common properties shown by entanglement in all these systems.

Then, the aforementioned setups can be though of as a paradigmatic system composed of n (one-dimensional) harmonic oscillators or *modes*. The latter is a nice example of a *continuous variable* (CV) system[i] in ordinary quantum mechanics [53; 191] (because their degrees of freedom take an infinite number of values), and it is formally described by the n-fold tensor product of the single-mode Hilbert space $\mathcal{H}_1 = L^2(\mathbb{R})$ (which represent the set of square-integrable complex functions), *i.e.* $\mathcal{H}_n = \bigotimes_{i=1}^{n} \mathcal{H}_1$. The m-th mode is described in terms of the canonical position $\hat{q}_m$ and momentum $\hat{p}_m$ operators. Equivalently, they may be described by their dimensionless counterparts $\hat{Q}_m = \hat{q}_m\sqrt{M\Omega/\hbar}$ and $\hat{P}_m = \hat{p}_m/\sqrt{M\Omega\hbar}$ defined in terms of a characteristic frequency Ω and mass M, this shall be employed in the dimensionless analysis of entanglement. Let us introduce the operator-valued vector $\hat{\boldsymbol{x}} = (\hat{q}_1, \hat{p}_1, \ldots, \hat{q}_n, \hat{p}_n)^T$ whose elements satisfy the canonical commutation relations $[\hat{\boldsymbol{x}}_m, \hat{\boldsymbol{x}}_l] = -i\hbar\,[\boldsymbol{J}_n]_{ml}$, with the symplectic matrices

$$\boldsymbol{J}_n = \bigoplus_{m=1}^{n} \boldsymbol{J}_1 \quad \text{and} \quad \boldsymbol{J}_1 = \begin{pmatrix} 0 & -1 \\ 1 & 0 \end{pmatrix},$$

of the composite system and a single subsystem. Despite of the mathematical subtleties

[i] In contrast to CV systems one may encounter "discrete systems" (for example spin systems), whose degrees of freedom take d discrete values, and are formally described by the complex vectorial space $\mathbb{C}^d$.

that may arise from dealing with infinite-dimensional Hilbert spaces[ii] [93], we can perform a complete study of the entanglement supported by CV systems (with finite mean energy) [77], however one may expect that such study will become rather involved as compared with the simpler case of discrete systems.

The successful development of quantum optics based on the Wigner-function method proved convenient to describe a continuous variable system in terms of the real symplectic space $(\mathbb{R}^{2n}, \boldsymbol{J}_n)$, *i.e.* phase space [77; 8], rather than the infinite dimensional complex Hilbert space $\mathcal{H}_n$. In this context, a quantum mechanical operator $\hat{A}$ is replaced by its Weyl symbol

$$W_A(\boldsymbol{x}) = \int_{\mathbb{R}^{2n}} e^{i\boldsymbol{x}^T \boldsymbol{J}_n \boldsymbol{\xi}} \mathrm{Tr}\left[\hat{A} e^{-i\hat{\boldsymbol{x}}^T \boldsymbol{J}_n \boldsymbol{\xi}}\right] \frac{d^{2n}\boldsymbol{\xi}}{(2\pi)^{2n}}, \tag{1.1}$$

which is a function of the classical phase space variables $\boldsymbol{x} = (q_1, p_1, ..., q_n, p_n)$ [190], and where we have defined the so-called Weyl operator as $\hat{D}(\boldsymbol{\xi}) = e^{-i\hat{\boldsymbol{x}}^T \boldsymbol{J}_n \boldsymbol{\xi}}$. The Weyl symbol of a density matrix $\hat{\varrho}$ is typically referred to as Wigner function, and it is denoted by $W(\boldsymbol{x})$ [250].

Eq.(1.1) supports the view of the Wigner function as the Fourier transform of $\mathrm{Tr}\left[\hat{\varrho}\hat{D}(\boldsymbol{\xi})\right]$. The latter plays a remarkable role in the phase-space methods, it is known as the characteristic function of $W(\boldsymbol{x})$, and it is usually denoted by $\chi_W(\boldsymbol{\xi})$. The importance of this mathematical object relies on the fact that the average of any symmetrized product between the operators of an arbitrary set of modes can be readily obtained from the characteristic function, *e.g.*

$$\left\langle \left\{ \hat{q}_i^r, \hat{p}_j^s \right\} \right\rangle = i^s (-i)^r \left(\frac{\partial}{\partial \xi_{p_i}} \right)^r \left(\frac{\partial}{\partial \xi_{q_j}} \right)^s \chi_W(\boldsymbol{\xi}) \Big|_{\boldsymbol{\xi} \to \vec{0}} \quad \text{for} \quad r, s \in \mathbb{N}, \tag{1.2}$$

where $\{\bullet, \bullet\}$ denotes the anti-commutator. In the following we shall refer to $\left\langle \left\{ \hat{q}_i^r, \hat{p}_j^s \right\} \right\rangle$ as the (r, s)-moment of the (i, j)-modes. Conversely, the coefficients of the Taylor expansion of the characteristic function around the origin can be, in principle, obtained from the knowledge of the set of all moments between the position and momentum operators of all the system constituents. From here and Eq.(1.1) it follows that one may determine the Wigner function from the full statistics of the position and momentum operators of the system modes.

Unfortunately, the full knowledge of the Wigner function for arbitrary quantum states can become a complex problem since the computation of all such moments is usually a rather difficult task in practice. Nonetheless, the situation simplifies considerably if we focus our attention on the so-called Gaussian states. By definition a quantum state $\hat{\varrho}$ is

[ii] An important property of CV-system Hilbert spaces is that they are separable. This means that they admit a countable orthonormal basis, e.g. any vector $|v\rangle \in \mathcal{H}_1$ can be written in terms of the basis $\{|m\rangle\}_{m=0}^{\infty}$ as follows $|v\rangle = \sum_{m=0}^{\infty} v_m |m\rangle$ [1]. For harmonic oscillators, such basis can be identified with the Fock or number basis, and $\mathcal{H}_n$ will correspond to the tensor product structure of infinite-dimensional Fock spaces.

Gaussian if its Wigner function is a Gaussian function, *i.e.*

$$W(\boldsymbol{x}) = \frac{e^{-\frac{1}{2}(\boldsymbol{x}-\bar{\boldsymbol{x}})^T \boldsymbol{V}^{-1}(\boldsymbol{x}-\bar{\boldsymbol{x}})}}{(2\pi)^n \sqrt{\det(\boldsymbol{V})}}, \tag{1.3}$$

where the vector $\bar{\boldsymbol{x}} = \mathrm{Tr}(\hat{\varrho}\hat{\boldsymbol{x}})$ contains the expectation values (first-moments) of the phase space variables, and $\boldsymbol{V}$ is the *covariance matrix* (CM) which is defined by

$$\boldsymbol{V}_{ml} = \frac{1}{2}\mathrm{Tr}\left(\hat{\varrho}\left\{[\hat{\boldsymbol{x}}]_m - [\bar{\boldsymbol{x}}]_m, [\hat{\boldsymbol{x}}]_l - [\bar{\boldsymbol{x}}]_l\right\}\right) . \tag{1.4}$$

In this case, W is completely characterized by the vector $\bar{\boldsymbol{x}}$ and the real symmetric $2n \times 2n$ matrix $\boldsymbol{V}$, *i.e.* by $2n^2 + n$ real parameters. According to the Heisenberg uncertainty relation, the covariance matrix of any quantum state must satisfy $\boldsymbol{V} \geq \frac{i\hbar}{2}\boldsymbol{J}_n$ [77], which implies the positive definiteness $\boldsymbol{V} > 0$. Equivalently, the uncertainty relation can be expressed in terms of the symplectic eigenvalues, denoted by $\{\nu_i\}_{i=1}^n$, of the covariance matrix $\boldsymbol{V}$ as $\nu_i > \hbar/2$ for $i = 1, \ldots, n$. It should be noticed that the symplectic eigenvalues of a $2n \times 2n$ real symmetric matrix $\boldsymbol{A}$ are directly obtained as the eigenvalues $\{\pm i\nu_i\}_{i=1}^n$ of the matrix $\boldsymbol{J}_n^T\boldsymbol{A}$. Furthermore, it will be seen that the entanglement is invariant under local unitary transformations [77]. Doing a translation in the phase space of each oscillator we can conveniently cancel out the mean values $\bar{\boldsymbol{x}}$ without changing the entanglement properties of the system (*i.e.*, we take $\bar{\boldsymbol{x}} = 0$ from now on).

Most recently, a considerable amount of research has been directed towards the study of CV states generated from Gaussian ones by operations made with photons [141], that is to say, by adding or subtracting photons to the modes composing the system. As a result, the state is no longer Gaussian but its Wigner function can be expressed in a compact form as follows,

$$W(\boldsymbol{x}) = \frac{F(\boldsymbol{x})e^{-\frac{1}{2}\boldsymbol{x}^T \boldsymbol{V}^{-1}\boldsymbol{x}}}{(2\pi)^n \sqrt{\det(\boldsymbol{V})}}, \tag{1.5}$$

where $F(\boldsymbol{x})$ is a polynomial function whose degree is roughly determined by the number of such manipulations that need to be applied to a Gaussian state to arrive at the state of interest. It should be emphasized that a broad set of non-Gaussian states are described by a Wigner function of the type (1.5) since we only require $F(\boldsymbol{x})$ to be an analytic function with domain in all the phase space.

Thorough the present dissertation we shall focus on Gaussian and non-Gaussian states characterized by Eq.(1.5). The importance of Gaussian quantum states also relies on the fact that they naturally appear in every quantum system which can be described, at least approximately, by a quadratic bosonic Hamiltonian, for which their ground or thermal equilibrium states are Gaussian [216]. Moreover, a great degree of accuracy has been achieved in the experimental creation and manipulation of Gaussian states with optical fields [149]. For these reasons a substantial part of quantum information theory for CV systems has been developed for such states [250]. On the other hand, recent investigations pointed out that the non-Gaussian states given in Eq.(1.5) display particularly strong non-classical properties, which make them convenient for experimentally testing puzzling ideas from quantum physics.

1.2 Quantum entanglement

The phenomenon of entanglement emerges in quantum systems composed by many parties or subsystems. These can be photons, qubits [iii], mechanical oscillators, or even different degrees of freedom of the same quantum object may, in principle, be conceived as a composite system which may support quantum entanglement [29] (for example the system consisting of the spatial displacement and spin of an atom). The simplest case is a bipartite system constituted by only two parties/subsystems. A prominent example is given by the two-qubit system, widely denoted by Alice (A) and Bob (B), within the quantum information community. Since all the relevant information about the system is encoded in the density operator $\hat{\varrho} \in \mathcal{H}_n$, entanglement is then a property related to the state, and we will say that the system is entangled when $\hat{\varrho}$ would show entanglement.

In this context, entanglement physically manifests as correlations between observables concerning different subsystems that cannot be reproduced by purely classical means. For example, Bell's inequalities constitute a feasible experimental test for these correlations in spin systems. However, Schrödinger pointed out that entanglement has a more profound implication on the *nature* of the system which is intimately related to the *information* encrypted by the state. Information is the central object of quantum information theory, and may be quantified by using the von Neumann entropy [34],

$$S(\hat{\varrho}) = -\mathrm{Tr}\hat{\varrho}\,\log_2\hat{\varrho}. \tag{1.6}$$

In his work [217], Schumacher provided an operational meaning (within a communication scheme) to the notion of information within quantum theory: Eq.(1.6) determines the mean number of qubits needed to faithfully transmit a statistical ensemble of pure quantum states. Contrary to the classical counterpart [iv], the entropy of a subsystem can be greater than the entropy of the total system when the state is entangled. More precisely, it has been proven that only entangled states violate the following entropic inequalities [128],

$$S(\hat{\varrho}_{AB}) \geq S(\hat{\varrho}_A), \quad S(\hat{\varrho}_{AB}) \geq S(\hat{\varrho}_B), \tag{1.7}$$

where $\hat{\varrho}_{A/B} = \mathrm{Tr}_{A/B}(\hat{\varrho}_{AB})$. In ordinary words, the violation of equation (1.7) means that in an entangled system the knowledge about its whole is greater than about either of its parts. Schrödinger noticed that this bizarre feature of entanglement leads to seemingly paradoxical situations as Einstein, Podolsky, and Rosen tried to show [215]. Aside the violation of Eq.(1.7), other quite important feature that has none classical counterpart is known as *monogamy* of entanglement [52; 121]. This property consists on a trade-off in

[iii] Recall that the qubit replaces the role of the classical binary digit in the extension of classical information theory to quantum systems, and thus, it represents a fundamental unit of information [66]. Physically, it is any two-state quantum system, such as spin-$\frac{1}{2}$ or an arbitrary superposition of two Fock states.

[iv] The classical counterpart of the von Neumann entropy is the Shannon entropy which is generally denoted by $H(\rho)$, where ρ is the probability distribution that describes the state. Unlike the former, the Shannon entropy of a bipartite state ρ_{AB} is never smaller than the entropy of the reduced states that represent the two subsystems alone, *i.e.* $H(\rho_{AB}) \geq H(\rho_A), H(\rho_B)$.

the amount of entanglement that the different constituents of a many-party system may share: Instead of appearing between the elementary subsystems, entanglement generally emerges stronger between groupings of those subsystems.

Further counter-intuitive aspects of entanglement are found in the realm of statistical physics concerning the mechanism whereby a quantum system and its environment, which is considered to be comparatively large, become eventually entangled due to their unavoidable interaction. Paradoxically, such entangling interaction is though to be the main responsible for the loss of coherence in quantum systems, and thus, it would be the reason why the macroscopic world seems to behave not quantum mechanically [265]. Remarkable enough, it was suggested that this entanglement is at the origin of thermalization of a small system in contact with an environment [201].

Though entanglement is considered to be the most prominent quantum correlation, it is not the only one that can be observed in many-party systems. Zurek, Ollivier & Zurek, and independently, Hernderson & Vedral introduced the quantum discord as a quantity which enables to measure the *quantumness* of correlations [120; 181]. In particular, they showed that quantum systems, even in absence of entanglement, may have non-zero discord, that is to say, they still contain non-classical correlations. Surprisingly enough, in Ref.[82] it was shown that almost all quantum states have non-zero discord. This result indicates that entanglement is comparatively a quantum correlation more difficult to be experimentally and theoretically observed.

Several equally intriguing questions about entanglement still remain open. Research pursuing to answer these questions form a research field on its own, framed within the quantum information theory and known as theory of entanglement [129]. For the present dissertation the main interest is put on the following issues: Can a meaningful picture of entanglement in a CV system be provided?, and second, Can this picture be readily characterized by simple and experimentally friendly tools? As a starting point, one may look only at the entanglement supported by a particular partition or decomposition in two groups of the n-mode system. That is, we rearrange the n modes in two larger subsystems, which shall be refereed to as $n_A \times n_B$-mode bipartition, and ask ourselves whether they are entangled. Since there are $2^{n-1}-1$ inequivalent such bipartitions[v], it takes little imagination to anticipate that the certification of entanglement becomes cumbersome with an increasing number of constituents, and that a complete answer to the first question represents a great endeavour due to the huge number of distinct ways in which a system

[v]Let us show how the number of bipartitions is obtained from the following result of combinatorial analysis,

$$\sum_{k=1}^{n-1} \binom{n-1}{k} = 2^{n-1} - 1.$$

Let us denote each partition by S_1 and S_2. If we consider that S_1 contains at least a single-mode, then $\binom{n-1}{k}$ gives the number of inequivalent ways in which we can split the n-mode system in a partition S_2 consisting on k modes and S_1. As this is true for any value of $k = 1, \ldots, n-1$, the total number of bipartitions is obtained by summing all of such partitions raging from the situation when S_2 only contains one mode and S_1 the rest ($k = 1$), and the converse situation ($k = n-1$). Clearly, this number is given by the mentioned result.

can be entangled. Indeed, a complete description of multipartite entanglement stands as one of the great challenges in the theory of entanglement. However, quantum information theory has provided numerous complementary partial answers to both questions by introducing the concept of *separable* states. In the following we shall show how this concept allows to formally define entanglement and gain a deep understanding in the quantitative and qualitative estimation of this quantum correlation. The following section culminates with the introduction of the separability criteria for multipartite continuous-variable states proposed in Ref.[A1], and a comparative study with others similar results.

1.2.1 The concept of (in)separability

Roughly speaking, entanglement are correlations that cannot be created by either local or classical means. A more rigorous definition requires a more precise description about which operations correspond to these 'classical means' within quantum theory. A priori, it does not seem a promising task to give a satisfactory answer to such issue, because the distinction between 'quantum' and 'classical' manipulations frequently leads to a heated debate. Nonetheless, the essential question may be thought of as follows: all those manipulations that are able to create or increase classical correlations must encompass these classical means, otherwise the latter could induce quantum correlations (entanglement). A step further, once one knows the explicit form of the density operators which are classically correlated, the foregoing question reduces to ask which operations preserve this form. Fortunately, Werner provided such form in Ref.[252], by characterizing the set of classically correlated states[vi] as the result of individual preparations in each party that share the same source of randomness. Nowadays, these classically-correlated states are widely refereed to as *separable* states [125].

Quantum information theory has classified those local and classical means under the name *local operations and classical communications* (LOCC) [170; 200]. This set comprises general local manipulations as well as all those which may be performed using classical communication. Intuitively, one may conveniently exchange (classical) information between different parties of a composed system using standard telecom technologies, and subsequently apply local operations conditioned to this information that may result in (classical) correlations. Mathematically, whereas local operations can be easily expressed in terms of a tensor product of unitary operators acting independently on each system party (for instance, in the bipartite case $\mathcal{E}_{loc}(\hat{\varrho}) = (\hat{u}_A^\dagger \otimes \hat{u}_B^\dagger)\hat{\varrho}(\hat{u}_A \otimes \hat{u}_B)$), LOCC are described by a much more complex expression that involves an operator sum of tensorial product of unitary (local) operators[vii] (see e.g. [68]). It is important to realize that entanglement

[vi] Remarkably, the introduction of the quantum discord showed later that the set of states which Werner initially called classically correlated may possess quantum correlations, however they have no entanglement [4].

[vii] As an example, in the bipartite case it looks like $\mathcal{E}_{LOCC}(\hat{\varrho}) = \sum_{ijk\ldots} \cdots (\hat{F}_3^{ijk} \otimes \mathbb{I}^A)(\mathbb{I}^B \otimes \hat{E}_2^{ij})(\hat{F}_1^i \otimes \mathbb{I}^A)\ \hat{\varrho}\ ((\hat{F}_1^i)^\dagger \otimes \mathbb{I}^A)((\hat{E}_2^{ij})^\dagger \otimes \mathbb{I}^B)((\hat{F}_3^{ijk})^\dagger \otimes \mathbb{I}^A)\cdots$, where $\sum_{ijk} \hat{F}_\alpha^{ijk}(\hat{F}_\alpha^{ijk})^\dagger = \mathbb{I}$ and $\sum_{ijk} \hat{E}_\alpha^{ijk}(\hat{E}_\alpha^{ijk})^\dagger = \mathbb{I}$ for any α and each sequence of indices $(i, j, k, \ldots)$ (and $\mathbb{I}^{A/B}$ is the unit operator acting on the Hilbert space $\mathcal{H}_{A/B}$).

remains invariant under unitary local manipulations (*i.e.*, local basis changes), whereas the action of a LOCC can vary the quantum correlations properties of the state (e.g. a pure state may not remain pure under LOCC).

In the bipartite case, it is immediate to see that the density matrix of any pure state produced by only doing local operations, is necessarily given by a tensor product between two reduced states, written as $|\Psi_{AB}\rangle = |\Psi_A\rangle \otimes |\Psi_B\rangle$, which describe independently the two subsystems. Since we have argued that entanglement can not be created by local operations, one may use this fact to define entanglement as follows: if the density operator can not be written as a tensorial product state, the state is bipartite entangled and by extension we say the bipartite system is entangled. One can go further by appealing to the property that any mixed state may be expressed as a convex sum of pure states, this leads in a natural way to the concept of separability. The state is called separable (in the sense of Werner) if and only if it can be expressed as a convex sum of product states[viii], *i.e.*

$$\hat{\varrho}_{AB} = \sum_i p_i \hat{\varrho}^i_A \otimes \hat{\varrho}^i_B, \tag{1.8}$$

where $\hat{\varrho}^i_{A/B} = |\Psi^i_{A/B}\rangle \langle\Psi^i_{A/B}|$, $p_i \geq 0$ $(\forall\ i)$ and $\sum_i p_i = 1$. The extremely important property of this state is that only LOCC are necessary to produce it [112]. By virtue of the preceding discussion, we may extend the previous definition of entanglement to mixed states as follows: the state is bipartite entangled if and only if it is not bipartite separable [126] (in terms of the definition Eq.(1.8)). Notice that the term non-separable or inseparable is widely used as a synonymous of entangled, and the issue of knowing whether $\hat{\varrho}_{AB}$ is separable is referred to as the separability problem.

Formally, from Eq.(1.8) follows that the separability problem consists essentially on stating whether $\hat{\varrho}_{AB}$ lies in the convex hull of product states. Unfortunately, this last point is in general a rather difficult problem to discern[ix], since there may exist, in principle, infinite ways to decompose the system in an ensemble of classical probabilities and pure states, say $\left\{p_i, |\Psi^i_{A/B}\rangle\right\}$. It will be seen that the solution of this problem can be obtained from applying optimization procedures which return a preferred decomposition that minimizes certain functional (see convex-roof measures) or the lowest mean value of certain observable among all separable states (see entanglement witness). More precisely, it has been shown that the separability problem is closely related to the optimization of some linear function $f(\boldsymbol{x}) = \boldsymbol{c}^T\boldsymbol{x}$, with $\boldsymbol{x} \in \mathbb{R}^t$ being the objective variable (t is determined by the specific problem), subjects to the constraint $\boldsymbol{F}_0 + \sum_{s=1}^{t} \boldsymbol{x}_s \boldsymbol{F}_s \geq 0$, where $\boldsymbol{F}_0,\ \boldsymbol{F}_1, \cdots,\ \boldsymbol{F}_s$ are Hermitian matrices of arbitrary dimensions [76]. These problems are called semi-definite programs. Hyllus and Eisert provided an example of the relation between the separability problem and semi-definite programs in the realm of continuous-variable systems [134].

[viii] From the Caratheodory theorem [129] follows that the number of terms in the convex sum appearing in Eq.(1.8) is bounded from above by the square of the dimension of the global Hilbert space $d_{AB} = \dim\mathcal{H}^2_{AB}$.

[ix] Gurvits showed that the separability problem in discrete systems is NP-hard (Non-deterministic Polynomial-time hard) [115]. Roughly speaking, a NP-hard problem is at least as hard as any decision problem for which an available solution can be efficiently tested by an algorithm which needs to do a number of operations that grows polynomially with the input size.

First, let us note that shortly before it was proved that any $n_A \times n_B$-mode bipartite state with CM $\boldsymbol{V}_0$ is separable if there exist two CMs $\boldsymbol{V}_A$, $\boldsymbol{V}_B$ such that $\boldsymbol{V}_0 \geq \boldsymbol{V}_A \oplus \boldsymbol{V}_B$ [253; 129], *i.e.*

$$\hat{\varrho}_{AB}, \text{ with CM } \boldsymbol{V}_0, \text{ separable } \Rightarrow \boldsymbol{V}_0 \geq \boldsymbol{V}_A \oplus \boldsymbol{V}_B \text{ with } \boldsymbol{V}_A \geq \frac{i}{2}\boldsymbol{J}_{n_A}, \boldsymbol{V}_B \geq \frac{i}{2}\boldsymbol{J}_{n_B}. \quad (1.9)$$

Hyllus and Eisert showed precisely that the solutions of some semi-definite optimization problems provide exactly efficient tests to certify the inequality (1.9). Interesting enough, Werner and Wolf realized that if the inequality is fulfilled for Gaussian states, then the state can be obtained by LOCC from the Gaussian state with covariance matrix $\boldsymbol{V}_A \oplus \boldsymbol{V}_B$, and therefore, the Ineq.(1.9) is also sufficient for separability on these states. Regarding the separability criteria proposed in Ref.[**A1**], its advantage, compared with other relative results, essentially relies upon the fact that it provides a readable optimization procedure to solve the semi-definite program corresponding to an analogous separability problem in multipartite CV systems, see Chapter 2 for further details.

In spite of the difficulty behind the separability problem, nowadays there is a considerable body of literature on the theory of entanglement [233; 77; 170; 34; 8; 200; 129; 112; 51; 9], whose major concern is to provide qualitative as well as quantitative estimators of entanglement, preferentially which would be experimentally accesible. Most of the important progress on this research area is related to the characterization of bipartite entanglement between a given decomposition of the many-party system onto two large subsystems. Although there are many significant results and contributions on this issue, we can roughly classified them into three fundamental approaches. Currently, the most efficient entanglement estimator, for either pure and mixed bipartite states, was proposed by Peres in the seminal work [192], and it is known as the Positive Partial Transposition criterion. Among the most important theoretical tools in the theory of entanglement is also the so-called Entanglement Witness, which represents a simple computational and experimentally feasible criteria to detect and quantify entanglement. Finally, entropy lies at the heart of the quantum correlations theory as it was previously emphasized, and it will be seen how entanglement can be quantified by entropy-based measures.

In what follows, we shall focus on the most relevant results for detecting and quantifying entanglement in a bipartite continuous-variable system, namely Alice (A) and Bob(B). We pay special attention to those results used in the analysis of entanglement performed in Refs. [**A2**], [**A3**], and [**A4**].

1. **Positive Partial Transposition** (PPT): it is in general a necessary criterion for separability, and is based on the observation that all density operator $\hat{\varrho}_{AB}$ describing a separable state must remain positive[x] under the partial transposition with respect to one of the indices corresponding to either the A or B subsystem, *i.e.*

$$\hat{\varrho}_{AB} \text{ separable} \Rightarrow \hat{\varrho}_{AB}^{T_B} \geq 0, \quad (1.10)$$

[x] A Hermitian operator is called positive if only if it has a non-negative spectrum. Similarly a map $\mathcal{E} : \hat{\varrho} \to \mathcal{E}(\hat{\varrho})$ is positive only if it preserves the Hermitian and positive properties of $\hat{\varrho}$.

where $\hat{\varrho}_{AB}^{T_B} = [\mathbb{I}_A \otimes T_B](\hat{\varrho}_{AB})$ is the partially transposed operator [187] defined by

$$\langle m| \langle \mu| \hat{\varrho}_{AB}^{T_B} |n\rangle |\nu\rangle = \langle m| \langle \nu| \hat{\varrho}_{AB} |n\rangle |\mu\rangle ,$$

and similarly for partial transposition on A. Any state satisfying the inequality in Eq.(1.10) is called PPT. Then, the criterion is equivalent to say that all states that are not PPT must be necessarily entangled. However, the other way around is not generally true, and there can be PPT states that are entangled. It has been shown that PPT entangled states posses essentially *bound* entanglement, which means that if we have N copies of the state then we cannot concentrate the entanglement in some (less) copies by doing certain manipulations involving only LOCC [129]. Behind the latter is the intuitive idea of 'distillation' of entanglement.

The PPT criterion can be though of as a particular case of a more general criterion in terms of positive maps,

$$\hat{\varrho}_{AB} \text{ separable} \Rightarrow [\mathbb{I}_A \otimes \mathcal{E}_B](\hat{\varrho}_{AB}) \geq 0, \tag{1.11}$$

where $\mathcal{E}_B$ may be any positive but not complete positive (CP) map [xi]. Remarkably enough Horodecki (M.), Horodecki (P.), and Horodecki (R.) showed that bipartite entanglement can be fully determined (it means a necessary and sufficient condition) by applying all positive but no CP maps to any given $\hat{\varrho}_{AB}$ [125]. In practice, however, the general form of all theses maps is essentially unknown and this approach becomes unfruitful.

Shchukin and Vogel found that the PPT criterion in continuous-variable systems may be nicely expressed in terms of an infinite series of inequalities concerning the moments of the quadrature variables [224; 172]. As an example, they showed that in the two-mode case these hierarchy of inequalities can be compactly expressed in terms of the following infinite Hermitian matrix of moments,

$$M(\hat{\varrho}_{AB}) = [M_{ij}(\hat{\varrho}_{AB})] ,$$

with

$$M_{ij}(\hat{\varrho}_{AB}) = \mathrm{Tr}\left(\hat{a}^{\dagger i_1}\hat{a}^{i_2}\hat{a}^{\dagger i_3}\hat{a}^{i_4} \otimes b^{\dagger j_1}b^{j_2}b^{\dagger j_3}b^{j_4}\hat{\varrho}_{AB}\right) ,$$

where $i = (i_1, i_2, i_3, i_4) \in \mathbb{N}^4$ and $j = (j_1, j_2, j_3, j_4) \in \mathbb{N}^4$, and a^α, b^β are the annihilation operators acting on A and B, respectively. It turns out that $\hat{\varrho}_{AB}$ is PPT if and only if all the principal minors of $M(\hat{\varrho}_{AB})$ are non-negative. Thus, a negative value of the latter reveals necessarily the entanglement in the state. This scheme reduces considerably in the case of a $n_A \times n_B$-mode Gaussian state, for which the PPT criterion can be formulated as follows [8],

$$\hat{\varrho}_{AB}, \text{ with CM } \boldsymbol{V}_{A|B}, \text{ separable} \Rightarrow \tilde{\boldsymbol{V}}_{A|B} \geq \frac{i}{2}\boldsymbol{J}_n \tag{1.12}$$

[xi] A positive map $\mathcal{E}$ is completely positive (CP) if its extension $\mathcal{E} \otimes \mathbb{I}$ is positive too, being $\mathbb{I}$ the identity map in any dimension. These kind of maps are extremely important in physics, since quantum operations are described by completely positive maps.

where $\tilde{\boldsymbol{V}}_{AB}$ stands for the partially transposed covariance matrix which is given by

$$\tilde{\boldsymbol{V}}_{A|B} = \boldsymbol{\Lambda}_{A|B}\boldsymbol{V}_{A|B}\boldsymbol{\Lambda}_{A|B}, \tag{1.13}$$

with

$$\boldsymbol{\Lambda}_{A|B} = \mathrm{diag}(\underbrace{1,1,1,1,\ldots,1,1}_{n_A},\underbrace{1,-1,1,-1,\ldots,1,-1}_{n_B}).$$

It should be noticed that the inequality in Eq.(1.12) can be equivalently expressed in terms of the symplectic eigenvalues, denoted by $\tilde{\nu}_i$, of $\tilde{\boldsymbol{V}}_{AB}$ as follows

$$\tilde{\nu}_i \geq \frac{1}{2} \text{ for } i \in \{1,\ldots,n\} \ . \tag{1.14}$$

Remarkably, PPT is also sufficient for separability in quantum Gaussian states describing bipartite systems composed by either $1_A \times n_B$ [227; 253], or $n_A \times n_B$ modes endowed with symmetry with respect to the permutation of A and B (bisymmetric Gaussian states) [221], being n_A and n_B arbitrary.

We would like to mention here that Giedke, Kraus, Lewenstein, and Cirac provided a necessary and sufficient operational criterion for separability of bipartite Gaussian states composed by an arbitrary number of modes. This does not rely on PPT at all, rather, in a non-linear map that transforms $\boldsymbol{V}$ in an appropriate CM $\boldsymbol{V}_N$ whose entanglement can be readable assessed by using the separability condition given in Eq.(1.9). If the original CM $\boldsymbol{V}$ is separable, then this criterion returns $\boldsymbol{V}_A$ and $\boldsymbol{V}_B$ [99].

2. **Entanglement Witness** (EW): An entanglement witness is any observable $\hat{W}$ that (i) has at least one negative eigenvalue (*i.e.* is not positive), and (ii) has non-negative mean values for all product states [125]. This approach relies on the mathematical properties of the set $\mathcal{S}_{AB}$ comprising all separable states: this is compact and convex[xii]. The latter and property (ii) guarantee that $\hat{W}$ has always non-negative mean values for separable states, *i.e.*

$$\hat{\varrho}_{AB} \text{ separable} \Rightarrow \mathrm{Tr}(\hat{W}\hat{\varrho}_{AB}) \geq 0. \tag{1.15}$$

Therefore, a negative expectation value of $\hat{W}$ signals the presence of entanglement. The main advantage of using EWs is that one may, in principle, design an experimental setup to assess the inequality given in Eq.(1.15) by decomposing $\hat{W}$ into a sum of locally measurable terms [112]. As compared with entanglement criteria based on PPT, entanglement witnesses may be more convenient in those situations where we do not have access to the full knowledge of the state. However, some a

[xii] Intuitively, this means that the connection line between any two points in the set $\mathcal{S}_{AB}$ lies also into the set. Consequently, there is always a plane separating an entangled state from the separable states. Within the EW approach, such plane is geometrically determined by $\mathrm{Tr}(\hat{W}\hat{\varrho}_{AB})$.

priori knowledge on the state is required (before applying the measurement scheme) in order to design successful EWs.

Remarkably enough, one may construct an entanglement witness $\hat{W}_{\mathcal{E}}$ based on any positive but not CP map $\mathcal{E}$ through the so-called Choi-Jamiołkowski isomorphism[xiii]. From the Horodecki result (as given in Eq.(1.11)), this implies that there exist a complete set of entanglement witnesses, denoted by $\mathcal{W}$, which are able to fully identify the bipartite entanglement for an arbitrary $\hat{\varrho}_{AB}$ [125]: For every entangled state there exists an entanglement witness enable to detect it. The problem of this approach, unfortunately, is that it does not exist yet a practicable recipe which tell us how to construct the suited witness in accordance with the specific entanglement properties exhibited by a given state. However, an important progress in this direction was made by Lewesntein, Krauss, Cirac and Horodecki. Their idea basically relies on *optimizing* the number of entangled states detectable by a general entanglement witness $\hat{W}$ by subtracting a positive operator P as $\hat{W}'(\lambda) = (1-\lambda)^{-1}(\hat{W}+\lambda P)$ (where $\lambda > 0$), such that the new witness $\hat{W}'(\lambda)$ is optimal in the sense that there is no other witness which is able to identify more entangled states than $\hat{W}'(\lambda)$ [155]. The problem here is that the determination of P involves the computation of an infimum that is hard to calculate (at least analytically). In an analogue approach Sperling and Vogel showed that any witness can be brought on the form[xiv]

$$\hat{W}_{\hat{O}} = \hat{O} - \inf\left\{\langle a,b|\,\hat{O}\,|a,b\rangle\right\}\mathbb{I}, \tag{1.16}$$

where $\hat{O}$ is some bounded Hermitian operator (which can be positive), $|a\rangle \in \mathcal{H}_A$, and $|b\rangle \in \mathcal{H}_B$. Unlike the Lewenstein and co-workers idea, the optimal witness here is obtained from the (separability) eigenvalue problem of $\hat{O}$ [229] that is apparently easier to deal with. Recently, this approach was successfully applied in the detection of multipartite entanglement in a large system of coupled harmonic oscillators [230].

Moreover, we may establish similar separability criteria that involve the variances or higher moments of some observables instead of their mean values, this may be followed from the idea that entanglement witnesses are enhanced by adding non-linear terms [110]. These have been proved to be very successful in detecting entanglement in continuous-variables systems, and some examples, among others, are Duan-Giedke-Cirac-Zoller [70] and Simon [227] criteria, which have been extensively used for Gaussian states, or Agarwal-Biswas [14], and Nha-Kim [177] criteria, which are specially useful for detecting entanglement in non-Gaussian states. Basically, these are inequalities that involved the second and quartic moments of the quadrature

[xiii] Roughly speaking, the Choi-Jamiołkowski isomorphism states that we can make an one-to-one correspondence between a (linear) CP map $\mathcal{E}: \mathcal{B}(\mathcal{H}_B) \to \mathcal{B}(\mathcal{H}_B)$ and a (linear) positive operator $\hat{A}_{\mathcal{E}}$, where $\mathcal{E}$ would act on the set of bounded operators $\mathcal{B}(\mathcal{H}_B)$ and $\hat{A}_{\mathcal{E}} \in \mathcal{B}(\mathcal{H}_A)\otimes\mathcal{B}(\mathcal{H}_B)$ [125; 97]. This mathematical result is very important in ordinary quantum mechanics, since it allows one to relate physical actions (CP maps) with physical states (trace-one positive operators).

[xiv] Whenever $\hat{W}_{\hat{O}}$ would have a negative eigenvalue, $\hat{W}_{\hat{O}}$ could be an EW by construction (see [236]).

operators, respectively. Remarkably enough, it has been shown that many of these criteria are covered by the above mentioned infinite series of inequalities that results from the PPT criterion [173], though they were not firstly derived from PPT. In particular, we shall show that the criterion proposed in Ref.[A1] reproduces exactly the results of the PPT criterion for arbitrary two-mode and pure three-mode Gaussian states. On the other hand, Hyllus and Eisert provided useful practical tools to obtain optimal entanglement witnesses concerning only second moments by following an alternative optimization procedure to the above [134].

Others non-linear entanglement witnesses are based on the entropic manifestation of entanglement. On one hand, the entropic inequalities given in Eq.(1.7) in terms of the von Neumann entropy of the states $\hat{\varrho}_{AB}$ and $\hat{\varrho}_{A/B}$ comprise a necessary condition for separability, in general. These inequalities hold even for alternative definitions of entropy[xv] like the Rényi-α entropy [128], or Tsallis entropy[238], which are simpler to compute in comparison with the von Neumann entropy. On the other hand, one may stablish analogous necessary separability criteria by deducing the entropic inequalities evaluated now in the probability distribution of global operators (for example, the mean position and momentum of the bipartite system), that any separable state must satisfy [213].

3. **Measures based on convex-roof extension**: Both PPT criterion and EW establish general sufficient conditions for entanglement, but they are not able by themselves to quantify the amount of entanglement contained in the state. Any meaningful quantifier or measure of entanglement must be endowed with (at least) two reasonable properties [244]: (I) non-increasing under LOCC[xvi], and (II) vanishing on separable states. Interesting enough, an entanglement quantifier, say $E(\hat{\varrho}_{AB})$, can be built up on an entanglement witness $\hat{W}$ as follows [39],

$$E(\hat{\varrho}_{AB}) = \max\left\{0, -\inf_{\hat{W}\in\mathcal{M}} \mathrm{Tr}(\hat{\varrho}_{AB}\hat{W})\right\}, \tag{1.17}$$

where $\mathcal{M} = \mathcal{W} \cap \mathcal{C}$, and $\mathcal{C}$ distinguishes different entanglement measures. Unfortunately, this approach will suffer from the mathematical drawback resulting from the optimization procedure discussed previously (see paragraph above Eq.(1.16)).

A prominent example of entanglement measure is represented by the entropy of entanglement $E_S(\Psi_{AB})$ which is nothing but the reduced von Neumann entropy for bipartite pure states [35],

$$E_S(\Psi_{AB}) = S(\mathrm{Tr}_A\left(|\Psi\rangle\langle\Psi|\right)) = S(\mathrm{Tr}_B\left(|\Psi\rangle\langle\Psi|\right)). \tag{1.18}$$

[xv] For $\alpha \geq 0$, the quantum Rényi-α entropy $S_\alpha(\hat{\varrho})$ is given by $S_\alpha(\hat{\varrho}) = (1-\alpha)^{-1}\ln \mathrm{Tr}\hat{\varrho}^\alpha$, whereas the Tsallis entropy reads $T_\alpha(\hat{\varrho}) = (\alpha-1)^{-1}(1-\mathrm{Tr}\hat{\varrho}^\alpha)$. The von Neumann entropy is recovered from both definitions in the limit $\alpha \to 1$.

[xvi] More precisely, any proper entanglement measure E must satisfy $E(\hat{\varrho}) \geq E(\mathcal{E}_{LOCC}(\hat{\varrho}))$. Behind this condition is the physical intuition that entanglement cannot be created by LOCC. A quantitative estimator of entanglement satisfying this conditions is also called entanglement *monotone*.

In fact, Eq.(1.18) constitutes a unique entanglement measure in the case of bipartite pure states: proper entanglement measures coincide, as a limiting case, with the entropy of entanglement[xvii] for pure states [68]. However, this measure fakes from quantifying correctly the entanglement contained in mixed states. To tackle this issue, one may constructively extend a given measure $E(\Psi)$ for pure states to the mixed case by exploiting the fact that any state can be decomposed as a convex sum in pure states. Then, an entanglement measure may be constructed as follows,

$$E(\hat{\varrho}_{AB}) = \inf \sum_i p_i E(\Psi^i_{AB}), \tag{1.19}$$

where the infimum is taken over all possible ensemble $\{p_i, \Psi^i_{AB}\}$ which satisfies $\hat{\varrho} = \sum_i p_i \left|\Psi_i\right\rangle \left\langle\Psi_i\right|$ (with $\sum_i p_i = 1$ and $p_i \geq 0$).

Entanglement estimators built following this recipe are generically called convex-roof extended measures, and an important example is the entanglement of formation $E_F(\hat{\varrho})$ which results from the entropy of entanglement. In practice it is needed to make some simplifying assumptions over the decomposition ensemble such that the convex-roof measure still remains a powerful tool to detect entanglement, since the evaluation of the infimum value in Eq.(1.19) is a difficult task for systems described by large Hilbert spaces[xviii]. This idea was successfully applied in the case of Gaussian states, Wolf *et al.* proposed to restrict the decomposition to pure Gaussian states (that is a Gaussian convex-roof extension), which resulted in the Gaussian entanglement of formation $E_G(\hat{\varrho})$ [257]. This allowed to find a closed form expression of E_G in the case of arbitrary two-mode Gaussian states, which constitutes an upper bound of the true entanglement of formation. More generally, Adesso and Illuminati showed that the Gaussian convex-roof extension enables to define generic Gaussian entanglement measures starting from *bona fide* measures of bipartite entanglement in pure Gaussian states [6]. In this direction Adesso, Girolami, and Serafini introduced the so-called Gaussian Renyi-2 entanglement [5], which is a convex-roof measure based on the Renyi-2 entropy $\mathcal{E}_2$ (analogous to E_G). The latter is specially interesting because it can be used to quantify the monogamy of entanglement in n-mode Gaussian states through the following inequality

$$\mathcal{E}_2(\hat{\varrho}_{S_1|S_2\ldots S_n}) - \sum_{i=2}^{n} \mathcal{E}_2(\hat{\varrho}_{S_1|S_i}) \geq 0, \tag{1.20}$$

where S_i denotes the ith constituent of the interesting system. Given a bipartition $A|B$ of the state, Ineq.(1.20) physically constraints the distribution of bipartite

[xvii] It is intuitive to see the reason for which the von Neumann entropy may work as an entanglement measure for pure states. Loosely speaking, this relies on the fact that the partial trace of a pure product state always returns a pure state. A positive value of the entropy of the reduced states $\hat{\varrho}_A$ or $\hat{\varrho}_B$ reveals that they are mixed, and then it entails that $\hat{\varrho}_{AB}$ is necessarily entangled.

[xviii] In discrete systems, it was shown that the running time of any algorithm for computing $E_F(\hat{\varrho})$ would grow exponentially with the dimension of the Hilbert space [132].

entanglement among different partitions of the system: the entanglement between the A and B parties as a whole will be greater than the entanglement that can be established between the constituents of A and B separately. Adesso and Illuminati showed that bipartite entanglement measures satisfying analogue inequalities to (1.20) may also provide proper quantifiers of multipartite entanglement [7] (see Sec.1.2.2). Surprisingly enough, not all entanglement measures obey an inequality analogue to Eq.(1.20).

4. **(Logarithmic) Negativity**: There is yet another family of entanglement measures that is straightforward to compute, specially in continuous-variable systems. The negativity $N(\hat{\varrho}_{AB})$ basically consists in quantifying the violation of the PPT criterion for separability, much in the spirit of Eq.(1.17), and may be formally defined as

$$N(\hat{\varrho}_{AB}) = \max\left\{0, -\sum_k \lambda_k^-\right\}, \tag{1.21}$$

where λ_k^- represents a negative eigenvalue of the partial transpose. Based on this measure, Vidal and Werner proposed the logarithmic negativity $E_N(\hat{\varrho}_{AB}) = \mathrm{Log}(1 + 2N(\hat{\varrho}_{AB}))$ [247], which constitutes a full entanglement monotone (this means that it satisfies the above condition (I) in the most strict sense) [195]. An important property of the logarithmic negativity is that it is an upper bound for the entanglement entropy, *i.e.* $E_N(|\Psi_{AB}\rangle\langle\Psi_{AB}|) \geq E_S(\Psi_{AB})$. Adesso and Illuminaty showed that the logarithmic negativity, in the case of a Gaussian state with CM $\boldsymbol{V}$, is readily obtained from [10; 8],

$$E_N(\boldsymbol{V}) = \begin{cases} \sum_k \log\tilde{\nu}_k & \text{for } k : \tilde{\nu}_k < 1, \\ 0 & \text{otherwise,} \end{cases} \tag{1.22}$$

where $\tilde{\nu}_i$ are the symplectic spectrum of the partial transpose CM $\tilde{\boldsymbol{V}}$ and which is computed from the Eq.(1.13). Recalling that PPT is a sufficient and necessary criterion for entanglement in $1_A \times n_B$ and bisymmetric $n_A \times n_B$ Gaussian states, Eq.(1.22) may be employed to properly quantify the bipartite entanglement of these states. Although the logarithmic negativity does not satisfy any analogue expression to equation (1.20) exhibiting monogamy, it is easier to compute for mixed states than the Renyi-2 entanglement, and it is used to analyse the entanglement in two-mode, and 1×2-mode Gaussian states in Refs. **[A2]**, **[A3]**, and **[A4]**.

In large harmonic chains and lattices maintained in the ground and thermal states and with nearest-neighbour interactions and periodic boundary conditions, logarithmic negativity has been successfully employed to quantify bipartite entanglement between a distinguished group or region I, whose boundary we denote by δI, an its exterior [27; 196; 20]. Remarkably enough, Audeneart and co-workers for harmonic chains, and later, Plenio and co-workers in optical lattices showed that the logarithmic negativity exhibits a linear dependence in the number of oscillators on the surface of the region,

say $E_N(\hat{\varrho}_I) \sim N_{\delta I}$. Subsequently, this permitted to prove that entanglement of the reduced system scales at most as the boundary area of the region, *i.e.* $E_S(\Psi_I) \leq N_{\delta I}$. This relation is referred to as an *area law* [75], and is of important relevance in many-body systems because it has been found in many realistic models [51]. Intuitively, an area law suggests that most of the quantum correlations decay rapidly in a finite number of neighbours, that is the correlation length is small enough such that the entanglement between the region I and its exterior are mainly established via its boundary surface [75]. However, the converse may not be true: we may have an area law even for an infinite correlation length.

As one may have probably appreciated the evaluation of any entanglement measure, including logarithmic negativity, requires the full knowledge of the density operator, which theoretically can be obtained from an ensemble of measurements on a complete set of observables, for instance by quantum state tomography. However, this ensemble grows rapidly with the Hilbert space dimension of the composite system under study, such that the required efforts to determine $\hat{\varrho}_{AB}$ may rapidly saturate experimental resources and then makes ultimately inaccessible the complete knowledge of the state in many practical situations. In those cases, an alternative strategy may consist in providing tight lower bounds of entanglement measures that are experimentally accessible in the spirit of entanglement witnesses [39; 74; 169]. Starting from Eq.(1.17) one may construct an entanglement witness $\hat{W}$ which reproduces some of the above entanglement measures $E(\hat{\varrho}_{AB})$, such that one obtains a lower bound $E(\hat{\varrho}_{AB}) \geq \max\left\{0, -\mathrm{Tr}(\hat{\varrho}_{AB}\hat{W})\right\}$. Although there are several papers studying this issue, we just like to mention two of them: in Ref.[111] Gühne, Reimpell, and Werner provided a method to obtain entanglement witnesses as lower bounds of generic entanglement measures (for instance convex-roof extended measures) subject to the available measurement data on certain set of observables, while Audenaert and Plenio pursuing essentially the same question provided lower bounds of several entanglement measures, for instance logarithmic negativity in discrete systems, compatible with given values of purity and correlations in the measurement record [28].

Finally we would like to notice here that, though, there are a number of entanglement measures for mixed states, which may be distinguished from their operational meaning and mathematical properties, this issue is not a drawback in the theory of entanglement, because each of them may be worthwhile to quantify entanglement in certain physical situation. Further, this issue is not characteristic from the quantumness of entanglement, since, for example, the classical conception of entropy allows analogously different quantitative measures which are axiomatically equivalent [34].

Before proceeding any further, we must mention that the definition of entangled states, as given by Eq.(1.8), does not apply to study indistinguishable particles, essentially because their wave functions must be symmetrized if we are dealing with bosons. In particular, it does not make sense to consider each elementary subsystem as parts of *distinct* partitions

of the whole system (all the bipartitions would be also indistinguishable). Throughout the present dissertation we always assume that each harmonic oscillator composing the system can be experimentally discriminate, though they satisfy a bosonic statistics. The entanglement in harmonic oscillators is termed as continuous variable entanglement in the specialized literature in order to distinguish from the study of entanglement appearing in indistinguishable bosonic particles, which is beyond the scope of this dissertation. Comprehensive overviews in this topic can be found in Refs.[19; 182].

Let now turn the attention on multipartite entanglement, which comprises bipartite entanglement as a particular case. As a starting point one may try to generalize the foregoing techniques to characterize entanglement in multipartite systems, however, it has been shown that this is not straightforward to do in several cases. On the other hand, the difficulty behind the evaluation of the previous quantities increases with the number of constituents, so that the problem may become intractable numerically. Furthermore, unlike the bipartite case where any state is either entangled or separable, the structure of entanglement in multipartite systems is much more richer occurring *inequivalent* classes of entanglement. These problems, among others, make difficult to obtain qualitative or quantitative estimators of multipartite entanglement so successful as those for bipartite entanglement. Even there is not a unique systematic characterization of multipartite entanglement: Instead it will be seen that one uses a specific scheme to identify entanglement depending on the inseparability properties exhibited by the state. This lack of a single classification is understood as there are several types and families of quantum entanglement when more than two parties are involved. We devote the next section to discuss the relevant results regarding this topic.

1.2.2 Multipartite entanglement

The above treatment on separability is not restricted to a specific number of constituents, and thus, the definition of entanglement based on Eq.(1.8) can be straightforwardly generalized to a multipartite system that decomposes into n elementary parties S_1, S_2,..., S_n. The notion of bipartite separability translates now into full n-partite separability [243], *i.e.* the state is fully (n-partite) separable iff it can be expressed as follows

$$\hat{\varrho} = \sum_i p_i \hat{\varrho}^i_{S_1} \otimes \hat{\varrho}^i_{S_2} \otimes \cdots \otimes \hat{\varrho}^i_{S_n}, \tag{1.23}$$

where $\hat{\varrho}^i_{S_j} = |\Psi^i_{S_j}\rangle \langle \Psi^i_{S_j}|$ represents the reduced state of the S_j subsystem. Then, all states that are not separable according to Eq.(1.23) are called n-partite entangled or inseparable. The condition Eq.(1.23) of full separability can be nicely reformulated for Gaussian states, as we showed previously for the bipartite case, in terms of their covariance matrix: a n-mode Gaussian state with CM $\boldsymbol{V}$ is fully separable if only if there exist a set of covariance matrices $\left\{\boldsymbol{V}_{S_1}, \ldots, \boldsymbol{V}_{S_n} : \boldsymbol{V}_{S_j} \geq \frac{i}{2}\boldsymbol{J}_1, \quad j = 1, \ldots, n\right\}$ such that [99]

$$\boldsymbol{V} \geq \boldsymbol{V}_{S_1} \oplus \boldsymbol{V}_{S_2} \oplus \cdots \oplus \boldsymbol{V}_{S_n}. \tag{1.24}$$

As before, this condition is just necessary for full separability in more general states than Gaussian.

Looking closely to the definition of full separability based on Eq.(1.23), it is seen that it does not provide a description of multipartite entanglement as meaningful as for bipartite entanglement. For instance, there may exist a partition $\{I_1, \ldots, I_k\}$ being I_i disjoint subsets of the set of indices $S = \cup_{i=1}^{n} S_i$, *i.e.*

$$S = I_1 \cup I_2 \cup \cdots \cup I_k \text{ with } I_i \cap I_j = \emptyset \text{ if } i \neq j, \tag{1.25}$$

in which a n-partite pure state may split in k parties as follows $|\Psi\rangle = |\Psi\rangle_{I_1} \otimes |\Psi\rangle_{I_2} \otimes \cdots \otimes |\Psi\rangle_{I_k}$, where $|\Psi\rangle_{I_i}$ is defined on the tensor product of all elementary Hilbert spaces belonging to the set I_i. This state is *partially* separable in some sense because it is separable with respect to the partition $\{I_1, \ldots, I_k\}$, though it is still entangled since it violates condition Eq.(1.23). On the other hand, another example of realistic state is that one can not be split in any bipartition, *i.e.* $|\Psi\rangle \neq |\Psi\rangle_{I_1} \otimes |\Psi\rangle_{I_2}$ for any two disjoint subsets I_1, I_2 such that $S = I_1 \cup I_2$, which would intuitively correspond to the physical situation when all the bipartitions are entangled. Although these two exemplary cases are distinct manifestations of entanglement in multipartite systems, the definition based on Eq.(1.23) is unable to capture the difference between them. However, one may generalize this definition in order to characterize these instances of entangled states and to provide versatile separability criteria for them. This leads basically to two different schemes that are known under the name k-separability and k-partite entanglement.

1.2.3 k-separability and k-partite entanglement

The direct generalization of the notion of full separability is the concept of k-separable states, which has a clear meaning in the case of pure states: A n-partite quantum state is called k-partite separable, if only if it can be expressed as a tensorial product of k substates (with $k \leq n$), written as $|\Psi_{k-sep}\rangle = |\Psi_1\rangle \otimes |\Psi_2\rangle \otimes \cdots \otimes |\Psi_k\rangle$. Similarly as before, we say that a mixed state is k-separable, if only if it has a decomposition into k-separable pure states [71; 91], *i.e.*

$$\hat{\varrho}_{k-sep} = \sum_i p_i \left|\Psi^{(i)}_{k-sep}\right\rangle \left\langle\Psi^{(i)}_{k-sep}\right|, \tag{1.26}$$

with $p_i \geq 0$ and $\sum_i p_i = 1$. One may see that the above definition of full (n-partite) separable state is now equivalent to n-separability. The other limiting case is when the state is 1-separable, or in other words, it is not 2-separable (bi-separable). Such state is also called *genuine* n-partite entangled [113; 133] in order to distinguish from biseparable (triseparable, etc) entanglement. Here, we should notice that there is not a well-established concept of genuine multipartite entanglement [36], and sometimes it is identified, independently of the condition Eq.(1.26), with the fact that the state is not separable with respect to any bipartition [159; 7]. Whenever we talk about genuine n-partite entangled states in the following, we shall refer to states which are not biseparable (neither triseparable, etc) according to Eq.(1.26). Since a state that is not biseparable must have a decomposition

only on pure n-partite entangled states, this definition is connected with the physical intuition that genuine entanglement cannot be devised without participation of all parties. It is important to mention that the latter is the most relevant class of entanglement from the operational point of view, for instance genuine multipartite entanglement is the essential resource in the success of the quantum communication and teleportation protocols.

Since the k-separable states entered in Eq.(1.26) are generally separable with respect to different partitions, $\hat{\rho}_{k-sep}$ must not be necessarily separable with respect to a specific partition. Looking first at pure states (and then employing the fact that mixed states are the convex combination of these), one may readily see that this approach yields a scheme of entanglement consisting on several classes that follows a hierarchical structure in the sense that each one is embedded on the subsequent: A k-separable state is automatically k'-separable for all $k' < k$. This hierarchy goes from fully separability, when the state is n-separable, to genuine n-partite entanglement. As similarly occurs in the bipartite case, it is a highly non-trivial problem to obtain reliable estimators of k-separability because there may exist infinite ways in which decompose the state according to Eq.(1.26). In Refs.[39; 230] and [92] have been presented necessary criteria for k-separability. Whereas the two former are based on the extension of entanglement witnesses according to the definition Eq.(1.26), the latter was derived from the following observation [91]: the tensorial product $|\Psi_{k-sep}\rangle \otimes |\Psi_{k-sep}\rangle$ of two copies of a pure k-separable state with respect to the partition $\{I_1, \ldots, I_k\}$ (conceived according to condition Eq.(1.25)), remains invariant under the interchange of all elementary subsystems contained in each subset I_i of such k-partition. Interesting enough, in Ref.[230] was presented an entanglement witness based on the Hamiltonian of interacting harmonic oscillators that can be successfully applied to study multipartite entanglement in the ground state of large harmonic systems. Similarly result were used to study inseparability of Gibbs states in harmonic linear lattices [20]. In particular, it allowed to derive a threshold temperature for which the Gibbs states of the lattices left to be n-partite entangled.

The another relevant approach to multipartite entanglement, which may be considered as a suitable generalization of definition Eq.(1.23), is devised from an operational point of view: a pure state of a n-partite system $|\Psi_{k,n}\rangle$ is called k-partite entangled if cannot be described without an at least k-partite entanglement contribution [228; 113; 154]. This definition implies that a subset of at least k parties of the system must be necessarily entangled. Going further, a mixed n-partite state is considered k-partite entangled if it can not be expressed as a statistical mixture of at most $(k-1)$-partite entangled states [154][**A1**], *i.e.*

$$\hat{\varrho}_{k,n} \neq \sum_{j=1}^{k-1} \int d\mu_j(a) \left|\Psi_{j,n}^{(a)}\right\rangle \left\langle\Psi_{j,n}^{(a)}\right|, \tag{1.27}$$

where $|\Psi_{j,n}^{(a)}\rangle$ are j-partite entangled n-partite states, and $\mu_j(a)$ are positive functions that satisfy $\sum_{j=1}^{k-1} \int d\mu_j(a) = 1$. Intuitively, this definition means that a k-partite entangled state can be realized by mixing different states that are at most k-partite entangled, but since the states that enter this average may carry entanglement between different groups of

subsystems, a k-partite entangled n-partite state is not necessarily separable with respect to a certain bipartition [154][A1]. Again, if the state is not at least 2-partite (bipartite) entangled, then it is fully separable, and conversely, n-partite entanglement (in n-partite systems) is equivalent to the previously defined genuine n-partite entanglement.

The multipartite-entanglement classification based on the k-separability and k-partite entanglement schemes share the property that both yield an analogue hierarchical structure of entanglement that goes from fully separability to genuine n-partite entanglement. Clearly, if a n-partite state is k-separable then it cannot be k'-partite entangled for all $k' > k$. Nonetheless, there is a difference which stems from the fact that, contrary to the former, the latter tells us how large is the largest entangled partition. This makes the idea of k-partite entanglement easier to be intuitively understood as compared with k-separability. Moreover, the k-partite entanglement scheme has proved to be more advantageous in the analysis of multipartite entanglement in discrete systems [113].

Fortunately, in Ref.[154] Levi and Mintert provided a successful hierarchy of separability criteria that establish sufficient conditions for k-partite entanglement. This is based on a previous result from Huber & Mintert and co-workers collected in Ref.[133], where they showed that genuine n-partite entanglement is identified through the condition,

$$\tau_n(\hat{\varrho}) = \underbrace{|\langle \Phi_1 | \, \varrho \, | \Phi_2 \rangle|}_{f(\hat{\varrho})} - \sum_{j=1}^{2^{n-1}-1} \underbrace{\sqrt{\langle \Phi_{1j} | \, \varrho \, | \Phi_{1j} \rangle \, \langle \Phi_{2j} | \, \varrho \, | \Phi_{2j} \rangle}}_{f_j(\hat{\varrho})} > 0 \ , \tag{1.28}$$

where $|\Phi_1\rangle = \bigotimes_{m=1}^{n} |\varphi_m\rangle$ and $|\Phi_2\rangle = \bigotimes_{m=1}^{n} |\varphi_{n+m}\rangle$ are two product vectors, and the vectors $|\Phi_{1i}\rangle$ and $|\Phi_{2i}\rangle$ are defined in terms of the inequivalent possibilities to divide the n-subsystems into two groups: the $2^{n-1}-1$ inequivalent bipartitions can be characterized by a vector $\boldsymbol{v}_j$ whose n elements adopt the values 0 or 1, and the groups are defined by the subsystems associated with the value 0 and 1 respectively [A1]. In terms of these vectors, we have the definition

$$|\Phi_{1j}\rangle = \bigotimes_{m=1}^{n} |\varphi_{m+n[\boldsymbol{v}_j]_m}\rangle \ , |\Phi_{2j}\rangle = \bigotimes_{m=1}^{n} |\varphi_{m+n-n[\boldsymbol{v}_j]_m}\rangle \ , \tag{1.29}$$

that is, the vectors $|\Phi_{1j}\rangle$ and $|\Phi_{2j}\rangle$ are obtained from the vectors $|\Phi_1\rangle$ and $|\Phi_2\rangle$ through a permutation of state vectors $|\varphi_m\rangle$ with $|\varphi_{n+m}\rangle$ that belong to those subsystems that are grouped together in the j-th bipartition. Going back to Eq.(1.28), if a pure state $\hat{\varrho} = |\Psi\rangle \langle \Psi|$ is separable with respect to the j-th bipartition, then $f(\hat{\varrho}) = f_j(\hat{\varrho})$ and τ_n must be non-positive. As this reasoning holds for any bipartition, and, in addition τ_n is convex, τ_n is indeed non-positive for any state $\hat{\varrho}$ that can be decomposed into bi-separable pure states. Remarkably enough, one may introduce the function

$$\tau_{bi,n}(\hat{\varrho}) = f(\hat{\varrho}) - (2^{n-1}-1)^{-1} \sum_{j=1}^{2^{n-1}-1} f_j(\hat{\varrho}),$$

whose positive value unveils a mixed state to be at least bi-partite entangled according to the above reasoning. Levi and Mintert realized that one may proceed further and introduce certain scalar factors $a_j^{(k,n)} \geq 0$ [154] for $n \geq k \geq 2$ such that

$$\tau_{k,n}(\hat{\varrho}) = f(\hat{\varrho}) - \sum_j a_j^{(k,n)} f_j(\hat{\varrho}), \tag{1.30}$$

can be positive only if $\hat{\varrho}$ is at least k-partite entangled. These coefficients are not unique and must be conveniently chosen to reliably detect the entanglement featured by the quantum states which one is concerned [154]. Based on Eq.(1.30), we propose in Ref.[A1] a versatile criterion of k-partite entanglement that can be straightforwardly apply to either Gaussian or non-Gaussian states characterized by Eq.(1.5). The obvious suggestion that we made was to consider Gaussian states as good candidates of probe vectors $\{|\varphi_m\rangle\}_{m=1}^{2n}$, as much in the spirit of the derivation of the Gaussian entanglement of formation. It will be seen that this consideration permits to simplify the optimization procedure involved in the appropriate election of the set of probe states for an accurate characterization of k-partite entanglement, see Sec.2.1 for further details.

Apart from the above schemes based on k-separability and k-partite entanglement, here we also discuss others strategies that have been proved to be useful to characterize multipartite entanglement. Quite remarkable Giedke, Kraus, Lewenstein and Cirac provided a sufficient and necessary criterion for full 3-partite separability in Gaussian states that relies on algebraic results of positive-definite (Hermitian) matrices [124]: Basically, they conveniently expressed the condition Ineq.(1.24) for three-mode Gaussian states in a mathematical form that is computationally easy to certify. Using this criterion these authors presented a characterization of tripartite Gaussian states based on a slightly different scheme to the above ones, and which consists on a complete classification into the following five distinct separability classes [100]:

(C1). *Fully inseparable* or tripartite entangled states, which are not separable in any of the three possible bipartitions.

(C2). *One-mode biseparable states*, which are separable in one out of those possible bipartitions.

(C3). *Two-mode biseparable states*, for which now two of the bipartitions are separable.

(C4). *Three-mode biseparable* or PPT entangled states, which are separable under all bipartitions, but does not satisfy condition Ineq.(1.24).

(C5). *Fully separable* or tripartite separable states, which unlike those of **(C4)**, satisfy condition Ineq.(1.24).

Since PPT criterion is a sufficient and necessary criterion for entanglement in 1×2-mode Gaussian states, it can be used to distinguish between the classes **(C1)**, **(C2)** and **(C3)**. Whereas states in class **(C4)** stand as non-trivial examples of bound entangled states. We

must clarify here that PPT is not able to identify genuine multipartite entanglement according to the definition based on the Eq.(1.26) (or equivalently on Eq.(1.27)), as a result, class **(C1)** will compress both genuine tripartite and biseparable (three-mode) entangled states [133]. As opposite to the above schemes based on k-separability and k-partite entanglement, this classification tells us which particular parties are entangled. We shall employ this classification to characterize the entanglement in a three-mode system subjected to independent **[A3]** or a common reservoir **[A2]**.

In the more general scenario of a n-mode system, analogue separability conditions to Ineqs. (1.15) and (1.11) can be extended to fully separable states, respectively, by a set of entanglement witnesses and positive but not completely positive maps [127; 138]. In this line, PPT criterion and entanglement witnesses concerning only the second moments of position and momentum operators were formulated as necessary criteria for full separability by extending condition Ineq.(1.10) [225] or Duan-Giedke-Cirac-Zoller criterion [159], respectively, to assess the separability of each one of the $2^{n-1}-1$ possible bipartitions. Moreover, Cramer, Plenio, and Wunderlich proposed accessible entanglement witnesses in many-body systems that work as necessary conditions for full separability, and which rely solely on measurements in neutron scattering for spin systems and time-of-flight imaging for cold atoms [58]. They have also proposed entanglement quantifiers of n-partite entanglement based on these witnesses as given by Eq.(1.17). Remarkably enough, the latter result has been successfully applied to quantify experimentally multipartite entanglement over large regions in optical lattices of $\sim 10^5$ sites composed by ultracold interacting bosons [57].

Unfortunately there is not known yet any proper entanglement measure, concerning continuous variable systems, which is able to quantify multipartite entanglement, either following the definition based on Eq.(1.26) or Eq.(1.27), and at the same time it is susceptible to be computed at least numerically. The most important progress in this direction was given by Adesso and co-workers, who proposed several bona fide measures of genuine tripartite Gaussian entanglement [7; 11; 5], among which is found the Renyi-2 entanglement $\mathcal{E}_2$. Their results rely on quantifying the genuine tripartite entanglement as the residual entanglement emerging form the monogamy inequality, e.g.

$$\mathcal{E}_2(\hat{\varrho}_{S_1|S_2|S_3}) = \mathcal{E}_2(\hat{\varrho}_{S_1|S_2S_3}) - \mathcal{E}_2(\hat{\varrho}_{S_1|S_2}) - \mathcal{E}_2(\hat{\varrho}_{S_1|S_3}). \tag{1.31}$$

These previous schemes like k-partite entanglement or classification (**C1**-**C5**) are not the only ones that we can use at the time to tackle the description of multipartite entanglement, nonetheless they are the most relevant from the perspective of the present dissertation. For the sake of completeness we also include a continuation a brief survey to other approaches that are susceptible to be used in the discussion of the concluding part.

1.2.4 SLOCC classification and others

A more illustrative example of the subtle that arises on the characterization of multipartite entanglement was provided by Dür, Vidal, and Cirac in the seminal work [72], where they

compared the entanglement of the classes of Greenberger-Horne-Zeilinger (GHZ) and W states [129; 112] in a three-qubit system. Let us denote each qubit by A, B, and C. Using the (computational) basis given by the tensorial product between the single-qubit basis $\{|0\rangle_i, |1\rangle_i\}$ (with $i = A, B, C$), the mentioned states read

$$|GHZ\rangle = \frac{1}{\sqrt{2}}(|000\rangle + |111\rangle), \quad |W\rangle = \frac{1}{\sqrt{3}}(|100\rangle + |010\rangle + |001\rangle).$$

Although, these states are formally genuine tripartite entangled according to the definition based either in Eq.(1.26) or in Eq.(1.27), they represent different physical situations. Whereas the GHZ state is considered to be the maximal tripartite entangled state, in the sense that the entanglement contained by such state is needed to prepare an arbitrary tripartite state [2], the entanglement in the W state is more robust in the reduced two-qubit state. The reduced density matrix $\hat{\varrho}_{AB} = Tr_C(|GHZ\rangle\langle GHZ|)$ resulting from the lost of the C-qubit in the GHZ state is separable, while the reduced state $\hat{\varrho}_{AB} = Tr_C(|W\rangle\langle W|)$ is two-mode entangled.

It was shown that these two classes of entangled states are inequivalent in the sense that one cannot transformed a GHZ into a W state, or vice versa, by doing stochastic LOCC, namely SLOCC, which consist on applying non-trace-preserving operations and classical communication [72]. Since these operations do not create entanglement at all, SLOCC equivalent states must contain essentially the same entanglement (in some sense they are 'equally' entangled). This result naturally suggests that SLOCC grants a reasonable scheme to classify n-partite entanglement: two pure states, say $|\Phi\rangle$ and $|\Psi\rangle$, belongs to the same SLOCC class if they can be transformed into each other with non-zero probability by means of LOCC [72]. This assertion is equivalent to say that there exist (local) invertible transformations $\hat{\mathcal{U}}_i$ such that [129]

$$|\Psi\rangle = \hat{\mathcal{U}}_1 \otimes \cdots \otimes \hat{\mathcal{U}}_n |\Phi\rangle . \tag{1.32}$$

For discrete systems represented by the n-fold tensor product of Hilbert spaces $\mathbb{C}^{d_1} \otimes \cdots \otimes \mathbb{C}^{d_n}$, it was shown that each $\hat{\mathcal{U}}_i$ belongs to the special linear group[xix] over each elementary subsystem, *i.e.* $\hat{\mathcal{U}}_i \in \mathrm{SL}(d_i, \mathbb{C})\ \forall\ i$.

Similarly multipartite entanglement may be classified according to their interconvertibility under other classes of transformations, provided the key observation that such transformations are unable to create entanglement. For example, a classification of pure states in terms of LOCC classes, instead of SLOCC, considers only local unitary transformations in Eq.(1.32) [129], *i.e.* $\hat{\mathcal{U}}_i \in \mathrm{SU}(d_i, \mathbb{C})\ \forall\ i$. Further approaches are based on transformations that permit a simpler mathematical (say coarse grained) characterization of multipartite entanglement [231; 171].

[xix] The general linear group over the complex vector space $\mathbb{C}^d$ is the set of $d \times d$ invertible matrices with entries from $\mathbb{C}$ and with a unitary determinant. Endowed with the matrix multiplication this set consists on a group denoted by $\mathrm{SL}(d, \mathbb{C})$. An important subgroup is composed by the set of unitary matrices, which is denoted by $\mathrm{SU}(d, \mathbb{C})$.

In the realm of continuous-variable systems, Giedke and Kraus have recently derived necessary and sufficient conditions for Gaussian states to be equivalent under either Gaussian local unitaries (GLU), *i.e.* the operators $\hat{\mathcal{U}}_i$ can be now any local unitary operation that preserves the set of Gaussian states [97], or a wider set of operations compressing Gaussian LOCC (GLOCC) [98]. Remarkably, they showed that the covariance matrix $\boldsymbol{V}$ of GLU-equivalent states can be brought into a *standard form* $\boldsymbol{V}_{SF}$, which is unique and can be easier characterized than the original covariance matrix, via a local symplectic transformation[xx] $\boldsymbol{S}$ (*i.e.*, $\boldsymbol{J}_n = \boldsymbol{S}^\dagger \boldsymbol{J}_n \boldsymbol{S}$). We can write the latter in the equivalent form,

$$(\boldsymbol{S}_1 \oplus \cdots \oplus \boldsymbol{S}_n)^\dagger \boldsymbol{V} (\underbrace{\boldsymbol{S}_1 \oplus \cdots \oplus \boldsymbol{S}_n}_{\boldsymbol{S}}) \longrightarrow \boldsymbol{V}_{SF}. \tag{1.33}$$

In essence, the standard form is obtained after deleting the irrelevant information for the characterization of entanglement from the original covariance matrix, then equation (1.33) allows one to translate the analysis of entanglement on studying the standard form irrespectively of the particular expression of the CM $\boldsymbol{V}$ of the system. Remarkably enough, Duan and co-workers, and Adesso and co-workers provided respectively such standard form for Gaussian two-mode and three-mode states in Refs. [70] and [11] (see also [220]). These have been proved to be convenient to show that the separability criterion proposed in Ref.[A1] reproduces the PPT results for arbitrary two-mode and pure three mode Gaussian states (see Sec.2.1). Furthermore, Adesso and co-workers also found that there is a unique family comprising both the extension of W (maximal reduced two-mode entangled) and GHZ (maximally tripartite genuine entangled) states onto continuous-variable states, which are denoted by GHZ/W states [11]. This set of states, though obeying the monogamy (Ineq.(1.20)), features simultaneously maximum tripartite and two-mode entanglement. Recently, Giedke and Krauss discovered that these states do not contain *maximal* entanglement in the sense that an arbitrary pure tripartite state cannot be achievable from a GHZ/W state by doing GLOCC.

Compared with the previous approaches based on k-separability or k-partite entanglement definitions, the characterization of multipartite entanglement in terms of SLOCC or similar provides a more physical insightful scheme since it reveals underlying symmetries in the entangled state [171], and further, constitutes a more elegant mathematical approach. Nonetheless, most of the important progress on this direction has been restricted to pure states [231; 184; 103; 249] and discrete systems [104], for which it was shown that the complexity behind determining the different classes grows rapidly with increasing number of constituents. From a practical point of view, and as we are concerned with entanglement in mixed states and large many-party systems, it is advisable to use the approach based on k-partite entanglement. Though this scheme is not able to identify different SLOCC-classes,

[xx] There is a one to one correspondence between a Gaussian unitary and an affine symplectic map acting on the phase space as follows $(\boldsymbol{S}, \boldsymbol{d}) : \boldsymbol{x} \to \boldsymbol{S}\boldsymbol{x} + \boldsymbol{d}$ [250]. Since entanglement remains invariant under local unitary manipulations, then a local symplectic transformation $\boldsymbol{S}$ will left intact the entanglement properties of the state. In this way (as it was mentioned in Sec.1.1), we can conveniently cancel out the mean value $\bar{\boldsymbol{x}}$ by means of a local displacement $\boldsymbol{d} = -\bar{\boldsymbol{x}}$.

it will see in Chapter 2 that it may provide meaningful information about the behaviour of entanglement in dissipative scenarios.

1.3 Modelling open quantum systems

In many realistic situations the quantum properties of the interesting system is unavoidably influenced by the interaction with a background or field, called *reservoir*, which is constituted by a large number of particles compared to the system and, as much in the sense of thermodynamics, only a few of its observable attributes (e.g. its temperature) are accessible[xxi]. This situation is ubiquitous in several areas of physics such as quantum optics (e.g. Lamb effect [96]), statistical physics (e.g. quantum Brownian motion [218; 12]), or condensed matter (e.g. dissipative quantum tunneling [46]), and further, it has been proposed as the key ingredient to understand the mechanism of decoherence as well as the emergence of classical behaviour from an underlying quantum world [265]. The study of such *open* systems, in which the physical interest on the reservoir is secondary, has lead to a considerable amount of research during the half past century, which has culminated on the birth of the theory of open quantum systems [160; 136; 47; 251; 266; 43; 96; 208].

It is well known that quantum *coherence* of experimentally accessible quantum systems is generally destroyed by the mentioned reservoir interaction, so that a meaningful description of their correlations properties, in particular entanglement, necessarily requires to take account such interaction. Here, we are concerned with a many-party system composed of harmonic oscillators that may reliably describe the modes of a radiation field into an optical or microwave cavity, or , on other hand, the center-of-mass motion of nanomechanical oscillators or ultracold atoms arranged in optical lattices. The reservoir influence on all these setups cannot be neglected. For instance, the mirrors of the cavity will always reflect the photons that arrive at them only if they are ideally perfect, otherwise there will be an irreversible loss of photons from the cavity [160]. Further, nanomechanical oscillators are relatively massive which makes difficult to isolate them from their solid-state substrates, and consequently, they will suffer from losses due to thermal excitations. Analogously, atoms in optical lattices may also experience certain damping due to spontaneous emission processes (e.g. see Doppler effect). Then the irreversible transference of energy, say dissipation [219], from the system into the reservoir is by no means negligible in all these systems. In the present dissertation we address the study of entanglement properties in those quantum systems where the reservoir influence consists mainly on the dissipative effects arising from the underlying vibrational degrees of freedom such as the normal modes (photons) of a radiation field or the low-energy modes (phonons) of a nanoscopic system. It should be mentioned that other sources of perturbation might be present in realistic

[xxi] A direct example is provided by the measurement theory, where the reservoir might represent the measurement instrument, and certain operator (e.g. position or momentum) of the quantum system is perturbed in order to be observed. On the other hand, if the reservoir has a well defined initial temperature T, then the system may eventually reach a thermal equilibrium state at such temperature. We shall say that the reservoir acts as a heat bath in those cases.

setups, as could be the loss of particles in ultracold atoms, such that quantum correlations can be influenced in a stronger manner by the reservoir interaction than we consider here.

A priori the standard quantum mechanics provides one with the essential tools (Schrödinger or Heisenberg equations) to derive the equations of motion of the reduced dynamics for the system interacting with the reservoir. However, this generally yields a hierarchical structure of equations [16; 17; 246] that becomes numerically intractable with increasing numbers of reservoir constituents and strong couplings. Unfortunately, there is no recipe which could be successfully applied to rigorously solve this intricate problem, instead, there are several strategies which ultimately rely upon making some approximations that permit to reduce consistently such hierarchy into a manageable set of equations. Only a few specific systems can be exactly solved, among which, we highlight the damped harmonic oscillator [107; 206; 116; 106; 193]. The latter represents the physical process whereby an oscillator reaches asymptotically a stationary state following a dissipative dynamics, that may correspond eventually to a thermal equilibrium state at the initial reservoir temperature.

Though it may look somehow artificial, the most successful approach to a formal description of the damped oscillator rest on an assumption about the microscopic form of the Hamiltonians describing the reservoir and system-reservoir interaction. This is commonly refereed to as the Caldeira-Leggett model [46; 67], and basically consists on assuming that the reservoir is composed by a large set of non-interacting harmonic oscillators linearly coupled to the system [86; 87; 251]. Starting from this model, the Heisenberg equation for the position of the damped oscillator results in a generalized Langevin equation (GLE), which has found remarkable applications in a broad range of research topics within the non-equilibrium statistical mechanics: in the study of the quantum Brownian motion [88], in the characterization of heat conduction in low dimensional systems [263; 264; 63] or thermalization in scalar fields [22], and in problems more closely related to condensed matter physics such as the description of fluctuations and dissipation around quantum phase transitions [166].

In a multimode scenario of damped harmonic oscillators several physical situations can be devised in which the dissipative dynamics differs substantially. For instance, the system oscillators can be very closed to each other such that they perceive essentially the same reservoir, this will correspond to the case in which all the oscillators are strictly in contact with a *common environment*. The opposite situation takes place when the system oscillators are far apart between them, then one could expect that each oscillator would see locally a different reservoir. The limiting case of *independent environments* occurs when each oscillator is interacting with a separate reservoir at an initially distinct temperature, which may give rise to thermal non-equilibrium situations contrary to the former scenario. Regrettably, the Caldeira-Legget model itself is unable to track the underlying differences that range between both scenarios for the simple reason that it does not contain an explicit dependence on the position of the system oscillators.

Based on physical grounds in what follows we propose a reliable, simple extension of the Caldeira-Leggett model enable to describe a n-mode system subjected to dissipative quantum dynamics which accounts for the aforementioned situations. Afterwards, we

shall see briefly that from such model one may derive a generalized Langevin equation which governs the evolution of the position operator for the oscillator system, and whose solution can provide the time-evolved covariance matrix of a Gaussian state with relatively little effort in general dissipative scenarios. In particular, this equation was exploited on the analysis of the time asymptotic properties of the multipartite Gaussian entanglement supported by a three-mode system in Refs. **[A2]**, **[A3]**, and **[A4]**. For more general states than Gaussian, as it is the case of the non-Gaussian state given in Eq.(1.5), it is convenient for our purposes to focus the study directly on the dynamics of the Wigner function instead of the position operators. This leads us to the time-independent Fokker-Planck equation which appears in many realistic situations [207; 266], and shall be used as a complement of the generalized Langevin equation to address the dissipative dynamics of continuous-variable systems. It will be shown in Chapter 2 that the general solution of such equation allows one to discuss in general terms the behaviour of the multipartite entanglement characterized by the separability criteria proposed in Ref. **[A1]**

Finally, we must mention that there are other ways to describe the quantum evolution of the system subjected to dissipative dynamics instead of using the generalized Langevin or Fokker-Planck equation. This basically consists on deriving an equation of motion for the density operator $\hat{\varrho}_S$ (in the Schrödinger picture) which is refereed to as the *master equation*. For the damped harmonic oscillator the exact form of this equation was derived by Hu, Paz, and Zhang in Ref.[130] (see also Ref.[84]). Several analogue studies to the present dissertation have exploited such equation to study entanglement. Comparing both approaches, the GLE formalism may be more advantageous for a faithful description of the dissipative dynamics in linear systems essentially because its exact solution can be numerically obtained as we will show, while to solve the master equation one very often needs to make certain approximations on either the system (e.g. considering equal frequencies for all the system oscillators) or the reservoir (e.g. high temperatures and weak couplings with the reservoir). In contrast, the master equation approach may be more convenient when the system exhibit non-linearities since a few results are known about the solution of non-linear generalized Langevin equations. Furthermore, the resolution of either the generalized Langevin or Fokker-Planck equations may be drastically complicated if the interesting system experiences external time-dependent forces, in that case one may recall to the non-equilibrium Green-function methods (which have been extensively applied in quantum transport problems [203]), or if such driving are periodic, the powerful Floquet theory can be used [144; 145]. Notice that the multipartite entanglement supported by linear and time-independent harmonic systems raises enough questions as to stimulate several works on this topic, and further investigation beyond of such systems is not the purpose of the present dissertation.

1.3.1 Microscopic approach to dissipative harmonic oscillators

To begin with, we set down certain prescription and notation which shall be used in the course of our treatment. Let us denote the system and reservoir by S and R, respectively. Generically the Hamiltonian of the system-plus-reservoir complex in dissipative quantum

mechanics can be decomposed as follows,

$$\hat{H} = \hat{H}_S + \hat{H}_R + \hat{H}_I,$$

where $\hat{H}_R$ and $\hat{H}_I$ corresponds respectively to the Hamiltonian of the reservoir and system-reservoir interaction, whereas $\hat{H}_S$ represents the Hamiltonian of the interesting system that can be expressed in terms of an interaction potential $\hat{U}$, *i.e.*

$$\hat{H}_S = \sum_{i=1}^{n} \frac{\hat{p}_i^2}{2m_i} + \hat{U}(\hat{x}_1, \cdots, \hat{x}_n).$$

where m_i denote the mass of the ith oscillator. Notice that the potential interaction in realistic setups may be non-quadratic, a prominent example is provided by the optomechanical systems. As a consequence, the system equations of motion will be non-linear in those cases, which leads to an unsolvable dynamics. However, one can use perturbative methods to approach $\hat{U}$ by a quadratic interaction potential in a low-energy treatment. This can be expressed as follows,

$$\hat{U} = \sum_{i,j=1}^{n} U_{ij}\hat{x}_i\hat{x}_j. \tag{1.34}$$

The so-called microscopic model will determine the explicit form of $\hat{H}_R$ and $\hat{H}_I$, which will basically consist on a (huge) set of interacting harmonic oscillators with a broad spectrum. Since the reservoir is unable to possess arbitrarily large amount of energy[xxii], we shall consider that the frequency of its most energetic mode is roughly bounded (from above) by a finite cut-off frequency ω_c. In the following, we shall also denote by ω_S a characteristic frequency of the evolution of the system alone, which can be the frequency of the most energetic oscillator for a non-interacting system, or the largest of normal-mode frequencies for an interacting one. Additionally, we will consider that the system-reservoir interaction strength is approximately characterized by a *dissipative rate* which shall be designated by the parameter γ (e.g. this parameter plays the role of the damping coefficient in the damp harmonic oscillator). Finally, we shall also consider that the modes composing the system are well located at positions $\boldsymbol{R}_\lambda = \boldsymbol{r}_\lambda^0 + \boldsymbol{r}_\lambda$, being $\boldsymbol{r}_\lambda^0$ and $\boldsymbol{r}_\lambda$ the equilibrium position and displacement of the λth oscillator. Notice that if the modes experience long-range interactions between them, then the interaction potential given by Eq.(1.34) will appear naturally after doing the harmonic approximation around its equilibrium positions [216].

Then we endeavour to derive a physical reasonable form for the Hamiltonians $\hat{H}_R$ and $\hat{H}_I$ in order to provide a reliable description, as general as possible, of the dissipative quantum dynamics followed by the system, and which, at the same time, allows one to access to the entanglement properties of the system. To do that we require the microscopic model to fulfil a few reasonable premises mainly based on physical grounds. We list such premises below:

[xxii] This fact stems from boundary conditions over the reservoir. For instance, in a microwave cavity, normal modes with wavelengths much larger than the cavity length will barely contribute to the electromagnetic field into the cavity.

(1). The Hamiltonian $\hat{H}$ encoding the microscopical model should be local U(1) gauge invariant. That is, the change in the Hamiltonian, given by $\hat{H}_{\Lambda(\boldsymbol{r}_\lambda^0)} = \hat{\mathcal{U}}^\dagger_{\Lambda(\boldsymbol{r}_\lambda^0)} \hat{H} \hat{\mathcal{U}}_{\Lambda(\boldsymbol{r}_\lambda^0)}$, corresponding to a gauge transformation of the global phase of the wave function, written as $|\Psi_{\Lambda(\boldsymbol{r}_\lambda^0)}\rangle = e^{\frac{i}{\hbar}\Lambda(\boldsymbol{r}_\lambda^0)} |\Psi\rangle = \hat{\mathcal{U}}_{\Lambda(\boldsymbol{r}_\lambda^0)} |\Psi\rangle$, leaves invariant the equations of motion of system-plus-reservoir observables [54].

(2). The reservoir is composed of a large number of modes, say N, compared to the n-mode system ($N \gg n$), and the energy spectrum of the latter must be completely embedded in the spectrum of the former. This implies that, first, the reservoir has practically a quasi-continuous distribution of modes in energy, and second, the largest reservoir frequency is much larger than the characteristic frequency of the system, *i.e.* $\omega_c \gg \omega_S$.

(3). Independently of the initial state of the system, and for a reservoir in a thermal equilibrium state at certain temperature T, the model eventually returns the relaxation of the system into a thermal equilibrium state with the temperature set by the reservoir, *i.e.* $\hat{\varrho}_S(t \to \infty) \to e^{-\hat{H}_S/k_BT}/\mathrm{Tr}(e^{-\hat{H}_S/k_BT})$. More precisely, we require that the microscopic model reduces to the Caldeira-Leggett model in the limit of a common reservoir.

(4). We claim simplicity of the model. As a starting point we require that the reservoir degrees of freedom can be analytically integrated out to obtain the reduced dynamics of the system. This means that the system-reservoir interaction should be linear on the reservoir degrees of freedom.

Several comments are in order. As it is well known, quantum theory establishes that the global phase of the wave function has no relevance on the observable properties of quantum systems, then one may recognize **(1)** as a basic condition in order to avoid spurious predictions coming from the specific choice of the coordinate-reference system.

From the premise **(3)** follows that the microscopic model will be at least as successful as the Caldeira-Leggett model in the description of dissipation, though we expect that new phenomena may emerge from the interaction of harmonic oscillator with the same reservoir. The condition **(3)** is then fundamentally a customary checkup to verify that, for a reservoir at thermal equilibrium, the system follows indeed an evolution governed by the dissipative quantum dynamics contained on the well-established Caldeira-Leggett model. On the other hand, the premise **(2)** is needed to give consistency to condition **(3)**: It guarantees that there will be an effective exchange of photons/phonons at the microscopic time scale ω_S^{-1}, albeit this flow of energy will be from the system to the reservoir on *average* due to the great number of reservoir modes interacting with the system modes. In addition, it will be seen that the premise **(2)** ensures that the system reaches a stationary state in the asymptotic time limit, such that its initial conditions are completely washed out by the interaction with the reservoir.

Though the premise **(4)** is omnipresent in any research field in physics, we prefer to explicitly include it in the above list because a simple and accurate description of the state

is desirable due to the complexity behind the characterization of entanglement, which we extensively illustrated in the previous section. The degree of accuracy of our description will clearly depend on the physical details included in the microscopic model, here we must keep in mind that our ultimate intention is to come to a deeper understanding of the phenomenon of entanglement in harmonic oscillator subjected to dissipative quantum dynamics. For instance, this entails in many cases to restrict the analysis to quadratic Hamiltonians because the application of entanglement measures for CV systems is usually limited to the set of Gaussian states.

To elucidate valid expressions for the Hamiltonians $\hat{H}_R$ and $\hat{H}_I$, which will be unlikely unique, is instructive to take a simple example which is found in scalar field theories. It is shown that a dissipative microscopic model satisfying the premises **(1)** and **(2)** may be expressed as the Hamiltonian of a set of harmonic oscillator interacting with a free bosonic field (e.g. the electromagnetic field in free space) by minimal coupling[xxiii] [143]. For this system, $\hat{H}_R$ clearly takes the form of the free Hamiltonian for the reservoir oscillators, whereas the interaction Hamiltonian acquires a more complicated expression. Let us consider for a clear exposition that all the oscillators are well confined such that they move practically in the x-direction. Hence, the interaction Hamiltonian may be expressed as follows [245]

$$\hat{H}_I = -\sum_{\lambda=1}^{n} \hat{x}_\lambda \sum_{\boldsymbol{k}} g_{\boldsymbol{k}} \Big(\hat{a}_{\boldsymbol{k}} e^{i\boldsymbol{k}\cdot\boldsymbol{R}_\lambda} + \hat{a}_{\boldsymbol{k}}^\dagger e^{-i\boldsymbol{k}\cdot\boldsymbol{R}_\lambda} \Big), \tag{1.35}$$

where $a_{\boldsymbol{k}}$ is the annihilation operator of the reservoir mode with wave vector $\boldsymbol{k} = (2\pi/L)\boldsymbol{n}$ with $\boldsymbol{n} \in \mathbb{Z}^d$, whereas d and L are respectively the dimension and a characteristic length of the reservoir field. Here, $g_{\boldsymbol{k}}$ mainly describes the coupling strength of the system oscillator with the $\boldsymbol{k}$th mode.

Looking at Eq.(1.35), $\hat{H}_I$ is not linear on the position of the system modes. Starting from the Heisenberg equations for the system-plus-reservoir oscillators, one may realize that, after tracing out the reservoir degrees of freedom, the Heisenberg equations governing the reduced dynamics will exhibit a non-linear dependence on $\hat{x}_\lambda$, which complicates the problem in general. We may circumvent this obstacle by considering the dipole or long-wavelength approximation, this means to restrict the study to those physical situations in which there is not appreciable change on the reservoir field in the displacement of the oscillator around the position equilibrium, *i.e.* $e^{i\boldsymbol{k}\cdot\boldsymbol{r}_\lambda} \ll 1$. Hence, the interaction Hamiltonian can be approximated as follows

$$\hat{H}_I \cong -\sum_{\lambda=1}^{n} \hat{x}_\lambda \sum_{\boldsymbol{k}} g_{\boldsymbol{k}} \Big(\hat{a}_{\boldsymbol{k}} e^{i\boldsymbol{k}\cdot\boldsymbol{r}_\lambda^0} + \hat{a}_{\boldsymbol{k}}^\dagger e^{-i\boldsymbol{k}\cdot\boldsymbol{r}_\lambda^0} \Big), \tag{1.36}$$

[xxiii] Loosely speaking, in field theory the interesting field that may be endowed with certain symmetries is coupled to a gauge field $\hat{A}_\mu$ in order to make the theory invariant under the group of transformations generated by such symmetries [18], e.g. quantum electrodynamics is a (gauge) theory with the symmetry group $U(1)$. Formally this can be done for a field with $U(1)$ symmetry by minimal coupling, which consist on doing the replacement in the Hamiltonian $\hat{p}_\mu \to \hat{p}_\mu - q\hat{A}_\mu$, where $\hat{p}_\mu$ denotes the kinematic momentum of the field particles.

which exhibits a bilinear coupling in position observables of both system and reservoir. This approximation is necessary to fulfil condition **(4)**. As an additional argument, the interaction Hamiltonian in the Caldeira-Leggett model is presumably linear in the coordinate operators of both system and reservoir. It is worth mentioning that the dipole approximation is well justified in our study because we are dealing with harmonic oscillators well localized in space.

Yet the Hamiltonian (1.36) has not an adequate form, following the Caldeira-Leggett model a counter term must be added in order to preserve the bare frequency of the system oscillator [251; 46]. For instance, if we do not include such counter term then the thermal equilibrium state returned by this model would involve a renomalization frequency instead of the actual frequency of the modes, as occurs in the damped harmonic oscillator [206; 116]. Interesting enough, such counter term stems from a more profound physical consequence: it arises naturally from the local $U(1)$ gauge invariance of the microscopic model [143]. Starting from the minimal coupling model of the system oscillators interacting with the free bosonic field, this can be shown by doing first the dipole approximation, as showed in Eq.(1.36), and second the Göppert-Mayer transformation[xxiv]. Then, the full oscillator-reservoir Hamiltonian $\hat{H}_B + \hat{H}_I \to \hat{H}_{BI}$ becomes [A2],

$$\begin{aligned}\hat{H}_{RI} = &\sum_{\boldsymbol{k}} \frac{1}{2m_{\boldsymbol{k}}}\left(\hat{\boldsymbol{p}}_{\boldsymbol{k}} + g_{\boldsymbol{k}}\sqrt{\frac{2m_{\boldsymbol{k}}}{\hbar\omega_{\boldsymbol{k}}}}\sum_{\lambda=1}^{n}\hat{x}_\lambda \sin(\boldsymbol{k}\cdot\boldsymbol{r}_\lambda^0)\right)^2 \\ &+\sum_{\boldsymbol{k}} \frac{m_{\boldsymbol{k}}\omega_{\boldsymbol{k}}^2}{2}\left(\hat{\boldsymbol{x}}_{\boldsymbol{k}} - \frac{g_{\boldsymbol{k}}}{\omega_{\boldsymbol{k}}^2}\sqrt{\frac{2\omega_{\boldsymbol{k}}}{m_{\boldsymbol{k}}\hbar}}\sum_{\lambda=1}^{n}\hat{x}_\lambda \cos(\boldsymbol{k}\cdot\boldsymbol{r}_\lambda^0)\right)^2,\end{aligned} \tag{1.37}$$

where we have introduced the bosonic annihilation operator,

$$\hat{a}_{\boldsymbol{k}} = (m_{\boldsymbol{k}}\omega_{\boldsymbol{k}}\hat{\boldsymbol{x}}_{\boldsymbol{k}} + i\hat{\boldsymbol{p}}_{\boldsymbol{k}})/\sqrt{2\hbar m_{\boldsymbol{k}}\omega_{\boldsymbol{k}}},$$

and its adjoint $\hat{a}_{\boldsymbol{k}}^\dagger$, with $\omega_{\boldsymbol{k}}$ and $m_{\boldsymbol{k}}$ respectively the frequency and mass of the mode with wave vector $\boldsymbol{k}$. From Eq.(1.37), it is immediate to see that the Hamiltonian $\hat{H}_{BI}$ reproduces the Caldeira-Leggett model in the limit of a common environment, *i.e.* $|\boldsymbol{r}_\lambda^0| \to 0\ \forall\ \lambda$. In appendix A, it is shown in more detail the derivation of Hamiltonian Eq.(1.37) starting from the aforementioned minimal coupling model.

We have thus far established that the microscopic model described by the Hamiltonian given in Eq.(1.37) is perhaps the simplest model satisfying all the above premises. Though it eventually describes a set of (non-relativistic and spinless) harmonic oscillators interacting with an electromagnetic field through a dipole-like interaction [211], this model also provides a general framework to investigate dissipative harmonic systems since it has been derived from first principles as much in the spirit of the derivation of the electromagnetism Lagrangian from requiring Lorentz invariance (covariance principle), and analogously gauge

[xxiv] In electrodynamics the Göppert-Mayer transformation leads to the Hamiltonian representation in which the $\hat{H}_I$ expresses as the dipole interaction [54]. For a single oscillator minimally coupled to a three-dimensional gauge field, say $\hat{\boldsymbol{A}}$, such transformation reads as $\hat{\mathcal{U}} = e^{\frac{i}{\hbar}\hat{\boldsymbol{x}}\cdot\hat{\boldsymbol{A}}}$.

transformation and simplicity [18]. Without need to refer to the actual microscopic details, we shall consider the expression (1.37) as an *effective* Hamiltonian to simulate both the reservoir and system-reservoir interaction for our interesting setups. Consequently, our future development will mainly provide an accurate description for the relevant or universal features of dissipation (for instance, the relaxation into a thermal equilibrium state) exhibited on such systems. It should be noticed that this issue is in agreement with our initial purpose of studying universal aspects of quantum entanglement. Nonetheless, the microscopic approach based on the Hamiltonian (1.37) is more insightful than one could expect, such that it may well represent the realistic physical situation for a broad range of dissipative quantum systems. Let us discuss below this issue in some detail.

At first sight the oscillator representation of the reservoir may seem a too restrictive condition, however Feynman and Vernon early showed that an arbitrary reservoir can be mapped, irrespectively of its internal structure, onto a system composed of independent oscillators when the strength of the interaction $\hat{H}_I$ is weak enough compared with the characteristic energies of the realistic reservoir [83]. This fundamental result relies upon the classical idea that the interaction potential over any particle having small displacements around a position equilibrium may well approximated by a quadratic series expansion in the displacements. Alternatively, such oscillator representation arises naturally in condensed matter physics by doing an effective low-energy description of the (bosonic) reservoirs, *i.e.* the so-called second quantization, which consists basically on casting the reservoir Hamiltonian in terms of a set of (bosonic) quasiparticles determined by its excitation spectrum [18]. This analysis can be sketched as follows

$$\left\{\begin{array}{c}\text{Reservoir}\\ \text{Reservoir constituents (e.g. atoms in a solid)}\\ \hat{H}_R(\hat{\boldsymbol{x}}_i,\hat{\boldsymbol{p}}_i)\end{array}\right. \longrightarrow \left\{\begin{array}{c}\text{Excitation spectrum}\\ \text{Quasi-particles (e.g. phonons)}\\ \sum_{\boldsymbol{k}}\omega_{\boldsymbol{k}}\hat{a}^\dagger_{\boldsymbol{k}}\hat{a}_{\boldsymbol{k}}\end{array}\right.$$

where the index i may enumerate the particle in the reservoir, or further possibilities. A prominent example is found in the dissipative nanomechanical oscillator, where its solid-state substrate at low temperatures can be though of as a gas of phonons, and whose dispersion relation will give the frequencies $\omega_{\boldsymbol{k}}$.

Aside the oscillator representation of the reservoir, the other questionable aspect of this model is related to the linear nature of the system-reservoir interaction. Even though the microscopic coupling (at the mode level) is weak, the global effects of the reservoir upon the system that turn into dissipation will be relevant as long as the number of reservoir oscillators is large. Intuitively, the dissipation in the system will essentially emerge from the fact that the Poncaré recurrence time of the system-plus-reservoir complex, which is the time in which this returns at its initial state, becomes very large as compared with the natural times of the system (ω_S^{-1}). According to the condition **(2)**, the frequency spectrum of the reservoir will be sufficiently dense as to produce an infinite recurrence time[xxv] [245].

[xxv] The observed revival time in the dynamics of the oscillators is roughly determined by the inverse of the minimum separation between energies [245]. In this way the interesting system, instead of dissipate, could be effectively excited by a reservoir with short number of oscillators.

On the other hand, the weak microscopic coupling seems to be a reasonable consideration because the interaction between the system and reservoir modes is normally proportional to the inverse of the reservoir volume [251].

Summarizing, the approach to dissipative dynamics based on the Hamiltonian (1.37) will also give a detailed microscopic description of those systems which make linear analysis valid. Remarkable enough this has been proved to be the case for the large class of open quantum systems for which the Caldeira-Legget model has been successfully applied[xxvi]. More generally, such linear analysis will be well justified essentially when both system and reservoir experience a low-energy evolution, which for mechanical systems means to maintain the whole setup at low enough temperatures. It is precisely in this regimen where we expect to observe most of the interesting features related to entanglement in harmonic oscillators.

Once we have the Hamiltonians of the reservoir and system-reservoir interaction, we may proceed further in the Heisenberg picture and derive the generalized Langevin equation. From Sec.1.1 we learnt that continuous variable states have a natural representation in terms of the Wigner function. We devote the next section to shortly show that one may conveniently use the generalized Langevin equation to determine the Wigner function of Gaussian (e.g. covariance matrix) or non-Gaussian states without requiring any fundamental approximation.

1.3.2 Generalized Langevin equation

Historically, the generalized Langevin equation appeared to study the quantum analogue of the classical Brownian motion [118], which corresponds to the *erratic* motion of large particles suspended in fluids (which may play the role of reservoirs). In this kind of systems, dissipation comes along with certain *noise* which causes such irregular motion on the particles. These observable effects were initially described in the context of the Langevin equation by a phenomenological friction and random forces. The macroscopic characteristics of such forces turn to be intimately related through the so-called *fluctuation-dissipation* relation when the strength of these forces over the "Brownian particle" is sufficiently weak [232]. Remarkable enough, this result can be straightforwardly extended to situations where the system is weakly perturbed by a thermodynamic force (e.g. induced by temperature gradients) or external fields (e.g. electric fields) (see linear response theory [18]). Further investigations in non-equilibrium statistical mechanics showed that the theory around Brownian motion could be applied successfully to many other phenomena [166] (even when the Brownian particle is not a particle at all).

In the present study, one finds that the generalized Langevin equation governs the time evolution of the position operators of the system oscillators in the Caldeira-Leggett model. It emerges naturally from the Heisenberg equations of motion for the position operators after tracing out the degrees of freedom of the reservoir oscillators [86; 87]. This basically

[xxvi] Here, it must be mentioned that there exist other successful models, among which one may find a reservoir consisting of spins particles (see Ref.[202] for a complete overview).

consists on substituting in the equation-of-motion system the solution of the Heisenberg equations of the reservoir degrees of freedom. Starting from the Hamiltonian (1.37), and defining the position-operator vector $\hat{\boldsymbol{X}} = (\hat{x}_1, \cdots, \hat{x}_n)^T$, one finds that the generalized Langevin equation can be cast in the following compact form [A2],

$$M\ddot{\hat{\boldsymbol{X}}} + \frac{\partial \hat{U}}{\partial \hat{\boldsymbol{X}}} + 2\tilde{\Omega}\hat{\boldsymbol{X}} + \frac{1}{\hbar}\int_{t_0}^{t} \chi(t-\tau)\hat{\boldsymbol{X}}(\tau)d\tau = \hat{\boldsymbol{F}}(t), \tag{1.38}$$

where t_0 denotes the instant in which reservoir and system are put in contact, M is a $n \times n$ diagonal matrix whose elements contain the masses of the system oscillators, and $\tilde{\Omega}$ is a $n \times n$ matrix which includes the aforementioned renormalization term. This is given by,

$$\tilde{\Omega}_{\lambda\mu} \;=\; \frac{1}{\hbar}\sum_{\boldsymbol{k}} \frac{g_{\boldsymbol{k}}^2}{\omega_{\boldsymbol{k}}} \cos\left(\boldsymbol{k}\cdot\Delta\boldsymbol{r}_{\lambda\mu}^0\right), \tag{1.39}$$

where we have defined the spatial separation $\Delta\boldsymbol{r}_{\lambda\mu}^0 := \boldsymbol{r}_{\lambda}^0 - \boldsymbol{r}_{\mu}^0$. At first sight, Eqs. (1.38) and (1.39) reveal that the renormalization matrix and $\chi(t)$ may play the role of effective interaction potentials between oscillators which are in contact with a common environment. In Ref.[A2] it is discussed in which conditions this environment-mediated interaction is able to generate entanglement between system oscillators which do not experience any direct coupling.

The matrix $\chi(t)$ that plays the role of a memory kernel in Eq.(1.38) regards the dissipative effects, and is usually known as the susceptibility, whereas the random force is represented by the vector $\hat{\boldsymbol{F}}(t)$. This possesses a linear dependence on the values of the position and momentum operators of the reservoir modes at time t_0 (see appendix in Ref.[A2]). Hence, the equation (1.38) shows a dependence on the initial conditions, and as a consequence, on the system-plus-reservoir state at time t_0, which we denote by $\hat{\varrho}_{SR}(t_0)$.

If the system and reservoir are decoupled at time t_0, then the initial system-plus-reservoir density operator may be written as a product state $\hat{\varrho}_{SR}(t_0) = \hat{\varrho}_S(t_0) \otimes \hat{\varrho}_R(t_0)$. Typically, the reservoir will have a well-defined temperature T and it is initially in a thermal equilibrium state irrespectively of the unperturbed state of the system, *i.e.* $\hat{\varrho}_{SR}(t_0) = \hat{\varrho}_S(t_0) \otimes Z_R^{-1} e^{-\hat{H}_R/k_B T}$. This state is commonly known as the Feynman-Vernon initial condition, and it is broadly used in the theory of open quantum systems because it is very convenient for computations[xxvii]. Unfortunately, this will match with the realistic situation only on highly controlled experiments, in which the interesting system has been maintained well isolated from its environment, otherwise, one must expect that the density operator $\hat{\varrho}_{SR}(t_0)$ would be a correlated state. In the case of the damped harmonic oscillator, Grabert, Schramm and Ingold, and independently, Karrlein and Grabert considered more general initial states than the mentioned Feynman-Vernon, where the interesting system is prepared after doing a set of measurements over an initial thermal equilibrium state

[xxvii] For instance, a factorized initial condition is a key ingredient on the powerful Kraus Theorem [187], which essentially says that any physically meaningful quantum operation (CP map) can be seen as the partial trace of a unitary evolution in a larger Hilbert space (for example, see LOCC in Sec.1.2.1).

of the system-plus-reservoir complex [106; 140]. They showed that a particular initial preparation mainly influences the transient dynamics, while interesting enough, the time asymptotic dynamics features independence of such preparation when the system and reservoir are weakly coupled [251]. This is in agreement with our intuition about dissipative dynamics: it is expected that the interaction with the huge number of reservoir particles effectively washes out the initial information about the system in the long-time limit. In any case, we may consider that the system and reservoir are putting in contact in the infinite past ($t_0 \to -\infty$), such that they would have barely interacted previously, and thus, the Feynman-Vernon initial condition would be well justified.

As we are mostly interested in the asymptotic properties of the dissipative system, we may consider the Feynman-Vernon initial condition without loss of generality. This choice has an immediate consequence on the statistics of the fluctuating force. The latter will be stationary and Gaussian due to, first, $\hat{\boldsymbol{F}}(t)$ features a linear dependence on both $\hat{\boldsymbol{x}}_{\boldsymbol{k}}(t_0)$ and $\hat{\boldsymbol{p}}_{\boldsymbol{k}}(t_0)$, and second, the thermal equilibrium state of the reservoir is Gaussian. Furthermore, the initial thermal equilibrium condition of the reservoir allows one to relate the matrix susceptibility with the force vector via the Kubo formula **[A2]**,

$$\chi_{\lambda\mu}(t-t') = -i\left\langle [\hat{F}_\lambda(t), \hat{F}_\mu(t')] \right\rangle_{\hat{\varrho}_R} \Theta(t-t'-|\Delta\boldsymbol{r}^0_{\lambda\mu}|/c), \tag{1.40}$$

where c denotes the sound velocity of the reservoir (or the speed of light, in a corresponding optical setup), and the Heaviside step function Θ reflects causality with a retardation stemming from the distance $\Delta\boldsymbol{r}^0_{\lambda\mu}$ between the oscillators λ and μ. This feature of causality is in agreement with our physical intuition about that two space-time separated oscillators cannot (indirectly) influence each other through the coupling with the reservoir[xxviii], and on the other hand, all the interaction between the system and reservoir vanishes before they are put in contact. This leads to that the matrix elements of the susceptibility are formally causality functions, *i.e.* $\chi_{\lambda\mu}(t) = 0$ for $t < |\Delta\boldsymbol{r}^0_{\lambda\mu}|/c$. This characteristic entails an important mathematical property[xxix]: the Fourier transforms of these elements, which we shall denote by $\chi_{\lambda\mu}(\omega)$, are analytic functions in the upper-complex half plane (Im $\omega > 0$), and as a consequence, its real $\mathrm{Re}(\chi_{\lambda\mu}(\omega))$ and imaginary $\mathrm{Im}(\chi_{\lambda\mu}(\omega))$ part must satisfy the Kramers-Kronig relation,

$$\mathrm{Re}\chi_{\lambda\mu}(\omega') = \frac{1}{\pi} P \int_{-\infty}^{\infty} \frac{\mathrm{Im}\chi_{\lambda\mu}(\omega)}{\omega - \omega'} d\omega, \tag{1.41}$$

where P is the Cauchy principal value.

[xxviii] Alternatively, the Heaviside step function in the expression for the susceptibility (1.40) comes from the fact that the forces operators $\hat{F}_\lambda(t)$ and $\hat{F}_\mu(t')$ must commute for space-like separations, *i.e.* $[\hat{F}_\lambda(t'), \hat{F}_\mu(t)] = 0$ if $|\boldsymbol{r}^0_\lambda - \boldsymbol{r}^0_\mu| > c|t-t'|$. This is usually known as microscopic causality, and it is fulfilled for a scalar field interacting with a harmonic oscillator [211].

[xxix] Other useful mathematical property of the susceptibility is that $\chi(\omega) = \chi^\dagger(-\omega)$ (where $M^\dagger$ is the conjugate transpose matrix of M), since $\chi(t)$ is a real-valued function. Moreover Ford, Lewis and O'Connell showed in the damped-harmonic-oscillator model that the second law of thermodynamics entails that the real part of the Fourier transform of the susceptibility is always positive [88].

Additionally, from the fact that the reservoir is initially in a thermal equilibrium state one finds that the power spectrum of the symmetrized forces correlation $\hat{F}_\lambda(t)\hat{F}_\mu(t')$ reads [A2]

$$\mathrm{Re}\left\langle \boldsymbol{F}(\omega)\boldsymbol{F}^T(\omega') + \boldsymbol{F}(\omega')\boldsymbol{F}^T(\omega)\right\rangle_{\hat{\varrho}_R} = 4\pi\hbar\delta\left(\omega+\omega'\right)\Gamma(\omega), \tag{1.42}$$

with the matrix $\Gamma(\omega)$ defined by its elements

$$\Gamma_{\lambda\mu}(\omega) = -\frac{1}{\hbar}\mathrm{Im}\chi_{\lambda\mu}(\omega)\coth\left(\frac{\hbar\omega}{2k_BT}\right) = J_{\lambda,\mu}(|\omega|)\coth\left(\frac{\hbar|\omega|}{2k_BT}\right). \tag{1.43}$$

Since the fluctuating force has Gaussian statistics, this can be fully determined from Eq.(1.42) (its mean value, designed by $\langle\hat{\boldsymbol{F}}(t)\rangle_{\hat{\varrho}_R}$, results to be zero because $\hat{\varrho}_R$ is a Gaussian distribution with mean value zero). Indeed, the expression (1.42) is a quantum fluctuation-dissipation relation because it associates the fluctuations, characterized by the anti-commutator $\langle\{\hat{F}_\lambda(t),\hat{F}_\mu(t')\}\rangle$, with the dissipation, given by the commutator $\langle\left[\hat{F}_\lambda(t),\hat{F}_\mu(t')\right]\rangle$ according to Eq.(1.40). It should be noticed that in the equation (1.43) it has been employed the following identity which directly derives from the Hamiltonian (1.37) without making any consideration,

$$-\frac{1}{\hbar}\mathrm{Im}\chi_{\lambda\mu}(\omega) = \Theta(\omega)J_{\lambda,\mu}(\omega) - \Theta(-\omega)J_{\lambda,\mu}(-\omega), \tag{1.44}$$

where $J_{\lambda,\mu}(\omega)$ is identified with the reservoir spectral density, and is given by [A2]

$$J_{\lambda,\mu}(\omega) = \frac{\pi}{\hbar}\sum_{\boldsymbol{k}} g_{\boldsymbol{k}}^2\cos\left(\boldsymbol{k}\cdot\Delta\boldsymbol{r}^0_{\lambda\mu}\right)\delta\left(\omega-\omega_{\boldsymbol{k}}\right). \tag{1.45}$$

The Eq.(1.45) coincides in the limit of equal environments ($\Delta\boldsymbol{r}^0_{\lambda\mu}\to 0$) with the usual definition derived from the Caldeira-Leggett model. It will be seen that the Fourier transform plays an important role in the resolution of the generalized Langevin equation, for that reason Eqs. (1.41), (1.44), and (1.45) will be of primary importance in further developments. Interestingly an analogous fluctuation-dissipation relation to Eq.(1.42) holds even when the reservoir is initially in a squeezed thermal state, see Refs. [186] and [A4].

Looking closely at expression (1.45), one may realize that the so-called spectral density plays a major role because it compactly encodes the information about the microscopic properties of the dissipative dynamics: the (microscopic) strength of the system-reservoir interaction (given by $g_{\boldsymbol{k}}$), and further, the frequencies of the reservoir modes (*i.e.* the reservoir spectrum energy). Indeed, once one knows the explicit form of $J_{\lambda,\mu}(\omega)$ the susceptibility and the statistical properties of the fluctuating force can be completely determined from Eqs. (1.41), (1.44), and by virtue of the fluctuation-dissipation relation (1.42), respectively. That is, the spectral density fully characterizes the open dynamics of those dissipative systems for which the Feynman-Vernon initial condition is satisfied [151]. Consequently, most of the difficulty in solving the generalized Langevin equation will depend on the (mathematical) properties of the spectral density. In principle, the spectral density could be measured experimentally (e.g. in nanomechanical oscillators [109]) or can

be deduced from a microscopic model (e.g. atom interacting with an electromagnetic field [245]). However, the coupling coefficients $g_{\boldsymbol{k}}$ are unknown in many practical situations and an appropriate phenomenological expression is usually adopted for the spectral density [151].

Therefore, the explicit expression of the spectral density will practically dictate the characteristics of the quantum evolution of the system of interest subjected to a dissipative quantum dynamics. In a more general context, the theory of open systems has devoted considerable attention to an important class of evolutions for which the treatment is considerably simplified. This is refereed to as the *Markovian* evolution, and equivalently, Markovian dynamics is used to designate the physical process which gives rise to such evolution [43; 96; 208]. Physically, this kind of evolution emerges when the characteristic time scale of the reservoir correlation functions is much shorter than the natural time scale associated with the evolution of the system, such that the *memory* of the system evolution over its history disappears [245]. Intuitively, the defining feature of a Markovian evolution is that only the present knowledge of $\hat{\boldsymbol{X}}$, and absolutely nothing of its past values, will influence the future values of $\hat{\boldsymbol{X}}$. This has an immediate consequence in the generalized Langevin equation: the susceptibility approaches at a Dirac delta function (*i.e.*, $\chi(t-\tau) \to \delta(t-\tau)$) in the Markovian limit, and consequently, its Fourier transform $\chi(\omega)$ must be practically constant. At first glance, Eqs.(1.41) and (1.44) reveal that a frequency-independent spectral density (*i.e.*, $J(\omega) \propto \gamma$) is necessary to induce a strict Markovian evolution. This is almost an idealization because it entails that the reservoir has no particular structure[xxx], however, surprisingly enough, the developed theory around the Markovian dynamics has been used very successfully in many areas of physics, such as quantum optics [96]. Regarding the damped harmonic oscillator, it was shown that an approximately Markovian dynamics holds either in the limit of weak or strong damping if the temperature is high enough in comparison with the dissipative rate, *i.e.* $\hbar\gamma \ll k_B T$ [105]. Since we are mainly interested in the physics that occurs near the ground state, the quantum evolution of the dissipative system will be mostly dominated by non-Markovian effects.

Going back to the equation (1.38), one may immediately see that the generalized Langevin equation is an integro-differential equation which is non-linear in the position operators except for a quadrature interaction potential $\hat{U}$. Such non-linearity makes rather difficult to obtain an exact solution of Eq.(1.38), as we have previously outlined. Depending on the mathematical properties of the memory kernel there are a few formal results about the existence and uniqueness of the (stationary) solution of this kind of non-linear equation. One practical way to handle these difficulties is to linearise the interaction potential by using perturbative methods, see for example the treatment for an optomechanical setup

[xxx] In the Brownian motion, non-structured reservoirs are identified with white-noise fluctuating forces, which is characterized by a power spectrum $\langle\{F(\omega), F(\omega')\}\rangle = 2\gamma k_B T \delta(\omega - \omega')$ [118]. The fluctuation-dissipation relation given in Eq.(1.42) shows that this consideration is opposite to the actual situation one finds in the quantum regime [96]. However, the same consideration has been satisfactorily used to study the damping of a radiation field into a cavity [160]. The reason of this success likely relies on the fact that the interaction between light and matter is very weak in Nature.

in Refs. [248; 61]. Nonetheless, the applicability of the obtained solutions is restricted to those physical situations in which the system interaction is weak. For the present study, we shall focus the attention on quadratic interaction potentials given by Eq.(1.34). Then the generalized Langevin equation becomes linear (more precisely, it corresponds to a linear Volterra equation of second kind), and thus, can be rigorously solved by using the methods based on the Green functions [45; 89; 84]. Doing so one obtains the following solution for the position-operator,

$$\hat{\boldsymbol{X}}(t) = \dot{\alpha}(t-t_0)M\hat{\boldsymbol{X}}(t_0) + \alpha(t-t_0)\hat{\boldsymbol{P}}(t_0) + \underbrace{\int_{t_0}^{t} \alpha(t-\tau)\hat{\boldsymbol{F}}(\tau)d\tau}_{\text{Stationary Solution}}, \tag{1.46}$$

where we have introduced the momentum-operator vector,

$$\hat{\boldsymbol{P}}(t) = M\dot{\hat{\boldsymbol{X}}}(t). \tag{1.47}$$

$\alpha(t)$ compactly denotes the matrix Green function of the generalized Langevin equation (which has been assumed to be linear in the position operators). It must be mentioned that we have used the fact that the memory kernel (or susceptibility) in Eq.(1.38) is stationary in the sense that $\chi(t,\tau) = \chi(t-\tau)$, and as a consequence, the Green function is also stationary [157]. Furthermore, this property of the memory kernel permits one to use the Laplace transform to convert the integro-differential equation (1.38) into an algebraic expression from which the matrix Green function may be straightforwardly obtained,

$$\mathcal{L}(\alpha(t))(s) = \left(Ms^2 + U + 2\tilde{\Omega} + \frac{1}{\hbar}\mathcal{L}(\chi(t))(s)\right)^{-1}, \tag{1.48}$$

where $\mathcal{L}(f(t))(s)$ denotes the Laplace transform of the function $f(t)$. Using the inversion formula of Laplace transform in Eq.(1.48) we may obtain the Green function in the time domain, and then, the time-dependent solution of the position-operator vector from Eq.(1.46). Nonetheless, in the future the interest is foremost in the stationary solution which by definition does not depend on the initial values of $\hat{\boldsymbol{X}}(t_0)$ and $\hat{\boldsymbol{P}}(t_0)$. Later we discuss in detail when this solution is guaranteed, now let us anticipate that in its derivation it is more convenient to use the Fourier transform of the Green function,

$$\alpha(t) = \int_{-\infty}^{\infty} \frac{e^{-i\omega t}}{-M\omega^2 + U + 2\tilde{\Omega} + \frac{1}{\hbar}\chi(\omega)} \frac{d\omega}{2\pi}, \tag{1.49}$$

where $\chi(\omega)$ stands for the Fourier transform of the matrix susceptibility, which is straightforwardly obtained from the Eqs. (1.44), and (1.41) once one knows the spectral density. Notice that to obtain $\alpha(\omega)$ we have previously took the limit $t_0 \to -\infty$ in the generalized Langevin equation.

At this point one may use the mathematical results related to the integral transforms

[xxxi] [79]. From here follows that if the Laplace transform of the susceptibility has an algebraic expression in terms of the (Laplace) variable s, then the elements of the matrix Green function in the time domain $\alpha_{\lambda\mu}(t)$ will be in general a combination of complex exponential functions whose exponents are given by the simple poles of its Laplace transform ($\mathcal{L}(\alpha_{\lambda\mu}(t))(s)$). This is the case for an Ohmic spectral density with Drude cut-off [107; 193]. Nonetheless, more complicated choices of the spectral density (for example, see **[A2]**) leads to complex non-polynomial expressions of the Laplace transform of the susceptibility which ultimately makes inaccessible to obtain analytically an expression for the matrix Green function of the generalized Langevin equation. This essentially occurs because an analytic form of the inverse Laplace transform of Eq.(1.48) is unknown. However one may use numerical methods related to integration in the complex plane (for example, see [258]) in order to compute numerically such inverse Laplace transform at any time and for an elected set of values for the problem parameters (e.g. temperature, oscillator frequency, etc). As a consequence, the problem of tracking the time evolution of the dissipative system may become in general computationally time-consuming.

As we have previously discussed, we expect that the interaction with the reservoir wipes out all the information about the initial state of the system in the long-time limit. More precisely, the reservoir will drive the system into a stationary state independent of its initial conditions. Paying attention to Eq.(1.46), it is deduced that the system reaches a stationary state as long as the matrix Green function vanishes in the asymptotic time limit, *i.e.* $\alpha_{\lambda\mu}(t \to \infty) \to 0 \ \forall \ \lambda, \mu$. One may use the Riemann-Lebesgue lemma[xxxii] in Eq.(1.49) to formally show that this will be certainly the case if the Fourier transform of the Green function $\alpha_{\lambda\mu}(\omega)$ decays as fast as $1/|\omega|^p$ for $p > 1$ [194]. Hence, this condition is guaranteed depending on the explicit form of the Fourier transform of the susceptibilities $\chi_{\lambda\mu}(\omega)$.

Dhar and Wagh pointed out that such condition is violated in particular if the system-plus-reservoir complex has a normal mode with a frequency Ω_b which is root of the denominator in Eq.(1.49) (see also Ref.[185]). In the damped harmonic oscillator this entails that the imaginary part of the Fourier transform of the susceptibility vanishes at the value Ω_b, *i.e.* $\mathrm{Im}\chi(\Omega_b) = 0$, which according to Eqs. (1.44) and (1.45) turns into that Ω_b lies outside the bandwidth of the reservoir modes [64]. Here, we recall the previous premise **(3)**, which establishes that the reservoir spectrum is quasi-continuous and fully comprises the system

[xxxi] One may invert both Laplace and Fourier transform by making use of the Residue Theorem on a contour integral in the complex plane. Then the starting point is the knowledge of its Laurent series, which will coincide directly with the partial fraction decomposition of the Laplace transform in the case of a polynomial expression.

[xxxii] Let $f(\omega)$ be an complex-valued function that is absolutely integrable on $\mathbb{R}$. Then the Riemann-Lebesgue lemma states that [50],

$$\lim_{|t|\to\infty} \int_{-\infty}^{\infty} f(\omega) e^{i\omega t} d\omega \to 0. \tag{1.50}$$

One says $f(\omega)$ is an absolutely integrable function on $\mathbb{R}$ if it is fulfil $\int_{-\infty}^{\infty} |f(\omega)| d\omega < 0$, or equivalently, if it belongs to the class of $L^1(\mathbb{R})$-functions. Clearly, the Riemann-Lebesgue lemma has an intuitive interpretation: the integrand becomes so highly oscillatory that everything cancels out.

spectrum, to ensure in our future development that there will not exist solutions of the kind Ω_b. Physically, this means that the interaction potential $\hat{U}$ contains neither inverted harmonic contributions nor infinite high potential barriers which prevent the system to effectively dissipate energy into the reservoir. In general, the mathematical condition upon $\alpha(\omega)$ required to satisfy the Riemann-Lebesgue lemma (this is $\alpha_{\lambda\mu}(\omega)$ decays as fast as $1/|\omega|^p$ for $p > 1$ and $\forall\ \lambda, \mu$) implies reasonable properties of *regularity* (e.g. uniform continuity and not take arbitrary large values) of the spectral densities $J_{\lambda,\mu}(\omega)$ from which is derived the Fourier transform of the susceptibility matrix. Formally, the spectral density is usually conceived as an analytic function except in a few isolated poles (mathematically known as meromorphic function). This also guarantees the existence of both the Laplace and Fourier transform of the susceptibility and of the Green function [84].

In the present dissertation, we are concerned with dissipative systems which arrive at stationary states in the asymptotic time limit, provided that the spectral densities $J_{\lambda,\mu}(\omega)$ (and then $\alpha(\omega)$) fulfil the previous properties. This will correspond to an equilibrium state if the reservoir is initially in thermal equilibrium **[A2]**, or more generally, to a (thermal) non-equilibrium state if the system is in contact with several environments at different temperatures **[A3]**. In both situations, it is preferable to use the Fourier transform to obtain the stationary solution of the generalized Langevin equation as we have mentioned above. The latter can be written in terms of the Fourier transform of the matrix Green function as follows,

$$\hat{\boldsymbol{X}}_{sta}(t) = \int_{-\infty}^{\infty} e^{-i\omega t}\ \alpha(\omega)\boldsymbol{F}(\omega)\frac{d\omega}{2\pi}, \tag{1.51}$$

where $\boldsymbol{F}(\omega)$ is the Fourier transform of the force vector, and the subscript 'sta' emphasizes that $\hat{\boldsymbol{X}}_{sta}$ is a stationary solution. One obtains the stationary solution of the momentum-operator vector by using Eq.(1.47).

By virtue of Eq.(1.1) and the characteristic function in Sec.1.1, the Wigner function of the system may be completely characterized from the knowledge of the moments and correlations (cross terms) of $\hat{\boldsymbol{X}}(t)$ and $\hat{\boldsymbol{P}}(t)$ (e.g. just their variances in the Gaussian case). On the other hand, from the Eqs. (1.46) and (1.47), one finds that such moments will acquire a complicated expression which involves time convolution integrals between the Green function $\alpha(t)$ and the moments of the system initial state and force vector $\hat{\boldsymbol{F}}(t)$. Successive symmetrized correlations of products among $\hat{\boldsymbol{X}}(t_0)$, $\hat{\boldsymbol{P}}(t_0)$, and $\hat{\boldsymbol{F}}(t)$ will appear with increasing degree of the moments. If the Wigner-function representation of the state involves an arbitrary number of these moments, then the computation of the time-dependent Wigner function may become in general a tedious and difficult task. However, if we consider that the initial state of the system is Gaussian, and further, thanks to the fact that the force vector has Gaussian statistics (given by the fluctuation-dissipation relation (1.42)), then moments of higher order can be written at any time in terms of the first and second moments of $\hat{\boldsymbol{X}}(t_0)$, $\hat{\boldsymbol{P}}(t_0)$, and $\hat{\boldsymbol{F}}(t)$, and correlations between them. That is, the time-evolved state will inherit the Gaussian statistics of the initial Gaussian states of both system and reservoir. This implies that the system state will remain Gaussian during all the evolution [107; 206; 116; 106]. Furthermore, from here, also follows that the

stationary state of the system will be Gaussian irrespectively of its initial state, since all the dependence on the latter will disappear in the long-time limit. These results are well-known from quantum optics [47; 96], and rely upon the fact that the Heisenberg equations of the system-plus-reservoir complex are linear [251]. We must mention that this feature of the solution of the generalized Langevin equation has been exploited to successfully analyse the stationary Gaussian entanglement in the Refs. **[A2]**, **[A3]**, and **[A4]**. Another interesting property of the generalized Langevin equation with quadratic interaction potentials is that it coincides exactly with its classical counterpart[xxxiii]. This indicates that the quantum mechanical properties of the dissipative system will be hidden in the initial condition of the system and the properties of the force vector statistics.

Then the study of the time asymptotic properties of the system reduces to compute the covariance matrix defined in Eq.(1.4). Replacing the solutions $\hat{\boldsymbol{X}}_{sta}(t)$ and $\hat{\boldsymbol{P}}_{sta}(t)$, given by Eq.(1.51), into expression (1.4) one finds that the elements of the covariance matrix are obtained as closed-form expressions involving frequency-variable integrals of products between $\alpha_{ij}(\omega)$ and the Fourier transform of the second moments of the force vector. For further details, see Eqs. (14), (15), and (16) in Ref.**[A2]**. More extensively, the stationary solution of the generalized Langevin equation provides us with more information than the covariance matrix, that is the two-time correlations functions between the position and momentum operators, *i.e.*

$$C_{\hat{\boldsymbol{A}}\hat{\boldsymbol{B}}}(t,t') = \frac{1}{2}\langle \hat{\boldsymbol{A}}(t)\hat{\boldsymbol{B}}^T(t') + \hat{\boldsymbol{B}}(t')\hat{\boldsymbol{A}}^T(t)\rangle_{\hat{\varrho}_S}, \tag{1.52}$$

with $\hat{\boldsymbol{A}}, \hat{\boldsymbol{B}} \in \{\hat{\boldsymbol{X}}, \hat{\boldsymbol{P}}\}$ and where $\hat{\varrho}_S$ symbolizes the stationary state. It should be noticed that one obtains the covariance matrix from Eq.(1.52) for correlations evaluated at equal times. Unfortunately, an analytic expression for equation (1.52) on time domain is generally unknown. Instead it can be written as a closed-form expression of an integral in the frequency domain. Then one will need to resort to numerical methods related to integration in the complex plane [258] in order to evaluate the latter numerically.

So far we have dealt with the generalized Langevin equation which governs the exact quantum evolution of the position operators of the system modes, which will be approximately Markovian only in certain special limits (e.g. weak coupling with the reservoir and high temperatures). In what follows, we turn our attention to the treatment of the open dynamics based on the time-independent Fokker-Planck equation. The conceptual jump resides essentially on that the solution of this equation directly provides the time-evolved Wigner function of the dissipative system. This has been proved to be very convenient when the n-mode system stars from a non-Gaussian state.

[xxxiii] For instance, it was shown in quantum optics that the classical Liouville equation of motion is identical to the quantum mechanical equation of motion of the Wigner function for quadratic interaction potentials [96].

1.3.3 Time-independent Fokker-Planck equation

In classical mechanics, Fokker-Planck equations are a form of Liouville equations used to study the dynamics of macroscopic but small systems subjected to fluctuations and dissipative effects produced by the interaction with their environments [207; 266]. Then, in the context of the statistical physics, these equations formally govern the time evolution of the phase-space distribution function, say $f(\boldsymbol{x},t)$, of the dissipative system. The Wigner function, namely $W(\boldsymbol{x},t)$, which is the central object in our treatment, is expected to approach $f(\boldsymbol{x},t)$ in the classical limit, what makes to think that the Fokker-Planck equation may have a quantum counterpart for $W(\boldsymbol{x},t)$. Early investigations in the theory of open quantum systems showed that this kind of equations arise naturally in the study of the famous quantum Brownian motion, e.g see [12]. Indeed, several Fokker-Planck equations that describe the dynamics of the quantum damped harmonic oscillator have been derived starting from the Caldeira-Leggett model [140], where they basically differ on the approximations made in the open-system dynamics. Regarding quantum information theory, these equations have been also employed (in the interaction picture) to study the effects of losses and thermal hopping over the entanglement in continuous-variable systems [222].

Let us express the Hamiltonian $\hat{H}_S$ of the n-mode system in terms of the phase-space variables through a $2n\times 2n$ real symmetrical matrix $\boldsymbol{H}$, such that $\hat{H}_S=\hat{\boldsymbol{x}}^T\boldsymbol{H}\hat{\boldsymbol{x}}$. Further, it should be noticed that there are few results about the solution of a Fokker-Planck equation whose coefficients are time-dependent functions (e.g., see [89]), however the situation changes substantially when they are constants, which shall be refer to as time-independent Fokker-Plank equations.

Rather than looking for a microscopical derivation of the system equations of motion, we ask for a physically meaningful quantum evolution, as general as possible, of the Wigner function consistent with a dissipative scheme. With that in mind, we shall consider that the open dynamics of the n-mode system is well described by a quite general time-independent Fokker-Planck equation. This leads us to the following Liouville-like equation for the Wigner function,

$$\frac{\partial W(\boldsymbol{x},t)}{\partial t}=-\left(\boldsymbol{x}^T\boldsymbol{H}\boldsymbol{J}_n\frac{\partial}{\partial\boldsymbol{x}}+\left(\frac{\partial}{\partial\boldsymbol{x}}\right)^T\left[\boldsymbol{J}_n^T\boldsymbol{H}-\boldsymbol{\Gamma}\right]\boldsymbol{x}-\left(\frac{\partial}{\partial\boldsymbol{x}}\right)^T\boldsymbol{D}\frac{\partial}{\partial\boldsymbol{x}}\right)W(\boldsymbol{x},t) \quad (1.53)$$

with $\left(\frac{\partial}{\partial\boldsymbol{x}}\right)^T=\bigoplus_{l=1}^n\left(\frac{\partial}{\partial q_l},\frac{\partial}{\partial p_l}\right)$, whereas $\boldsymbol{\Gamma}$ and $\boldsymbol{D}$ are $2n\times 2n$ real symmetric matrices that encode all the interaction with the environment. For the present, no specific form for $\boldsymbol{\Gamma}$, $\boldsymbol{D}$, and $\boldsymbol{H}$ is assumed, we only require that they may provide a physically consistent description of certain dissipative scenario. In general, the Heisenberg uncertainty relations imply the condition $\boldsymbol{V}(t)\geq i\boldsymbol{J}_n/2$ for $t\geq 0$ which is necessary for any physical non-Gaussian state, whereas it is necessary and sufficient for any physical Gaussian state. The only consideration made is that the matrix $\boldsymbol{D}$ is positive-definite, and second the eigenvalues of the matrix $\boldsymbol{J}_n^T\boldsymbol{H}-\boldsymbol{\Gamma}$ all have non-zero real negative parts, *i.e.*

$$\boldsymbol{D} > 0, \quad (1.54)$$

$$H(\boldsymbol{J}_n^T\boldsymbol{H}-\boldsymbol{\Gamma}) < 0, \quad (1.55)$$

where $H(\boldsymbol{J}_n^T\boldsymbol{H}-\boldsymbol{\Gamma}) = 1/2(\boldsymbol{J}_n^T\boldsymbol{H}-\boldsymbol{\Gamma}+(\boldsymbol{J}_n^T\boldsymbol{H}-\boldsymbol{\Gamma})^\dagger)$ [124]. Both conditions (1.54) and (1.55) guarantee that Eq.(1.53) has no singularities or run-away solutions [207; 48], and consequently, we expect that the Wigner function reaches a stationary solution in the long-time limit, in agreement with a dissipative dynamics. Physically, such conditions exclude the possibility that the interaction potential of the system would have inverted harmonic contributions nor infinite high potential barriers as before.

Before embarking in the derivation of the solution of the Eq.(1.53), let us make a brief comment about the relation between the open-system formalism we are dealing with now and the previous one. In the case of the damped harmonic oscillator, it is well-known that a time-independent Fokker-Planck equation can be associated with a memoryless Langevin equation for a strict Markovian dynamics [266; 150]. However, the global evolution of a many-particle system may be non-Markovian even though each particle follows a 'reduced' Markovian dynamics (e.g., a combination of continuous Markov processes is often not by itself Markovian) [101]. This prevents us to establish a formal, as well as general, relation between the generalized Langevin equation given in Eq.(1.38) and the Fokker-Planck equation (1.53). Nonetheless, this does not exclude the possibility that both equations may describe the same evolution of the dissipate system in certain limits (see Refs. [101] and [85]), though further development in this direction is beyond of the scope of the present dissertation. We must expect in those cases that the matrix $\boldsymbol{\Gamma}$ and $\boldsymbol{D}$ will be given in terms of the matrix susceptibility $\chi(t)$ and force vector $\hat{\boldsymbol{F}}(t)$, respectively, as occurs in the damped harmonic oscillator. Consequently, $\boldsymbol{\Gamma}$ regards the dissipative effects, while $\boldsymbol{D}$ characterizes the noise influence in the dissipative dynamics.

Since the interaction potential is quadratic, the time-independent Fokker-Planck equation is linear in the phase-space variables. As before, this allows one to use the Green function method to obtain a general solution of such equation. Starting from the knowledge of the initial state of the system $W(\boldsymbol{x},0)$, the Wigner function at later times is given by,

$$W(\boldsymbol{x},t) = \int_{\mathbb{R}^{2n}} W(\boldsymbol{x}',0)G(\boldsymbol{x},\boldsymbol{x}',t)d^{2n}\boldsymbol{x}'. \tag{1.56}$$

where now the Green function is denoted by $G(\boldsymbol{x},\boldsymbol{x}',t)$, and takes the form (see [12; 48])

$$G(\boldsymbol{x},\boldsymbol{x}',t) = \frac{1}{(2\pi)^n\sqrt{\det(\boldsymbol{\sigma}(t))}}e^{-\frac{1}{2}(\boldsymbol{x}-\boldsymbol{b}(t)\boldsymbol{x}')^T\boldsymbol{\sigma}(t)^{-1}(\boldsymbol{x}-\boldsymbol{b}(t)\boldsymbol{x}')} \tag{1.57}$$

where

$$\begin{aligned}\boldsymbol{b}(t) &= e^{(2\boldsymbol{J}_n^T\boldsymbol{H}-\boldsymbol{\Gamma})t},\\ \boldsymbol{\sigma}(t) &= \boldsymbol{\sigma}(\infty) - e^{(2\boldsymbol{J}_n^T\boldsymbol{H}-\boldsymbol{\Gamma})t}\boldsymbol{\sigma}(\infty)e^{(2\boldsymbol{H}\boldsymbol{J}_n-\boldsymbol{\Gamma})t}.\end{aligned} \tag{1.58}$$

The matrix $\boldsymbol{\sigma}(\infty)$ will determine the stationary solution of Eq.(1.53), and is obtained from solving the Lyapunov equation,

$$(2\boldsymbol{J}_n^T\boldsymbol{H}-\boldsymbol{\Gamma})\boldsymbol{\sigma}(\infty)+\boldsymbol{\sigma}(\infty)(2\boldsymbol{H}\boldsymbol{J}_n-\boldsymbol{\Gamma}) = -2\boldsymbol{D}. \tag{1.59}$$

It must be mentioned that the stationary solution will be unique due to the uniqueness of the matrix $\boldsymbol{\sigma}(\infty)$. The latter can be easily seen from Eq.(1.59) by appealing to a standard theorem of linear algebra which states that the solution $\boldsymbol{X}$ of $\boldsymbol{RX}-\boldsymbol{XS}=\boldsymbol{T}$ is uniquely determined if the matrices $\boldsymbol{R}$ and $\boldsymbol{S}$ have no common eigenvalues [263]. Here, $\boldsymbol{R}=2\boldsymbol{J}_n^T\boldsymbol{H}-\boldsymbol{\Gamma}$ and $\boldsymbol{S}=-(2\boldsymbol{J}_n^T\boldsymbol{H}-\boldsymbol{\Gamma})^T$ might only have a common eigenvalue zero, which, however, has been excluded from our study by the requirement Eq.(1.55).

Doing the integral in Eq.(1.56) after substituting the Wigner function of an initial non-Gaussian state given by Eq.(1.5), one finds that the time-evolved Wigner function can be cast in terms of the matrices $\boldsymbol{b}(t)$ and $\boldsymbol{\sigma}(t)$ as follows,

$$W(\boldsymbol{x},t)=\frac{e^{-\frac{1}{2}\boldsymbol{x}^T\boldsymbol{\sigma}(t)^{-1}\boldsymbol{x}}}{(2\pi)^n\sqrt{\det\left(\boldsymbol{b}(t)\boldsymbol{V}(0)\boldsymbol{b}(t)^T+\boldsymbol{\sigma}(t)\right)}}\times \left[e^{\frac{1}{2}\left(\frac{\partial}{\partial\boldsymbol{x}'}+\boldsymbol{b}(t)^T\boldsymbol{\sigma}(t)^{-1}\boldsymbol{x}\right)^T\left(\boldsymbol{V}(0)^{-1}+\boldsymbol{b}(t)^T\boldsymbol{\sigma}(t)^{-1}\boldsymbol{b}(t)\right)^{-1}\left(\frac{\partial}{\partial\boldsymbol{x}'}+\boldsymbol{b}(t)^T\boldsymbol{\sigma}(t)^{-1}\boldsymbol{x}\right)}F(\boldsymbol{x}')\right]_{\boldsymbol{x}'=\vec{0}}, \tag{1.60}$$

where $\boldsymbol{V}(0)$ is the initial covariance matrix in Eq.(1.5), and the exponential differential operator must be understood as a power sum. In particular, if the system starts from a Gaussian state (*i.e.*, $F(\boldsymbol{x})=1$), Eq.(1.60) transforms in,

$$W(\boldsymbol{x},t)=\frac{e^{-\frac{1}{2}\boldsymbol{x}^T\left(\boldsymbol{b}(t)(\boldsymbol{V}(0)-\boldsymbol{\sigma}(\infty))\boldsymbol{b}(t)^T+\boldsymbol{\sigma}(\infty)\right)^{-1}\boldsymbol{x}}}{(2\pi)^n\sqrt{\det\left(\boldsymbol{b}(t)(\boldsymbol{V}(0)-\boldsymbol{\sigma}(\infty))\boldsymbol{b}(t)^T+\boldsymbol{\sigma}(\infty)\right)}}, \tag{1.61}$$

where we have used the identity (1.58). Clearly, this Wigner function corresponds to a Gaussian state whose covariance matrix evolves as $\boldsymbol{V}(t)=\boldsymbol{b}(t)(\boldsymbol{V}(0)-\boldsymbol{\sigma}(\infty))\boldsymbol{b}(t)^T+\boldsymbol{\sigma}(\infty)$. It must be noticed that the Wigner function given by Eq.(1.60) corresponds to a non-Gaussian of the form we are dealing in the present dissertation (and which is defined in Eq.(1.5)).

Paying attention to Eq.(1.60) (and Eq.(1.61)), one may realize that the solutions of the Fokker-Planck and generalized Langevin equations share two important properties. The first one follows from Eq.(1.61), which is that the initial Gaussian characteristic of the state is maintained during all the evolution. The second property is related to the stationary state that reaches the system, this will be always Gaussian with covariance matrix $\boldsymbol{\sigma}(\infty)$. The latter follows from the fact that $\boldsymbol{b}(t)$ goes to zero in the long-time limit in agreement with the condition (1.55). As a consequence, the covariance matrix in the exponential appearing in Eq.(1.60) approaches to $\boldsymbol{\sigma}(\infty)$ in the long-time limit (see Eq.(1.58)), whereas the polynomial part reduces to evaluate the successive derivatives of $F(\boldsymbol{x})$ at the origin, which reduces to the unity.

In the present study, we address the dissipative dynamics of the system through the Fokker-Planck equation with the goal of obtaining a simple and reliable description of the time-evolved Wigner function. Without specifying the matrices $\boldsymbol{H}$, $\boldsymbol{\Gamma}$ and $\boldsymbol{D}$, the equation (1.60) provides us with a quite general quantum evolution of the Wigner function when the n-mode system is subjected to dissipative quantum dynamics, and it starts from an initial non-Gaussian state. Similarly reasoning applied to the Eq.(1.61) instead if the

system is initially in a Gaussian state. It will show in the Chapter 2 that these results permit to analyse the transient evolution of multipartite entanglement characterized by the separability criteria proposed in Ref.[A1]. In particular, both formulas have been used in that work to analyse the dynamics of entanglement in specific dissipative scenarios.

Chapter 2

Entanglement dynamics

Quantum mechanics is not a theory about reality,
it is a prescription for making the best possible predictions about the future
if we have certain information about the past.
-Gerard't Hooft (Extracted from [122])

The evolution of entanglement under environmental influence has been proved to be very rich at short time scales, e.g. quantum correlations exhibit death and re-birth [197; 164; 32; 135; 158; 241; 94], while at long times it commonly shows a downgrading tendency [234], which may end up in a completely loss of inseparability properties. Most of the research concerning entanglement in open systems has mainly focused, on one hand, on finding robust states against harmful dissipative and noisy effects, and on the other hand, on designing strategies to actively counteract such effects. Among the latter, one can find novel tools based on the so-called error-correction schemes [60] or quantum Zenon effect, which both consist essentially on performing a set of measurements and unitary manipulations on the system that effectively shield its quantum correlations from the environmental influence. Other strategies rely on conveniently engineering the system and system-reservoir interaction with the aim of either effectively decoupling collective degrees of freedom of the system from the reservoir [188; 189; 165], or driving precisely the system onto preferred entangled states by dissipation [256; 139] or correlated quantum noise [240; 123; 261; 167]. Interestingly, further investigation in harmonic oscillators has shown that a parametric driving between two modes is able to generate robust stationary entanglement at relatively high temperatures [95]. Nonetheless, the preceding methods are generally hampered by the following issues: they may be unsuccessfully applied due to a poor treatment of the actual environmental influence (e.g. it is usually assumed, without clear evidences, that the system follows a Markovian evolution), or more generally, their performance requires of an accurate degree of control over the system and reservoir.

The present chapter pursues to explore the dynamics of multipartite entanglement which underlies when CV systems are driven at low enough temperatures, making the linear treatment of the open-system dynamics (exposed in Sec.1.3) consistent. It is our intention

to get insight about such *low-energy* dynamics in general dissipative scenarios from the perspective that the aforementioned methods are unfeasible. Unlike foregoing works, none restrictions (e.g. we assume arbitrary frequencies) on the interesting system or reservoir will be imposed in our analysis. With this in mind, it should be recalled from the previous chapter that an attempt to provide a meaningful description of entanglement becomes more complicate as either the mixedness of the system state (separability problem) or the number of the system constituents (a family of several types of entanglement emerges) grows. Unfortunately, the meeting of both circumstances prevents us of gaining an "universal" picture of the multipartite entanglement dynamics in realistic dissipative scenarios, and as a consequence, the scope of future discussions will be centred on simple, but rather insightful, physical situations that make the inseparability properties of the system accessible to qualitative or quantitative analysis.

At short time scales, we shall address the inseparability properties of Gaussian and non-Gaussian states when they are subjected to purely dissipative effects (e.g., photon losses and thermal hopping), remember that it is of particular interest how much and for how long entanglement persists. At this respect, Gaussian entangled states themselves have shown very robust under environmental influence [15; 3], see also Refs. [178] and [212]. To monitor the evolution of entanglement we will employ the inseparability criterion proposed in Ref.[**A1**], which shall be introduced in more detail in what follows.

The stationary inseparability properties of the dissipative system deserve special attention since in many experimental setups the system has been unavoidably interacting with the reservoir for a long time. We shall focus this study on two simple schemes which widely capture most of the relevant physics behind multipartite dissipative scenarios, this can be roughly classified on a common environment or independent environments. The former shall consist on three uncoupled modes which are in contact with the same reservoir, and whose open-system dynamics is determined by the Hamiltonian given in Eq.(1.37). This will permit us to shed light on the mechanism whereby the (a priori decoherent) reservoir interaction is able to create entanglement among non-directly interacting oscillators, and further, which are the main characteristic of this generated entanglement. The second scheme shall deal with an one-dimensional open (harmonic) chain composed of three oscillators, each of which is in contact with an independent reservoir at a priori initial different temperature. This second setup allows one to analyse entanglement supported by thermal out-of-equilibrium systems, which has been recently subjected to intensive investigation [161; 55; 33; 31; 56; 210], and may be particularly useful to elucidate if the establishment of stationary energy currents may come along with a buildup of the quantum correlations.

2.1 Separability criteria for CV multipartite entanglement

In the Sec.1.2 it was extensively illustrated that most successful entanglement estimators in the arena of CV systems entails an optimization of an entropy-like functional like a

convex-roof construction, the proper choice of a set of observables that witness the entanglement for a broad class of states, or the suitable election of a finite or infinite series of inequalities which are mainly based on the well-known criterion of PPT. Unfortunately, the technical difficulties involved in all these methods make the evaluation of entanglement a hard computational task in many cases, what ultimately forces us to focus the analysis on a set of entangled states smaller than those which are susceptible to be detected, for instance pure or Gaussian states.

Additionally, there is no a conception of the separability problem in the realm of multipartite states as clear and precise as in the bipartite case, instead, there are several complementary definitions of entanglement that are chosen depending on the specific properties exhibited by the quantum state in which we are interested in. Among the most meaningful definitions is found the so-called k-partite entanglement which is formulated in Eq.(1.27) and results in a hierarchical classification of the quantum correlation that goes from fully separability to genuine (n-partite) entanglement. Intuitively, this tells us how large is the largest entangled partition of the system. Fortunately, the separability criteria recently introduced by Levi and Mintert, which is exposed in the Eq.(1.30) (see also Eq.(1.28)) and generically designated as $\tau_{k,n}$, permits to perform a comparatively simple analysis of k-partite entanglement for highly mixed states, which makes it particularly interesting for our present purposes. Recall that in such criteria an accurate characterization of entanglement relies primarily on an appropriate choice of $2n$ probe states over which the only constraint is that they must be pure, written as $\{|\varphi_m\rangle\}_{m=1}^{2n}$. Though in certain cases one may deduce an optimal form of the latter by looking at the particular properties of the state of interest, these are encountered in general by doing an optimization procedure to obtain a maximum of the function $\tau_{k,n}(\hat{\varrho})$, whose positive value would undoubtedly reveal the k-partite entanglement.

Accordingly these probe states transform in complex-valued functions in the realm of CV systems, such that the aforementioned optimization procedure will consist on the maximization of certain functional, in which converts $\tau_{k,n}$, and for which the optimization domain corresponds now to such $2n$ functions. At first glance Eq.(1.30) (and Eq.(1.28)) reveals us that this functional is non-linear in these functions. Then, unless we make some simplifying assumptions over the set of probe states, the characterization of k-partite entanglement through $\tau_{k,n}$ in large-particle systems does not seem to be a promising endeavour. As we are dealing with general CV states whose Wigner functions exhibit certain Gaussian structure (see Eq.(1.3) and Eq.(1.5)), we propose that a reasonable choice for $\{|\varphi_m\rangle\}_{m=1}^{2n}$ is the set of Gaussian states. Indeed, there are several previous examples in the theory of entanglement, like the Gaussian entanglement of formation or Gaussian convex-roof measures mentioned in Sec.1.2, that proved that we can gain some understanding on the quantitative estimation of bipartite entanglement by doing this Gaussian-like assumption. Further investigation on this direction shows that such consideration permits one to get a closed-form expression for $\tau_{k,n}$ as a parametric function of the first and second moments of the probe states, and which provides a reliable characterization of k-partite entanglement for a broad class of Gaussian and non-Gaussian states given by Eq.(1.5). In what follows we expose the main results of this investigation which can be found in further detail in

Ref.[A1].

2.1.1 A Gaussian-like assumption

In analogy to the concept of Gaussian entanglement of formation, we require that all probe vectors to be Gaussian. Each Gaussian probe state $|\varphi_m\rangle$ is then characterized by its first and second moments,

$$\bar{\boldsymbol{x}}_m = (\bar{q}_m, \bar{p}_m), \text{ and} \tag{2.1}$$

$$\boldsymbol{\Sigma}_m = \begin{bmatrix} \sigma_{xx}^{(m)} & \sigma_{xp}^{(m)} \\ \sigma_{xp}^{(m)} & \sigma_{pp}^{(m)} \end{bmatrix}, \tag{2.2}$$

with $\det(\boldsymbol{\Sigma}_m) = 1/4$, $\sigma_{xx}^{(m)} \geq 0$ and $\sigma_{pp}^{(m)} \geq 0$. It should be noticed that $\bar{q}_m$, $\bar{p}_m$, $\sigma_{xx}^{(m)}$, $\sigma_{pp}^{(m)}$, and $\sigma_{xp}^{(m)}$ play the role of free parameters which form the optimization domain. Clearly, the set of these parameters grows linearly with the number of system constituents, *i.e.* it grows as $8n$. From here follows that $|\Phi_{1/2}\rangle$ and $|\Phi_{1j/2j}\rangle$ can be expressed as tensorial product states in terms of the probe states according to Eq.(1.29), and thus they inherit the Gaussian character. Then the first moments of the vectors $|\Phi_1\rangle$ and $|\Phi_1\rangle$ take the form

$$\boldsymbol{X}_{\Phi_1} = \bigoplus_{m=1}^{n} \bar{\boldsymbol{x}}_m, \tag{2.3}$$

$$\boldsymbol{X}_{\Phi_2} = \bigoplus_{m=1}^{n} \bar{\boldsymbol{x}}_{n+m}. \tag{2.4}$$

and the covariance matrices are given by

$$\boldsymbol{\Sigma}_{\Phi_1} = \bigoplus_{m=1}^{n} \boldsymbol{\Sigma}_m, \tag{2.5}$$

$$\boldsymbol{\Sigma}_{\Phi_2} = \bigoplus_{m=1}^{n} \boldsymbol{\Sigma}_{n+m}. \tag{2.6}$$

Let us designate the maximum of $\tau_{k,n}$ over all possible probe states,

$$\mathcal{T}_{k,n}(\hat{\varrho}) = \max_{\Phi_1,\Phi_2} \tau_{k,n}(\hat{\varrho}).$$

Recall that a positive value of $\mathcal{T}_{k,n}(\hat{\varrho})$ reveal us that $\hat{\varrho}$ is k-partite entangled. Notice that one can say nothing about the converse assertion in general.

With this at hand and starting from the equation (1.5) for the Wigner function of $\hat{\varrho}$, one finds that the matrix elements $\langle \Phi_1 \,|\, \hat{\varrho} \,|\, \Phi_2 \rangle$, $\langle \Phi_{1j} \,|\, \hat{\varrho} \,|\, \Phi_{1j} \rangle$ and $\langle \Phi_{2j} \,|\, \hat{\varrho} \,|\, \Phi_{2j} \rangle$, involved in the evaluation of $\tau_{k,n}(\hat{\varrho})$, entail an integral with a Gaussian kernel in the domain $\mathbb{R}^{2n}$. The suitable form of $W(\hat{\varrho})$ as a product between a polynomial $F(\boldsymbol{x})$ and a Gaussian function

with CM $\boldsymbol{V}$ permits to compute analytically such integrals. Hence, we may obtain closed-form expressions for the mentioned elements as functions of $\bar{\boldsymbol{x}}_m$ and $\boldsymbol{\Sigma}_m$.

One can proceed further and conveniently manipulate these expressions in order to write $\tau_{k,n}$ in the following compact form,

$$\tau_{k,n}(\hat{\varrho}) \;=\; \frac{e^{-\frac{\alpha}{2}}\,|\mathsf{f}_{\Phi_{21}}|}{\sqrt[4]{\det\left(\boldsymbol{\Sigma}_{\Phi_1}+\boldsymbol{\Sigma}_{\Phi_2}\right)}} - \sum_j a_j^{(k,n)} e^{-\frac{\beta_j}{4}} \sqrt{\mathsf{f}_{\Phi_{1j}}\mathsf{f}_{\Phi_{2j}}}\;, \tag{2.7}$$

with

$$\mathsf{f}_u = \frac{\exp\left(\frac{1}{2}K^T\left(\boldsymbol{V}^{-1}+\boldsymbol{\Sigma}_u^{-1}\right)^{-1}K\right)F(\boldsymbol{x})\Big|_{\boldsymbol{x}=\vec{0}}}{\sqrt{\det\left(\boldsymbol{\Sigma}_u+\boldsymbol{V}\right)}}, \tag{2.8}$$

and where $K=\left(\frac{\partial}{\partial \boldsymbol{x}}+\boldsymbol{\Sigma}_u^{-1}\boldsymbol{X}_u\right)$ for $u=\Phi_{21},\Phi_{1j},\Phi_{2j}$. The quantities

$$\alpha = \mathrm{Re}\left(\boldsymbol{X}_{\Phi_{21}}^T\boldsymbol{\Sigma}_{\Phi_{21}}^{-1}\boldsymbol{X}_{\Phi_{21}}\right) + (\boldsymbol{X}_{\Phi_1}-\boldsymbol{X}_{\Phi_2})^T\boldsymbol{J}_n^T\mathrm{Re}(\boldsymbol{\Sigma}_{\Phi_{21}})\boldsymbol{J}_n(\boldsymbol{X}_{\Phi_1}-\boldsymbol{X}_{\Phi_2}) \tag{2.9}$$

and

$$\beta_j = \boldsymbol{X}_{\Phi_{1j}}^T\boldsymbol{\Sigma}_{\Phi_{1j}}^{-1}\boldsymbol{X}_{\Phi_{1j}} + \boldsymbol{X}_{\Phi_{2j}}^T\boldsymbol{\Sigma}_{\Phi_{2j}}^{-1}\boldsymbol{X}_{\Phi_{2j}}\;, \tag{2.10}$$

are quadratic functions of the first-moment vectors. Furthermore, $\boldsymbol{\Sigma}_{\Phi_{1j/2j}}$, and $\boldsymbol{\Sigma}_{\Phi_{21}}$ are $2n\times 2n$ (complex) matrices that are determined from the matrices $\boldsymbol{\Sigma}_m$ by simple algebraic expressions, and similarly occurs for the $2n$-vectors $\boldsymbol{X}_{\Phi_{1j/2j}}$, and $\boldsymbol{X}_{\Phi_{21}}$, which are given in terms of the vectors $\bar{\boldsymbol{x}}_m$.

Though equation (2.7) still seems to be a complicated expression a first sight, it supposes a rather convenient form of $\tau_{k,n}$ in order to carry out the optimization procedure. The Heisenberg uncertainty relation over the probe states guarantees that the above matrices (the real part in the case of $\boldsymbol{\Sigma}_{\Phi_{21}}$) are positive-definite. This translates into that Eq.(2.7) has non-singular values in all the real domain corresponding to the free parameters. Furthermore, Eq.(2.7) is a real continuous function thanks to the fact that $F(\boldsymbol{x})$ is analytic in all the phase space. These features make that the maximum of $\tau_{k,n}$ would be accessible in the majority of cases by using standard optimization procedures [258].

The situation simplifies when $\hat{\varrho}$ is a Gaussian state, *i.e.* $F(\boldsymbol{x})=1$. In that case, one may try to envisage the form of the matrices $\boldsymbol{\Sigma}_m$ by looking at the shape of the Gaussian Wigner function, which is rotational invariant with respect to an axis passing through the origin. The latter leads us to make the suggestion $\boldsymbol{\Sigma}_{\Phi_1}=\boldsymbol{\Sigma}_{\Phi_2}=\boldsymbol{\Sigma}$, which entails $\boldsymbol{\Sigma}_{\Phi_{21}}=\boldsymbol{\Sigma}$. Thankfully, from this observation and employing some algebraic identities, it is analytically shown that the maximum is attained when $\boldsymbol{X}_{\Phi_1}=-\boldsymbol{X}_{\Phi_2}=\boldsymbol{X}$. With this, we arrive at

$$\tilde{\mathcal{T}}_{k,n} = \max_{\boldsymbol{X},\boldsymbol{\Sigma}}\;\tilde{\tau}_{k,n},$$

with

$$\tilde{\tau}_{k,n}(\hat{\varrho}) = \frac{e^{-2\boldsymbol{X}^T\boldsymbol{J}_n^T\frac{1}{\boldsymbol{\Sigma}^{-1}+\boldsymbol{V}^{-1}}\boldsymbol{J}_n\boldsymbol{X}}}{\sqrt{\det\left(\boldsymbol{\Sigma}+\boldsymbol{V}\right)}} - \sum_j a_j^{(k,n)}\frac{e^{-\frac{1}{2}\boldsymbol{X}^T(\boldsymbol{P}_j)^T\frac{1}{\boldsymbol{\Sigma}+\boldsymbol{V}}\boldsymbol{P}_j\boldsymbol{X}}}{\sqrt{\det\left(\boldsymbol{\Sigma}+\boldsymbol{V}\right)}}\;, \tag{2.11}$$

and

$$\boldsymbol{P}_j = \bigoplus_{m=1}^{n} (-1)^{[\boldsymbol{v}_j]_m} \boldsymbol{I} \ , \tag{2.12}$$

where $\boldsymbol{I}$ is the two-dimensional identity matrix, and $\boldsymbol{v}_j$, which is defined in the context of Eq.(1.29), characterizes the bipartition j.

Accordingly, the number of free parameters involved in the optimization procedure for Gaussian states reduces to $4n$ parameters which consist on the entries of $\boldsymbol{\Sigma}$ and $\boldsymbol{X}$. It is important to realize that we have obtained these results by just assuming that each pair of probe states, $|\varphi_m\rangle$ and $|\varphi_{n+m}\rangle$, share the same covariance matrix ($\boldsymbol{\Sigma}_m = \boldsymbol{\Sigma}_{n+m}$), which has then lead to that the maximum is recovered when they are symmetrically localized in the phase space ($\bar{\boldsymbol{x}}_m = -\bar{\boldsymbol{x}}_{n+m}$).

The expression (2.11) provides us with more information about the optimal choice of probe states. To see this, we observe that according to this equation the inequality

$$4\boldsymbol{J}_n^T \frac{1}{\boldsymbol{\Sigma}^{-1} + \boldsymbol{V}^{-1}} \boldsymbol{J}_n \geq (\boldsymbol{P}_j)^T \frac{1}{\boldsymbol{\Sigma} + \boldsymbol{V}} \boldsymbol{P}_j \ , \tag{2.13}$$

is satisfied for any mixed Gaussian state that is biseparable with respect to the partition j. This is deduced by just comparing the exponentials in Eq.(2.11), and using the fact that their arguments are positive-definite quadratic forms in terms of $\boldsymbol{X}$. It is worthwhile noting that if inequality (2.13) is violated in all the bipartitions, then $\hat{\varrho}$ is genuine multipartite entangled.

Curiously, the Ineq.(2.13) resemblances to the PPT criterion (see the inequality in Eq.(1.12)), though a priori they arise from different observations: PPT is based on that partial transposition maps separable states onto separable states, whereas $\tau_{k,n}$ identifies entanglement by looking at certain symmetries that any k-partite separable state must satisfy. Indeed, we find mathematically that the Ineq.(2.13) reproduces the results of PPT criterion for either arbitrary two-mode Gaussian states or pure three-mode Gaussian states, when all the probe states $|\varphi_m\rangle$ are chosen to be pure infinitely-squeezed states, with covariance matrix with $\sigma_{pp}^m \to 0$ ($\forall m$) for squeezing in momentum, or $\sigma_{xx}^m \to 0$ ($\forall m$) for squeezing in position. Let us briefly sketch how this comes about. First, one must realize that the inequality (2.13) can be translated into the eigenvalue problem of the product matrix [124],

$$\boldsymbol{Z}_j = 4(\boldsymbol{P}_j)^T (\boldsymbol{\Sigma} + \boldsymbol{V}) \boldsymbol{P}_j \boldsymbol{J}_n^T \left(\boldsymbol{\Sigma}^{-1} + \boldsymbol{V}^{-1}\right)^{-1} \boldsymbol{J}_n, \tag{2.14}$$

such that, inequality (2.13) is not violated as long as all of the eigenvalues of $\boldsymbol{Z}_j$ are greater than the unity.

We do not assume any particular form of $\boldsymbol{V}$, instead this is expressed in terms of the corresponding standard form[i] for equivalent entangled states without any loss of generality. In the Ineq.(2.13), $\boldsymbol{V}$ is then substituted by the standard form for the two-mode and pure

[i]Recall from Sec.1.2.4 that the covariance matrices of GLU-equivalent classes of entangled states can be brought into a standard form $\boldsymbol{V}_{SF}$ (see Eq.(1.33)). This guarantees that the characteristic polynomial of $\boldsymbol{Z}_j$ given in Eq.(2.14) will be exactly the same for these equivalent classes, and irrespective of whether we take other specific form of $\boldsymbol{V}$.

three-mode Gaussian states, and analogously, $\boldsymbol{\Sigma}$ is replaced by the covariance matrix of a n-mode single-mode squeezed state. After taking the limit of infinite-squeezed probe states one finds that n roots of the characteristic polynomial of $\boldsymbol{Z}_j$ coincide with the unity, and more interestingly, the other n roots are given by $4\tilde{\nu}_i^2$ $(i = 1, \ldots, n)$, where $\tilde{\nu}_i$ coincides with the symplectic eigenvalues of the partial transpose of $\boldsymbol{V}$ with respect the j bipartition and which appears in the symplectic formulation of the PPT criterion (1.14). Then PPT and the Ineq.(2.13) provide the same results related to entanglement in two-mode and pure three-mode Gaussian states. Remembering that PPT is a necessary and sufficient separability criterion for those states, this result means that $\tilde{\tau}_{k,n}$ is able to detect completely the Gaussian two-mode and pure three-mode entanglement.

Furthermore, we encounter that such assertion is no longer true for three-mode mixed Gaussian states, which is in agreement with the fact that PPT basically discerns fully inseparability in those states whereas $\tau_{3,3}$ identifies genuine tripartite entanglement. However, exhaustive numerical studies show that $\tau_{2,3}$ still detects entanglement on the vast majority of bipartite three-mode entangled states. Importantly, that the results from PPT and $\tau_{k,n}$ coincide practically for the previous studied states (recalling the coincidence is exact for two-mode and pure three-mode Gaussian states) outlines that the strength of the latter to detect entanglement remains almost intact after doing the Gaussian-like assumption.

In order to test the strength of the Eq.(2.7) in a further extent, we have also carried out an extensive study about the ability of $\tau_{k,n}$ to reveal the entanglement encapsulated in non-Gaussian states. In particular, we have assessed the entanglement of those non-Gaussian states known as coherently photon-subtracted two-mode squeezed vacuum states (CPS-TSVS). We will go back to these states later, let just anticipate that they have an important characteristic which is: the PPT criterion based on the second-order correlations fails to unveil the entanglement of these states when squeezing is zero [14]. This led Agarwal and Biswas to develop a new criteria based on higher order correlations which has been proved to be an 'optimized' criterion for the inseparability of certain classes of non-Gaussian states [177]. Remarkably enough, the expression (2.7) is able to detect this purely non-Gaussian entanglement in agreement with the Agarwal-Biswas criterion.

From the foregoing discussion we may draw two conclusions: first the Gaussian-like assumption made over the set of probe states yields a simple as well as a strong criteria for assessing the separability of either Gaussian and non-Gaussian states, and second, an optimal choice of the probe states are the set of infinitely-squeezed Gaussian states for which the pairs $|\varphi_m\rangle$ and $|\varphi_{n+m}\rangle$ are symmetrically localized in phase space. The latter conclusion has a more profound consequence in the detection of entanglement at the experimental level as the expression of $\tau_{k,n}$ for Gaussian states admits an operational interpretation in terms of Gaussian measurements. Let us briefly discuss how the hierarchies (2.7) and (2.11) can be implemented with experimental data.

Experimental quantification

The standard procedure would be based on the experimental reconstruction of the Wigner function in terms of quantum state tomography [162] or a measurement scheme specially

designed for multicomponent CV systems, followed by the analytical evaluation of Eqs.(2.7) and (2.11). However, the hierarchies for Gaussian states (2.11) may be also directly accessed by performing Gaussian measurements, modelled in terms of a positive-valued operators with Gaussian Weyl symbol [77; 180], which will be characterized by a covariance matrix $\boldsymbol{\sigma}_M$ and first-moment vector $\boldsymbol{X}_M$ that plays the role of the outcome of the measurement. If one performs such a measurement on the whole n-mode system, the probability of the outcome $\boldsymbol{X}_M$ is given by [180],

$$p(\boldsymbol{X}_M;\boldsymbol{\sigma}_M)=\frac{e^{-\frac{1}{2}\boldsymbol{X}_M^T\frac{1}{\boldsymbol{\sigma}_M+\boldsymbol{V}}\boldsymbol{X}_M}}{(2\pi)^n\sqrt{\det\left(\boldsymbol{\sigma}_M+\boldsymbol{V}\right)}}.$$

One may immediately identify the second term in Eq.(2.11) as $(2\pi)^n p(\boldsymbol{P}_j\boldsymbol{X};\boldsymbol{\Sigma})$, this is due to the fact that this term comes originally from matrix elements that play the role of projective measurements. On the other hand, the first term in Eq.(2.11), which results from off-diagonal matrix elements, may be expressed in terms of the Fourier transform $\hat{p}(\boldsymbol{\omega};\boldsymbol{\Sigma})$ of the probability distribution $p(\boldsymbol{X};\boldsymbol{\Sigma})$, *i.e.*

$$\tilde{p}(\boldsymbol{\omega};\boldsymbol{\Sigma})=\frac{1}{(2\pi)^n}\int_{\mathbb{R}^{2n}}d^{2n}\boldsymbol{X}e^{-i\boldsymbol{\omega}^T\boldsymbol{X}}\ p(\boldsymbol{X};\boldsymbol{\Sigma}),$$

such that Eq.(2.11) may be written as follows

$$\begin{aligned}\tilde{\tau}_{k,n}(\hat{\varrho}) &= e^{-2\boldsymbol{X}^T\boldsymbol{J}_n^T\boldsymbol{\Sigma}\boldsymbol{J}_n\boldsymbol{X}}\int_{\mathbb{R}^{2n}}d^{2n}\boldsymbol{\omega}e^{-2\boldsymbol{\omega}^T\boldsymbol{\Sigma}\boldsymbol{J}_n\boldsymbol{X}}\tilde{p}(\boldsymbol{\omega};\boldsymbol{\Sigma})\\ &- (2\pi)^n\sum_j a_j^{(k,n)}p(\boldsymbol{P}_j\boldsymbol{X};\boldsymbol{\Sigma}).\end{aligned}\tag{2.15}$$

This expression relates $\tilde{\tau}_{k,n}$ directly to the measurement statistics of a Gaussian measurement with the covariance matrix $\boldsymbol{\Sigma}$.

Since the projection of $\hat{\varrho}$ onto a one-mode pure infinitely-squeezed state models an ideal homodyne measure in the mth mode of the system [162; 78; 97], the previous results indicate that one may *completely* certify the inseparability of arbitrary two-mode and pure three-mode Gaussian states by a collective of simultaneous (ideal) homodyne measures on each mode of the system. At this respect, it was shown that it is possible to completely reconstruct, without having a full tomographic knowledge, the covariance matrix of a two-mode Gaussian state by locally manipulating the modes [59; 205], that is to say by means of a measurement scheme based on single homodyne measures and passive operations.

In practice, one will need an ensemble of identically prepared quantum states of the system in order to obtain a reliable statistics $p(\boldsymbol{X};\boldsymbol{\Sigma})$ to perform the Fourier transform involved in Eq.(2.15). Note that we have considered ideal Gaussian measurements, however they may contain errors due to the implicit imperfections of the experimental scheme. In order to avoid spurious conclusions from the experimental evaluation of expression (2.15), these systematic errors must be treated at the level of measurement statistics. Unfortunately, this method has certain disadvantages when is compared with previously mentioned

entanglement witnesses (see Sec.1.2.1), since it entails practically to perform quantum state tomography. Nevertheless, whereas such results may return quantitative estimations of bipartite entanglement based on measurement data, Eq.(2.15) is more general in the sense that it can be, in principle, applied to experimentally certify the *multipartite* entanglement of Gaussian states.

Finally, we would like to remark that one may address the problem of characterizing the multipartite entanglement without requiring a Gaussian conjecture on the probe states. This will lead to another function $\tau_{k,n}$ different from Eq.(2.7), which would probably identify the entanglement of other class of continuous-variable states, maybe a broader class than the one we considered here. However, the resulting hierarchy will be, as a consequence, rather involved as compared with the expression (2.7). This reflects the underlying idea at the base of the vast majority of existing tools designed to detect and estimate entanglement at theoretical as well as experimental level: it is necessary to get a compromise between the set of entangled states to be detected and the required computational and experimental efforts.

2.2 Entanglement dynamics in dissipative scenarios

Endowed with the expression (2.7) (and also Eq.(2.11)) for the separability criteria $\tau_{k,n}$, and the results of the entanglement theory and dissipative dynamics previously exposed in Chapter 1, we are ready to address the entanglement dynamics influenced by dissipative effects. Now we turn the attention to the time evolution of entanglement of a generic n-mode system in a dissipative scenario. In order to get some taste about the entanglement dynamics we first discuss, in general terms, the inseparability properties during a general quantum evolution of the Wigner function of the dissipative system.

Let us focus on the simple but non-trivial case of Gaussian entanglement characterized by the $\tau_{k,n}$ criterion. Here we may employ the result of Sec.1.3.3 related to the time evolution of the covariance matrix of an initial Gaussian state (see Eq.(1.61)) when the dissipative dynamics is simulated by a time-independent Fokker-Planck equation. This yields the following evolution for the CM,

$$\boldsymbol{V}(t) = e^{(2\boldsymbol{J}_n^T\boldsymbol{H}-\boldsymbol{\Gamma})t}(\boldsymbol{V}(0)-\boldsymbol{V}(\infty))e^{(2\boldsymbol{J}_n^T\boldsymbol{H}-\boldsymbol{\Gamma})^T t}+\boldsymbol{V}(\infty), \tag{2.16}$$

where $\boldsymbol{V}(\infty)$ is the stationary covariance matrix, whereas $\boldsymbol{H}$, and $\boldsymbol{\Gamma}$ and $\boldsymbol{D}$ are related respectively to the coherent evolution of system oscillators, and the system-reservoir coupling and characteristic properties of the reservoir. Substituting Eq.(2.16) into the Eq.(2.11) and after some straightforward algebra, the time evolution of $\tau_{k,n}$ can be cast into the form,

$$\tilde{\tau}_{k,n}(\hat{\varrho}(t)) \propto g(t)e^{-2\boldsymbol{X}^T\boldsymbol{J}_n^T\frac{1}{\boldsymbol{\Sigma}^{-1}+\boldsymbol{V}^{-1}(\infty)}\boldsymbol{J}_n\boldsymbol{X}}-\sum_j a_j^{(k,n)}f_j(t)e^{-\frac{1}{2}\boldsymbol{X}^T(\boldsymbol{P}_j)^T\frac{1}{\boldsymbol{\Sigma}+\boldsymbol{V}(\infty)}\boldsymbol{P}_j\boldsymbol{X}}, \tag{2.17}$$

where we have defined the functions,

$$\begin{aligned}
\boldsymbol{C}(t) &= e^{(2\boldsymbol{J}_n^T\boldsymbol{H}-\boldsymbol{\Gamma})t}\left(\boldsymbol{V}(0)-\boldsymbol{V}(\infty)\right)e^{(2\boldsymbol{H}\boldsymbol{J}_n-\boldsymbol{\Gamma})t},\\
g(t) &= e^{2\boldsymbol{X}^T\boldsymbol{J}_n^T\frac{1}{\boldsymbol{\Sigma}^{-1}+\boldsymbol{V}^{-1}(\infty)}\frac{1}{(\boldsymbol{\Sigma}^{-1}+\boldsymbol{V}^{-1}(\infty))^{-1}-\boldsymbol{V}(\infty)-\boldsymbol{V}(\infty)\boldsymbol{C}^{-1}(t)\boldsymbol{V}(\infty)}\frac{1}{\boldsymbol{\Sigma}^{-1}+\boldsymbol{V}^{-1}(\infty)}\boldsymbol{J}_n\boldsymbol{X}},\\
f_j(t) &= e^{\frac{1}{2}\boldsymbol{X}^T(\boldsymbol{P}_j)^T\frac{1}{\boldsymbol{\Sigma}+\boldsymbol{V}(\infty)}\frac{1}{(\boldsymbol{\Sigma}+\boldsymbol{V}(\infty))^{-1}+\boldsymbol{C}^{-1}(t)}\frac{1}{\boldsymbol{\Sigma}+\boldsymbol{V}(\infty)}\boldsymbol{P}_j\boldsymbol{X}}.
\end{aligned}$$

Looking closely at these expressions, it is seen that $\boldsymbol{C}(t)$ vanishes asymptotically according to the conditions (Eqs. (1.54) and (1.55)) for which the reservoir drives the system towards the stationary state $\boldsymbol{V}(\infty)$. As a result, it follows that $g(t\to\infty)\to 1$ and $f_j(t\to\infty)\to 1$ $(\forall\ j)$ irrespectively of the initial condition $\boldsymbol{V}(0)$. In this way, one recovers from Eq.(2.17) the expression (2.11) evaluated at the stationary state in the long-time limit. Importantly, the eigenvalues of $2\boldsymbol{J}_n^T\boldsymbol{H}-\boldsymbol{\Gamma}$ will be complex in general, and therefore the matrix exponential in the term $\boldsymbol{C}(t)$ will have an oscillatory contribution determined by the characteristic frequency ω_S of the isolated evolution of the system, but which is dominated by an exponentially decaying evolution in the natural time scale γ^{-1} in which evolves the open system. In whole, $g(t)$ and $f_j(t)$ must inherit this decaying oscillatory behaviour, and consequently, $\tilde{\tau}_{k,n}(\hat{\varrho}(t))$ will exhibit an exponential-decaying oscillatory evolution in time.

Then Eq.(2.17) provides us with a rough description of the entanglement evolution that one should observe in dissipative scenarios. First, entanglement may experience a transient dynamics with a generally oscillatory behaviour (of decreasing amplitude) at short times scales (in comparison with γ^{-1}), when the effects of the coherent evolution are still important compared to dissipative effects. This is consistent with the observed deaths and re-births of entanglement in the transient evolution. In addition, entanglement presents an exponentially decay at large times, that will approach asymptotically at certain constant value. This stationary entanglement will be distinct from zero depending on the characteristics of the interaction between the system modes, and the system-reservoir coupling.

Nonetheless, the above general picture does not give information about the time in which entanglement disappears or whether the stationary state becomes entangled. As outlined in the introduction of this chapter, we must focus the study on realistic dissipative scenarios in order to go deeper into these questions. We will divide the future discussion into two main parts. We devote the first part to study the transient dynamics of entanglement when the system is initially in several important examples of Gaussian and non-Gaussian states, whereas the stationary dynamics in the mentioned three-mode systems is addressed in the second part.

2.2.1 Transient Entanglement

To begin with, we analyse the consequences of losses and thermal hopping effects on the fate of entanglement at short time scales. The simplest dissipative scenario that accounts for such reservoir influence corresponds to the case when each system oscillator is in contact with an independent heat bath, whose temperature is determined by the average photon

number $N_{th}^{(i)}$ and the system-reservoir coupling strength which is roughly characterized by the dissipative rate γ_i. Notice that this is the case for many implementations of quantum information tasks [223; 222]. For a clear exposition, we shall consider that all the heat baths are at the same temperature $N_{th}^{(i)} = N_{th}$ and have the same dissipative rate $\gamma_i = \gamma$ (for $i = 1, \ldots, n$). Furthermore, we shall translate the analysis to the interaction picture as the interest is mainly in the evolution of entanglement under purely dissipative effects. In the open-system formalism based on the time-independent Fokker-Planck equation, the latter corresponds to ignore the Hamiltonian contribution, designated as $\boldsymbol{H}$, in Eq.(1.53). Hence, the evolution of the Wigner function is governed by the time-independent Fokker-Plank equation characterized by

$$\boldsymbol{\Gamma} = \frac{\gamma}{2}\boldsymbol{I}_{2n}, \tag{2.18}$$

$$\boldsymbol{D} = \frac{\gamma(1+2N_{th})}{4}\boldsymbol{I}_{2n}. \tag{2.19}$$

where $\boldsymbol{I}_{2n}$ stands for the $2n \times 2n$ identity matrix. As an immediate consequence of this choice, the state of the system will approach to the symmetrical separable thermal (Gaussian) state in the asymptotic time limit. This is consistent with the fact that the system modes evolve independently, and then, it is expected that the system reaches a separable stationary state.

With expressions (2.18) and (2.19) at hand, we can use the results of Sec.1.3.3 to obtain the time evolution of the Wigner function of the system. As it was shown, this can be roughly classified into Gaussian or non-Gaussian depending whether the initial state of the system is Gaussian or not. A continuation, we focus the attention in several important examples of both characteristic evolutions.

Gaussian Evolution

We devote special attention to the *genuine* multipartite entanglement in mixed states. Recall that the PPT criterion cannot detect such entanglement in general, in contrast to the $\tau_{k,n}$ criteria. Let us consider that the system is initially in a mixed genuine entangled state with the following covariance matrix [99],

$$\boldsymbol{V}(0) = \boldsymbol{V}_{GHZ} + g\boldsymbol{I}_{2n} \text{ with } \; g \geq 0, \tag{2.20}$$

where g plays the role of a mixing parameter, and $\boldsymbol{V}_{GHZ}$ stands for the $2n \times 2n$ covariance matrix of a continuous-variable analogue of the GHZ states,

$$\boldsymbol{V}_{GHZ} = \frac{1}{2}\begin{pmatrix} a & 0 & -c & 0 & -c & 0 & \cdots \\ 0 & b & 0 & c & 0 & c & \\ -c & 0 & a & 0 & -c & 0 & \\ 0 & c & 0 & b & 0 & c & \\ -c & 0 & -c & 0 & a & 0 & \\ 0 & c & 0 & c & 0 & b & \\ \vdots & & & & & & \ddots \end{pmatrix}, \tag{2.21}$$

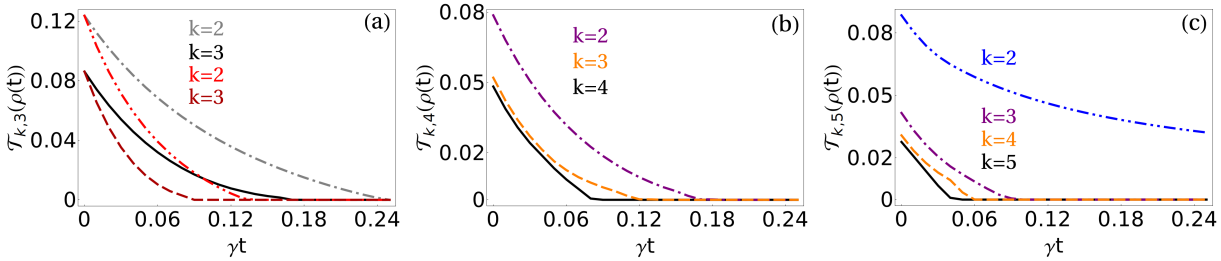

Figure 2.1: It is illustrated the entanglement characterized by the hierarchy $\mathcal{T}_{k,n}$ as a function of time, and for an initial Werner-type state given in Eq.(2.20) with $r = 0.9$ and $g = 0.1$. Figure (a) shows the time-evolution of three-mode entanglement when the reservoir has both a photon number occupation $N_{th} = 1$ (black-solid and gray-dot-dashed line) and $N_{th} = 2$ (red-dashed and red-dot-dot-dashed line). Similarly, figures (b) and (c) depict respectively the hierarchy for a four- and five- mode system coupled to a reservoir with $N_{th} = 1$.

with

$$
\begin{aligned}
a &= \frac{2}{n}\left(\frac{n-2}{2}e^{2r} + \cosh(2r)\right), \\
b &= \frac{2}{n}\left(\frac{n-2}{2}e^{-2r} + \cosh(2r)\right), \\
c &= \frac{2}{n}\sinh(2r),
\end{aligned}
$$

whereas $r \geq 0$ is a squeezing parameter. Notice that a and b are always positive since $n \geq 2$. This state has attracted special attention on quantum communication. Importantly, it was shown in Ref.[A1] that the genuine entanglement in these states degrades with increasing mixing g.

Figure 2.1 illustrates the decay of entanglement in systems composed by three, four, and five modes. The dissipation degrades in a similar way the different degrees of entanglement: k-partite entanglement vanishes after a finite period of time roughly determined by γ. However, we appreciate that the initial genuine entanglement of the state gets more fragile when increasing the number of modes of the system (see the black-solid line in figures (2.1) (a), (b) and (c)). This is consistent with known results for analogous GHZ states in discrete systems, where they exhibit an exponential decay with the number of constituents [23] (e.g. GHZ becomes separable when one of the constituents is lost). On the contrary, the state becomes wealthy in bi-partite multimode entanglement (e.g. see the lines with $k = 2$). This feature is related to the fact that the number of (small) entangled partitions that turn into such entanglement may be substantially large with increasing number of constituents. This could ultimately make this class of entanglement more resilient to dissipative effects compared with genuine entanglement. On the other hand, from figure 2.1 (a) follows that temperature effects (*i.e.*, thermal noise) characterized by the parameter

N_{th} boost the decay of entanglement as one could expect since it induces additional mixing.

Non-Gaussian Evolution

We now investigate in parallel the inseparability properties of two important instances of non-Gaussian states influenced by the losses and thermal hopping effects. For the seek of simplicity, let us focus on two-mode systems. First, we consider that the latter is initially in the previously mentioned coherent photon-subtracted two single-mode squeezed vacuum states (CPS-TSVS). These states derive from the locally squeezed two-mode vacuum state by applying the operator $(\alpha\hat{a}_1 + \beta\hat{a}_2)^u$, where $\hat{a}_l$ $(l = 1, 2)$ is the photon-annihilation operator of the lth mode and $|\alpha|^2 + |\beta|^2 = 1$ [114]. For simplicity, we shall consider the states obtained for $u = 1$ and symmetrically squeezed in both modes. The covariance matrix $\boldsymbol{V}$ and the polynomial function F that define the Wigner function via Eq.(1.3) take the form, $\boldsymbol{V}(0) = \frac{1}{2}\mathrm{diag}(e^{-2r}, e^{2r}, e^{-2r}, e^{2r})$, and

$$\begin{aligned} F(\boldsymbol{x},0) &= 2\cosh^2(r)\Big((x_1^2+p_1^2)|\alpha|^2 + (x_2^2+p_2^2)|\beta|^2 + 2\mathrm{Re}((x_1-ip_1)(x_2+ip_2)\alpha^*\beta)\Big) \\ &+ 2\sinh^2(r)\Big((x_1^2+p_1^2)|\alpha|^2 + (x_2^2+p_2^2)|\beta|^2 + 2\mathrm{Re}((x_1+ip_1)(x_2-ip_2)\alpha^*\beta)\Big) \\ &- 4\cosh(r)\sinh(r)\Big(|\alpha p_1 + \beta p_2|^2 - |\alpha x_1 + \beta x_2|^2\Big) - 1. \end{aligned} \tag{2.22}$$

Notice that these states only have entanglement in the non-Gaussian degrees of freedom (*i.e.* in $F(\boldsymbol{x})$) since the covariance matrix is completely separable. In some sense, these states only contain non-Gaussian entanglement.

Furthermore, we shall also consider that the system starts from the the so-called photon-added two-mode (globally) squeezed states, whose entanglement properties have been recently studied for the pure [175] and mixed [131; 262] cases. They are obtained by operating with $(a_1^\dagger)^u(a_2^\dagger)^v$ over the two-mode symmetrically squeezed state. We shall treat the states with $u = 1$ and $v = 0$, which coincide with the two-variable Hermite polynomial states [259]. According to the definition (1.3), these states are determined by the following covariance matrix,

$$\boldsymbol{V}(0) = \frac{(1+2N_0)}{2}\begin{pmatrix} \cosh(2r) & 0 & \sinh(2r) & 0 \\ 0 & \cosh(2r) & 0 & -\sinh(2r) \\ \sinh(2r) & 0 & \cosh(2r) & 0 \\ 0 & -\sinh(2r) & 0 & \cosh(2r) \end{pmatrix}, \tag{2.23}$$

and the polynomial function,

$$\begin{aligned} F(\boldsymbol{x},0) &= \Big((p_2 + 2N_0p_2 + p_2\cosh(2r) + p_1\sinh(2r))^2 \\ &+ (x_2 + 2N_0x_2 + x_2\cosh(2r) - x_1\sinh(2r))^2 \\ &- 2(1+2N_0)(N_0 + \cosh(r)^2)\Big) \Big/ \Big(2(1+2N_0)^2(\cosh^2(r) + N_0\cosh(2r)\Big) \end{aligned} \tag{2.24}$$

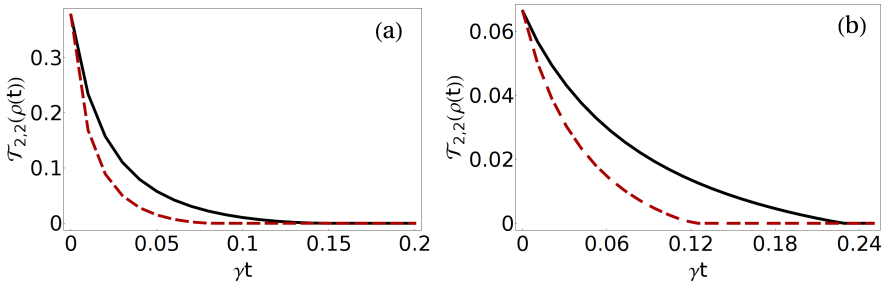

Figure 2.2: Figure (a): $\mathcal{T}_{2,2}(\hat{\rho}(t))$ as a function of time when the system is initially in the CPS-TSVS state with $|\alpha| = 0.5$ and $r = 0$. Figure (b): Similarly, $\mathcal{T}_{2,2}(\hat{\rho}(t))$ as a function of time when the system is initially in a SPS-TVS state with $r = 2$ (and $N_0 = 0$). In both figures the black-solid and red-dashed lines correspond to the cases when the reservoirs have an average photon number $N_{th} = 2$ and $N_{th} = 4$, respectively.

Here, N_0 and r play the role of mixing and squeezing parameters, respectively. For the particular value $N_0 = 0$, these states coincide with the single photon-subtracted two-mode vacuum squeezed (SPS-TVS) states studied in Ref.[13]. It is important to realize that the SPS-TVS states given by Eqs. (2.23) and (2.24) contain entanglement in the Gaussian degrees of freedom, contrary to the above mentioned CPS-TSVS states.

According to the results of Sec.1.3.3 (see Eq.(1.60)), one finds that the covariance matrix evolves as follows,

$$\boldsymbol{V}(t) = \boldsymbol{\varepsilon}(t) + \boldsymbol{\sigma}(t), \tag{2.25}$$

with

$$\begin{aligned} \boldsymbol{\varepsilon}(t) &= \frac{e^{-\gamma t}}{2}\boldsymbol{V}(0), \\ \boldsymbol{\sigma}(t) &= (1-e^{-\gamma t})\frac{1+2N_{th}}{2}\left(\boldsymbol{I}\oplus\boldsymbol{I}\right), \end{aligned}$$

and the polynomial part $F(\boldsymbol{x},t)$ is given by

$$\begin{aligned} F(\boldsymbol{x},t) &= F\left(e^{\frac{\gamma}{2}t}(\boldsymbol{\varepsilon}^{-1}(t)\boldsymbol{\sigma}(t)+\boldsymbol{I}_2)^{-1}\boldsymbol{x},0\right) \\ &+ \frac{1}{2}\sum_{l,m}\left(\boldsymbol{\varepsilon}^{-1}(t)+\boldsymbol{\sigma}^{-1}(t)\right)^{-1}_{lm}\left.\frac{\partial^2 F(e^{\frac{\gamma}{2}t}\boldsymbol{x},0)}{\partial\left[\boldsymbol{x}\right]_l\partial\left[\boldsymbol{x}\right]_m}\right|_{\boldsymbol{x}=\vec{0}}, \end{aligned} \tag{2.26}$$

For $t = 0$, Eq.(2.26) returns the initial expression (either Eq.(2.22) or Eq.(2.24)) for the previous states ($F(\boldsymbol{x}, t \to 0) \to F(\boldsymbol{x}, 0)$), whereas in the long time ($F(\boldsymbol{x}, t \to \infty) \to 1$) the system evolves asymptotically into the symmetrical separable thermal (Gaussian) state.

Figure (2.2) (a) and (b) show the time evolution of $\mathcal{T}_{2,2}$ when the system is initially in a CPS-TSVS and SPS-TVS state, respectively. A first sight, one may appreciate that the evolution of entanglement is different in both situations. Interestingly, the pure non-Gaussian entanglement of the CPS-TSVS states is degraded *asymptotically* in time, *i.e.* it

suffers an exponential decay, while the two-mode entanglement in the initial SPS-TVS state clearly vanishes at a finite time scale, similarly to the foregoing Gaussian example. In both situations, the decay of entanglement is faster for increasing values of the initial reservoir temperature as a consequence of the increase of thermal noise. Though not showed here, we find a similar behaviour for other choice of parameters for the states $\{|\alpha|, N_0, r\}$ and the reservoirs $\{\gamma, N_{th}\}$.

Remarkable enough, the direct comparison between the previous states suggests that the purely non-Gaussian entanglement encoded in $F(\boldsymbol{x}, t)$ is more robust against the losses and dissipative effects than the entanglement encapsulated in the covariance matrix $\boldsymbol{V}(t)$. Looking at Eqs. (2.25) and (2.26), this observation must be related to the fact that the covariance matrix approaches exponentially to its stationary expression while the polynomial part exhibits a more complicated decay (to the unity). Unfortunately, we cannot extract further information from these equations, together with the expression (2.17), which could shed light on this issue. This is a basic consequence of the fact that separability criteria generally exhibit a non-linear dependence on $\hat{\varrho}$, which substantially complicates the static and dynamic analysis of entanglement.

In summary, we have observed that multipartite entanglement under purely dissipative effects tend irreversibly to disappear in a finite time (compared with the dissipative rates of the reservoirs) for Gaussian states, or asymptotically for certain classes of non-Gaussian entangled states. A priori, the latter result may be of particular interest for implementing quantum communication protocols. A reliable conclusion on this aspect deserves further investigation beyond the scope of the present dissertation.

To conclude this section, we would like to remark that these previous examples also illustrate that Eq.(2.7) may provide a meaningful description of multipartite CV entanglement in realistic dissipative scenarios. As the hierarchy (2.7) deals with Gaussian and non-Gaussian states at the same footing, it is of particular interest to study the time evolution of k-partite entanglement when the state evolves from Gaussian to non-Gaussian, or vice-versa.

2.2.2 Stationary three-mode Gaussian entanglement

In this section we present results on stationary entanglement supported by a three-mode system in contact with a common or independent environments. The main results of this investigation have been published in the Refs. **[A2]** and **[A3]**. In what follows, it can be found a summary of the main conceptual developments and findings.

Recall that the stationary state of the system will be Gaussian thanks to the linearity of the system-plus-reservoir Heisenberg equations. As we extensively illustrated in Sec.1.3.2 how to obtain its covariance matrix from solving the generalized Langevin equation (see Eq.(1.52)), we will go directly to the discussion of the results. As estimators of entanglement we shall use the logarithmic negativity (see Eq.(1.22)) to measure two-mode entanglement, and the qualitative classification of tripartite entanglement proposed by Giedke, Kraus, Lewenstein and Cirac (see classification (**C1**-**C5**)), both tools were introduced in Sec.1.2.

Common environment

At first glance the generalized Langevin equation (1.38) reveals that the system oscillators in contact with a common environment will experience an effective interaction mediated by the renormalization matrix $\tilde{\Omega}$ (given in Eq.(1.39)), which shall refer to as the renormalization potential, and the susceptibility matrix $\chi(t)$. Interestingly, it will be seen how this environment-mediated interaction is responsible for the generation of stationary entanglement between system oscillators which do not experience any direct coupling, *i.e.* $U_{\lambda\mu} = m_\lambda \omega_\lambda^2 \delta_{\lambda\mu}$. At this respect, previous works (e.g. see Refs.[226; 139]) have pointed out that such appearance of entanglement may be due to the Hamiltonian of the system of interest possesses normal modes which do not suffer from the dissipative dynamics, instead they follow free coherence evolutions. In this way, a great part of the entanglement contained in the initial state of the system can be isolated from dissipative effects by conveniently encoding it in such degrees of freedom. This is precisely the idea behind the methods aiming to protect entanglement based on free-decoherence subspaces. In our study, a rapid analysis of the normal modes shows that all of them will be subjected to dissipation and noise unless all oscillators have the same frequency and are located at the same place[ii]. In the future discussion we are mostly interested in arbitrary arrangements of the system oscillator, in which the λth mode is well localized around at an equilibrium position $\boldsymbol{r}_\lambda^0$, so that the created entanglement will be indeed induced by the system-reservoir interaction that turns into dissipative quantum effects.

As a consequence, the coupling strength with the reservoir should be strong enough in order to observe the generation of entanglement, what entails to drive the system into the strong dissipative regimen. This circumstance, combined with low temperatures, yields that the evolution of the system of interest will be dominated by non-Markovian effects. As a matter of fact, if the system would follow a Markovian evolution we should expect that each system oscillator would eventually reach its own thermal equilibrium state and thus the stationary state would be separable (recalling the oscillators are uncoupled). Then it is important to realize that the *non-Markovian character* of the open-system dynamics is crucial for the appearance of entanglement in the dissipative system. As we saw in Sec.1.3.2, the characteristics of a non-Markovian evolution is determined by the explicit form of the reservoir spectral density given in Eq.(1.45), which contains the reservoir spectrum $\omega_{\boldsymbol{k}}$ and system-reservoir interaction parameters written as $g_{\boldsymbol{k}}$. In what follows, we make reasonable approximations over these magnitudes which provide reliable phenomenological expressions for the spectral density. This will be the starting point of the subsequent study.

Let us denote each mode by $\mathcal{A}$, $\mathcal{B}$, and $\mathcal{C}$. Let also focus on the cases of one-dimensional (1D) and three-dimensional (3D) environments. We shall assume for the environmental

[ii]The position-operator vector of the normal modes is found to be governed by a transformed generalized Langevin equation in which now the potential term and memory kernel are given respectively by the transformed matrix of $\tilde{\Omega} + U$ and $\chi(t)$. Formally, the aforementioned physical situation will correspond to the case in which all the entries of both matrices ($\tilde{\Omega} + U$ and $\chi(t)$) separately become identical. By arguments from linear algebra concerned with the diagonalization of matrices, one may see that this permits the possibility that the dissipative and fluctuation terms may become identically to zero in the transformed GLE.

field the linear dispersion $\omega_{\boldsymbol{k}} = c|\boldsymbol{k}|$, which comprises the physical cases of acoustic phonons in a solid-state substrate and a free electromagnetic field. Furthermore, we consider an isotropic coupling between the oscillators and the environment, which is given by

$$g_{\boldsymbol{k}}^2 = m\hbar\gamma(\omega_{\boldsymbol{k}}/\omega_c^{d-1})c^d V_{\boldsymbol{k}}(d)e^{-\omega/\omega_c},$$

where d is the dimension of the environment, $V_{\boldsymbol{k}}$ is the number of field modes per d-dimensional $\boldsymbol{k}$-space volume, γ roughly determines the coupling strength with the environment, and ω_c is a cut-off frequency for the environmental spectrum. Replacing $g_{\boldsymbol{k}}$ and $\omega_{\boldsymbol{k}}$ in the expression for the reservoir spectral density and taking the quasi-continuum limit $V_{\boldsymbol{k}} \to 0$, one obtains

$$J_{\lambda,\mu}^{1D}(\omega) = \pi m\gamma\omega e^{-\omega/\omega_c}\cos(\omega|\Delta\boldsymbol{r}_{\lambda\mu}^0|/c), \tag{2.27}$$

$$J_{\lambda,\mu}^{3D}(\omega) = \frac{4\pi^2 mc}{|\Delta\boldsymbol{r}_{\lambda\mu}^0|}\Big(\frac{\omega}{\omega_c}\Big)^2 e^{-\omega/\omega_c}\sin(\omega|\Delta\boldsymbol{r}_{\lambda\mu}^0|/c). \tag{2.28}$$

Accordingly to Eq.(1.39), the renormalization potentials become

$$\tilde{\Omega}_{\lambda\mu}^{1D} = \frac{m\gamma\omega_c}{1+(\omega_c|\Delta\boldsymbol{r}_{\lambda\mu}^0|/c)^2}, \tag{2.29}$$

$$\tilde{\Omega}_{\lambda\mu}^{3D} = \frac{8m\pi\gamma\omega_c}{[1+(\omega_c|\Delta\boldsymbol{r}_{\lambda\mu}^0|/c)^2]^2}. \tag{2.30}$$

Additionally, the susceptibility may be deduced from expressions (1.41) and (1.44), and the knowledge of the reservoir spectral density, to give

$$\chi_{\lambda\mu}^{1D}(t) = 4m\,\gamma\,\hbar\,\omega_c^2\Theta\left(t-|\Delta\boldsymbol{r}_{\lambda\mu}^0|/c\right)\frac{\omega_c|\Delta\boldsymbol{r}_{\lambda\mu}^0|/c-t\omega_c}{[1+(\omega_c|\Delta\boldsymbol{r}_{\lambda\mu}^0|/c-t\omega_c)^2]^2}, \tag{2.31}$$

$$\chi_{\lambda\mu}^{3D}(t) = 8\pi m\,\gamma\,\hbar\,\frac{\omega_c c}{|\Delta\boldsymbol{r}_{\lambda\mu}^0|}\Theta(t-|\Delta\boldsymbol{r}_{\lambda\mu}^0|/c) \times\left(\frac{1-3(\omega_c|\Delta\boldsymbol{r}_{\lambda\mu}^0|/c+t\omega_c)^2}{[1+(\omega_c|\Delta\boldsymbol{r}_{\lambda\mu}^0|/c+t\omega_c)^2]^3}-\frac{1-3(\omega_c|\Delta\boldsymbol{r}_{\lambda\mu}^0|/c-t\omega_c)^2}{[1+(\omega_c|\Delta\boldsymbol{r}_{\lambda\mu}^0|/c-t\omega_c)^2]^3}\right). \tag{2.32}$$

The aforementioned non-Markovian character of the quantum evolution is reflected in the non-exponential time decay followed by the susceptibilities (memory kernels). The dimensionless parameter $|\Delta\boldsymbol{r}_{\lambda\mu}^0|\omega_c/c$, appearing in the above equations, compares two different time scales, on one hand $|\Delta\boldsymbol{r}_{\lambda\mu}^0|/c$, that is the time of flight of a phonon or photon between two oscillators, and on the other hand ω_c^{-1} which roughly represents the time scale during which memory effects disappears. Surprisingly, the spatial algebraic decay of the environment-mediated interaction, inherent in the susceptibilities and in the renormalization potential, indicates that an effective coupling between oscillators that are far apart may be established. Notice that such decay goes at least as $\sim(|\Delta\boldsymbol{r}_{\lambda\mu}^0|\omega_c/c)^3$ and $\sim(|\Delta\boldsymbol{r}_{\lambda\mu}^0|\omega_c/c)^8$ for the 1D and 3D environment, respectively.

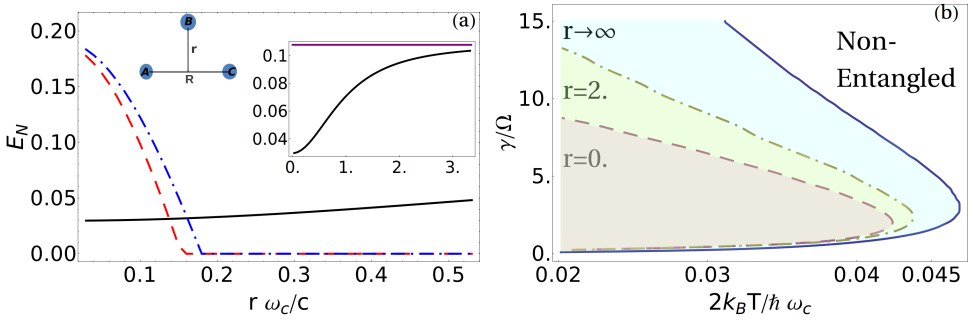

Figure 2.3: (a) Stationary two-mode entanglement measured by the logarithmic negativities $E_N(\boldsymbol{V}_{\mathcal{AC}})$ (black solid line), $E_N(\boldsymbol{V}_{\mathcal{AB}})$ (red dashed line), and $E_N(\boldsymbol{V}_{\mathcal{BC}})$ (blue dash-dotted line) for the triangular geometry as function of the displacement r. The inset provides an extended picture of $E_N(\boldsymbol{V}_{\mathcal{AC}})$, where the purple flat line marks the value in the absence of oscillator $\mathcal{B}$. (b) Phase diagram for fixed R and various values of r as function of coupling strength γ and temperature T. In the shaded areas, the oscillators $\mathcal{A}$ and $\mathcal{B}$ exhibit stationary entanglement. The outer blue line marks the limit $r \to \infty$, which is equivalent to the absence of oscillator $\mathcal{B}$. As oscillator $\mathcal{B}$ comes closer, the area with entanglement shrinks.

Although this environmental-mediated interaction possesses a long-range feature, it is found that the characteristic length of the entanglement correlation is roughly determined by $R_0 = c/\omega_c$, in agreement with a central result of Ref. [261]. The induced two-mode and bipartite three-mode entanglement vanish at a finite distance R_0 which mainly depends on temperature, being almost independent of the dissipation strength γ. However a larger γ supports the effective interaction required for entanglement creation, but also increases decoherence which acts towards separability. Nevertheless, as expected, entanglement eventually disappears with increasing γ. Furthermore, we observe that two-mode entanglement decays faster for the 3D environment than the 1D case when the spatial separation between oscillators increases. This is in agreement with the fact that the susceptibility $\chi^{3D}(t)$ decreases with the distance much faster than $\chi^{1D}(t)$. A simple analytical estimation of R_0 when all the correlation interaction is only through the renormalization potential reveals that this is larger than the value followed from the numerical data. Though the renormalization potential is still relevant for the transient evolution of entanglement, this observation suggests that in the long-time limit the mechanism behind the generation of entanglement mainly relies on memory effects (Eqs. (2.31) and (2.32)) rather than on the renormalization term (Eqs. (2.29) and (2.30)). We may infer from the latter that the environment-induced interaction represents a kind of feedback between oscillators which is predominantly coherent when only low energy environmental modes are thermally excited, i.e., for $k_BT \ll \hbar\omega_c$.

Remarkable enough, we found that the two-mode entanglement between any pair of modes ($\mathcal{AB}$, $\mathcal{AC}$, or $\mathcal{BC}$) is negatively affected by the presence of the remaining oscillator,

which shall refer to as "passive" oscillator. To see this more clearly, we focus on a triangular arrangement of the oscillators in contact with a 3D environment: the oscillators $\mathcal{A}$ and $\mathcal{C}$ are placed at distance $\Delta \boldsymbol{r}^0_{\mathcal{AC}} = R$, but the passive oscillator $\mathcal{B}$ is shifted by a distance r perpendicular to the line connecting $\mathcal{A}$ and $\mathcal{C}$. The black-solid line in figure (2.3) (a) represents the two-mode entanglement between $\mathcal{AC}$ oscillators measured by the logarithmic negativity as a function of the distance r. As one may appreciate, $E_N(\boldsymbol{V}_{\mathcal{AC}})$ is eventually destroyed when $\mathcal{B}$ is close enough to the pair ($r \to 0$), whereas in the opposite limit ($r \to \infty$), $E_N(\boldsymbol{V}_{\mathcal{AC}})$ approaches the value of two-mode entanglement when the oscillator pair $\mathcal{AC}$ evolves independent of $\mathcal{B}$. Indeed, figure (2.3) (b) clearly illustrates that the parameter space of entangled states shrinks significantly by the presence of the passive oscillator. Furthermore, this shows that the oscillators effectively interact even at distances greater than the correlation length of two-mode entanglement, which entails that the environment-induced interaction has a long range in space in agreement with Eqs. from (2.29) to (2.32).

Furthermore, figure (2.3) (a) shows that the oscillator $\mathcal{B}$ becomes entangled with $\mathcal{A}$ and $\mathcal{C}$ almost simultaneously at small distance, in agreement with the foregoing discussion. That is, $E_N(\boldsymbol{V}_{\mathcal{AB}})$ and $E_N(\boldsymbol{V}_{\mathcal{BC}})$ increase while $E_N(\boldsymbol{V}_{\mathcal{AC}})$ becomes smaller. Then it is seems that there is a trade-off between $E_N(\boldsymbol{V}_{\mathcal{AC}})$, $E_N(\boldsymbol{V}_{\mathcal{AB}})$, and $E_N(\boldsymbol{V}_{\mathcal{BC}})$ what resemblances the monogamy property of entanglement[iii]. Nonetheless, the competition between these three two-mode entanglements is characteristic for our environment-induced entanglement mechanism, mainly because the logarithmic negativity (i) is a bona fide measure that generally does not satisfy monogamy and (ii) becomes increasingly manifested by raising the coupling strength γ.

One must expect that this tendency towards separability might be enhanced by adding further oscillators. However, even though $E_N(\boldsymbol{V}_{\mathcal{AC}})$ may be reduced or vanish in the presence of oscillator $\mathcal{B}$, we find that there is still the possibility of an emerging tripartite entangled state analogous to a GHZ-like state. This emergence of tripartite entanglement on the expense of smaller two-mode entanglement may be interpreted as consequence of an effective three-body interaction whereby all three oscillators effectively interact simultaneously via the same bath. Further investigation on the tripartite entanglement reveals that certain geometries of the oscillators favour the resilience of the bipartite three-mode entanglement (classes **(C1)**-**(C3)**) to increasing values of the initial environmental temperature. For instance, it is seen that for identical oscillators fully inseparable states are more robust when they are equally spaced forming a triangle. This feature relies essentially on the fact that the oscillators with smaller frequencies will be more affected by thermal noise, such that one may conveniently arrange the oscillator to increase the environment-mediated interaction with the rest to counteract this effect.

In conclusion, our findings underline that non-Markovian effects are relevant for a deeper understanding of the appearance of stationary multipartite entanglement in a common environment. It will be seen that this is in contrast to the behavior of subsystems coupled to independent heat baths, for which thermal relaxation dominates. An interesting

[iii] Recall that, in some sense the property monogamy of entanglement says that if two modes have a considerable amount of entanglement, they will share substantially less entanglement with a third mode.

consequence of our results in the realm of quantum information may be found in setups for quantum communication and teleportation. Considering the model studied as a simplified quantum network, our result for two-mode entanglement in the presence of a passive oscillator implies the need for sufficient microscopic control of the reservoir influence and interaction between all constituents.

Independent environments

Now we turn the attention to the scheme of independent environments[iv]. In this case, the dissipative system consists on an one-dimensional open chain composed by three harmonic oscillator designated as $\mathcal{L}$ (left), $\mathcal{C}$ (center), and $\mathcal{R}$ (right). Each of them is in contact with an independent reservoir at an initial temperature given by T_i (with $i \in \mathcal{L}, \mathcal{C}, \mathcal{R}$). Contrary to the foregoing scheme, they are coupled through a nearest-neighbour interaction which is contained in the potential,

$$U = \frac{1}{2}\begin{pmatrix} k + m\omega_{\mathcal{L}}^2 & -k & 0 \\ -k & 2k + m\omega_{\mathcal{C}}^2 & -k \\ 0 & -k & k + m\omega_{\mathcal{R}}^2 \end{pmatrix},$$

where k play the role of a springlike coupling strength. To analyse the open-system dynamics we shall consider Ohmic spectral densities with Lorentz-Drude high frequency cutoff

$$J_i(\omega) = \frac{m\gamma_i\omega}{1 + \omega^2/\omega_c^2},$$

where γ_i stands for the dissipation rate of the ith heat bath (which carries the order of magnitude of the system-bath interaction) and ω_c is the cutoff frequency. For seek of simplicity, we consider each oscillator equally coupled to its reservoir (*i.e.*, $\gamma_i = \gamma$ for $i \in \mathcal{L}, \mathcal{C}, \mathcal{R}$). As a consequence of the chosen spectral density, the matrix renormalization term takes the form $\tilde{\Omega}_{ij} = \delta_{ij}\gamma\omega_c/2$, whereas the susceptibility is given by,

$$\chi_{ij}(t) = \Theta(t)\delta_{ij}m\hbar\gamma\omega_c^2 e^{-\omega_c t}.$$

The fact that the non-diagonal elements of the susceptibility matrix and renormalization term are zero reflects the fact that each oscillator is interacting with an independent environment. Unlike the previous example, here all the interaction is through a springlike coupling between $\mathcal{L} \leftrightarrow \mathcal{C}$ and $\mathcal{C} \leftrightarrow \mathcal{R}$. Let denote by Ω a characteristic frequency of oscillators in the chain.

We find that for initial thermal equilibrium conditions, that is $T_i = T$ for $i \in \mathcal{L}, \mathcal{C}, \mathcal{R}$, the system eventually reaches a Gibbs state with the temperature T. To be more precise, the stationary state approaches to the Gibbs state in the limit of weak dissipative rate, which is in agreement with the result found for the damped harmonic oscillator in Refs. [107] and [116]. This state is wealthy in fully inseparable entanglement (class **(C1)**

[iv] The microscopic model of independent environments consists essentially in coupling each oscillator to a large set of non-intercating harmonic oscillators as occurs in the Caldeira-Leggett model.

entanglement) for high coupling strengths (e.g. $k/m\Omega^2 \sim 0.1$) and comparatively low temperatures (e.g. $k_BT/\hbar\Omega \approx 0.4$). However, such inseparability is damaged for increasing dissipative rates, so that larger values of the coupling strength k are required to establish stationary fully inseparable entanglement. Interestingly enough, we find that the chain ground state undergoes a structural transition between different schemes of entanglement: its inseparability properties are downgrading to a lower class of entanglement (within the classification (**C1**-**C5**)) as the dissipation grows stronger.

In the strong dissipative regime, the stationary entanglement between the bipartition $\mathcal{C}|(\mathcal{LR})$ exhibits more resilience to noise than in either $\mathcal{L}|(\mathcal{CR})$ or $\mathcal{R}|(\mathcal{LC})$, which relies on the fact that the mode $\mathcal{C}$ is in direct interaction with the remaining two. Although all the bipartite entanglement finally disappears for relatively high temperatures $k_BT/\hbar\omega_i \sim 0.5$, it is seen that a stationary fully inseparable state is recovered by increasing the strength of the springlike coupling, what seems reasonable. Moreover, we study the influence of the oscillator frequencies on the fate of entanglement. Doing so, we consider several arrangements of the frequencies, e.g. $\omega_{\mathcal{L},\mathcal{R}} = \Omega$, and $\omega_{\mathcal{C}} = \Omega + \delta$. As before, the dependence of the quantum correlations on the oscillator frequencies, at a constant temperature, it is seen on the fact that the dynamics of the modes becomes more insensitive to thermal noise for higher frequency values. For instance, fully inseparable entanglement is favoured by increasing values of δ, however very large values of the central frequency may cause an effective decoupling of the central mode from the rest as $k/m\omega_{\mathcal{C}}$ becomes smaller. In general, a compromise between shielding the system from thermal noise and keeping the effective interaction between chain modes provides a rich variety of stationary entanglement (classes **(C1)**-**(C4)**).

Finally, we analyse the inseparability properties when a stationary energy transport flows from the left ($\mathcal{L}$) to the right ($\mathcal{R}$) heat bath, induced by a temperature gradient ΔT. This corresponds with the initial configuration $T_{\mathcal{L}} = T + \Delta T$, $T_{\mathcal{C}} = T$, and $T_{\mathcal{R}} = T - \Delta T$. Interestingly, the temperature gradient proves detrimental to the buildup of stationary bipartite three-mode entanglement (classes **(C1)**-**(C3)**). This occurs due to the intensification of thermal noise at the hot end of the chain rather than as a consequence of the stationary energy currents established across the system. This observation mainly relies on the fact that the magnitude of the stationary energy current remains comparable when a rich dynamics of bipartite entanglement appears (by conveniently manipulating the frequency of chain oscillators). Nonetheless, the question about the role of quantum correlations in the energy current deserves more attention. The next section is devoted to this question.

Stationary entanglement and energy current

Before proceeding any further it should be mentioned that the details of the forthcoming discussion can be found in Ref.[**A4**].

Given the increasing interest in quantum systems subjected to thermal non-equilibrium conditions at the quantum level, one might naturally rises the question whether and in which way the stationary response of the system to a temperature gradient may be influ-

enced by the presence of (genuine) multipartite entanglement. Here, we pursue to elucidate whether the average and fluctuations of the stationary energy current across a harmonic chain are sensitive to the appearance of two-mode and *genuine* tripartite entanglement in the system. In the realm of quantum networks composed by spin systems, there have been important progresses which indicate, on one hand, that the presence of bipartite entanglement does not play an important role on the excitation transport [199], and on the other hand, they show a strong correlation between quantum coherence and transport efficiency [255]. We center the analysis in the same setup as before, but now the initial configuration of temperatures is given as follows $T_{\mathcal{L}} = T + \delta T$, $T_{\mathcal{C}} = T + \Delta T$, and $T_{\mathcal{R}} = T - \delta T$. Notice that there are now two temperatures gradients: δT establishes a stationary energy transport along the chain, whereas ΔT permits us to induce a rich variety of quantum correlations between chain oscillators.

Let us denote by $\hat{j}_{ij}$ the energy current from the jth oscillator to the ith oscillator. Looking at the Hamiltonian of the chain, one obtains the following expressions for the energy currents between oscillators,

$$\hat{j}_{\mathcal{RC}}(t) = \frac{k}{4m}\Big(\{\hat{x}_{\mathcal{C}}(t), \hat{p}_{\mathcal{C}}(t)\} - \{\hat{x}_{\mathcal{R}}(t), \hat{p}_{\mathcal{R}}(t)\} + \underbrace{(\{\hat{x}_{\mathcal{C}}(t), \hat{p}_{\mathcal{R}}(t)\} - \{\hat{x}_{\mathcal{R}}(t), \hat{p}_{\mathcal{C}}(t)\})}_{\text{Correlation Terms}} \Big), \tag{2.33}$$

$$\hat{j}_{\mathcal{CL}}(t) = \frac{k}{4m}\Big(\{\hat{x}_{\mathcal{L}}(t), \hat{p}_{\mathcal{L}}(t)\} - \{\hat{x}_{\mathcal{C}}(t), \hat{p}_{\mathcal{C}}(t)\} + \underbrace{(\{\hat{x}_{\mathcal{L}}(t), \hat{p}_{\mathcal{C}}(t)\} - \{\hat{x}_{\mathcal{C}}(t), \hat{p}_{\mathcal{L}}(t)\})}_{\text{Correlation Terms}} \Big), \tag{2.34}$$

whereas the total energy current through the chain is given by

$$\hat{J}(t) = \hat{j}_{\mathcal{RC}}(t) + \hat{j}_{\mathcal{CL}}(t). \tag{2.35}$$

From here it is immediate to obtain the average of the energy currents, e.g.

$$\left\langle \hat{j}_{ij} \right\rangle = \frac{k}{2m}\left(C_{x_j p_j}(t,t) - C_{x_i p_i}(t,t) + (C_{x_j p_i}(t,t) - C_{x_i p_j}(t,t)) \right), \tag{2.36}$$

where the two-time correlations functions, e.g. $C_{x_i p_j}(t,t)$, are obtained from Eq.(1.52) which was illustrated in Sec.1.3.2. Analogously, the fluctuations of the energy current can be expressed from the current-current correlation function,

$$K_{j_{ij} j_{lm}}(t+\tau, t) = \frac{1}{2}\left\langle \left\{ \hat{j}_{ij}(t+\tau), \hat{j}_{lm}(t) \right\} \right\rangle - \left\langle \hat{j}_{ij}(t+\tau) \right\rangle \left\langle \hat{j}_{lm}(t) \right\rangle. \tag{2.37}$$

Interestingly, from the linear response theory it is known that Eq.(2.37) may characterize the response of the (energy or electric) transport to an external weak field [203]. Hence, we could expect that it may gauge a change in the average properties of the energy current due to the appearance of entanglement. Thanks to the Gaussian statistics of the stationary state, it is easy to show that the current-current correlation functions will be also given in

terms of the above mentioned two-time correlations functions defined in Eq.(1.52). It is important for the forthcoming discussion to realize that the average energy current depends linearly in such correlation functions, while the current-current correlation exhibits a non-linear dependence. Finally let us mention that we have performed the subsequent study for Ohmic and super-Ohmic dissipations, which are characterized by the spectral densities $J^{(Oh)}(\omega) = \pi m\gamma\omega/2e^{-\omega/\omega_c}$, and $J^{(SOh)}(\omega) = \pi m\gamma\omega^2/2\omega_c e^{-\omega/\omega_c}$, respectively. Here, it should be pointed out that, as a consequence of this choice, the non-Makovian effects will be more pronounced in the latter than in the former. Further, notice that $K_{j_{ij}j_{lm}}(t+\tau,t)$ will return the same value for an arbitrary choice of the initial time t since the system is in a stationary state.

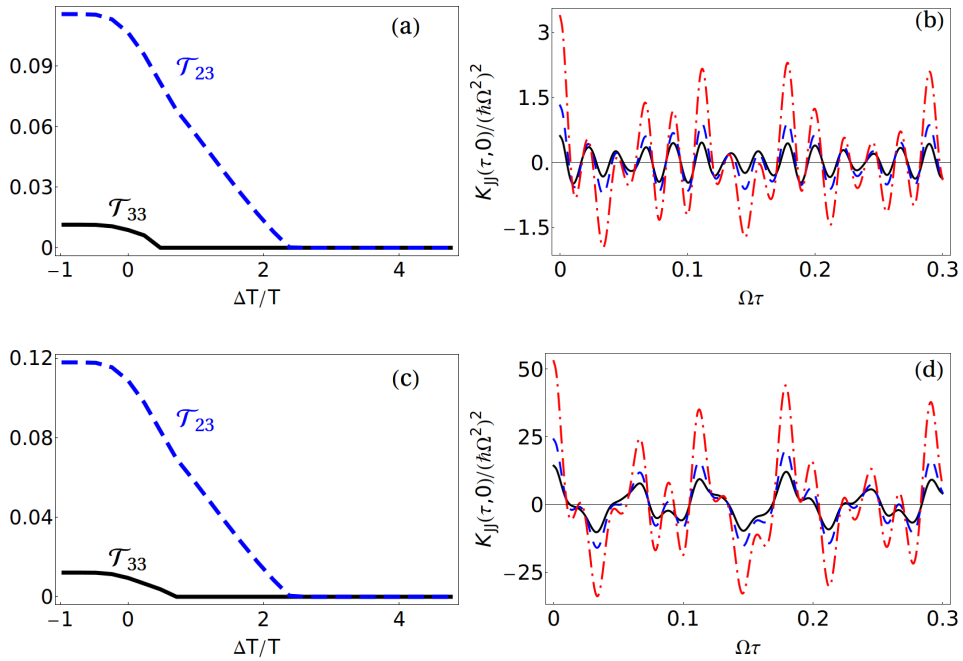

Figure 2.4: Figures (a) and (c) show the criterion $\mathcal{T}_{k,3}$ as a function of the temperature gradient for the Ohmic and super-Ohmic dissipation, respectively. Analogously, figures (b) and (d) illustrate the current-current correlation of the energy current across the chain as a function of time for Ohmic and super-Ohmic dissipation, and for different values of the temperature gradient ΔT: the solid-black line depicts $K_{JJ}(\tau,0)$ when the system is genuine entangled ($\Delta T/T = -0.95$), and similarly, the blue-dashed line illustrates $K_{JJ}(\tau,0)$ when the system is bipartite three-mode entangled ($\Delta T/T = 1.9$). The red-dot-dashed line corresponds to the case when the system is likely separable in all the three-mode bipartitions ($\Delta T/T = 4.3$).

The expressions for the energy current exhibit an explicit dependence on the correlations between position and momentum operators of chain oscillators (see Eqs. (2.33) and (2.34)). As the quantum correlations shared by the system modes are partially encoded on those

correlations, one might expect that the energy current would also display a counterpart feature. If this were the case, one could expect that the energy current would experience an observable change in its average properties, determined by Eqs. (2.33)-(2.37), when entanglement is present in the chain. Hence, the performed investigation has essentially consisted on an extensive numerical analysis of the average properties of the energy current when a rich variety of entanglement emerges by conveniently manipulating ΔT. Let just illustrate here the results for the current-current correlations (or equivalently, fluctuations) of the energy current across the chain.

Figures (2.4) (a) and (b) illustrate the bipartite three-mode ($\kappa = 2$) and genuine tripartite ($\kappa = 3$) entanglement measured by the previously exposed criteria $\mathcal{T}_{\kappa,3}$ when the temperature gradient ΔT changes. In the low temperature and strong coupling (between chain oscillators) regime, the three-mode system exhibits genuine tripartite entanglement, though this feature rapidly disappears for positive values of ΔT. A similar behaviour occurs for two-mode entanglement. Interestingly enough, the system is still bipartite three-mode entangled for relatively high temperatures gradients ($\Delta T/T \approx 2$). Notice that we recover practically the same results concerning entanglement for both Ohmic and super-Ohmic dissipation.

In parallel, figures (2.4) (c) and (d) illustrate the current-current correlation as a function of time when the system features genuine tripartite entanglement (see black-solid line in figs. (2.4) (c) and (d)), and bipartite three-mode entanglement (see blue-dashed line in figs. (2.4) (c) and (d)). Clearly, the energy current fluctuations exhibit an oscillatory behaviour with several peaks at short times τ. This should be effectively suppressed at times $\hbar/2\pi k_B T < \tau$ according to the results of Ref.[137], where it was shown that at low temperatures the two-time correlations functions (given in Eq.(1.52)) for the damped harmonic oscillator (at a temperature T) display an exponential decay in the long time limit.

In the figures we appreciate that there is no a substantial change on the current-current correlations when the system evolves from genuine tripartite to bipartite three-mode entangled: such oscillatory behaviour is essentially the same in both situations. The only difference is in the amplitude of the oscillations, which is attributable to thermal fluctuations present when the temperature gradient increases. Moreover, one may observe that such characteristic oscillatory behaviour of the fluctuations remains even for values of temperature gradients ($\Delta T/T \gtrsim 4$) when the system is expected to be separable in all the three-mode bipartitions (see red-dashed-dot line). The comparison of the current-current correlations in different parameters regimes, in which the system features various types of multipartite entanglement, shows that the fluctuations of the energy current along the harmonic chain are apparently insensitive to the existence of tripartite genuine or bipartite three-mode entanglement. Importantly, we have found similar results for the average energy current across the chain in presence of two-mode entanglement and even general quantum correlations measured by discord, which point out that the average properties of the energy current are insensitive to the emergence of entanglement, or equivalently, they are unable to reveal the quantum correlations established in the harmonic chain. Furthermore, it should be mentioned that the behaviour of these average properties are determined

by the temperature gradients, and it can be explained without resorting to the existence of quantum correlations.

If entanglement were exclusively responsible of the behaviour of the average and fluctuations of the energy current, we may expect that the latter would witness the appearance of the former. In this way, we argue that our findings related to the mean values of the energy current can be, at least, qualitatively understood by recalling that entanglement estimators typically exhibit a non-linear dependence on the density operators as was extensively illustrated in Sec.1.2, and thus they will express in principle as non-linear functionals in terms of the aforementioned two-time correlations functions (e.g. see logarithmic negativity). That is to say, entanglement features a non-linear dependence in the correlations appearing in Eq.(2.36) contrary to the energy values $\langle \hat{j}_{ij} \rangle$ (with $i, j \in \mathcal{L}, \mathcal{R}, \mathcal{C}$), such that the latter are unable to manifest themselves entanglement. Though we do not appreciate the appearance of entanglement in the fluctuations (see figure (2.4)), this argument do not close the door to the current-current correlation could manifest the appearance of quantum correlations, because its expression depends non-linearly on the correlation functions between all the system oscillators. In essence, such argument rests on the idea that the reliable observation of entanglement relies on the ability to measure non-linear properties of the quantum state [168; 169].

In summary, we do not observe that the presence of (non-equilibrium) entanglement has significant consequences in the average properties of the energy current across the chain. We also find the same scenario when the system oscillators share other quantum correlations, such as discord, instead of entanglement. In overall, the mean value and fluctuations of the energy current show little structure (these is mainly determined by the temperature gradients) in comparison with the rich variety of quantum correlations exhibited by the system oscillators: two-mode discord and entanglement, bipartite three-mode and genuine tripartite entanglement. These observations find partial support on the fact that the average energy currents exhibit a linear dependence on the two-time correlation functions which carry the quantum correlations. Such dependence is more intricate in the case of the fluctuations, which makes more complicate to elucidate their possible relation to quantum correlations. Interesting enough, the results obtained for quantum correlations are practically the same whether the system suffers Ohmic or super-Ohmic dissipation, suggesting that non-Markovian effects do not induce substantial changes in the stationary quantum correlations compared with the Markovian case.

Chapter 3

Conclusion and prospects

Our imagination is stretched to the utmost,
not, as in fiction, to imagine things which are not really there,
but just to comprehend those things which are there.
-Richard P. Feynman (Extracted from "The Character of Physical Law")

Let us recall that we started the present dissertation from the premise that a meaningful (theoretical) description of entanglement demands, firstly, the elaboration of easy-handling estimators of quantum correlations, and secondly, a reliable treatment of the open-system dynamics which makes attainable the analysis of entanglement.

To sum up, we have reported the development of a readable (theoretical) tool which is able to characterize multipartite entanglement in continuous-variable states, as well as the *low-energy* dynamics of continuous-variable entanglement in quite general dissipative scenarios (ranging from a common environment to independent environments). To be more precise, we list the main results drawn from the research program of this thesis:

1. A hierarchy of separability criteria for multimode continuous-variable systems is proposed. They allow to study in a unified way the k-partite entanglement of broad classes of Gaussian and non-Gaussian states. From this criterion follows that Gaussian entanglement in two-mode and pure three-mode states can be completely assessed by performing local homodyne measurements.

2. Using the foregoing hierarchy, we found that quantum correlations in certain non-Gaussian states are as resilient as in Gaussian ones under purely dissipative effects: the entanglement encapsulated in the non-Gaussian degrees of freedom of the Wigner function shows an exponential decay. In general, the bipartite multimode entanglement gets more robust with an increasing number of constituents, though it tends to disappear in the long time limit.

3. Nonetheless, a highly non-Markovian interaction mediated by a common environment is able to induce stationary Gaussian two-mode and tripartite entanglement between

uncoupled oscillators. Although such environment-induced interaction represents an effective many-party interaction with a spatial long-range feature, the generated multipartite entanglement has a finite size in the spatial degree of freedom. Remarkably enough, we found that the presence of a passive oscillator is detrimental for stationary two-mode entanglement. Our findings suggest that the environment-induced entanglement mechanism corresponds to an uncontrolled feedback which is predominantly coherent at low temperatures and for moderate oscillator-environment coupling as compared to the oscillator frequency.

4. We also found that a compromise among thermal non-equilibrium conditions, oscillator frequencies, and springlike couplings yields a rich variety of stationary tripartite entanglement supported by a harmonic chain. These results apply to regimes of low and comparatively high temperatures, as well as weak and relatively strong dissipative rates. Interestingly, it was shown that the entanglement structure of the chain ground state is degraded as dissipation grows: it is downgraded from fully inseparable to bipartite three-mode entangled. Furthermore, we found that establishing stationary energy currents across the harmonic chain does not favour the buildup of stationary quantum correlations, instead, a temperature gradient eventually destroys the entanglement shared by the system oscillators as a consequence of the growth of thermal fluctuations.

5. More precisely, an extensive numerical analysis indicates that the stationary mean value and fluctuations of the energy current remain insensitive to the emergence of a rich variety of quantum correlations. Contrary to most entanglement estimators, the average energy current depends linearly on the correlation terms (between position and momentum operators) which carry the quantum correlations. We argue that this observation partially supports the numerical findings. Interestingly, the results obtained for quantum correlations are practically the same for Ohmic or super-Ohmic dissipations.

In overall, the above results underline that the behaviour of entanglement under dissipation may be very different when we pass either from two- to multi- mode systems, or from a common to independent environments. The physics behind the entanglement phenomenon goes *non-linearly* with the number of system constituents. This feature reflects itself in the dynamics of multipartite entanglement, and ultimately may become the entanglement evolution under dissipation somehow unexpected. As an example of the latter aspect, we observed that, instead to enrich the entanglement shared by the oscillators, a passive oscillator in a common environment is harmful for the appearance of two-mode quantum correlations. On the other hand, our findings concerning independent environments indicate that the *stationary* entanglement is barely changed by non-Markovian effects (in such dissipative scenario) as compared with a Markovian evolution, in which thermal relaxation dominates. In contrast, the non-Markovian character of the open dynamics is crucial for a deeper understanding of stationary multipartite entanglement in a common environment. At this respect, an still open question is how multipartite entangled states larger than

tripartite would be influenced by non-Markovian effects. As a follow-up project, it is appealing to confirm the tendency to separability between uncoupled oscillators predicted by the above results, which is that the two-mode entanglement and eventually bipartite multimode entanglement will disappear, and further, how this feature influences the quantum correlations between direct interacting oscillators. This will likely help to design better strategies to shield entanglement from the dissipative effects since we have gained a more accurate description of the environmental influence.

It is important to emphasize that we have performed an exact treatment on the open-system dynamics of the harmonic oscillators, so that our results are essentially grounded in the physical reasonable statements concerning the microscopic model which describes the environment and system-environment interaction. In spite of the fact that we have carried out the study for specific configurations of the environment and (linear) interaction between oscillators, one must expect to see an analogous dynamics of entanglement in other dissipative scenarios, since the emergence of quantum correlations in linear CV systems composed by a large (and finite) number of constituents essentially stems from the proximity of the system to the ground state.

Nonetheless, the study of non-linear CV systems deserves further attention. A prominent example is given by the recent optomechanical setups, which represent a non-linear coupling between both a light and mechanical degree of freedom. So far the lack of readable estimators for non-Gaussian entanglement (in highly mixed states) has practically limited the study of quantum correlations in such setups to the linear regimen for which the state follows a Gaussian evolution. It would be of particular interest to apply the entanglement estimator developed in this thesis to analyse the dynamics of non-Gaussian entanglement in this kind of systems in order to see, for instance, whether they manifest resilience to dissipation and thermal noise. From the above results, we may anticipate that the quantum correlations encoded in the non-linear degrees of freedom may be as robust as the largely explored Gaussian entanglement.

Finally, we would like to remark that all above investigation lies on the crossover of quantum information and open quantum systems theory. Nonetheless, entanglement is a rather general feature of quantum systems, and thus, it may be related to others fields of physics. For instance, it has been shown that quantum entanglement may serve as an order parameter for characterizing (quantum) ordinary [183; 204], or topological phase transitions [142; 153; 62]. These examples point out that the symmetries of the ground states of matter are intimately related to their entanglement structure, which is in agreement with the fact that equivalently entangled states share certain symmetries. Importantly, these recent results also support the thinking that a deeper understanding of quantum entanglement may come from the study of quantum correlations in the physics of many-body systems.

Remarkably, novel research on quantum simulation in cold atoms is paving the way to study fundamental aspects of condensed matter, and in general, about Physics [237]. The success of the latter relies on the fact that (as much in the sense of the present dissertation) the effective low-energy dynamics of atoms in optical lattices, forming a many-body lattices systems, coincides with that of a many-body system, or equivalently, an interacting quantum field theory. Interestingly quantum simulation with artificial gauge

fields promises to access a new physical phenomena [102], for instance the creation of effective magnetic fields for photons [239; 81] or the negative refraction of light in photonic resonator lattices [80]. Then it is expected that future investigation on entanglement will likely concern on the dynamics of quantum correlations supported by continuous variable systems driving by artificial gauge fields. However, an attempt to do this will be stricken by certain issues, on one hand, the lack of experimental-friendly criteria to characterize entanglement, and on the other hand, the open-system treatment becomes involved with an explicit time-dependence of the system-field interaction. We hope that the work presented here may help to stimulate further research in this direction.

Chapter 4

Compendium

An expert is a man who has made all the mistakes which can be made, in a narrow field.
-Attributed to Niels Bohr

Article 1

HIERARCHIES OF MULTIPARTITE ENTANGLEMENT FOR CONTINUOUS-VARIABLE STATES

Antonio A. Valido, Federico Levi, and Florian Mintert

Phys. Rev. A 90, 052321 (2014)

PHYSICAL REVIEW A **90**, 052321 (2014)

Hierarchies of multipartite entanglement for continuous-variable states

Antonio A. Valido,[1,*] Federico Levi,[2] and Florian Mintert[2,3]

[1]*Instituto Universitario de Estudios Avanzados (IUdEA) and Departamento de Física, Universidad de La Laguna, E-La Laguna 38203, Spain*

[2]*Freiburg Institute for Advanced Studies, Albert-Ludwigs University of Freiburg, Albertstraße 19, D-79104 Freiburg, Germany*

[3]*Department of Physics, Imperial College London, London SW7 2AZ, United Kingdom*

(Received 18 September 2014; published 14 November 2014)

We derive a hierarchy of separability criteria for multimode continuous-variable systems. They permit one to study in a unified way the k-partite entanglement of broad classes of Gaussian and non-Gaussian states. With specific examples we demonstrate the strength of the criteria, and we discuss their assessment based on data obtained from Gaussian measurements.

DOI: 10.1103/PhysRevA.90.052321 PACS number(s): 03.67.Mn, 03.65.Ud, 03.67.Bg

I. INTRODUCTION

Entanglement has proven to be a central resource in quantum information processing using either discrete or continuous-variable (CV) systems (such as field modes of light, nanomechanical oscillators or cold atomic gases) [1]. Any attempt to create an entangled state is limited by the residual noise and decoherence, and proper tools to verify entanglement are needed to evidence the success of an experiment. In CV systems these tools can roughly be divided into those that apply to Gaussian states [2–6] (see [7] for a complete review), and those that apply to more general states [8,9]. Most tools entail an optimization of an entropylike functional like a convex roof construction [10,11], the proper choice of a set of observables that witness the entanglement for a broad class of states [12–18], or the suitable selection of a finite [19–24] or infinite [25,26] series of inequalities (concerning moments of the quadrature variables) which are mainly based on the well-known criterion of positive partial transposition (PPT) [1,27]. The need to optimize or accurately choose a tool in accordance with the specific properties of a quantum state makes the characterization of entanglement a computationally intricate problem [28], which becomes even more involved as the mixedness of the state or the number of constituents of the system grows.

Entanglement shared by two subsystems has been realized experimentally in various systems [29], but increasing the number of entangled components is a big experimental challenge, such that the preparation of states with more than bipartite entanglement has been achieved in few systems only [30–32]. The limitations due to noise and decoherence typically get increasingly severe with the growing number of entangled subsystems. Under given imperfect conditions it might not be possible to create a genuinely n-partite entangled state in an n-partite system, whereas the preparation of a bipartite entangled state might still be feasible. Tools to verify bipartite or genuine n-partite entanglement have been explored in detail [33], but tools that analyze the range in between have been established only recently [8,34–37]. Only those tools, however, will help us to gauge experimental progress and eventually achieve the creation of genuine n-partite entanglement.

We build up here on a hierarchy of separability criteria that detect k-partite entanglement in n-partite discrete systems [36], and extend this approach to the case of contiuous-variable systems. Based on this hierarchy, we present versatile hierarchies of separability criteria that apply to Gaussian and non-Gaussian states such as photon-added or -subtracted states [38] that display particularly strong nonclassical correlation properties [39–44].

The paper is organized as follows: We start with an introduction to CV systems and hierarchies of separability criteria in Sec. II. The formulation of these hierarchies for CV systems is presented in Sec. III, which is accompanied with a discussion of the similarities with the PPT criterion (see Sec. III A). We apply these hierarchies to Gaussian and non-Gaussian states in Sec. IV, and the possible experimental assessment of the criterion is discussed in Sec. V.

II. BASIC DEFINITIONS

A. Phase space representation

The Hilbert space $\mathcal{H}_n$ of a quantum system composed by n modes results from the n-fold tensor product of the single-mode Hilbert space $\mathcal{H}_1 = \mathrm{L}^2(\mathbb{R})$, and all the physical information about the system is encoded in the density operator $\hat{\rho}$. The mth mode is described in terms of the canonical operators, i.e., position $\hat{Q}_m$ and momentum $\hat{P}_m$. Equivalently it may be described by their dimensionless counterparts $\hat{q}_m = \hat{Q}_m\sqrt{M\Omega/\hbar}$ and $\hat{p}_m = \hat{P}_m/\sqrt{M\Omega\hbar}$ defined in terms of the frequency Ω and and mass M. From now on we will use only the dimensionless operators and define the operator-valued vector $\hat{\boldsymbol{x}} = (\hat{q}_1, \hat{p}_1, ..., \hat{q}_n, \hat{p}_n)^T$ whose elements satisfy the canonical commutation relations $[\hat{\boldsymbol{x}}_m, \hat{\boldsymbol{x}}_l] = -i[\boldsymbol{J}_n]_{ml}$, with the symplectic matrices,

$$\boldsymbol{J}_n = \bigoplus_{m=1}^{n} \boldsymbol{J}_1 \quad \text{and} \quad \boldsymbol{J}_1 = \begin{pmatrix} 0 & -1 \\ 1 & 0 \end{pmatrix},$$

of the composite system and a single subsystem.

It is convenient to describe a continuous-variable system in terms of the real symplectic space $(\mathbb{R}^{2n}, \boldsymbol{J}_n)$, i.e., phase space [7,27], rather than the infinite dimensional complex Hilbert space $\mathcal{H}_n$. Quantum mechanical operators $\hat{A}$ are then

*aavalido@ull.es

replaced by their Weyl symbol,

$$W_A(\boldsymbol{x}) = \int_{\mathbb{R}^{2n}} \frac{d^{2n}\boldsymbol{\xi}}{(2\pi)^{2n}} e^{i\boldsymbol{x}^T \boldsymbol{J}_n \boldsymbol{\xi}} \mathrm{Tr}\big[\hat{A} e^{-i\hat{\boldsymbol{x}}^T \boldsymbol{J}_n \boldsymbol{\xi}}\big], \tag{1}$$

i.e., functions $W_A(\boldsymbol{x})$ of classical phase space variables $\boldsymbol{x} = (q_1, p_1, \ldots, q_n, p_n)$ [45]. The Weyl symbol of a density matrix $\hat{\rho}$ is typically referred to as the Wigner function, and it is denoted by $W(\boldsymbol{x})$ [46].

The Wigner function $W(\boldsymbol{x})$ of a Gaussian state $\hat{\rho}$ has the particularly simple form [46],

$$W(\boldsymbol{x}) = \frac{e^{-\frac{1}{2}(\boldsymbol{x}-\bar{\boldsymbol{x}})^T \boldsymbol{V}^{-1}(\boldsymbol{x}-\bar{\boldsymbol{x}})}}{(2\pi)^n \sqrt{\det(\boldsymbol{V})}},$$

where the vector $\bar{\boldsymbol{x}} = \mathrm{Tr}(\hat{\rho}\hat{\boldsymbol{x}})$ contains the expectation values (first moments) of the dimensionless phase space variables, and the covariance matrix $\boldsymbol{V}$ is defined by

$$\boldsymbol{V}_{ml} = \tfrac{1}{2}\mathrm{Tr}(\hat{\rho}\{[\hat{\boldsymbol{x}}]_m - [\bar{\boldsymbol{x}}]_m, [\hat{\boldsymbol{x}}]_l - [\bar{\boldsymbol{x}}]_l\}),$$

where $\{.,.\}$ denotes the anticommutator. In this case, W is completely characterized by the vector $\bar{\boldsymbol{x}}$ and the real symmetric $2n \times 2n$ matrix $\boldsymbol{V}$, i.e., by $2n^2 + n$ real parameters. According to the Heisenberg uncertainty relation, the covariance matrix of any quantum state must satisfy $\boldsymbol{V} \geqslant \frac{i}{2}\boldsymbol{J}_n$ [27,46], which implies the positive definiteness $\boldsymbol{V} > 0$. Since the entanglement of the system is invariant under local unitary displacements [27], we shall take the first-moment vector equal to zero ($\bar{\boldsymbol{x}} = 0$) from now on.

Here, we are concerned with the class of entangled states $\hat{\rho}$ whose Wigner function may be expressed as the product of a polynomial function $F(\boldsymbol{x})$ and the Wigner function of a Gaussian state with the covariance matrix $\boldsymbol{V}$, i.e.,

$$W(\boldsymbol{x}) = \frac{F(\boldsymbol{x}) e^{-\frac{1}{2}\boldsymbol{x}\boldsymbol{V}^{-1}\boldsymbol{x}}}{(2\pi)^n \sqrt{\det(\boldsymbol{V})}}. \tag{2}$$

Direct examples of this kind of state are those states which are generated by a series of photon-creation [47] or photon-subtraction operations [44,48,49], or more general, a coherent superposition of both [20,50]. We shall refer to the latter as photon-manipulated states. In that case, the degree of the polynomial corresponds to the number of such manipulations that need to be applied to a Gaussian state to arrive at the state in question. We should, however, stress that $F(\boldsymbol{x})$ may be also an analytic function with domain in all the phase space (a function with a convergent Taylor series), such that the set of non-Gaussian states with Wigner function (2) may comprise a broader class of CV states than the photon-manipulated states, as, for example, Schrödinger cat states.

B. Hierarchy of separability criteria

A pure state of an n-partite quantum system is considered n-partite entangled if it cannot be written as a simple tensor product of two state vectors each of which describes a part of the subsystems only. If an n-partite quantum state cannot be written as a simple tensor product of k_i-partite entangled k_i-partite state vectors with $k_i < k$, then the state is k-partite entangled.

A mixed n-partite state $\hat{\rho}$ is considered k-partite entangled if it cannot be represented as an average over projectors onto pure states that are less than k-partite entangled, i.e.,

$$\hat{\rho} \neq \sum_{j=1}^{k-1} \int d\mu_j(a) \big|\Psi_{j,n}^{(a)}\big\rangle\big\langle\Psi_{j,n}^{(a)}\big|, \tag{3}$$

where $|\Psi_{j,n}^{(a)}\rangle$ are j-partite entangled n-partite states, $\mu_j(a)$ are positive functions that satisfy $\sum_{j=1}^{k-1}\int d\mu_j(a) = 1$, and the summation is restricted to values $j < k$. Physically, this definition means that a k-partite entangled state can be realized by mixing different states that are at most k-partite entangled, but since the states that enter this average may carry entanglement between different groups of subsystems, a k-partite entangled n-partite state is not necessarily separable with respect to a certain bipartition.

Our starting point to detect k-partite entanglement is a hierarchy of separability criteria $\tau_{k,n}$. It is based on a comparison between several matrix elements of the density operator in question with respect to some product states. As shown in [51], genuine n-partite entanglement is identified through the condition,

$$\tau_n(\hat{\rho}) = \underbrace{|\langle\Phi_1|\varrho|\Phi_2\rangle|}_{f(\varrho)} - \sum_{j=1}^{2^{n-1}-1} \underbrace{\sqrt{\langle\Phi_{1j}|\varrho|\Phi_{1j}\rangle\langle\Phi_{2j}|\varrho|\Phi_{2j}\rangle}}_{f_j(\varrho)} > 0, \tag{4}$$

where $|\Phi_1\rangle = \bigotimes_{m=1}^n |\varphi_m\rangle$ and $|\Phi_2\rangle = \bigotimes_{m=1}^n |\varphi_{n+m}\rangle$ are two product vectors, and the vectors $|\Phi_{1i}\rangle$ and $|\Phi_{2i}\rangle$ are defined in terms of the inequivalent possibilities to divide the n subsystems into two groups: There are $2^{n-1} - 1$ inequivalent such bipartitions, each of which that can be characterized by a vector $\boldsymbol{v}_j$ whose n elements adopt the values 0 or 1, and the groups are defined by the subsystems associated with the value 0 and 1, respectively. In terms of these vectors, we have the definition,

$$|\Phi_{1j}\rangle = \bigotimes_{m=1}^n \big|\varphi_{m+n[\boldsymbol{v}_j]_m}\big\rangle, \quad |\Phi_{2j}\rangle = \bigotimes_{m=1}^n \big|\varphi_{m+n-n[\boldsymbol{v}_j]_m}\big\rangle, \tag{5}$$

that is, the vectors $|\Phi_{1j}\rangle$ and $|\Phi_{2j}\rangle$ are obtained from the vectors $|\Phi_1\rangle$ and $|\Phi_2\rangle$ through a permutation of state vectors $|\varphi_m\rangle$ with $|\varphi_{n+m}\rangle$ that belong to those subsystems that are grouped together in the jth bipartition.

If a pure state $\hat{\rho} = |\Psi\rangle\langle\Psi|$ is separable with respect to the jth bipartition, then $f(\hat{\rho}) = f_j(\hat{\rho})$. Since the $f_j(\hat{\varrho})$ are nonnegative, this implies that τ_n is nonpositive. As this reasoning holds for any bipartition, and, in addition, τ_n is convex, τ_n is indeed nonpositive for any state ϱ that can be decomposed into biseparable pure states.

A fully separable pure state is biseparable with respect to all bipartitions; accordingly, one may introduce the function $\tau_{bi,n}(\hat{\rho}) = f(\varrho) - (2^{n-1}-1)^{-1}\sum_{j=1}^{2^{n-1}-1} f_j(\varrho)$, and a positive value of $\tau_{bi,n}$ identifies a mixed state to be at least bipartite entangled. In the same fashion, one can introduce scalar factors $a_j^{(k,n)} \geqslant 0$ [36] for $n \geqslant k \geqslant 2$ such that

$$\tau_{k,n}(\hat{\rho}) = f(\varrho) - \sum_j a_j^{(k,n)} f_j(\varrho) \tag{6}$$

can be positive only if $\hat{\rho}$ is at least k-partite entangled.

In order to detect entanglement properties as reliably as possible, a suitable choice of *probe vectors* $|\varphi_i\rangle$ is in order. In practice, it is desirable to find an optimal set of normalized such vectors that maximize $\tau_{k,n}$. Advantageously, the number of probe vectors scales only linearly with n, but a full optimization over the infinite-dimensional vectors without simplifying assumptions does not seem to be a fruitful endeavor. Similarly to the concept of Gaussian entanglement of formation [10], we therefore require that all probe vectors are Gaussian. Each Gaussian probe state $|\varphi_m\rangle$ is then characterized by it first and second moments,

$$\bar{\boldsymbol{x}}_m = (\bar{q}_m, \bar{p}_m), \text{ and} \tag{7}$$

$$\boldsymbol{\Sigma}_m = \begin{bmatrix} \sigma_{xx}^{(m)} & \sigma_{xp}^{(m)} \\ \sigma_{xp}^{(m)} & \sigma_{pp}^{(m)} \end{bmatrix}, \tag{8}$$

with $\det(\boldsymbol{\Sigma}_m) = 1/4$, $\sigma_{xx}^{(m)} \geqslant 0$ and $\sigma_{pp}^{(m)} \geqslant 0$. In the following we will identify choices for these parameters that yield strong criteria. Remarkably enough, this allows us to reproduce the PPT criterion for two-mode and pure three-mode Gaussian states. Beyond that, even with this simplifying assumption, Eq. (6), is able to detect non-Gaussian entanglement [20], for which criteria only based on the second moments of the quadrature variables fail. Both observations demonstrate that assuming Gaussian probe states makes the present hierarchy an easily accessible but strong tool.

III. HIERARCHIES OF INSEPARABILITY CRITERIA FOR CV SYSTEMS

The $\tau_{k,n}$ are parametrized by the first and second moments of the Weyl symbols of the operators $|\Phi_1\rangle\langle\Phi_1|$, $|\Phi_2\rangle\langle\Phi_2|$, $|\Phi_{1j}\rangle\langle\Phi_{1j}|$, and $|\Phi_{2j}\rangle\langle\Phi_{2j}|$. Let us denote their vectors of first moments by $\boldsymbol{X}_{\Phi_1}$, $\boldsymbol{X}_{\Phi_2}$, $\boldsymbol{X}_{\Phi_{1j}}$, and $\boldsymbol{X}_{\Phi_{2j}}$, and their matrices of second moments by $\boldsymbol{\Sigma}_{\Phi_1}$, $\boldsymbol{\Sigma}_{\Phi_2}$, $\boldsymbol{\Sigma}_{\Phi_{1j}}$, and $\boldsymbol{\Sigma}_{\Phi_{2j}}$. Since also the matrix element $\langle\Phi_1|\,\hat{\rho}\,|\Phi_2\rangle$ enters the definition of $\tau_{k,n}$, it is convenient to introduce also moments,

$$\boldsymbol{X}_{\Phi_{21}} = \frac{\int d^{2n}\boldsymbol{x}\; \boldsymbol{x}\; W_{|\Phi_2\rangle\langle\Phi_1|}(\boldsymbol{x})}{\int d^{2n}\boldsymbol{x}\; W_{|\Phi_2\rangle\langle\Phi_1|}(\boldsymbol{x})}, \tag{9}$$

and $\boldsymbol{\Sigma}_{\Phi_{12}}$ defined analogously, where the explicit normalization is introduced because the overlap between $|\Phi_1\rangle$ and $|\Phi_2\rangle$ is typically not unity.

As shown in Eq. (A6) in Appendix A, $\boldsymbol{\Sigma}_{\Phi_{21}}$ can easily be constructed from the covariance matrices $\boldsymbol{\Sigma}_m$ defined in Eq. (8) via the prescription,

$$\boldsymbol{\Sigma}_{\Phi_{21}} = \bigoplus_{m=1}^{n} \boldsymbol{\Sigma}_{m,n+m}, \tag{10}$$

with

$$\boldsymbol{\Sigma}_{m,n+m} = \frac{\boldsymbol{\Sigma}_m + \boldsymbol{\Sigma}_{n+m}}{2\det(\boldsymbol{\Sigma}_m + \boldsymbol{\Sigma}_{n+m})} + i\,\frac{\boldsymbol{\Sigma}_m \boldsymbol{J}_1^T \boldsymbol{\Sigma}_{n+m} - \boldsymbol{\Sigma}_{n+m}\boldsymbol{J}_1^T\boldsymbol{\Sigma}_m}{2\det(\boldsymbol{\Sigma}_m + \boldsymbol{\Sigma}_{n+m})}.$$

The first moments are then given by [52]

$$\boldsymbol{X}_{\Phi_{21}} = \frac{\boldsymbol{X}_{\Phi_1} + \boldsymbol{X}_{\Phi_2}}{2} + i\,\boldsymbol{\Sigma}_{\Phi_{21}}\boldsymbol{J}_n\big(\boldsymbol{X}_{\Phi_1} - \boldsymbol{X}_{\Phi_2}\big). \tag{11}$$

As it is extensively illustrated in Appendix A, one may express $\tau_{k,n}$ in a rather compact form,

$$\tau_{k,n}(\hat{\rho}) = \frac{e^{-\frac{\alpha}{2}}\left|\mathsf{f}_{\Phi_{21}}\right|}{\sqrt[4]{\det\left(\boldsymbol{\Sigma}_{\Phi_1} + \boldsymbol{\Sigma}_{\Phi_2}\right)}} - \sum_j a_j^{(k,n)} e^{-\frac{\beta_j}{4}}\sqrt{\mathsf{f}_{\Phi_{1j}}\mathsf{f}_{\Phi_{2j}}}, \tag{12}$$

with

$$\mathsf{f}_u = \frac{\exp\left(\frac{1}{2}K^T\left(\boldsymbol{V}^{-1} + \boldsymbol{\Sigma}_u^{-1}\right)^{-1}K\right)F(\boldsymbol{x})\big|_{\boldsymbol{x}=\vec{0}}}{\sqrt{\det(\boldsymbol{\Sigma}_u + \boldsymbol{V})}}, \tag{13}$$

and $K = (\frac{\partial}{\partial \boldsymbol{x}} + \boldsymbol{\Sigma}_u^{-1}\boldsymbol{X}_u)$ for $u = \Phi_{21}, \Phi_{1j}, \Phi_{2j}$. The quantities,

$$\alpha = \mathrm{Re}\big(\boldsymbol{X}_{\Phi_{21}}^T\boldsymbol{\Sigma}_{\Phi_{21}}^{-1}\boldsymbol{X}_{\Phi_{21}}\big) + \big(\boldsymbol{X}_{\Phi_1} - \boldsymbol{X}_{\Phi_2}\big)^T\boldsymbol{J}_n^T\mathrm{Re}\big(\boldsymbol{\Sigma}_{\Phi_{21}}\big) \times \boldsymbol{J}_n\big(\boldsymbol{X}_{\Phi_1} - \boldsymbol{X}_{\Phi_2}\big), \tag{14}$$

and

$$\beta_j = \boldsymbol{X}_{\Phi_{1j}}^T\boldsymbol{\Sigma}_{\Phi_{1j}}^{-1}\boldsymbol{X}_{\Phi_{1j}} + \boldsymbol{X}_{\Phi_{2j}}^T\boldsymbol{\Sigma}_{\Phi_{2j}}^{-1}\boldsymbol{X}_{\Phi_{2j}}, \tag{15}$$

are quadratic functions of the first-moment vectors, and Re denotes the real part. We provide the expressions for the vectors $\boldsymbol{X}_{\Phi_1}$, $\boldsymbol{X}_{\Phi_2}$, $\boldsymbol{X}_{\Phi_{1j}}$, and $\boldsymbol{X}_{\Phi_{2j}}$, as well as for the covariance matrices $\boldsymbol{\Sigma}_{\Phi_1}$, $\boldsymbol{\Sigma}_{\Phi_2}$, $\boldsymbol{\Sigma}_{\Phi_{1j}}$, and $\boldsymbol{\Sigma}_{\Phi_{2j}}$ in Eqs. (B1)–(B8) in Appendix B.

The general expression Eq. (12) holds for any state whose Wigner function can be cast in the form of Eq. (2). If $F(\boldsymbol{x}) = 1$ in Eq. (2), i.e., if $\hat{\rho}$ is Gaussian, then f_u defined in Eq. (13) takes the simpler form,

$$\mathsf{f}_u^{(G)} = \frac{\exp\left(\frac{1}{2}(\boldsymbol{X}_u)^T\boldsymbol{\Sigma}_u^{-1}\left(\boldsymbol{V}^{-1} + \boldsymbol{\Sigma}_u^{-1}\right)^{-1}\boldsymbol{\Sigma}_u^{-1}\boldsymbol{X}_u\right)}{\sqrt{\det(\boldsymbol{\Sigma}_u + \boldsymbol{V})}}.$$

In order to identify general properties of the states $|\Phi_i\rangle$ that yield potentially maximal values for $\tau_{k,n}$, we will make the assumption,

$$\boldsymbol{\Sigma}_{\Phi_1} = \boldsymbol{\Sigma}_{\Phi_2} = \boldsymbol{\Sigma}, \tag{16}$$

i.e., we assume that $|\varphi_m\rangle$ and $|\varphi_{n+m}\rangle$ (for $m = 1, \ldots, n$) have the same covariance matrix. With this assumption Eqs. (14) and (15) reduce to $\alpha = \alpha'$ and $\beta_j = \beta_j'$ with

$$\beta_j' = 2\alpha' + \tfrac{1}{2}\big(\boldsymbol{X}_{\Phi_1} - \boldsymbol{X}_{\Phi_2}\big)^T\boldsymbol{P}_j^T\boldsymbol{\Sigma}^{-1}\boldsymbol{P}_j\big(\boldsymbol{X}_{\Phi_1} - \boldsymbol{X}_{\Phi_2}\big),$$

and

$$\alpha' = 1/4(\boldsymbol{X}_{\Phi_1} + \boldsymbol{X}_{\Phi_2})^T\boldsymbol{\Sigma}^{-1}(\boldsymbol{X}_{\Phi_1} + \boldsymbol{X}_{\Phi_2}),$$

with

$$\boldsymbol{P}_j = \bigoplus_{m=1}^{n}(-1)^{[\boldsymbol{v}_j]_m}\boldsymbol{I}, \tag{17}$$

where $\boldsymbol{I}$ is the two-dimensional identity matrix, and $\boldsymbol{v}_j$, which is defined in the context of Eq. (5), characterizes the bipartition j. With the help of the following identity valid for quadratic matrices [53],

$$\frac{1}{\boldsymbol{\Sigma} + \boldsymbol{V}} = \boldsymbol{\Sigma}^{-1} - \boldsymbol{\Sigma}^{-1}(\boldsymbol{V}^{-1} + \boldsymbol{\Sigma}^{-1})\boldsymbol{\Sigma}^{-1}, \tag{18}$$

one may easily show that the hierarchy $\tau'_{k,n}$ resulting from the assumption Eq. (16) can be expressed as

$$\tau'_{k,n}(\hat{\rho}) = \frac{e^{-\frac{1}{8}(\boldsymbol{X}_{\Phi_1}+\boldsymbol{X}_{\Phi_2})^T \frac{1}{\boldsymbol{\Sigma}+\boldsymbol{V}}(\boldsymbol{X}_{\Phi_1}+\boldsymbol{X}_{\Phi_2})}}{\sqrt{\det(\boldsymbol{\Sigma}+\boldsymbol{V})}} h_{k,n},$$

where $h_{k,n}$ is a function which does not depend on $(\boldsymbol{X}_{\Phi_1} + \boldsymbol{X}_{\Phi_2})$, i.e., $h_{k,n} = h_{k,n}(\boldsymbol{\Sigma}, \boldsymbol{X}_{\Phi_1} - \boldsymbol{X}_{\Phi_2})$.

Since $\boldsymbol{\Sigma}$ and $\boldsymbol{V}$ are positive definite, the exponent is nonpositive, such that $\tau'_{k,n}$ adopts its maximum only if $\boldsymbol{X}_{\Phi_1} + \boldsymbol{X}_{\Phi_2} = 0$. That is, assuming Gaussian probe vectors and Eq. (16) permits one to perform an essential part of the maximization of $\tau_{k,n}$ analytically, which eases the reliable estimation of $\mathcal{T}_{k,n} = \max_{\Phi_1,\Phi_2} \tau_{k,n}$ substantially. With this, we arrive at

$$\tilde{\mathcal{T}}_{k,n} = \max_{\boldsymbol{X},\boldsymbol{\Sigma}} \tilde{\tau}_{k,n},$$

with

$$\tilde{\tau}_{k,n}(\hat{\rho}) = \frac{e^{-2\boldsymbol{X}^T \boldsymbol{J}_n^T \frac{1}{\boldsymbol{\Sigma}^{-1}+\boldsymbol{V}^{-1}} \boldsymbol{J}_n \boldsymbol{X}}}{\sqrt{\det(\boldsymbol{\Sigma}+\boldsymbol{V})}} - \sum_j a_j^{(k,n)} \frac{e^{-\frac{1}{2}\boldsymbol{X}^T (\boldsymbol{P}_j)^T \frac{1}{\boldsymbol{\Sigma}+\boldsymbol{V}} \boldsymbol{P}_j \boldsymbol{X}}}{\sqrt{\det\left(\boldsymbol{\Sigma}+\boldsymbol{V}\right)}}, \tag{19}$$

which can readily be optimized numerically.

A. Resemblance to the PPT Criterion

Since Eq. (19) is the result of several restrictions that potentially weaken the hierarchy, a critical assessment of its strength is in order. Since most of the existing separability criteria are concerned with separability with respect to a given bipartition, we focus for the moment on this question. According to Eq. (19), the inequality,

$$e^{-\frac{1}{2}\boldsymbol{X}^T (\boldsymbol{P}_j)^T \frac{1}{\boldsymbol{\Sigma}+\boldsymbol{V}} \boldsymbol{P}_j \boldsymbol{X}} \geqslant e^{-2\boldsymbol{X}^T \boldsymbol{J}_n^T \frac{1}{\boldsymbol{\Sigma}^{-1}+\boldsymbol{V}^{-1}} \boldsymbol{J}_n \boldsymbol{X}},$$

is satisfied for any mixed Gaussian state that is biseparable with respect to the bipartition j. Since this scalar inequality is satisfied for any choice of $\boldsymbol{X}$, it implies the matrix inequality [54],

$$4\boldsymbol{J}_n^T \frac{1}{\boldsymbol{\Sigma}^{-1}+\boldsymbol{V}^{-1}} \boldsymbol{J}_n \geqslant (\boldsymbol{P}_j)^T \frac{1}{\boldsymbol{\Sigma}+\boldsymbol{V}} \boldsymbol{P}_j. \tag{20}$$

In the following, we will show that this permits us to recover the ppt criterion for mixed two-mode and pure three-mode Gaussian states, when all the probe states $|\varphi_m\rangle$ are chosen to be pure infinitely squeezed states, with covariance matrix with $\sigma^m_{pp} \to 0$ $(\forall m)$ for squeezing in momentum, or $\sigma^m_{xx} \to 0$ $(\forall m)$ for squeezing in position. It is worthwhile noting that if inequality (20) is violated in all the bipartitions, then $\hat{\rho}$ is genuine multipartite entangled.

1. Two-mode case

The covariance matrix $\boldsymbol{V}$ of any two-mode Gaussian state can be expressed in the standard form (C1), in terms of four coefficients $a,b,c,d \in \mathbb{R}$ [7].

According to the ppt criterion, a two-mode Gaussian state is separable if and only if the symplectic eigenvalues $\{\tilde{\nu}_1, \tilde{\nu}_2\}$ of the partial transpose of the covariance matrix $\tilde{\boldsymbol{V}}_j$ with respect to the bipartition j satisfy [7,21]

$$\tilde{\nu}_1, \tilde{\nu}_2 \geqslant \tfrac{1}{2}. \tag{21}$$

These are directly obtained from the roots $\{\pm i\tilde{\nu}_1, \pm i\tilde{\nu}_2\}$ of the characteristic polynomial of the matrix $\boldsymbol{J}_2^T \tilde{\boldsymbol{V}}_j$, which is given by

$$\lambda^4 + \tilde{\Delta}_1^2 \lambda^2 + \tilde{\Delta}_2^2 = 0, \tag{22}$$

with $\tilde{\Delta}_1^2 = \frac{1}{4}(a^2 + b^2 - 2cd)$, $\tilde{\Delta}_2^2 = \frac{1}{16}(ab - c^2)(ab - d^2)$, which are the symplectic invariants.

On other hand, inequality (20) in the two-mode case may be translated into the eigenvalue problem of the product matrix [54],

$$\boldsymbol{Z}_1 = 4\boldsymbol{P}_1\left(\boldsymbol{\Sigma}+\boldsymbol{V}\right)\boldsymbol{P}_1 \boldsymbol{J}_2^T (\boldsymbol{\Sigma}^{-1} + \boldsymbol{V}^{-1})^{-1} \boldsymbol{J}_2, \tag{23}$$

such that inequality (20) is not violated as long as all of the eigenvalues $\{\lambda_z^{(i)}; i = 1,2,3,4\}$ of $\boldsymbol{Z}_1$ are non-negative, i.e., $\lambda_z^{(i)} \geqslant 1 \quad \forall i$.

Using the standard form (C1) and substituting $\boldsymbol{\Sigma}_m$ by the covariance matrix of a pure squeezed state [see Eq. (C2)], $\boldsymbol{Z}_1$ results in the matrix $\boldsymbol{Z}_1(r)$ defined in Eq. (C3) whose entries are given in terms of rational functions in the squeezing parameter r, as discussed in more detail in Appendix C.

In the limit of infinite squeezing in momentum ($r \to 0$), we find that $\boldsymbol{Z}_1$ [see Eq. (C4)] has $\lambda_z^{(1)} = \lambda_z^{(2)} = 1$ as the doubly degenerate eigenvalue, and the other two are given by the characteristic polynomial,

$$\left(\frac{\lambda_z}{4}\right)^2 - \tilde{\Delta}_1^2 \left(\frac{\lambda_z}{4}\right) + \tilde{\Delta}_2^2 = 0. \tag{24}$$

Since the roots of Eq. (24) are related with the roots of Eq. (22) through the expression $\lambda = \pm i\sqrt{\lambda_z}/2$, the conditions $\lambda_z^{(3)} \geqslant 1$ and $\lambda_z^{(4)} \geqslant 1$ are indeed equivalent to Eq. (21). That is, given the optimal choice of probe states with $|\varphi_m\rangle = |\varphi_{n+m}\rangle$ $(m = 1, \ldots, n)$ and infinitely squeezed covariance matrix, we recover exactly the necessary and sufficient PPT criterion from the inequality (20). It is straightforwardly to show that this assertion also holds if we consider infinite squeezing in position ($r \to \infty$) [see Eq. (C5)].

2. Three-mode case

The foregoing discussion sets the stage of the procedure that one has to follow in order to show the analog result for pure three-mode Gaussian states. In this case, the comparison between the inequalities (20) and (21) has to be in terms of the three possible bipartitions of the system, such that the characteristic polynomial of the matrices $\boldsymbol{Z}_j$ $(j = 1,2,3)$ leads to the characteristic polynomial of the matrices $\boldsymbol{J}_3^T \tilde{\boldsymbol{V}}_j$. We defer the details of the proof to Appendix C.

We may apply the same procedure to study the case of mixed tripartite-entangled states, but one finds that this assertion is no longer true. For mixed three-mode Gaussian states inequality (20) cannot be expected to reproduce the PPT criterion, since PPT basically discerns fully inseparability in the case of mixed states [5,32], whereas $\tau_{3,3}$ identifies genuine tripartite entanglement. However, we found that $\tau_{2,3}$ still detects entanglement of the vast majority of three-mode bipartite entangled states.

IV. EXAMPLES

We now turn the attention to illustrate how expression (12) provides reliable estimates of k-partite entanglement in Gaussian and non-Gaussian states.

A. Mixed genuine tripartite entangled states

Let us start analyzing the inseparability properties of a mixed tripartite Gaussian entangled state, whose covariance matrix may be expressed as follows,

$$\boldsymbol{V} = \boldsymbol{V}_{\rm GHZ} + g\boldsymbol{I}_3, \quad \text{with} \quad g \geqslant 0, \tag{25}$$

where $\boldsymbol{I}_n = \bigoplus_{m=1}^{n} \boldsymbol{I}$, and

$$\boldsymbol{V}_{\rm GHZ} = \frac{1}{2}\begin{pmatrix} a & 0 & -c & 0 & -c & 0 \\ 0 & b & 0 & c & 0 & c \\ -c & 0 & a & 0 & -c & 0 \\ 0 & c & 0 & b & 0 & c \\ -c & 0 & -c & 0 & a & 0 \\ 0 & c & 0 & c & 0 & b \end{pmatrix}, \tag{26}$$

with

$$a = \tfrac{1}{2}[e^{2r} + \cosh(2r)], \quad b = \tfrac{1}{2}[e^{-2r} + \cosh(2r)],$$
$$c = \tfrac{1}{2}\sinh(2r),$$

the covariance matrix of the continuous-variable analog of the GHZ states [5]. Here, g plays the role of a mixing parameter, while $r \geqslant 0$ is the squeezing parameter. We compare the hierarchies $\tau_{2,3}$ and $\tau_{3,3}$ with the PPT criterion applied to the bipartition $1|23$ [5].

As one can see in Fig. 1, $\tau_{3,3}$ detects that this state is genuinely tripartite entangled in a substantial part in the parameter regime, and for sufficiently strong squeezing, even substantially mixed states are still genuinely tripartite entangled. States that are too strongly mixed to be genuinely tripartite entangled can still be identified to be bipartite entangled via $\tau_{2,3}$, which detects nearly as many states as the ppt criterion.

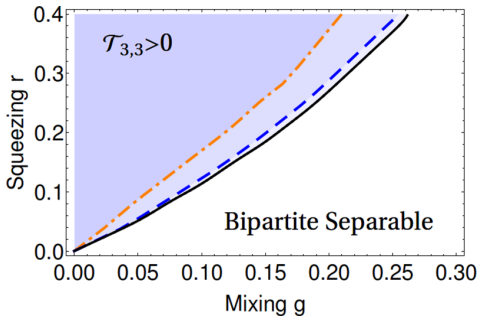

FIG. 1. (Color online) Density map of the inseparability properties of the Werner-type GHZ state defined in Eq. (25) in terms of the mixing g and squeezing parameter r. The black solid line depicts the border between bipartite entangled (blue region) and separable states according to the PPT criterion. Within the former, the blue dashed and orange dot-dashed lines delimit the region of the states for which the hierarchies $\mathcal{T}_{2,3}$ and $\mathcal{T}_{3,3}$ return positive values, respectively.

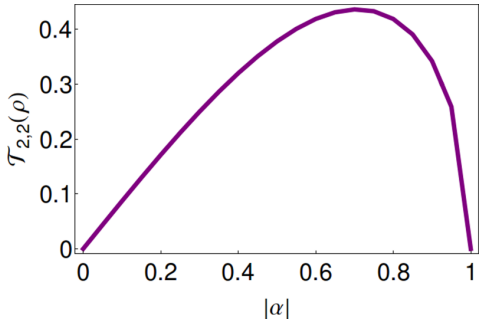

FIG. 2. (Color online) $\mathcal{T}_{2,2}(\hat{\rho})$ as a function of the amplitude $|\alpha|$ for the CPS-TSVS defined in Eq. (27) with $r = 0$, $\alpha = |\alpha|e^{i\frac{\sqrt{5}}{2}}$, and $\beta = |\beta|e^{i\frac{\pi}{2}}$.

B. Coherent photon-added or -subtracted two-mode states

To demonstrate the performance on non-Gaussian states we investigate the inseparability properties of coherently photon-subtracted two-mode squeezed vacuum states (CPS-TSVS). These states derive from the locally squeezed two-mode vacuum state by applying the operator $(\alpha\hat{a}_1 + \beta\hat{a}_2)^u$, where $\hat{a}_l$ ($l = 1,2$) is the photon-annihilation operator of the lth mode and $|\alpha|^2 + |\beta|^2 = 1$ [50]. For simplicity, we shall consider the states obtained for $u = 1$ and symmetrically squeezed in both modes. The covariance matrix $\boldsymbol{V}$ and the polynomial function F that define the Wigner function via Eq. (2) take the form, $\boldsymbol{V} = \frac{1}{2}\mathrm{diag}(e^{-2r}, e^{2r}, e^{-2r}, e^{2r})$, and

$$\begin{aligned} F(\boldsymbol{x}) = {} & 2\cosh^2(r)\big(\big(x_1^2 + p_1^2\big)|\alpha|^2 + \big(x_2^2 + p_2^2\big)|\beta|^2 \\ & + 2\mathrm{Re}((x_1 - ip_1)(x_2 + ip_2)\alpha^*\beta)\big) \\ & + 2\sinh^2(r)\big(\big(x_1^2 + p_1^2\big)|\alpha|^2 + \big(x_2^2 + p_2^2\big)|\beta|^2 \\ & + 2\mathrm{Re}((x_1 + ip_1)(x_2 - ip_2)\alpha^*\beta)\big) \\ & - 4\cosh(r)\sinh(r)(|\alpha p_1 + \beta p_2|^2 - |\alpha x_1 + \beta x_2|^2) - 1. \end{aligned} \tag{27}$$

In [20] it is shown that the PPT criterion based on the second-order correlations fails to unveil the entanglement of this state for $r = 0$, what makes this state particularly interesting to demonstrate the strength of the hierarchy. Remarkably enough, Fig. 2 shows that expression (12) is able to detect this purely non-Gaussian entanglement in agreement with [20]. Figure 2 corresponds to a specific choice of the phases of the complex parameters α and β, but we found $\tau_{2,2}$ to perform equally well for any other choice of phases.

C. Time evolution of an initially non-Gaussian entangled state

Finally, the tractable form of the hierarchy (12) also permits one to study the time evolution of the k-partite entanglement under the influence of environmental noise. Let us investigate how the two-mode non-Gaussian entanglement of the foregoing example is influenced when each mode is in contact with an independent heat bath. To be specific we assume the environmental coupling of both modes to be modeled with the same rate γ, and both baths to have the same temperature characterized by the mean photon number $N_{\rm th}$. The open

system dynamics is governed by a Fokker-Plank equation in the interaction picture [see Eq. (D1) in Appendix D], which has been extensively employed to study the effects of losses and thermal hopping in CV systems [55].

The time-dependent Wigner function is obtained from the Green function of the Fokker-Plank equation (see Appendix D for further details). In the interaction picture, one finds that the covariance matrix evolves according to

$$\boldsymbol{V}(t) = \boldsymbol{\varepsilon}(t) + \boldsymbol{\sigma}(t), \tag{28}$$

with

$$\boldsymbol{\varepsilon}(t) = \frac{e^{-\gamma t}}{2}\boldsymbol{V}(0), \quad \boldsymbol{\sigma}(t) = (1 - e^{-\gamma t})\boldsymbol{V}_{(N_{\rm th},0)},$$

where $\boldsymbol{V}(0) = \frac{1}{2}\mathrm{diag}(e^{-2r}, e^{2r}, e^{-2r}, e^{2r})$, $\boldsymbol{V}_{(N_{\rm th},0)} = \frac{1+2N_{\rm th}}{2}(\boldsymbol{I} \oplus \boldsymbol{I})$, and the polynomial part $F(\boldsymbol{x},t)$ is given by

$$F(\boldsymbol{x},t) = F(e^{\frac{\gamma}{2}t}[\boldsymbol{\varepsilon}^{-1}(t)\boldsymbol{\sigma}(t) + \boldsymbol{I}_2]^{-1}\boldsymbol{x}) + \frac{1}{2}\sum_{l,m}(\boldsymbol{\varepsilon}^{-1}(t) + \boldsymbol{\sigma}^{-1}(t))^{-1}_{lm}\frac{\partial^2 F(e^{\frac{\gamma}{2}t}\boldsymbol{x})}{\partial[\boldsymbol{x}]_l \partial[\boldsymbol{x}]_m}\bigg|_{\boldsymbol{x}=\vec{0}}, \tag{29}$$

For $t = 0$, Eq. (29) returns the initial expression Eq. (27) for the state ($F(\boldsymbol{x},0) = F(\boldsymbol{x})$), whereas in the long time ($F(\boldsymbol{x},t \to \infty) \to 1$) the system evolves asymptotically into the symmetrical separable thermal (Gaussian) state.

One may appreciate from Fig. 3 that the initial non-Gaussian entanglement is degraded *asymptotically* in time: The hierarchies shows that the two-mode entanglement features an exponential decay.

This example illustrates that Eq. (12) may provide an accurate description of multipartite CV entanglement in realistic dissipative scenarios. As the hierarchy deals with Gaussian and non-Gaussian states at the same footing, Eq. (12) is particularly of interest to study the time evolution of k-partite entanglement when the state evolves from Gaussian to non-Gaussian, or vice versa.

V. EXPERIMENTAL QUANTIFICATION

Let us now briefly discuss how the hierarchies (12) and (19) can be assessed with experimental data. The standard procedure would be based on the experimental reconstruction of the Wigner function in terms of quantum state tomography [56,57] or a measurement scheme especially designed for multicomponent CV systems [58], followed by the analytical evaluation of Eqs. (12) and (19). However, the hierarchies for Gaussian states (19) may be also directly accessed by performing Gaussian measurements, modeled in terms of positive-valued operators with the Gaussian Weyl symbol [27,59], which will be characterized by a covariance matrix $\boldsymbol{\sigma}_M$ and first-moment vector $\boldsymbol{X}_M$ that plays the role of the outcome of the measurement. If one performs such a measurement on the whole n-mode system, the probability of the outcome $\boldsymbol{X}_M$ is given by [59]

$$p(\boldsymbol{X}_M; \boldsymbol{\sigma}_M) = \frac{e^{-\frac{1}{2}\boldsymbol{X}_M^T \frac{1}{\boldsymbol{\sigma}_M + \boldsymbol{V}}\boldsymbol{X}_M}}{(2\pi)^n\sqrt{\det(\boldsymbol{\sigma}_M + \boldsymbol{V})}}.$$

One may immediately identify the terms in the sum in Eq. (19) as $(2\pi)^n p(\boldsymbol{P}_j\boldsymbol{X}; \boldsymbol{\Sigma})$, since these terms are derived from diagonal matrix elements [see Eqs. (A2) and (A3)]. On the other hand, the first term in Eq. (19), which results from off-diagonal matrix elements [see Eq. (A1)], may be expressed in terms of the Fourier transform $\hat{p}(\boldsymbol{\omega}; \boldsymbol{\Sigma})$ of the probability distribution $p(\boldsymbol{X}; \boldsymbol{\Sigma})$, i.e.,

$$\hat{p}(\boldsymbol{\omega}; \boldsymbol{\Sigma}) = \frac{1}{(2\pi)^n}\int_{\mathbb{R}^{2n}} d^{2n}\boldsymbol{X} e^{-i\boldsymbol{\omega}^T\boldsymbol{X}} p(\boldsymbol{X}; \boldsymbol{\Sigma}),$$

such that Eq. (19) may be brought in the form,

$$\tilde{\tau}_{k,n}(\hat{\rho}) = e^{-2\boldsymbol{X}^T\boldsymbol{J}_n^T\boldsymbol{\Sigma}\boldsymbol{J}_n\boldsymbol{X}}\int_{\mathbb{R}^{2n}} d^{2n}\boldsymbol{\omega} e^{-2\boldsymbol{\omega}^T\boldsymbol{\Sigma}\boldsymbol{J}_n\boldsymbol{X}}\hat{p}(\boldsymbol{\omega}; \boldsymbol{\Sigma}) - (2\pi)^n\sum_j a_j^{(k,n)} p(\boldsymbol{P}_j\boldsymbol{X}; \boldsymbol{\Sigma}), \tag{30}$$

as we extensively show in Appendix E. This expression relates $\tilde{\tau}_{k,n}$ directly to the measurement statistics of a Gaussian measurement with covariance matrix $\boldsymbol{\Sigma}$.

Since the projection of $\hat{\rho}$ onto a one-mode pure infinitely squeezed state [whose covariance matrix we illustrate in (C2)] models an (ideal) homodyne measure in the mth mode of the system [57,60,61], the results of Sec. III A indicate that one may *completely* certify the inseparability of arbitrary two-mode and pure three-mode Gaussian states by a collective of simultaneous (ideal) homodyne measures on each mode of the system.

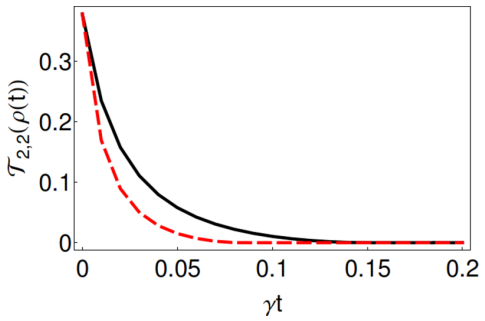

FIG. 3. (Color online) Time evolution of $\mathcal{T}_{2,2}(\hat{\rho}(t))$ when the system is initially in the CPS-TSVS state plotted in Fig. 2 with $|\alpha| = 0.5$, and it is in contact with independent thermal reservoirs with $N_{\rm th} = 2$ (black solid line) and with $N_{\rm th} = 4$ (red dashed line).

VI. CONCLUDING REMARKS AND OUTLOOK

The strength of the hierarchy as demonstrated by the explicit examples in Sec IV and the prospect to obtain a fine-grained characterization of multimode entanglement properties even for non-Gaussian states based only on Gaussian measurements underlines the practical value of the separability criteria presented here. In particular, the recent development of optomechanical experiments [62,63] that permit the realization of controlled interactions between massive degrees of freedom [64] and light call for tools that permit one to verify experimental achievements. Whereas experiments on continuous-variable entangled systems were in the realm of Gaussian states for a long time, this new generation of experiments permits one

to realize sizable nonlinear interactions which result in the generation of non-Gaussian entangled states.

This prospect to create and probe entangled states that were out of reach until recently, highlights the demand for theoretical tools for the analysis of entanglement properties beyond the Gaussian theory. In particular with the capacity to probe entanglement properties also in multimode systems, the present separability criteria promise to be a valuable theoretical support for a series of experiments to come.

ACKNOWLEDGMENTS

The authors acknowledge useful discussions with D. Alonso, and Ł. Rudnicki. A.A.V would like to thank D. Alonso and S. Kohler for their wise advice, and he is grateful to C. Dittrich, J. Pähle, and the group of "Coherent many-body quantum dynamics" at the Freiburg Institute for Advanced Studies for their warm hospitality throughout his visit in Freiburg. Financial support from the European Research Council under the project Odycquent, and from the Spanish MICINN (Grant No. FIS2010-19998) are gratefully acknowledged. A.A.V. acknowledges financial support from the Government of the Canary Islands through an ACIISI fellowship (85% co-financed by the European Social Fund), and from Vicerectorado de Investigación de la Universidad de La Laguna.

APPENDIX A: DERIVATION OF EQ. (12)

In this Appendix we illustrate the derivation of expression (12) starting from the formulation Eq. (6) of the hierarchy $\tau_{k,n}(\hat{\rho})$ in $\mathcal{H}_n$. The latter involves the following three matrix elements:

$$\langle\Phi_1|\hat{\rho}|\Phi_2\rangle, \tag{A1}$$

$$\langle\Phi_{1j}|\hat{\rho}|\Phi_{1j}\rangle, \tag{A2}$$

$$\langle\Phi_{2j}|\hat{\rho}|\Phi_{2j}\rangle, \tag{A3}$$

with $|\Phi_1\rangle$, $|\Phi_2\rangle$, $|\Phi_{1j}\rangle$, and $|\Phi_{2j}\rangle$ defined in Eqs. (4) and (5). One may compute these matrix elements by using the trace product rule [65],

$$\begin{aligned}\langle\boldsymbol{\phi}|\hat{\rho}|\boldsymbol{\psi}\rangle &= \mathrm{Tr}(\hat{\rho}|\boldsymbol{\psi}\rangle\langle\boldsymbol{\phi}|)\\ &= (2\pi)^n\int d^{2n}\boldsymbol{x}\, W(\boldsymbol{x})W_{|\boldsymbol{\psi}\rangle\langle\boldsymbol{\phi}|}(\boldsymbol{x}).\end{aligned} \tag{A4}$$

Hence, we must first derive the Weyl symbol $W_{|\Phi_2\rangle\langle\Phi_1|}$ corresponding to the n-fold tensor product operator $|\Phi_2\rangle\langle\Phi_1| = \bigotimes_{m=1}^{n}|\varphi_{n+m}\rangle\langle\varphi_m|$. According to the definition in Eq. (1), this may be expressed as

$$W_{|\Phi_2\rangle\langle\Phi_1|}(\boldsymbol{x}) = \prod_{m=1}^{n} W_{|\varphi_{n+m}\rangle\langle\varphi_m|}(q,p). \tag{A5}$$

Moreover, $W_{|\varphi_{n+m}\rangle\langle\varphi_m|}$ may be directly derived by using the classical formulation of the Wigner function [65], and the expression for the wave function of any single-mode pure Gaussian state, i.e.,

$$\phi_m(q) = \sqrt{\frac{2\sigma_{pp}^{(m)}}{\pi\left(1+4\left(\sigma_{xp}^{(m)}\right)^2\right)}}\, e^{-\frac{\sigma_{pp}^{(m)}(q-\bar{q}_m)^2}{1+2i\sigma_{xp}^{(m)}}+iq\bar{p}_m}.$$

Doing so, one arrives at the Gaussian function,

$$W_{|\varphi_l\rangle\langle\varphi_m|}(q,p) = N_{m,l}e^{-\frac{1}{2}((q,p)-\boldsymbol{X}_{m,l})^T\boldsymbol{\Sigma}_{m,l}^{-1}((q,p)-\boldsymbol{X}_{m,l}))}, \tag{A6}$$

with first-moment $\boldsymbol{X}_{m,l} = 1/2((\bar{q}_m,\bar{p}_m)+(\bar{q}_l,\bar{p}_l))^T + i\boldsymbol{\Sigma}_{m,l}\boldsymbol{J}_1((\bar{q}_m,\bar{p}_m)-(\bar{q}_l,\bar{p}_l))^T$ and the covariance matrix as given in Eq. (10), where the absolute value of the normalizing factor is given by

$$|N_{m,l}| = \frac{e^{\frac{-1}{4\det(\boldsymbol{\Sigma}_m+\boldsymbol{\Sigma}_l)}((\boldsymbol{X}^-)^T\boldsymbol{J}_1^T(\boldsymbol{\Sigma}_m+\boldsymbol{\Sigma}_l)\boldsymbol{J}_1\boldsymbol{X}^-)}}{\pi\sqrt[4]{\det(\boldsymbol{\Sigma}_m+\boldsymbol{\Sigma}_l)}},$$

with $\boldsymbol{X}^- = (\bar{q}_m,\bar{p}_m)-(\bar{q}_l,\bar{p}_l)$. Notice that, from Eq. (10) it is deduced that $\boldsymbol{\Sigma}_{\Phi_{21}}$ is a complex symmetric matrix which in general is not Hermitian. One may follow the same recipe to obtain the other Weyl symbols corresponding to the operators $|\Phi_{1j}\rangle\langle\Phi_{1j}|$, and $|\Phi_{2j}\rangle\langle\Phi_{2j}|$.

By virtue of the trace product rule (A4), the matrix element (A1) takes the form,

$$\begin{aligned}\langle\Phi_1|\hat{\rho}|\Phi_2\rangle &= \frac{N_{\Phi_{21}}}{\sqrt{\det(\boldsymbol{V})}}\int_{\mathbb{R}^{2n}} d^{2n}\boldsymbol{x}\; F(\boldsymbol{x})e^{-\frac{1}{2}\boldsymbol{x}^T\boldsymbol{V}^{-1}\boldsymbol{x}}e^{-\frac{1}{2}(\boldsymbol{x}-\boldsymbol{X}_{\Phi_{21}})^T\boldsymbol{\Sigma}_{\Phi_{21}}^{-1}(\boldsymbol{x}-\boldsymbol{X}_{\Phi_{21}})}\\ &= \frac{N_{\Phi_{21}}}{\sqrt{\det(\boldsymbol{V})}}\int_{\mathbb{R}^{2n}} d^{2n}\boldsymbol{x}\Big(F(\boldsymbol{x})e^{\frac{1}{2}(\boldsymbol{x}^T\boldsymbol{\Sigma}_{\Phi_{21}}^{-1}\boldsymbol{X}_{\Phi_{21}}+\boldsymbol{X}_{\Phi_{21}}^T\boldsymbol{\Sigma}_{\Phi_{21}}^{-1}\boldsymbol{x}-\boldsymbol{X}_{\Phi_{21}}^T\boldsymbol{\Sigma}_{\Phi_{21}}^{-1}\boldsymbol{X}_{\Phi_{21}})}\Big)e^{-\frac{1}{2}\boldsymbol{x}^T(\boldsymbol{V}^{-1}+\boldsymbol{\Sigma}_{\Phi_{21}}^{-1})\boldsymbol{x}}\\ &= \frac{(2\pi)^n N_{\Phi_{21}}e^{-\frac{1}{2}\boldsymbol{X}_{\Phi_{21}}^T\boldsymbol{\Sigma}_{\Phi_{21}}^{-1}\boldsymbol{X}_{\Phi_{21}}}}{\sqrt{\det\left(\boldsymbol{V}^{-1}+\boldsymbol{\Sigma}_{\Phi_{21}}^{-1}\right)\det(\boldsymbol{V})}}\Big[e^{\frac{1}{2}(\frac{\partial}{\partial\boldsymbol{x}})^T(\boldsymbol{V}^{-1}+\boldsymbol{\Sigma}_{\Phi_{21}}^{-1})^{-1}(\frac{\partial}{\partial\boldsymbol{x}})}\Big(F(\boldsymbol{x})e^{\boldsymbol{X}_{\Phi_{21}}^T\boldsymbol{\Sigma}_{\Phi_{21}}^{-1}\boldsymbol{x}}\Big)\Big]_{\boldsymbol{x}=\vec{0}},\end{aligned}$$

where we made use of the symmetry property of the pseudocovariance matrix $\boldsymbol{\Sigma}_{\Phi_{21}} = \boldsymbol{\Sigma}_{\Phi_{21}}^T$. In this expression, $\boldsymbol{x}$ is a $2n$-dimensional real vector. Since the exponential of the differential operator describes a shift in phase space (see Appendix E), we can conveniently manipulate this expression to obtain

$$\langle\Phi_2|\hat{\rho}|\Phi_1\rangle = \frac{\pi^n N_{\Phi_{21}}e^{-\frac{1}{2}\boldsymbol{X}_{\Phi_{21}}^T\boldsymbol{\Sigma}_{\Phi_{21}}^{-1}\boldsymbol{X}_{\Phi_{21}}}}{\sqrt{\det\left(\boldsymbol{V}+\boldsymbol{\Sigma}_{\Phi_{21}}\right)}}\Big[e^{\frac{1}{2}(\frac{\partial}{\partial\boldsymbol{x}}+\boldsymbol{\Sigma}_{\Phi_{21}}^{-1}\boldsymbol{X}_{\Phi_{21}})^T(\boldsymbol{V}^{-1}+\boldsymbol{\Sigma}_{\Phi_{21}}^{-1})^{-1}(\frac{\partial}{\partial\boldsymbol{x}}+\boldsymbol{\Sigma}_{\Phi_{21}}^{-1}\boldsymbol{X}_{\Phi_{21}})}F(\boldsymbol{x})\Big]_{\boldsymbol{x}=\vec{0}}. \tag{A7}$$

Similarly, one may derive the analog expression for the matrix elements given in Eqs. (A2) and (A3) by substituting the pair $\boldsymbol{X}_{\Phi_{21}}$, $\boldsymbol{\Sigma}_{\Phi_{21}}$ for the corresponding pair $\boldsymbol{X}_{\Phi_{1j}}$, $\boldsymbol{\Sigma}_{\Phi_{1j}}$, and $\boldsymbol{X}_{\Phi_{2j}}$, $\boldsymbol{\Sigma}_{\Phi_{2j}}$ in Eq. (A7) (and by taking $N_{\Phi_{21}}$ equal to π^{-n}). After replacing the result for each matrix element in Eq. (6) and some straightforward algebra, one arrives at expression Eq. (12) for the hierarchy that is valid as long as the Wigner function of the system can be expressed as in Eq. (2).

APPENDIX B: FIRST-MOMENT VECTORS AND COVARIANCE MATRICES ASSOCIATED WITH THE BIPARTITION J

In this Appendix we describe in more detail how to obtain the vectors $\boldsymbol{X}_{\Phi_{1j}}$ and $\boldsymbol{X}_{\Phi_{2j}}$, and the matrices $\boldsymbol{\Sigma}_{\Phi_{1j}}$, $\boldsymbol{\Sigma}_{\Phi_{2j}}$, and $\boldsymbol{P}_j$ associated with the bipartition labeled by j. In Sec. II, we stated that $|\Phi_{1j}\rangle$ and $|\Phi_{2j}\rangle$ are obtained from $|\Phi_1\rangle$ and $|\Phi_2\rangle$ by interchanging the one-mode states $|\varphi_m\rangle$ with $|\varphi_{m+n}\rangle$ corresponding to those subsystems that are grouped together in the bipartition j [see Eq. (5)]. On the other hand, from Eqs. (11) and (10) one obtains that the first-moment vectors of $|\Phi_1\rangle$ and $|\Phi_2\rangle$ are given by

$$\boldsymbol{X}_{\Phi_1} = \bigoplus_{m=1}^{n} \bar{\boldsymbol{x}}_m, \tag{B1}$$

$$\boldsymbol{X}_{\Phi_2} = \bigoplus_{m=1}^{n} \bar{\boldsymbol{x}}_{n+m}, \tag{B2}$$

and the covariance matrices are given by

$$\boldsymbol{\Sigma}_{\Phi_1} = \bigoplus_{m=1}^{n} \boldsymbol{\Sigma}_m, \tag{B3}$$

$$\boldsymbol{\Sigma}_{\Phi_2} = \bigoplus_{m=1}^{n} \boldsymbol{\Sigma}_{n+m}. \tag{B4}$$

Analogously, one may deduce the covariance matrices $\boldsymbol{\Sigma}_{\Phi_{1j}}$ and $\boldsymbol{\Sigma}_{\Phi_{2j}}$ by permuting the corresponding matrices $\boldsymbol{\Sigma}_m$ and $\boldsymbol{\Sigma}_{n+m}$ in the expressions (B3) and (B4), respectively. Doing so, one obtains

$$\boldsymbol{\Sigma}_{\Phi_{1j}} = \bigoplus_{m=1}^{n} \boldsymbol{\Sigma}_{m+n[\boldsymbol{v}_j]_m}, \tag{B5}$$

$$\boldsymbol{\Sigma}_{\Phi_{2j}} = \bigoplus_{m=1}^{n} \boldsymbol{\Sigma}_{m+n-n[\boldsymbol{v}_j]_m}. \tag{B6}$$

The same reasoning may be applied to derive the first-moment vectors, where one interchanges the corresponding vectors $\bar{\boldsymbol{x}}_m$ and $\bar{\boldsymbol{x}}_{n+m}$ in Eqs. (B1) and (B2). These permutations may be expressed in a compact way with the matrix P defined in Eq. (17), such that $\boldsymbol{X}_{\Phi_{1j}}$ and $\boldsymbol{X}_{\Phi_{2j}}$ may be written as [52]

$$\boldsymbol{X}_{\Phi_{1j}} = \frac{\boldsymbol{X}_{\Phi_1} + \boldsymbol{X}_{\Phi_2}}{2} + \frac{1}{2}\boldsymbol{P}_j\big(\boldsymbol{X}_{\Phi_1} - \boldsymbol{X}_{\Phi_2}\big), \tag{B7}$$

$$\boldsymbol{X}_{\Phi_{2j}} = \frac{\boldsymbol{X}_{\Phi_1} + \boldsymbol{X}_{\Phi_2}}{2} - \frac{1}{2}\boldsymbol{P}_j\big(\boldsymbol{X}_{\Phi_1} - \boldsymbol{X}_{\Phi_2}\big). \tag{B8}$$

APPENDIX C: RESEMBLANCE TO THE PPT CRITERION

1. Two-mode Gaussian case

The standard form of the covariance matrix of any two-mode Gaussian state reads [7]

$$\boldsymbol{V} = \frac{1}{2}\begin{pmatrix} a & 0 & c & 0 \\ 0 & a & 0 & d \\ c & 0 & b & 0 \\ 0 & d & 0 & b \end{pmatrix}, \quad \{a,b,c,d\} \in \mathbb{R}^4, \tag{C1}$$

whereas the covariance matrix of a one-mode pure squeezed state may be expressed as follows:

$$\boldsymbol{\Sigma}(r) = \operatorname{diag}\left(\frac{1}{4r}, r\right), \tag{C2}$$

where r is the squeezing parameter.

After substituting Eqs. (C1) and (C2) in the expression for the matrix (23), one obtains that the latter takes the following form:

$$\boldsymbol{Z}_1(r) = \begin{pmatrix} \frac{(1+2ar)(a(b+2r)-d^2)-4cdr^2}{(a+2r)(b+2r)-d^2} & 0 & \frac{2r(2r(ad-bc)+d(1+cd)-abc)}{(a+2r)(b+2r)-d^2} & 0 \\ 0 & \frac{(a+2r)(a(1+2rb)-2rc^2)-cd}{(1+2ar)(1+2br)-4c^2r^2} & 0 & \frac{2r(c(1+cd)-abd)+ac-bd}{(1+2ar)(1+2br)-4c^2r^2} \\ \frac{2r(2r(bd-ac)+d(1+cd)-abc)}{(a+2r)(b+ar)-d^2} & 0 & \frac{(1+2br)(b(a+2r)-d^2)-4cdr^2}{(a+2r)(b+2r)-d^2} & 0 \\ 0 & \frac{2r(c(1+cd)-abd)+bc-ad}{(1+2ar)(1+2br)-4c^2r^2} & 0 & \frac{(b+2r)(b(1+2ra)-2rc^2)-cd}{(1+2ar)(1+2br)-4c^2r^2} \end{pmatrix}. \tag{C3}$$

As one may see, the entries of the matrix $\boldsymbol{Z}_1(r)$ are rational functions in terms of the squeezing parameter r, and the limit $r \to 0$ reads

$$\lim_{r\to 0} \boldsymbol{Z}_1(r) = \begin{pmatrix} 1 & 0 & 0 & 0 \\ 0 & a^2-cd & 0 & ac-bd \\ 0 & 0 & 1 & 0 \\ 0 & bc-ad & 0 & b^2-cd \end{pmatrix}. \tag{C4}$$

Similarly, one may derive the expression for $\boldsymbol{Z}_1(r)$ in the limit $r \to \infty$, which corresponds to an infinite squeezing in position. Doing so, one may replace r in (C3) by $1/r$, and then take the limit $r \to 0$, i.e.,

$$\lim_{r\to 0} \boldsymbol{Z}_1\left(\frac{1}{r}\right) = \begin{pmatrix} a^2-cd & 0 & -bc+ad & 0 \\ 0 & 1 & 0 & 0 \\ -ac+bd & 0 & b^2-cd & 0 \\ 0 & 0 & 0 & 1 \end{pmatrix}. \tag{C5}$$

Both (C4) and (C5) have $\lambda_z^{(1)} = \lambda_z^{(1)} = 1$ as a doubly degenerate eigenvalue. The other two eigenvalues are given by $\lambda_z^{(3)} = 4\tilde{\nu}_1^2$ and $\lambda_z^{(3)} = 4\tilde{\nu}_1^2$, as we point out in Sec. III A. This illustrates that the hierarchy expressed in terms of the inequality (20) reproduces the results of the PPT criterion when we choose infinitely squeezed probe states either in momentum or position.

2. Three-mode Gaussian case

The standard form of a pure three-mode Gaussian state reads [7]

$$\boldsymbol{V} = \frac{1}{2}\begin{pmatrix} a_1 & 0 & e_{12}^{+} & 0 & e_{13}^{+} & 0 \\ 0 & a_1 & 0 & e_{12}^{-} & 0 & e_{13}^{-} \\ e_{12}^{+} & 0 & a_2 & 0 & e_{23}^{+} & 0 \\ 0 & e_{12}^{-} & 0 & a_2 & 0 & e_{23}^{-} \\ e_{13}^{+} & 0 & e_{23}^{+} & 0 & a_3 & 0 \\ 0 & e_{13}^{-} & 0 & e_{23}^{-} & 0 & a_3 \end{pmatrix}, \tag{C6}$$

where $a_1,a_2,a_3 \in \mathbb{R}$, and $e_{12}^{\pm}$, $e_{13}^{\pm}$, $e_{23}^{\pm}$ are simple functions of a_1,a_2, and a_3.

The characteristic polynomial reads $\lambda^6 + \tilde{\Delta}_1^3\lambda^4 + \tilde{\Delta}_2^3\lambda^2 + \tilde{\Delta}_3^3 = 0$, and the symplectic invariants $\{\tilde{\Delta}_l^3\}$ $(l = 1,2,3)$ are obtained from [21]

$$\tilde{\Delta}_l^3 = M_{2l}\left(\boldsymbol{J}_3^T\tilde{\boldsymbol{V}}_1^2\right),$$

where $M_{2l}(\boldsymbol{J}_3^T\tilde{\boldsymbol{V}}_1^2)$ is the principal minor of order $2l$ of the matrix $\boldsymbol{J}_3^T\tilde{\boldsymbol{V}}_1^2$, i.e., it is the sum of all the determinants of all the $2l \times 2l$ submatrices obtained by deleting $6-2l$ rows and the corresponding $6-2l$ columns [21]. Since one has to follow the same procedure for each bipartition, we illustrate here only the case for $S_1|S_2S_3$, where S_m symbolizes the mth mode $(m = 1,2,3)$. Although the whole expression of $\boldsymbol{Z}_{S_1|S_2S_3}(r)$ is straightforwardly derived from (23) by replacing $\boldsymbol{\Sigma}_m = \boldsymbol{\Sigma}(r)$ for $m = 1,2,3$ (its entries are again rational functions in terms of the squeezing parameter r), it is rather lengthy so that we only provide the final expression after taking the limit $r \to 0$,

$$\lim_{r\to 0}\boldsymbol{Z}_{S_1|S_2S_3}(r) = \begin{pmatrix} 1 & 0 & 0 & 0 & 0 & 0 \\ 0 & a_1^2 - e_{13}^{+}e_{13}^{-} - e_{12}^{+}e_{12}^{-} & 0 & a_1e_{12}^{+} - a_2e_{12}^{-} - e_{13}^{-}e_{23}^{+} & 0 & a_1e_{13}^{+} - a_3e_{13}^{-} - e_{12}^{-}e_{23}^{+} \\ 0 & 0 & 1 & 0 & 0 & 0 \\ 0 & a_2e_{12}^{+} - a_1e_{12}^{-} + e_{13}^{+}e_{23}^{-} & 0 & a_2^2 - e_{12}^{+}e_{12}^{-} + e_{23}^{+}e_{23}^{-} & 0 & a_2e_{23}^{+} + a_3e_{23}^{-} - e_{12}^{-}e_{13}^{+} \\ 0 & 0 & 0 & 0 & 1 & 0 \\ 0 & a_3e_{13}^{+} - a_1e_{13}^{-} + e_{12}^{+}e_{23}^{-} & 0 & a_3e_{23}^{+} + a_2e_{23}^{-} - e_{13}^{-}e_{12}^{+} & 0 & a_3^2 - e_{13}^{+}e_{13}^{-} + e_{23}^{-}e_{23}^{+} \end{pmatrix}. \tag{C7}$$

This matrix has $\lambda_z^{(1)} = \lambda_z^{(2)} = \lambda_z^{(3)} = 1$ as a three-times degenerate eigenvalue, and the other eigenvalues are the roots of the polynomial,

$$-\left(\frac{\lambda_z}{4}\right)^3 + \tilde{\Delta}_1^3\left(\frac{\lambda_z}{4}\right)^2 - \tilde{\Delta}_2^3\left(\frac{\lambda_z}{4}\right) + \tilde{\Delta}_3^3 = 0. \tag{C8}$$

As we have already seen for the two-mode case, the roots of the characteristic polynomial of $\boldsymbol{J}_3^T\tilde{\boldsymbol{V}}_1^2$ are related to those of (C8) through the expression $\lambda = \pm i\sqrt{\lambda_z}/2$. Hence, the inequality (20) applied in the bipartition $S_1|S_2S_3$ reproduces the PPT criterion for pure three-mode Gaussian states.

Analogously, one may show that this assertion holds for the other bipartitions $S_2|S_1S_3$ and $S_3|S_1S_2$. Now the roots of the corresponding characteristic polynomial are $\{1,1,1,4\tilde{\nu}_{S_2|S_1S_3,1}^2, 4\tilde{\nu}_{S_2|S_1S_3,2}^2, 4\tilde{\nu}_{S_2|S_1S_3,3}^2\}$ and $\{1,1,1,4\tilde{\nu}_{S_3|S_1S_2,1}^2, 4\tilde{\nu}_{S_3|S_1S_2,2}^2, 4\tilde{\nu}_{S_3|S_1S_2,3}^2\}$, in terms of the symplectic eigenvalues of the partially transpose covariance matrix corresponding to the bipartitions $S_2|S_1S_3$ and $S_3|S_1S_2$, respectively.

Once again, it is important to note that the assertion also holds for infinite squeezing in position ($r \to \infty$). One gets at the following matrix for $\boldsymbol{Z}_1(r)$, which is analog to (C7),

$$\lim_{r\to 0}\boldsymbol{Z}_{S_1|S_2S_3}\left(\frac{1}{r}\right) = \begin{pmatrix} a_1^2 - e_{13}^{+}e_{13}^{-} - e_{12}^{+}e_{12}^{-} & 0 & a_1e_{12}^{-} - a_2e_{12}^{+} - e_{13}^{+}e_{23}^{-} & 0 & a_1e_{13}^{-} - a_3e_{13}^{+} - e_{12}^{+}e_{23}^{-} & 0 \\ 0 & 1 & 0 & 0 & 0 & 0 \\ a_2e_{12}^{-} - a_1e_{12}^{+} + e_{13}^{-}e_{23}^{+} & 0 & a_2^2 - e_{12}^{+}e_{12}^{-} + e_{23}^{+}e_{23}^{-} & 0 & a_2e_{23}^{-} + a_3e_{23}^{+} - e_{12}^{+}e_{13}^{-} & 0 \\ 0 & 0 & 0 & 1 & 0 & 0 \\ a_3e_{13}^{-} - a_1e_{13}^{+} + e_{12}^{-}e_{23}^{+} & 0 & a_3e_{23}^{-} + a_2e_{23}^{+} - e_{13}^{+}e_{12}^{-} & 0 & a_3^2 - e_{13}^{+}e_{13}^{-} + e_{23}^{-}e_{23}^{+} & 0 \\ 0 & 0 & 0 & 0 & 0 & 1 \end{pmatrix}, \tag{C9}$$

from which one obtains the same characteristic polynomial as given in (C8).

APPENDIX D: TIME EVOLUTION OF THE WIGNER FUNCTION

We consider the time evolution of an n-mode system governed by the Fokker-Plank equation in the interaction picture [55,66],

$$\frac{\partial W(\boldsymbol{x},t)}{\partial t} = \left(\left(\frac{\partial}{\partial \boldsymbol{x}}\right)^T \boldsymbol{\Gamma}\boldsymbol{x} + \left(\frac{\partial}{\partial \boldsymbol{x}}\right)^T \boldsymbol{D}\frac{\partial}{\partial \boldsymbol{x}}\right) W(\boldsymbol{x},t), \tag{D1}$$

with $(\frac{\partial}{\partial \boldsymbol{x}})^T = \bigoplus_{l=1}^{n}(\frac{\partial}{\partial q_l}, \frac{\partial}{\partial p_l})$; $\boldsymbol{\Gamma}$ and $\boldsymbol{D}$ are $2n \times 2n$ real symmetric matrices that encode the interaction with the environment. In the case of interest here, these take the form $\boldsymbol{\Gamma} = \gamma/2(\boldsymbol{I} \oplus \boldsymbol{I})$ and $\boldsymbol{D} = \gamma(1 + 2N_{\text{th}})/4(\boldsymbol{I} \oplus \boldsymbol{I})$, where N_{th} is the mean photon number of the baths.

Equation (D1) is a linear Fokker-Plank equation with time-independent coefficients that can be straightforwardly solved by using the Green function method [67], that permit one to relate $W(\boldsymbol{x},t)$ and $W(\boldsymbol{x},0)$ via

$$W(\boldsymbol{x},t) = \int_{\mathbb{R}^{2n}} d^{2n}\boldsymbol{x}'\; W(\boldsymbol{x}',0)G(\boldsymbol{x},\boldsymbol{x}',t), \tag{D2}$$

in terms of the Green function $G(\boldsymbol{x},\boldsymbol{x}',t)$ which takes the form (see [67,68]),

$$G(\boldsymbol{x},\boldsymbol{x}',t) = \frac{1}{(2\pi)^n\sqrt{\det(\boldsymbol{\sigma}(t))}} e^{-\frac{1}{2}(\boldsymbol{x}-\boldsymbol{b}(t)\boldsymbol{x}')^T\boldsymbol{\sigma}(t)^{-1}(\boldsymbol{x}-\boldsymbol{b}(t)\boldsymbol{x}')}, \tag{D3}$$

where

$$\boldsymbol{b}(t) = e^{-\boldsymbol{\Gamma}t}, \quad \boldsymbol{\sigma}(t) = \boldsymbol{\sigma}(\infty) - e^{-\boldsymbol{\Gamma}t}\boldsymbol{\sigma}(\infty)e^{-\boldsymbol{\Gamma}t},$$

and $\boldsymbol{\sigma}(\infty)$ is the stationary solution of Eq. (D1), which is obtained from solving

$$\boldsymbol{\Gamma}\boldsymbol{\sigma}(\infty) + \boldsymbol{\sigma}(\infty)\boldsymbol{\Gamma} = 2\boldsymbol{D}.$$

The integration of expression (D2) with the Wigner function $W(\boldsymbol{x},0)$ of the CPS-TSVS state results in the solutions depicted in Eqs. (28) and (29).

APPENDIX E: EXPERIMENTAL QUANTIFICATION

In this section we will show the derivation of the following identity:

$$\begin{aligned}\langle\Phi_1|\hat{\rho}|\Phi_2\rangle &= (2\pi)^n \int_{\mathbb{R}^{2n}} d^{2n}\boldsymbol{x}\; W(\boldsymbol{x})W_{|\Phi_2\rangle\langle\Phi_1|}(\boldsymbol{x}) \\ &= e^{-2X^T\boldsymbol{J}_n^T\boldsymbol{\Sigma}\boldsymbol{J}_n X}\int_{\mathbb{R}^{2n}} d^{2n}\boldsymbol{\omega}\; e^{-2\omega^T\boldsymbol{\Sigma}\boldsymbol{J}_n X}\,\hat{p}(\boldsymbol{\omega};\boldsymbol{\Sigma}),\end{aligned} \tag{E1}$$

which has been used to obtain Eq. (30) of Sec. V. To start with, the probability distribution $p(\boldsymbol{X};\boldsymbol{\Sigma})$, corresponding a Gaussian measurement with covariance matrix $\boldsymbol{\Sigma}$ and first-moment vector $\boldsymbol{X}$ on an n-mode system with Wigner function $W(\boldsymbol{x})$, is given by

$$p(\boldsymbol{X};\boldsymbol{\Sigma}) = \int_{\mathbb{R}^{2n}} d^{2n}\boldsymbol{x}\; W(\boldsymbol{x})\frac{e^{-\frac{1}{2}(\boldsymbol{x}-\boldsymbol{X})^T\boldsymbol{\Sigma}^{-1}(\boldsymbol{x}-\boldsymbol{X})}}{(2\pi)^n\sqrt{\det(\boldsymbol{\Sigma})}}. \tag{E2}$$

Introducing a unitary transformation $\boldsymbol{U}$, such that $\boldsymbol{D} = \boldsymbol{U}^T\boldsymbol{\Sigma}\boldsymbol{U}$ (or $\boldsymbol{D}^{-1} = \boldsymbol{U}^T\boldsymbol{\Sigma}^{-1}\boldsymbol{U}$) is a diagonal matrix, permits one to rephrase this as

$$p(\boldsymbol{U}\tilde{\boldsymbol{X}};\boldsymbol{D}) = \int_{\mathbb{R}^{2n}} d^{2n}\tilde{\boldsymbol{x}}\; W(\boldsymbol{U}\tilde{\boldsymbol{x}})\frac{e^{-\frac{1}{2}(\tilde{\boldsymbol{x}}-\tilde{\boldsymbol{X}})^T\boldsymbol{D}^{-1}(\tilde{\boldsymbol{x}}-\tilde{\boldsymbol{X}})}}{(2\pi)^n\sqrt{\det(\boldsymbol{D})}},$$

with $\boldsymbol{x} = \boldsymbol{U}\tilde{\boldsymbol{x}}$ and $\boldsymbol{X} = \boldsymbol{U}\tilde{\boldsymbol{X}}$, where we have used $d^{2N}\tilde{\boldsymbol{x}} = d^{2N}\boldsymbol{x}$ since the Jacobian determinant $|\det(\boldsymbol{U})| = 1$. From here it becomes clear that $p(\boldsymbol{X};\boldsymbol{\Sigma})$ can be considered a multidimensional convolution transform with a Gaussian kernel, and its inverse formula is well established [69]. Using the latter for Eq. (E2), one obtains

$$W(\boldsymbol{X}) = \exp\left(-\frac{1}{2}\left(\frac{\partial}{\partial \boldsymbol{X}}\right)^T\boldsymbol{\Sigma}\left(\frac{\partial}{\partial \boldsymbol{X}}\right)\right)p(\boldsymbol{X};\boldsymbol{\Sigma}).$$

We may derive a more suitable form for this expression by using the Fourier transform of the Dirac delta function, that is,

$$\begin{aligned}W(\boldsymbol{x}) &= \exp\left(-\frac{1}{2}\left(\frac{\partial}{\partial \boldsymbol{x}}\right)^T\boldsymbol{\Sigma}\left(\frac{\partial}{\partial \boldsymbol{x}}\right)\right)\int_{\mathbb{R}^{2n}} d^{2n}\boldsymbol{u}\; p(\boldsymbol{u};\boldsymbol{\Sigma})\delta(\boldsymbol{x}-\boldsymbol{u}) \\ &= \frac{1}{(2\pi)^{2n}}\int_{\mathbb{R}^{2n}}\int_{\mathbb{R}^{2n}} d^{2n}\boldsymbol{u}d^{2n}\boldsymbol{\omega}\; p(\boldsymbol{u};\boldsymbol{\Sigma})\exp\left(-\frac{1}{2}\left(\frac{\partial}{\partial \boldsymbol{x}}\right)^T\boldsymbol{\Sigma}\left(\frac{\partial}{\partial \boldsymbol{x}}\right)\right)\exp(i\boldsymbol{\omega}^T(\boldsymbol{x}-\boldsymbol{u})) \\ &= \frac{1}{(2\pi)^{2n}}\int_{\mathbb{R}^{2n}}\int_{\mathbb{R}^{2n}} d^{2n}\boldsymbol{u}d^{2n}\boldsymbol{\omega}\; p(\boldsymbol{u};\boldsymbol{\Sigma})\exp\left(\frac{1}{2}\boldsymbol{\omega}^T\boldsymbol{\Sigma}\boldsymbol{\omega}\right)\exp(i\boldsymbol{\omega}^T(\boldsymbol{x}-\boldsymbol{u})).\end{aligned} \tag{E3}$$

On the other hand, the phase-space counterpart of $|\Phi_2\rangle\langle\Phi_1|$ is given by

$$W_{|\Phi_2\rangle\langle\Phi_1|}(\boldsymbol{x}) = \frac{1}{(2\pi)^n\sqrt{\det(\boldsymbol{\Sigma})}} e^{-2X^T\boldsymbol{J}_n^T\boldsymbol{\Sigma}\boldsymbol{J}_n X} e^{-\frac{1}{2}(\boldsymbol{x}-2i\boldsymbol{\Sigma}\boldsymbol{J}_n X)^T\boldsymbol{\Sigma}^{-1}(\boldsymbol{x}-2i\boldsymbol{\Sigma}\boldsymbol{J}_n X)}, \tag{E4}$$

according to Eqs. (A5) and (A6) in Appendix A. By replacing Eqs. (E3) and (E4) in the expression for the matrix element (E1), one obtains

$$\begin{aligned}
\langle\Phi_1|\hat{\rho}|\Phi_2\rangle &= (2\pi)^n \int_{\mathbb{R}^{2n}} d^{2n}\boldsymbol{x}\; W(\boldsymbol{x}) W_{|\Phi_2\rangle\langle\Phi_1|}(\boldsymbol{x}) \\
&= \frac{1}{(2\pi)^n} \int_{\mathbb{R}^{2n}} \int_{\mathbb{R}^{2n}} d^{2n}\boldsymbol{\omega} d^{2n}\boldsymbol{u}\; p(\boldsymbol{u};\boldsymbol{\Sigma}) e^{-i\boldsymbol{\omega}^T\boldsymbol{u}} e^{\frac{1}{2}\boldsymbol{\omega}^T\boldsymbol{\Sigma}\boldsymbol{\omega}} e^{-2\boldsymbol{X}^T\boldsymbol{J}_n^T\boldsymbol{\Sigma}\boldsymbol{J}_n\boldsymbol{X}} \\
&\quad \times \frac{1}{(2\pi)^n\sqrt{\det(\boldsymbol{\Sigma})}} \int_{\mathbb{R}^{2n}} d^{2n}\boldsymbol{x}\; e^{i\boldsymbol{\omega}^T\boldsymbol{x}} e^{-\frac{1}{2}(\boldsymbol{x}-2i\boldsymbol{\Sigma}\boldsymbol{J}_n\boldsymbol{X})^T\boldsymbol{\Sigma}^{-1}(\boldsymbol{x}-2i\boldsymbol{\Sigma}\boldsymbol{J}_n\boldsymbol{X})} \qquad \text{(E5)} \\
&= \frac{1}{(2\pi)^n} \int_{\mathbb{R}^{2n}} \int_{\mathbb{R}^{2n}} d^{2n}\boldsymbol{\omega} d^{2n}\boldsymbol{u}\; p(\boldsymbol{u};\boldsymbol{\Sigma}) e^{-i\boldsymbol{\omega}^T\boldsymbol{u}} e^{\frac{1}{2}\boldsymbol{\omega}^T\boldsymbol{\Sigma}\boldsymbol{\omega}} \frac{1}{(2\pi)^n\sqrt{\det(\boldsymbol{\Sigma})}} \int_{\mathbb{R}^{2n}} d^{2n}\boldsymbol{x}\; e^{-\frac{1}{2}\boldsymbol{x}^T\boldsymbol{\Sigma}^{-1}\boldsymbol{x}+i(\boldsymbol{\omega}+2\boldsymbol{J}_n\boldsymbol{X})^T\boldsymbol{x}} \qquad \text{(E6)} \\
&= \frac{1}{(2\pi)^n} \int_{\mathbb{R}^{2n}} \int_{\mathbb{R}^{2n}} d^{2n}\boldsymbol{\omega} d^{2n}\boldsymbol{u}\; p(\boldsymbol{u};\boldsymbol{\Sigma}) e^{-i\boldsymbol{\omega}^T\boldsymbol{u}} e^{\frac{1}{2}\boldsymbol{\omega}^T\boldsymbol{\Sigma}\boldsymbol{\omega}} (e^{-\frac{1}{2}(\boldsymbol{\omega}+2\boldsymbol{J}_n\boldsymbol{X})^T\boldsymbol{\Sigma}(\boldsymbol{\omega}+2\boldsymbol{J}_n\boldsymbol{X})}) \qquad \text{(E7)} \\
&= e^{-2\boldsymbol{X}^T\boldsymbol{J}_n^T\boldsymbol{\Sigma}\boldsymbol{J}_n\boldsymbol{X}} \int_{\mathbb{R}^{2n}} d^{2n}\boldsymbol{\omega}\; e^{-2\boldsymbol{\omega}^T\boldsymbol{\Sigma}\boldsymbol{J}_n\boldsymbol{X}} \left(\frac{1}{(2\pi)^n} \int_{\mathbb{R}^{2n}} d^{2n}\boldsymbol{u}\; e^{-i\boldsymbol{\omega}^T\boldsymbol{u}} p(\boldsymbol{u};\boldsymbol{\Sigma}) \right), \qquad \text{(E8)}
\end{aligned}$$

as we wanted to show. To derive Eq. (E8), one can separate the $\boldsymbol{x}$-dependent function from functions that depend on $\boldsymbol{\omega}$ and $\boldsymbol{u}$ only. Using $\boldsymbol{\Sigma} = \boldsymbol{\Sigma}^T$, one then arrives at Eq. (E6). Performing the integration of $\boldsymbol{x}$ results in Eq. (E7); rearranging terms yields to the desired form Eq. (E8). Substituting the explicit expression $p(\boldsymbol{u};\boldsymbol{\Sigma}) = \frac{\exp(-\frac{1}{2}\boldsymbol{u}^T(\boldsymbol{V}+\boldsymbol{\Sigma})^{-1}\boldsymbol{u})}{(2\pi)^n\sqrt{\det(\boldsymbol{V}+\boldsymbol{\Sigma})}}$ in Eq. (E8), and performing the integrals, we recover

$$|\langle\Phi_1|\hat{\rho}|\Phi_2\rangle| = \frac{e^{-2\boldsymbol{X}^T\boldsymbol{J}_n^T\frac{1}{\boldsymbol{\Sigma}^{-1}+\boldsymbol{V}^{-1}}\boldsymbol{J}_n\boldsymbol{X}}}{\sqrt{\det(\boldsymbol{\Sigma}+\boldsymbol{V})}},$$

which is the first term in Eq. (19).

[1] R. Horodecki, P. Horodecki, M. Horodecki, and K. Horodecki, Rev. Mod. Phys. **81**, 865 (2009).
[2] L.-M. Duan, G. Giedke, J. I. Cirac, and P. Zoller, Phys. Rev. Lett. **84**, 2722 (2000).
[3] R. Simon, Phys. Rev. Lett. **84**, 2726 (2000).
[4] R. F. Werner and M. M. Wolf, Phys. Rev. Lett. **86**, 3658 (2001).
[5] G. Giedke, B. Kraus, M. Lewenstein, and J. I. Cirac, Phys. Rev. Lett. **87**, 167904 (2001); Phys. Rev. A **64**, 052303 (2001).
[6] G. Adesso, A. Serafini, and F. Illuminati, Phys. Rev. A **73**, 032345 (2006).
[7] G. Adesso and F. Illuminati, J. Phys. A: Math. Theor. **40**, 7821 (2007); G. Adesso, S. Ragy, and A. R. Lee, Open Syst. Inf. Dyn. **21**, 1440001 (2014).
[8] A. Gabriel, M. Huber, S. Radic, and B. C. Hiesmayr, Phys. Rev. A **83**, 052318 (2011).
[9] L. Z. Jiang, X. Y. Chen, P. Yu, and M. Tian, Phys. Rev. A **89**, 012332 (2014).
[10] M. M. Wolf, G. Giedke, O. Kruger, R. F. Werner, and J. I. Cirac, Phys. Rev. A **69**, 052320 (2004).
[11] G. Adesso, D. Girolami, and A. Serafini, Phys. Rev. Lett. **109**, 190502 (2012).
[12] P. Hyllus and J. Eisert, New J. Phys. **8**, 51 (2006).
[13] F. Mintert, Phys. Rev. A **75**, 052302 (2007).
[14] S. P. Walborn, B. G. Taketani, A. Salles, F. Toscano, and R. L. de Matos Filho, Phys. Rev. Lett. **103**, 160505 (2009); D. S. Tasca, L. Rudnicki, R. M. Gomes, F. Toscano, and S. P. Walborn, *ibid.* **110**, 210502 (2013).
[15] A. Saboia, F. Toscano, and S. P. Walborn, Phys. Rev. A **83**, 032307 (2011).
[16] H. Nha, S.-Y. Lee, S.-W. Ji, and M. S. Kim, Phys. Rev. Lett. **108**, 030503 (2012).
[17] C. Zhang, S. Yu, Q. Chen, and C.H. Oh, Phys. Rev. Lett. **111**, 190501 (2013).
[18] J. Sperling and W. Vogel, Phys. Rev. Lett. **111**, 110503 (2013); Phys. Rev. A **79**, 022318 (2009).
[19] P. van Loock and A. Furusawa, Phys. Rev. A. **67**, 052315 (2003).
[20] G. S. Agarwal and A. Biswas, New J. Phys. **7**, 211 (2005).
[21] A. Serafini, Phys. Rev. Lett. **96**, 110402 (2006).
[22] M. Hillery and M. S. Zubairy, Phys. Rev. Lett. **96**, 050503 (2006); Z.-G. Li, S.-M. Fei, Z.-X. Wang, and K. Wu, Phys. Rev. A **75**, 012311 (2007); M. Hillery, H. T. Dung, and H. Zheng, *ibid.* **81**, 062322 (2010).
[23] H. Nha and J. Kim, Phys. Rev. A **74**, 012317 (2006); H. Nha, *ibid.* **76**, 014305 (2007); J. Gillet, T. Bastin, and G. S. Agarwal, *ibid.* **78**, 052317 (2008); R. Namiki, *ibid.* **85**, 062307 (2012).
[24] Q. Sun, H. Nha, and M. S. Zubairy, Phys. Rev. A **80**, 020101 (2009).
[25] E. Shchukin and W. Vogel, Phys. Rev. Lett. **95**, 230502 (2005); Phys. Rev. A **74**, 030302 (2006); A. Miranowicz and M. Piani, Phys. Rev. Lett. **97**, 058901 (2006); see also A. Miranowicz, M. Piani, P. Horodecki, and R. Horodecki, Phys. Rev. A **80**, 052303 (2009).
[26] H. Nha and M. S. Zubairy, Phys. Rev. Lett. **101**, 130402 (2008).
[27] J. Eisert and M. B. Plenio, Int. J. Quantum. Inform. **01**, 479 (2003).
[28] Y. Huang, New J. Phys. **16**, 033027 (2014).

[29] L. Li, Y. O. Dudin, and A. Kuzmich, Nature (London) **498**, 466 (2013); A. Dousse *et al.*, *ibid.* **466**, 217 (2010).
[30] D. Leibfried *et al.*, Nature (London) **438**, 639 (2005).
[31] H. Häffner *et al.*, Nature (London) **438**, 643 (2005).
[32] L. K. Shalm, D. R. Hammel, Z. Yan, C. Simon, K. J. Resch, and T. Jennewein, Nature Physics **9**, 19 (2013).
[33] M. Bourennane, M. Eibl, C. Kurtsiefer, S. Gaertner, H. Weinfurter, O. Gühne, P. Hyllus, D. Bruß, M. Lewenstein, and Anna Sanpera, Phys. Rev. Lett **92**, 087902 (2004).
[34] O. Gühne, G. Tóth, and H. J. Briegel, New J. Phys. **7**, 229 (2005).
[35] G. Vitagliano, P. Hyllus, I. L. Egusquiza, and G. Tóth, Phys. Rev. Lett. **107**, 240502 (2011).
[36] F. Levi and F. Mintert, Phys. Rev. Lett. **110**, 150402 (2013).
[37] M. Huber, M. Perarnau-Llobet, and J. I. de Vicente, Phys. Rev. A **88**, 042328 (2013).
[38] M. S. Kim, J. Phys. B: At. Mol. Opt. Phys. **41**, 133001 (2008).
[39] A. Kitagawa, M. Takeoka, M. Sasaki, and A. Chefles, Phys. Rev. A **73**, 042310 (2006).
[40] Y. Yang and F.-L. Li, Phy. Rev. A **80**, 022315 (2009).
[41] C. Navarrete-Benlloch, R. García-Patrón, J. H. Shapiro, and N. J. Cerf, Phys. Rev. A **86**, 012328 (2012).
[42] T. J. Bartley, P. J. D. Crowley, A. Datta, J. Nunn, L. Zhang, and I. Walmsley, Phys. Rev. A **87**, 022313 (2013).
[43] H.-J. Kim, J. Kim, and H. Nha, Phys. Rev. A **88**, 032109 (2013).
[44] P. Chowdhury, T. Pramanik, A. S. Majumdar, and G. S. Agarwal, Phys. Rev. A **89**, 012104 (2014).
[45] A. Perelomov, *Generalized Coherent States and their Applications* (Springer-Verlag, Berlin, 1986).
[46] C. Weedbrok, S. Pirandola, R. García-Patrón, N. J. Cerf, T. C. Ralph, J. H. Shapiro, and S. Lloyd, Rev. Mod. Phys. **84**, 621 (2012).
[47] G. S. Agarwal, New J. Phys. **13**, 073008 (2011).
[48] L. Y. Hu, F. Jia, and Z. M. Zhang, J. Opt. Soc. Am. B **29**, 1456 (2012).
[49] Y. J. Xu and X. G. Meng, Int. J. Theor. Phys. **52**, 3066 (2013).
[50] Q. Guo, L. Huang, L. Y. Hu, X. X. Xu, and H. L. Zhang, Int. J. Theor. Phys. **52**, 2886 (2013).
[51] M. Huber, F. Mintert, A. Gabriel, and B. C. Hiesmayr, Phys. Rev. Lett. **104**, 210501 (2010).
[52] F. Mintert and E. J. Heller, Europhys. Lett. **86**, 50006 (2009).
[53] K. R. Petersen and M. S. Pedersen, *The Matrix Cookbook* (Technical University of Denmark, Lyngby, 2012).
[54] R. A. Horn and C. R. Johnson, *Matrix Analysis* (Cambridge University Press, Cambridge, 1985).
[55] A. Serafini, F. Illuminati, M. G. A. Paris, and S. De Siena, Phys. Rev. A **69**, 022318 (2004); A. Serafini, M. G. A. Paris, F. Illuminati, and S. De Siena, J. Opt. B: Quantum Semiclass. Opt. **7**, R19 (2005).
[56] J. Rehacek, S. Olivares, D. Mogilevtsev, Z. Hradil, M. G. A. Paris, S. Fornaro, V. DAuria, A. Porzio, and S. Solimeno, Phys. Rev. A **79**, 032111 (2009).
[57] A. I. Lvovsky and M. G. Raymer, Rev. Mod. Phys. **81**, 299 (2009).
[58] T. Tufarelli, A. Ferraro, M. S. Kim, and S. Bose, Phys. Rev. A **85**, 032334 (2012).
[59] S. Olivares, Eur. Phys. Special Topics **203**, 3 (2012).
[60] J. Eisert, S. Scheel, and M. B. Plenio, Phys. Rev. Lett. **89**, 137903 (2002).
[61] G. Giedke and J. I. Cirac, Phys. Rev. A **66**, 032316 (2002).
[62] S. Gröblacher, K. Hammerer, M. R. Vanner, and M. Aspelmeyer, Nature (London) **460**, 724 (2009).
[63] G. A. Brawley *et al.*, arXiv:1404.5746.
[64] M. Aspelmeyer, T. J. Kippenberg, and F. Marquardt, arXiv:1303.0733.
[65] W. P. Schleich, *Quantum Optics in Phase Spaces* (Wiley-VCH Verlag, Berlin, 2001).
[66] H. Risken, *The Fokker-Planck Equation: Methods of Solution and Applications* (Springer-Verlag, Berlin, 1996).
[67] H. J. Carmichael, *Statistical Methods in Quantum Optics* (Springer-Verlag, New York, 2002).
[68] G. S. Agarwal, Phys. Rev. A **4**, 739 (1971).
[69] A. D. Polyanin and A. V. Manzhirov, *Handbook of Mathematics for Engineers and Scientist* (Chapmam Hall/CRC, Taylor Francis Group, Boca Raton, 2007).

Article 2

GAUSSIAN ENTANGLEMENT INDUCED BY AN EXTENDED THERMAL ENVIRONMENT

Antonio A. Valido, Daniel Alonso, and Sigmund Kohler

Phys. Rev. A 88, 042303 (2013)

PHYSICAL REVIEW A **88**, 042303 (2013)

Gaussian entanglement induced by an extended thermal environment

Antonio A. Valido,[1,2,*] Daniel Alonso,[1,3,†] and Sigmund Kohler[4,‡]

[1]*Instituto Universitario de Estudios Avanzados (IUdEA), Universidad de La Laguna, La Laguna 38203, Spain*

[2]*Departamento de Física Fundamental II, Universidad de La Laguna, La Laguna 38203, Spain*

[3]*Departamento de Física Fundamental, Experimental, Electrónica y Sistemas, Universidad de La Laguna, La Laguna 38203, Spain*

[4]*Instituto de Ciencia de Materiales de Madrid, CSIC, Cantoblanco, 28049 Madrid, Spain*

(Received 17 July 2013; published 3 October 2013)

We study stationary entanglement between three harmonic oscillators which are dipole coupled to a one-dimensional or a three-dimensional bosonic environment. The analysis of the open-system dynamics is performed with generalized quantum Langevin equations which we solve exactly in a Fourier representation. The focus lies on Gaussian bipartite and tripartite entanglement induced by the highly non-Markovian interaction mediated by the environment. This environment-induced interaction represents an effective many-party interaction with a spatial long-range feature: A main finding is that the presence of a passive oscillator is detrimental for stationary two-mode entanglement. Furthermore, our results indicate that the environment-induced entanglement mechanism corresponds to uncontrolled feedback which is predominantly coherent at low temperatures and for moderate oscillator-environment coupling as compared to the oscillator frequency.

DOI: 10.1103/PhysRevA.88.042303 PACS number(s): 03.67.Mn, 03.65.Yz, 03.67.Bg, 42.50.Lc

I. INTRODUCTION

Entanglement is a subtle feature of composite quantum systems, which is invariant under local operations, i.e., operations that act solely upon one constituent. Not considering protocols for entanglement swapping, entangling two subsystems requires an interaction between them [1]. Such an interaction need not be direct, but may be mediated by a further quantum system or even a heat bath, despite the fact that environmental degrees of freedom generally cause decoherence [2], which is detrimental to entanglement. For example, the interaction with a common heat bath can entangle two otherwise uncoupled systems even in the weakly dissipative Markovian regime [3–6] by making use of decoherence-free subspaces that include entangled states [7–11] or by correlated quantum noise that provides non-Markovian effects [12–16]. Also more involved system-environment interactions such as an exponential-like coupling [17,18], as well as dissipative engineering techniques [19], have been proposed for this issue. Given these multifaceted behaviors, it is intriguing to investigate entanglement between quantum systems in a more general dissipative scenario.

In the present paper, we investigate the setup sketched in Fig. 1and explore the influence of thermal relaxation on the creation of stationary entanglement between three independent oscillators whose equilibrium positions are spatially separated, such that the indirect interaction mediated by the bath is retarded. In particular we address two issues. The first one is the bath-induced entanglement formation between two oscillators in the presence of a further oscillator. The second one is the characterization of the resulting stationary tripartite entanglement. We investigate both one-dimensional (1D) and three-dimensional (3D) environments, where the former is restricted to a linear arrangement of the three oscillators. Our model does not possess decoherence-free subspaces and thus any emerging entanglement must stem from the environment-mediated interaction which at the same time induces decoherence and quantum dissipation. A most important feature of an extended environment is its dispersion relation which implies a finite signal transmission velocity and thus causes retardation effects. They may lead to an entanglement decay in several stages [7,11] or to a limiting distance for bath-induced two-mode entanglement [13]. Moreover, the dissipative quantum dynamics acquires an additional non-Markovian influence, which in our case is rather crucial because otherwise each oscillator would eventually reach its own Gibbs state and thus the total state would be separable.

Our paper is organized as follows. In Sec. II we define our model and derive within a quantum Langevin approach the main expressions and concepts used later for the numerical computations, which are presented and discussed in Sec. III. There two-mode and three-mode entanglement is studied as a function of the main parameters of the model. Conclusions are drawn in Sec. IV. Some rather lengthy derivations have been deferred to the Appendixes.

II. THE MODEL SYSTEM AND EQUILIBRIUM STATE

We employ a generalized Caldeira-Leggett model [20–22] to capture thermal relaxation of the oscillators, which can be derived from first principles [23,24]. We focus on the resulting stationary Gaussian entanglement that stems from the quadratic form of the Hamiltonian. The microscopic model will be approximately quadratic if the oscillators remain in their equilibrium positions (which is compatible with the presence of the environment-interaction effects), such that we can take the long-wave approximation at lowest order. The choice of a Gaussian initial state for the reservoir guarantees the Gaussian nature of the final stationary state. We assume a sudden switch-on of the interaction between the oscillators and the bath, such that the initial state of the full system (oscillator modes plus environment) is a product state $\rho_0 = \rho \otimes \rho_B$.

*aavalido@ull.es
†dalonso@ull.es
‡sigmund.kohler@icmm.csic.es

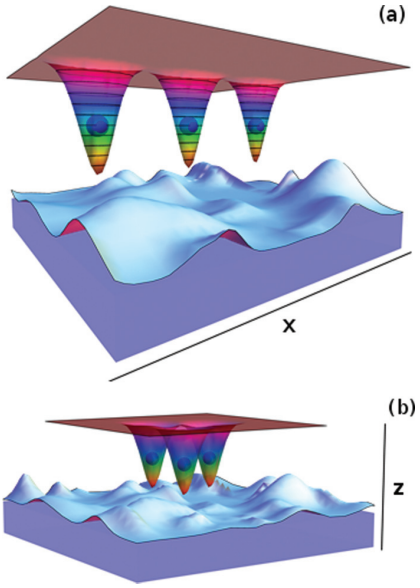

FIG. 1. (Color online) Oscillator-environment configuration considered in this paper. Three oscillators are confined to the direction indicated by the arrow; in the 1D arrangement (a) the oscillators move only in the x direction, while in the 3D configuration (b), the oscillators move only along the z direction. The interaction between the oscillators is mediated by a bosonic field, which also causes decoherence and quantum dissipation.

In the case of a system composed by N harmonic modes, a Gaussian state is determined up to irrelevant local displacements by the four $N \times N$ correlation matrices

$$C_{\boldsymbol{AB}}(t-t') = \tfrac{1}{2}\langle \boldsymbol{A}(t)\boldsymbol{B}^T(t') + \boldsymbol{B}(t')\boldsymbol{A}^T(t)\rangle_\rho,$$

with $\boldsymbol{A},\boldsymbol{B} \in \{\boldsymbol{X},\boldsymbol{P}\}$ and where $\boldsymbol{X}$ and $\boldsymbol{P}$ denote column vectors with the position and momentum operators of the oscillators. Thus, the stationary state is characterized by the $2N \times 2N$ covariance matrix

$$G = \begin{bmatrix} C_{\boldsymbol{XX}}(0) & C_{\boldsymbol{XP}}(0) \\ C_{\boldsymbol{PX}}(0) & C_{\boldsymbol{PP}}(0) \end{bmatrix}, \tag{1}$$

which contains the full information about the system fluctuations. To compute $C_{\boldsymbol{AB}}$, we employ the quantum Langevin equation formalism widely used in the study of Brownian motion [22,25], which we adapt to our case of an extended environment. Regarding the study of entanglement, remarkable achievements have been reported concerning its classification and quantification for Gaussian states [26,27]. Recently a similar analysis has been carried out for three identical harmonic oscillators in an equilateral triangular arrangement that are directly coupled and in contact with a common bosonic field at zero temperature [28]. In the opposite scenario of infinitely separated oscillators, each is surrounded by independent environments, possibly at different temperatures, which affects the entanglement [29].

A. Generalized Langevin equation

We consider three harmonic oscillators located at $\boldsymbol{R}_\lambda = \boldsymbol{r}^0_\lambda + \boldsymbol{r}_\lambda$, where $\lambda = 1,2,3$, while $\boldsymbol{r}^0_\lambda$ and $\boldsymbol{r}_\lambda$ denote equilibrium positions and displacements, respectively. We attribute to each displacement a conjugate momentum $\boldsymbol{p}_\lambda$, and employ the notations $\boldsymbol{r}_\lambda := (x_\lambda, y_\lambda, z_\lambda)$ and $\boldsymbol{p}_\lambda := (p_{x,\lambda}, p_{y,\lambda}, p_{z,\lambda})$. The oscillators are assumed to be independent of each other with anisotropic confinement. This situation can be modeled by coupling the oscillators to a free bosonic field. Following the above considerations, we model our setup by the system-bath Hamiltonian $H_0 = H_S + H_B + H_I$, with the system and the bath contributions

$$H_S = \sum_{\lambda=1}^{3}\left[\frac{\boldsymbol{p}_\lambda^2}{2m_\lambda} + \frac{1}{2}m_\lambda\left(\omega_{x,\lambda}^2 x_\lambda^2 + \omega_{y,\lambda}^2 y_\lambda^2 + \omega_{z,\lambda}^2 z_\lambda^2\right)\right], \tag{2}$$

$$H_B = \sum_{\boldsymbol{k}} \hbar\omega_{\boldsymbol{k}} a^\dagger_{\boldsymbol{k}} a_{\boldsymbol{k}}, \tag{3}$$

respectively, where $a^\dagger_{\boldsymbol{k}}$ and $a_{\boldsymbol{k}}$ are the usual bosonic creation and annihilation operators for the bath mode with wave vector $\boldsymbol{k} = (2\pi/L)\mathbb{Z}^D$. We assume that only one degree of freedom per oscillator is coupled to the bosonic field and thus experiences decoherence. While in 1D, this assumption appears natural, it can be realized in the 3D case by a strong anisotropy, $\omega_{x,\lambda} \ll \omega_{y,\lambda}, \omega_{z,\lambda}$, such that the motion in the y and z directions is frozen and can be ignored. The interaction between the central oscillators and the environment then takes the form

$$H_I = -\sum_{\lambda=1}^{3} x_\lambda \sum_{\boldsymbol{k}} g_{\boldsymbol{k}}(a_{\boldsymbol{k}} e^{i\boldsymbol{k}\cdot\boldsymbol{R}_\lambda} + a^\dagger_{\boldsymbol{k}} e^{-i\boldsymbol{k}\cdot\boldsymbol{R}_\lambda}), \tag{4}$$

with the coupling constants $g_{\boldsymbol{k}}$ [7]. A technically important simplification is provided by the assumption that $e^{i\boldsymbol{k}\cdot\boldsymbol{r}_\lambda} \ll 1$, which physically corresponds to the long-wave limit or the dipole approximation for which we find

$$H_I \cong -\sum_{\lambda=1}^{3} x_\lambda \sum_{\boldsymbol{k}} g_{\boldsymbol{k}}(a_{\boldsymbol{k}} e^{i\boldsymbol{k}\cdot\boldsymbol{r}^0_\lambda} + a^\dagger_{\boldsymbol{k}} e^{-i\boldsymbol{k}\cdot\boldsymbol{r}^0_\lambda}). \tag{5}$$

When coupling the bosonic field to the oscillators a counterterm must be added if one desires to preserve the bare oscillator potential of Eq. (3). Finally, the full oscillator-environment Hamiltonian $H_B + H_I \to H_{BI}$ becomes

$$H_{BI} = \sum_{\boldsymbol{k}} \frac{1}{2m_{\boldsymbol{k}}}\left[p_{\boldsymbol{k}} + g_{\boldsymbol{k}}\sqrt{\frac{2m_{\boldsymbol{k}}}{\hbar\omega_{\boldsymbol{k}}}}\sum_{\lambda=1}^{3} x_\lambda \sin\left(\boldsymbol{k}\cdot\boldsymbol{r}^0_\lambda\right)\right]^2 + \sum_{\boldsymbol{k}} \frac{m_{\boldsymbol{k}}\omega_{\boldsymbol{k}}^2}{2}\left[x_{\boldsymbol{k}} - \frac{g_{\boldsymbol{k}}}{\omega_{\boldsymbol{k}}^2}\sqrt{\frac{2\omega_{\boldsymbol{k}}}{m_{\boldsymbol{k}}\hbar}}\sum_{\lambda=1}^{3} x_\lambda \cos\left(\boldsymbol{k}\cdot\boldsymbol{r}^0_\lambda\right)\right]^2. \tag{6}$$

We have introduced the usual bosonic annihilation operator $a_{\boldsymbol{k}} = (m_{\boldsymbol{k}}\omega_{\boldsymbol{k}} x_{\boldsymbol{k}} + i\, p_{\boldsymbol{k}})/\sqrt{2\hbar m_{\boldsymbol{k}}\omega_{\boldsymbol{k}}}$ and its adjoint $a^\dagger_{\boldsymbol{k}}$. The coupling together with the counterterms in our Hamiltonian (6) can be interpreted as minimal coupling theory with $U(1)$ gauge symmetry [24]. Moreover, in field theoretical terms, the oscillators are coupled to the velocity of the bosonic field [23], which guarantees that the energy remains positive definite and prevents "runaway" solutions [30].

Associated with Hamiltonian (6) are equations of motion for the degrees of freedoms of both the oscillators and the environment. The dynamics of those of the oscillators, conditioned to the environmental state, is given by a quantum Langevin equation which follows from the exact Heisenberg equation of motion for $\boldsymbol{X} := (x_1, x_2, x_3)$ and which, after tracing out the environmental degrees of freedoms, reads [22] (for details see Appendix A)

$$M\ddot{\boldsymbol{X}} + \phi\boldsymbol{X} + \frac{1}{\hbar}\int_{-\infty}^{t} d\tau\, \chi(t-\tau)\boldsymbol{X}(\tau) = \boldsymbol{F}(t), \tag{7}$$

where here the mass matrix M is proportional to the unit matrix, $M_{\lambda\mu} = m\delta_{\lambda\mu}$, while the counterterm $\tilde{\Omega}_{\lambda\mu}$ is part of the potential matrix $\phi_{\lambda\mu} = m\omega_\lambda^2\delta_{\lambda\mu} + 2\tilde{\Omega}_{\lambda\mu}$. The memory-friction kernel $\chi(t)$ has the form of a 3×3 matrix, and $\boldsymbol{F}$ is the column vector with the fluctuating forces $F(\boldsymbol{r}_\lambda^0, t) := F_\lambda(t)$ that act upon each oscillator. These forces depend on the position of the oscillators and the environment. Owing to their quantum nature, the forces are operators and commute with each other only for timelike separations, i.e., $[F_\lambda(t'), F_\mu(t)] = 0$ if $|\boldsymbol{r}_\lambda^0 - \boldsymbol{r}_\mu^0| > c|t-t'|$, where c is the sound velocity of the environment (or the speed of light, in a corresponding optical setup) which enters via the dispersion relation $\omega_{\boldsymbol{k}} = c|\boldsymbol{k}|$. It relates to the memory-friction kernel via the Kubo formula

$$\chi_{\lambda\mu}(t-t') = -i\left\langle [F_\lambda(t), F_\mu(t')]\right\rangle_{\rho_B}\Theta\left(t-t'-\left|\Delta\boldsymbol{r}_{\lambda\mu}^0\right|/c\right), \tag{8}$$

where the Heaviside step function Θ reflects causality with a retardation stemming from the distance $\Delta\boldsymbol{r}_{\lambda\mu}^0 := \boldsymbol{r}_\lambda^0 - \boldsymbol{r}_\mu^0$ between the oscillators λ and μ. The average has been taken with respect to the Gibbs state ρ_B with temperature T, which ensures the Gaussian property exploited below. In the frequency domain, the real part of the symmetrized forces correlation $F_\lambda(t)F_\mu(t')$ reads

$$\mathrm{Re}\langle \boldsymbol{F}(\omega)\boldsymbol{F}^T(\omega') + \boldsymbol{F}(\omega')\boldsymbol{F}^T(\omega)\rangle_{\rho_B} = 4\pi\hbar\delta(\omega+\omega')\Gamma(\omega), \tag{9}$$

with the matrix Γ defined by its elements

$$\begin{aligned}\Gamma_{\lambda\mu}(\omega) &= -\frac{1}{\hbar}\,\mathrm{Im}\,\chi_{\lambda\mu}(\omega)\coth\left(\frac{\hbar\omega}{2k_BT}\right)\\ &= J_{\lambda,\mu}(|\omega|)\coth\left(\frac{\hbar|\omega|}{2k_BT}\right).\end{aligned} \tag{10}$$

This expression relates the real part of $\langle[F_\lambda(t), F_\mu(t')]\rangle$ (commutator) to $\langle\{F_\lambda(t), F_\mu(t')\}\rangle$ (anticommutator), and thus implies a quantum fluctuation-dissipation relation for the force operators. Moreover, we have introduced the bath spectral density

$$J_{\lambda,\mu}(\omega) = \frac{\pi}{\hbar}\sum_{\boldsymbol{k}} g_{\boldsymbol{k}}^2\cos\left(\boldsymbol{k}\cdot\Delta\boldsymbol{r}_{\lambda\mu}^0\right)\delta\left(\omega-\omega_{\boldsymbol{k}}\right), \tag{11}$$

which allows us to write the renormalization terms in the convenient form

$$\begin{aligned}\tilde{\Omega}_{\lambda\lambda} &= \frac{1}{\hbar}\sum_{\boldsymbol{k}}\frac{g_{\boldsymbol{k}}^2}{\omega_{\boldsymbol{k}}} = \frac{1}{\pi}\int_0^\infty \frac{J_{\lambda,\lambda}(\omega)}{\omega}d\omega,\\ \tilde{\Omega}_{\lambda\mu} &= \frac{1}{\hbar}\sum_{\boldsymbol{k}}\frac{g_{\boldsymbol{k}}^2}{\omega_{\boldsymbol{k}}}\cos\left(\boldsymbol{k}\cdot\Delta\boldsymbol{r}_{\lambda\mu}^0\right) = \frac{1}{\pi}\int_0^\infty \frac{J_{\lambda,\mu}(\omega)}{\omega}d\omega.\end{aligned} \tag{12}$$

With these relations, we can express the impact of the bath on the oscillators and their effective interaction, as well as non-Markovian memory effects in terms of the spectral density (11).

The nondiagonal potential renormalization (12) couples the oscillator coordinates x_λ which thus are no longer the normal modes of our problem. Therefore, we introduce the transformation matrix O which maps to the normal modes of the coupled oscillators, $\boldsymbol{Q} = O\boldsymbol{X}$. Together with the according transformation for our matrices, we obtain for $\boldsymbol{Q}$ the Langevin equation

$$M\ddot{\boldsymbol{Q}} + \phi_D\boldsymbol{Q} + \frac{1}{\hbar}\int_{-\infty}^{t} d\tau\,\Xi(t-\tau)\boldsymbol{Q}(\tau) = \boldsymbol{D}(t), \tag{13}$$

with the invariant mass matrix $M = OMO^T$, the potential matrix $\phi_D = O\phi O^T$, the susceptibility $\Xi(t) = O\chi(t)O^T$, and the fluctuation forces $\boldsymbol{D}(t) = O\boldsymbol{F}(t)$, while the fluctuation-dissipation relation becomes

$$\mathrm{Re}\langle \boldsymbol{D}(\omega)\boldsymbol{D}^T(\omega') + \boldsymbol{D}(\omega')\boldsymbol{D}^T(\omega)\rangle_{\rho_B} = 4\pi\hbar\delta(\omega+\omega')\Upsilon(\omega),$$

with $\Upsilon(\omega) = -(1/\hbar)\,\mathrm{Im}\,\Xi(\omega) = O^T\Gamma(\omega)O$. While the conservative part of the transformed Langevin equation (13) is now diagonal, the modes may still couple via the dissipation kernel $\Xi(t)$, unless the latter is diagonal as well. This can be achieved if ϕ and $\chi(t)$ commute at all times, which is the case if all oscillators have the same fundamental frequencies and are equally spaced, i.e., ϕ and $\chi(t)$ commute when the equilibrium positions of the oscillators form a equilateral triangle ($\Delta\boldsymbol{r}_{\lambda\mu}^0 = R$ for all $\lambda \neq \mu$) because they are symmetric matrices and their product is also symmetric [28]. A further particular geometry is given when the oscillators are placed in an isosceles triangle. Then the normal mode corresponding to the relative motion of the oscillators placed at the ends of the unequal side of the triangle and the center-of-mass dynamics are independent of each other. We consider these distinct geometries in Sec. III. Furthermore, it follows from the rank-nullity theorem [31] that the evolution of all normal modes will be subject to dissipation and noise unless all oscillators have the same frequency and are at the same place. Then their relative coordinate forms a decoherence-free subspace [8,10]. In general, however, i.e., for any other geometry, the oscillator-bath Hamiltonian does not possess a decoherence-free subspace.

One may also compute the normal modes of the total Hamiltonian H_0, e.g., by the Fano diagonalization technique [32]. Since, owing to the counterterm, the oscillator-environment Hamiltonian (6) is positive definite, its eigenvalues are positive as well. This implies that the Hamiltonian does not have any localized mode that may induce a non-Markovian dynamics, as is the case for atomic cavities [32–34]. Indeed, our environmental noise is characterized by the bath spectral density, so that non-Markovian effects stem from a non-Ohmic frequency dependence.

Having developed the formal solution of the quantum Langevin equation (7), we are able to evaluate the covariance matrix (1) whose entries read

$$C_{\boldsymbol{XX}}(0) = \hbar\int\frac{d\omega}{2\pi}\alpha(\omega)\Gamma(\omega)\alpha(-\omega)^T, \tag{14}$$

$$C_{\boldsymbol{XP}}(0) = C_{\boldsymbol{PX}}(0) = m\hbar\int\frac{d\omega}{2\pi}i\omega\,\alpha(\omega)\Gamma(\omega)\alpha(-\omega)^T, \tag{15}$$

$$C_{\boldsymbol{PP}}(0) = m^2\hbar \int \frac{d\omega}{2\pi}\omega^2\,\alpha(\omega)\Gamma(\omega)\alpha(-\omega)^T, \tag{16}$$

where $\alpha(\omega)$ corresponds to the Fourier transformed of the left-hand side of the quantum Langevin equation (7). All the covariances contain the integration kernel $K(\omega) = \alpha(\omega)\Gamma(\omega)\alpha(-\omega)^T$, while from the quantum fluctuation-dissipation relation (9) it follows that $K(\omega)$ is completely characterized by the generalized spectral density $J_{\lambda,\mu}(\omega)$.

B. Generalized spectral density and integration kernel $K(\omega)$

We assume for the bosonic field the linear dispersion $\omega_{\boldsymbol{k}} = c|\boldsymbol{k}|$, which comprises the physical cases of acoustic phonons and a free electromagnetic field. Then it is possible to construct the spectral densities $J_{\lambda,\mu}(\omega)$ as a necessary step for computing the full covariance matrix (1). A detailed derivation for the expressions introduced in this section can be found in Appendix B.

We shall focus on 1D and 3D environments with isotropic coupling between the oscillators and the bosonic field. For the coupling we choose $g_{\boldsymbol{k}}^2 = m\hbar\gamma(\omega_{\boldsymbol{k}}/\omega_c^{d-1})c^d V_{\boldsymbol{k}}(d)e^{-\omega/\omega_c}$, where d is the dimension of the environment, $V_{\boldsymbol{k}}$ is the number of field modes per d-dimensional $\boldsymbol{k}$-space volume, γ is the coupling strength coupling, and ω_c is the cutoff frequency of the environmental spectrum. Eventually, the continuum limit $V_{\boldsymbol{k}} \to 0$ will be taken. Hence, we obtain the spectral densities

$$J_{\lambda,\mu}^{1\mathrm{D}}(\omega) = \pi m\gamma\omega e^{-\omega/\omega_c}\cos\left(\omega\left|\Delta\boldsymbol{r}_{\lambda\mu}^0\right|/c\right), \tag{17}$$

$$J_{\lambda,\mu}^{3\mathrm{D}}(\omega) = \frac{4\pi^2 mc}{\left|\Delta\boldsymbol{r}_{\lambda\mu}^0\right|}\left(\frac{\omega}{\omega_c}\right)^2 e^{-\omega/\omega_c}\sin\left(\omega\left|\Delta\boldsymbol{r}_{\lambda\mu}^0\right|/c\right). \tag{18}$$

Accordingly, the potential renormalizations become

$$\Omega_{\lambda\mu}^{1\mathrm{D}} = \frac{m\gamma\omega_c}{1+\left(\omega_c\left|\Delta\boldsymbol{r}_{\lambda\mu}^0\right|/c\right)^2}, \tag{19}$$

$$\Omega_{\lambda\mu}^{3\mathrm{D}} = \frac{8m\pi\gamma\omega_c}{\left[1+\left(\omega_c\left|\Delta\boldsymbol{r}_{\lambda\mu}^0\right|/c\right)^2\right]^2}. \tag{20}$$

The imaginary part of the susceptibilities follows by inserting the spectral densities into Eq. (10), while their real parts are conveniently obtained via the Kramers-Kronig relations, so that we obtain

$$\begin{aligned}\chi_{\lambda\mu}^{1\mathrm{D}}(t) &= 4m\,\gamma\,\hbar\,\omega_c^2\Theta\left(t-\left|\Delta\boldsymbol{r}_{\lambda\mu}^0\right|/c\right)\\ &\quad\times\frac{\omega_c\left|\Delta\boldsymbol{r}_{\lambda\mu}^0\right|/c - t\omega_c}{\left[1+\left(\omega_c\left|\Delta\boldsymbol{r}_{\lambda\mu}^0\right|/c - t\omega_c\right)^2\right]^2},\end{aligned} \tag{21}$$

$$\begin{aligned}\chi_{\lambda\mu}^{3\mathrm{D}}(t) &= 8\pi m\,\gamma\,\hbar\,\frac{\omega_c c}{\left|\Delta\boldsymbol{r}_{\lambda\mu}^0\right|}\Theta\left(t-\left|\Delta\boldsymbol{r}_{\lambda\mu}^0\right|/c\right)\\ &\quad\times\left(\frac{1-3\left(\omega_c\left|\Delta\boldsymbol{r}_{\lambda\mu}^0\right|/c + t\omega_c\right)^2}{\left[1+\left(\omega_c\left|\Delta\boldsymbol{r}_{\lambda\mu}^0\right|/c + t\omega_c\right)^2\right]^3}\right.\\ &\quad\left.-\frac{1-3\left(\omega_c\left|\Delta\boldsymbol{r}_{\lambda\mu}^0\right|/c - t\omega_c\right)^2}{\left[1+\left(\omega_c\left|\Delta\boldsymbol{r}_{\lambda\mu}^0\right|/c - t\omega_c\right)^2\right]^3}\right).\end{aligned} \tag{22}$$

The nonexponential decay in time obeyed by the susceptibilities (memory kernels) describes non-Markovian dissipation [35], which will turn out as an essential ingredient for stationary entanglement in our system. Moreover, the dimensionless parameter $|\Delta\boldsymbol{r}_{\lambda\mu}^0|\omega_c/c$ is also involved in the renormalization terms and the generalized spectral densities. It compares two different time scales, on the one hand, $|\Delta\boldsymbol{r}_{\lambda\mu}^0|/c$, which is the time of flight of a phonon or photon between two oscillators, and on the other hand, ω_c^{-1}, which represents the time scale during which memory effects decay. Surprisingly, the environment-mediated interaction, inherent in the susceptibilities and in the renormalization term, establishes an effective coupling between all oscillators irrespective of their distance. At fixed time, they decay polynomially in space at least as $\sim(|\Delta\boldsymbol{r}_{\lambda\mu}^0|\omega_c/c)^3$ and $\sim(|\Delta\boldsymbol{r}_{\lambda\mu}^0|\omega_c/c)^8$ for the 1D and the 3D reservoir, respectively. Although this interaction possesses long-range features, we shall see that the characteristic length of the entanglement correlation is determined by $|\Delta\boldsymbol{r}_{\lambda\mu}^0|\omega_c/c$, in agreement with Ref. [13].

With the susceptibilities and the renormalization terms at hand, we find that the matrices $\alpha(\omega)$ read

$$\begin{aligned}\alpha_{\lambda\mu}^{1\mathrm{D}}(\omega) &= m\left(\omega_\lambda^2-\omega^2\right)\delta_{\lambda\mu} - m\gamma\omega\,\mathrm{Re}\left[g(\omega)-g(-\omega)\right]\\ &\quad+\pi m\,\gamma\,\omega\,\mathrm{Im}\left[\Theta(\omega)e^{-\left(1/\omega_c - i\left|\Delta\boldsymbol{r}_{\lambda\mu}^0\right|/c\right)\omega}\right.\\ &\quad\left.-\Theta(-\omega)e^{\left(1/\omega_c - i\left|\Delta\boldsymbol{r}_{\lambda\mu}^0\right|/c\right)\omega}\right]\\ &\quad-i\pi m\gamma\omega\cos\left(\left|\Delta\boldsymbol{r}_{\lambda\mu}^0\right|\omega/c\right)e^{-|\omega|/\omega_c},\end{aligned} \tag{23}$$

$$\begin{aligned}\alpha_{\lambda\mu}^{3\mathrm{D}}(\omega) &= m\left(\omega_\lambda^2-\omega^2\right)\delta_{\lambda\mu} - i4\pi^2 m\gamma\left(c/\left|\Delta\boldsymbol{r}_{\lambda\mu}^0\right|\right)\left(\frac{\omega}{\omega_c}\right)^2\\ &\quad\times\sin\left(\omega\left|\Delta\boldsymbol{r}_{\lambda\mu}^0\right|/c\right)e^{-|\omega|/\omega_c}\\ &\quad-\frac{4\pi\,m\,\gamma\,c\,\omega^2}{\omega_c^2\left|\Delta\boldsymbol{r}_{\lambda\mu}^0\right|}\,\mathrm{Im}\left[g(\omega)+g(-\omega)\right]\\ &\quad-\frac{4\pi^2\,m\,\gamma\,c\,\omega^2}{\omega_c^2\left|\Delta\boldsymbol{r}_{\lambda\mu}^0\right|}\,\mathrm{Re}\left[\Theta(\omega)e^{-\left(1/\omega_c - i\left|\Delta\boldsymbol{r}_{\lambda\mu}^0\right|/c\right)\omega}\right.\\ &\quad\left.+Theta(-\omega)e^{\left(1/\omega_c - i\left|\Delta\boldsymbol{r}_{\lambda\mu}^0\right|/c\right)\omega}\right],\end{aligned} \tag{24}$$

where

$$g(\omega) = e^{-(1-i\omega_c\left|\Delta\boldsymbol{r}_{\lambda\mu}^0\right|/c)\omega/\omega_c}\Gamma\left[0,-\left(1-i\omega_c\left|\Delta\boldsymbol{r}_{\lambda\mu}^0\right|/c\right)\omega/\omega_c\right],$$

and $\Gamma(0,x)$ is the incomplete gamma function. With these expressions, we readily obtain the elements of the stationary correlation matrix. Moreover, the dimension-dependent integration kernels $K(\omega)$ become

$$\begin{aligned}K_{\eta,\beta}^{1\mathrm{D}}(\omega) &= \pi m\gamma\,\omega\coth\left(\frac{\hbar\omega}{2k_BT}\right)e^{-|\omega|/\omega_c}\\ &\quad\times\sum_{\lambda,\mu}\cos\left(\omega|\Delta\boldsymbol{r}_{\lambda\mu}^0|/c\right)\\ &\quad\times\frac{\{\mathrm{adj}[\alpha^{1\mathrm{D}}(\omega)]\}_{\eta\lambda}\{\mathrm{adj}[\alpha^{1\mathrm{D}}(-\omega)^T]\}_{\mu\beta}}{|\alpha^{1\mathrm{D}}(\omega)||\alpha^{1\mathrm{D}}(-\omega)^T|},\end{aligned} \tag{25}$$

$$\begin{aligned}K_{\eta,\beta}^{3\mathrm{D}}(\omega) &= 4\pi^2 m\gamma\left(\frac{\omega}{\omega_c}\right)^2\coth\left(\frac{\hbar\omega}{2k_BT}\right)e^{-|\omega|/\omega_c}\\ &\quad\times\sum_{\lambda,\mu}\left(c/\left|\Delta\boldsymbol{r}_{\lambda\mu}^0\right|\right)\sin\left(\omega\left|\Delta\boldsymbol{r}_{\lambda\mu}^0\right|/c\right)\\ &\quad\times\frac{\{\mathrm{adj}[\alpha^{3\mathrm{D}}(\omega)]\}_{\eta\lambda}\{\mathrm{adj}[\alpha^{3\mathrm{D}}(-\omega)^T]\}_{\mu\beta}}{|\alpha^{3\mathrm{D}}(\omega)||\alpha^{3\mathrm{D}}(-\omega)^T|},\end{aligned} \tag{26}$$

where adj[α] and $|\alpha|$ are the adjoint and the determinant of α. With these expressions, we have achieved a closed, albeit quite complicated, form for the susceptibilities. Nevertheless, the analytic expressions certainly facilitate the numerical evaluation of the covariance matrices (14)–(16).

III. THERMAL ENTANGLEMENT INDUCED BY ISOTROPIC SUBSTRATES

Having derived the solution of the quantum Langevin equations, we turn to the entanglement among the oscillators induced by the non-Markovian dissipative dynamics. We focus on the quantum regime which requires low temperatures, $k_B T \ll \hbar\omega_\lambda$. In order to have the environment playing a constructive role, it must couple strongly to the oscillators, such that the quality factors $Q_\lambda = \omega_\lambda/\gamma \sim 1$–$10$ are rather small. In this regime, the dissipative oscillator dynamics is strongly non-Markovian. In the numerical evaluations of our analytical expressions, we use the typical units for nano-oscillators, i.e., for masses $m = 10^{-16}$ kg, for frequencies $\Omega = 1$ GHz, and for distances $R = 10$ nm. Realistic values for an environment realized by a solid-state substrate are a cutoff frequency (Debye frequency) corresponding to $\hbar\omega_c = 6.58 \times 10^{-2}$ meV and $c = 3000$ m/s for the speed of sound.

We characterize the Gaussian entanglement between two generic modes $\mathcal{X}$ and $\mathcal{Y}$ by the logarithmic negativity [36]

$$E_N(\rho_{\mathcal{X}\mathcal{Y}}) = \max\{0, -\ln(2\nu_-)\}, \tag{27}$$

where $\mathcal{X}$ and $\mathcal{Y}$ represent one of the three oscillators, henceforth labeled by $\mathcal{A}$, $\mathcal{B}$, and $\mathcal{C}$. Here, ν_- is the lowest symplectic eigenvalue of the partial transpose covariance matrix $G^{T_\mathcal{Y}}$ corresponding to the reduced density matrix $\rho_{\mathcal{X}\mathcal{Y}}$ of the two modes. Regarding the analysis of three-mode Gaussian entanglement, there is no generally accepted measure of tripartite entanglement for arbitrary mixed states. Nonetheless it is possible to characterize it by a classification scheme that assigns each state to one of five separability classes [26], which range from fully inseparable states (class 1) to mixed tripartite product states (class 5). For details, see Appendix D.

Even though our focus lies on entanglement, we investigate for completeness also the quantum fidelity $\mathcal{F}(\rho,\rho^C)$ of the thermal state $\rho^C \propto e^{-H_S/k_B T}$ as a function of the spatial degrees of freedom and temperature. In Ref. [37] an analytical expression for $\mathcal{F}(\rho,\rho')$ was found for arbitrary n-mode Gaussian states. In our case, it becomes

$$\mathcal{F}(\rho,\rho^C) = \prod_{i=1}^{n} \frac{2}{(\nu_i+\nu_i^C)^2}\left[\nu_i\nu_i^C + \frac{1}{4} + \sqrt{\left(\nu_i^2-\frac{1}{4}\right)\left((\nu_i^C)^2-\frac{1}{4}\right)}\right], \tag{28}$$

where ν_i and ν_i^C are the symplectic eigenvalues of the covariance matrix of ρ and ρ^C, respectively. Notice that here the symplectic eigenvalues are different from those used for the logarithmic negativity, because they are derived without partial transposition.

In previous works [17,18] on environment-induced entanglement, it was found that when the oscillators are very close each other, the most significant influence of the environment is to mediate an effective interaction between the oscillators, while decoherence becomes relevant mainly at higher temperatures. Moreover, it has been pointed out that for identical oscillators, entanglement creation may stem from a decoherence-free subspace [8,10]. Here, by contrast, we consider oscillators with different frequencies. Additionally, the Hamiltonian has no symmetries that would support decoherence-free subspaces unless the distance between the oscillators vanishes. This implies that the stationary entanglement has its roots in an environment-mediated interaction. From the Langevin equation (7), we see that this interaction enters as a renormalization potential or via dissipative effects, which we interpret as stochastic feedback between the oscillators.

A. Two-mode entanglement

We start by addressing the two-mode entanglement between the oscillators $\mathcal{A}$ and $\mathcal{C}$, placed at a distance $\Delta\boldsymbol{r}^0_{\mathcal{A}\mathcal{C}} = R$, in the absence of oscillator $\mathcal{B}$. This is equivalent to putting oscillator $\mathcal{B}$ at infinite distance, $\Delta\boldsymbol{r}^0_{\mathcal{A}\mathcal{B}} = \Delta\boldsymbol{r}^0_{\mathcal{B}\mathcal{C}} \to \infty$. Figure 2 depicts $E_N(\rho_{\mathcal{A}\mathcal{C}})$ for this case as a function of the distance R and the temperature T for a 1D and a 3D environment, respectively. Although the environment induces a long-range interaction [cf. the susceptibilities (23) and (24)] with a polynomial decay in both space and time, we recover a central result of

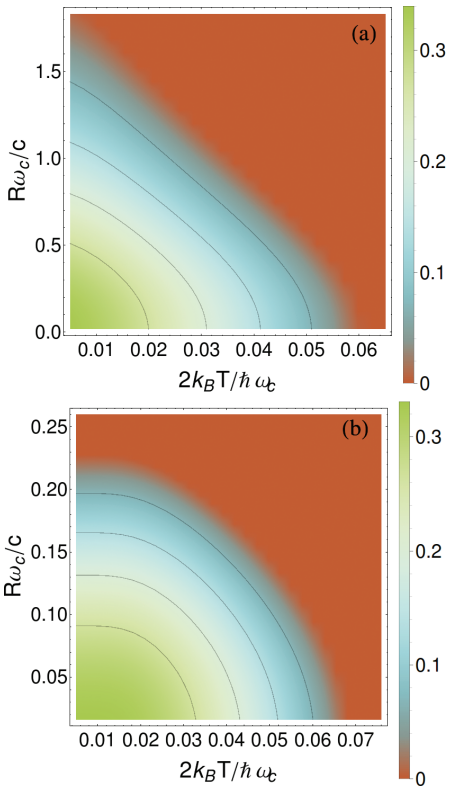

FIG. 2. (Color online) Stationary two-mode entanglement measured by the logarithmic negativity (27) as a function of oscillator distance R and temperature T for a (a) 1D and a (b) 3D environment. The oscillator frequencies are $\omega_\mathcal{A} = 7.2\ \Omega$, and $\omega_\mathcal{B} = 13.2\ \Omega$, while the dissipation is $\gamma = 5\ \Omega$.

Ref. [13]: The correlation length is given by $R \approx \omega_c/c$, while the entanglement vanishes at a finite distance R_0, which mainly depends on the temperature while being almost independent of the dissipation strength γ. Still a larger γ supports the effective interaction required for entanglement creation [12,17], but also increases decoherence which acts towards separability. Nevertheless, as expected, entanglement eventually disappears with increasing γ.

In 3D, entanglement generally appears to be more robust against thermal fluctuations, which is consistent with previous findings for qubits [7,11]. A qualitative explanation for this is the super-Ohmic character of the 3D spectral density of the bath which leads to stronger memory effects [38]. In turn, in the 1D case, entanglement is less affected by increasing the spatial separation R, which relates to the decay of the susceptibility as a function of the distance as we mentioned above: As a function of R, the susceptibility $\chi^{3D}(t)$ decreases, at least, five orders stronger than $\chi^{1D}(t)$. Thus, the effective interaction at large distance in 3D is weaker than in 1D. In both cases, the well-defined finite distance between the entangled oscillators indicates that our mechanism for two-mode entanglement relies on memory effects. Otherwise, we would expect a polynomial or exponential decay of the two-mode correlations with increasing distance. This supports the idea that the environment-induced interaction represents a kind of feedback between oscillators which is predominantly coherent when only low-energy environmental modes are thermally excited, i.e., for $k_B T \ll \hbar\omega_c$. Moreover, depending on the separation, the coupling strength with the environment is not too large to cause strong decoherence.

As discussed above, the effective interaction potential provided by the renormalization term $\tilde{\Omega}$ is crucial, but cannot explain fully the amount of entanglement observed. In order to underline this statement, let us assume that dissipation and noise are negligible, so that the problem reduces to two harmonic oscillators at thermal equilibrium with interaction potential ϕ. Then identical oscillators with equal frequencies $\omega_{\mathcal{A}} = \omega_{\mathcal{C}} = \Omega$, coupled at an equal position to a substrate ($R \to 0$), will be entangled under a condition [39] that in our case can be written as

$$(2N_+^{1D}+1)(2N_-^{1D}+1)\left(1-\frac{2\gamma\omega_c}{\Omega^2[1+(\omega_c R/c)^2]}\right)<1, \tag{29}$$

$$(2N_+^{3D}+1)(2N_-^{3D}+1)\left(1-\frac{16\pi\gamma\omega_c}{\Omega^2[1+(\omega_c R/c)^2]^2}\right)<1, \tag{30}$$

where $N_\pm^{1D,3D} = [e^{\hbar\Omega_\pm^{1D,3D}/k_B T}-1]^{-1}$ denotes the bosonic thermal occupation of normal modes with the frequencies

$$\Omega_\pm^{1D} = \Omega\sqrt{1+\frac{2\gamma\omega_c}{\Omega^2} \pm \frac{2\gamma\omega_c}{\Omega^2[1+(\omega_c R/c)^2]}}, \tag{31}$$

$$\Omega_\pm^{3D} = \Omega\sqrt{1+\frac{16\pi\gamma\omega_c}{\Omega^2} \pm \frac{16\pi\gamma\omega_c}{\Omega^2[1+(\omega_c R/c)^2]^2}}. \tag{32}$$

Notice that the conditions (29) and (30) result from an expansion of the symplectic eigenvalues to first order in $\gamma\omega_c/\Omega^2$, implying $\gamma\omega_c < \Omega^2$, for which the left-hand side of these expressions is strictly positive when neglecting dissipation and quantum noise [40]. These conditions demonstrate that R plays an important role for the entanglement creation, as can be appreciated in Fig. 2. Still, these analytic considerations overestimate the influence of R_0, as a quantitative comparison with the numerically evaluated expressions demonstrates (not shown). Although we find that the available entanglement generated by the effective potential $\tilde{\Omega}$ does not display most of the characteristics of the stationary entanglement discussed above, it is still relevant in the transient dynamics [6]. In the long-time limit, both the numerical data and the analytical results for the susceptibilities indicate that the mechanism behind entanglement creation may be interpreted as uncontrolled feedback (encoded in the susceptibility) which relies on the non-Markovian dissipation.

B. Two-mode entanglement in the presence of a third oscillator

We have already seen that the coupling to a common environment induces an effective interaction between oscillators and may create two-mode entanglement. In the case where three or more oscillators are in contact with the bath, we expect that additional effective interactions between any pair of oscillators emerge, provided that the oscillators are sufficiently close to each other, i.e., for distances $R \ll c/\omega_c$. It has been shown [41,42] that for three qubits in contact with a common environment, the two-qubit entanglement for certain initial states persists in the long-time limit when coupling a further qubit to the substrate. Hence, the question arises as to how two-mode entanglement is affected by the presence of a third oscillators. We study two different configurations: The first one is a linear arrangement in which the three oscillators are coupled to a 1D environment with separations $\Delta\boldsymbol{r}_{\mathcal{AC}}^0 = R$, $\Delta\boldsymbol{r}_{\mathcal{AB}}^0 = R/2 + r$, and $\Delta\boldsymbol{r}_{\mathcal{BC}}^0 = R/2 - r$, where $0 < r < R/2$, as sketched in Fig. 3. We fix R such that the outer oscillators $\mathcal{A}$ and $\mathcal{C}$ may be entangled or separable, depending on the other parameters. In the second configuration, the oscillators are in contact with a 3D reservoir. The oscillators $\mathcal{A}$ and $\mathcal{C}$ are again at distance $\Delta\boldsymbol{r}_{\mathcal{AC}}^0 = R$, but oscillator $\mathcal{B}$ is shifted by r perpendicular to the line connecting $\mathcal{A}$ and $\mathcal{C}$ (see the sketch in Fig. 4). Thus, $\Delta\boldsymbol{r}_{\mathcal{BC}}^0 = \Delta\boldsymbol{r}_{\mathcal{AB}}^0 = [r^2 + (R/2)^2]^{1/2}$.

For the linear arrangement, we start by placing the oscillators $\mathcal{A}$ and $\mathcal{C}$ at a distance R, and choose the other parameters such that both are separable in the absence of oscillator $\mathcal{B}$, while for $r = 0$, $\mathcal{B}$ is entangled with $\mathcal{A}$ in the absence of $\mathcal{C}$ (and vice versa). Then one might expect that the "passive" oscillator in the middle would give rise to an enhanced effective interaction between $\mathcal{A}$ and $\mathcal{C}$, similar to what is found in harmonic chains with nearest-neighbor interactions at thermal equilibrium [43]. However, we find the opposite (not shown), namely, that in the presence of oscillator $\mathcal{B}$, one has to reduce the distance R even below the limit found above for the two-oscillator setup. Thus, the presence of oscillator $\mathcal{B}$ is even harmful for entanglement between the other two oscillators. Therefore, we chose for R in the data shown in Fig. 3 a smaller value such that $0 < E_N(\rho_{\mathcal{AC}}) \ll 1$. As expected, oscillator $\mathcal{B}$ is stronger entangled with the oscillator that is closer, which is in accordance with our findings in the last section. The entanglement between the outer oscillators stays rather small

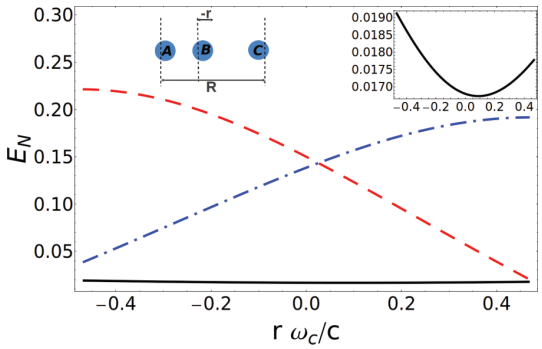

FIG. 3. (Color online) Stationary two-mode entanglement in the linear arrangement quantified by the logarithmic negativities $E_N(\rho_{\mathcal{AC}})$ (black solid line), $E_N(\rho_{\mathcal{AB}})$ (red dashed), and $E_N(\rho_{\mathcal{BC}})$ (blue dashed-dotted) for $R\omega_c/c = 0.933$. Temperature and damping are $k_BT/\hbar\omega_c = 0.026$, $\gamma = 5\Omega$, respectively, while the frequencies are $\omega_{\mathcal{A}} = 7.2\Omega$, $\omega_{\mathcal{B}} = 10.1\Omega$, and $\omega_{\mathcal{C}} = 13.2\Omega$, where $\Omega = 1$ GHz. The asymmetry between $E_N(\rho_{\mathcal{AB}})$ and $E_N(\rho_{\mathcal{BC}})$ is a consequence of choosing different oscillator frequencies. The entanglement between $\mathcal{A}$ and $\mathcal{B}$ is less sensitive to a moderate increase of temperature (not shown), because it involves the oscillators with the highest frequencies. The inset is a zoom that demonstrates the small quadratic increase of $E_N(\rho_{\mathcal{AC}})$.

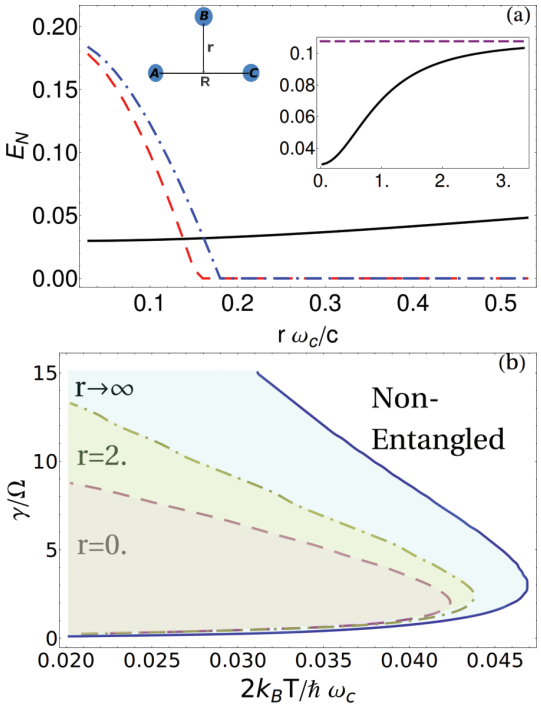

FIG. 4. (Color online) (a) Stationary two-mode entanglement measured by the logarithmic negativities $E_N(\rho_{\mathcal{AC}})$ (black solid line), $E_N(\rho_{\mathcal{AB}})$ (red dashed line), and $E_N(\rho_{\mathcal{BC}})$ (blue dashed-dotted line) for the triangular geometry with $R\omega_c/c = 0.167$ as a function of the displacement r. All other parameters are as in Fig. 3. The inset provides an extended picture of $E_N(\rho_{\mathcal{AC}})$, where the dotted line marks the value in the absence of oscillator $\mathcal{B}$. (b) Phase diagram for fixed R and various values of r as a function of coupling strength γ and temperature T. In the shaded areas, the oscillators $\mathcal{A}$ and $\mathcal{B}$ exhibit stationary entanglement. The outer blue line marks the limit $r \to \infty$, which is equivalent to the absence of oscillator $\mathcal{B}$. As oscillator $\mathcal{B}$ comes closer, the area with entanglement shrinks.

and remains almost unaffected by the position of the third oscillator. The small change can be appreciated in the inset of Fig. 3, which shows that $E_N(\rho_{\mathcal{AC}})$ assumes its minimum when $\mathcal{B}$ is roughly in the middle.

Our results for the triangular arrangement go into the same direction: We also encounter that the third oscillator reduces the two-mode entanglement between $\mathcal{A}$ and $\mathcal{C}$. This generic behavior is in contrast to the one found for setups that allow for decoherence-free subspaces [41,42]. The corresponding logarithmic negativity is plotted in Fig. 4(a) as a function of the position of $\mathcal{B}$. In fact, the parameter space with entangled states shrinks significantly by the presence of oscillator $\mathcal{B}$: Figure 4(b) demonstrates that $E_N(\rho_{\mathcal{AC}})$ is eventually destroyed when $\mathcal{B}$ is close enough to the pair. Then the oscillator $\mathcal{B}$ becomes entangled with $\mathcal{A}$ and $\mathcal{C}$ almost simultaneously. That is, $E_N(\rho_{\mathcal{AB}})$ and $E_N(\rho_{\mathcal{BC}})$ increase while $E_N(\rho_{\mathcal{AC}})$ becomes smaller. There is a trade-off between $E_N(\rho_{\mathcal{AC}})$, $E_N(\rho_{\mathcal{AB}})$, and $E_N(\rho_{\mathcal{BC}})$ resembling the monogamy property of correlations [1]. The competition between these three bipartite entanglements is characteristic for our environment-induced entanglement mechanism, mainly because the logarithmic negativity (i) is a bona fide measure that generally does not satisfy monogamy and (ii) becomes increasingly manifest by raising the coupling strength γ, as can be seen in Fig. 4(b). This feature is independent of whether the three oscillators have equal or different frequencies. Furthermore, in the limit $r \to \infty$, $E_N(\rho_{\mathcal{AC}})$ approaches the value of two-mode entanglement when the oscillator pair $\mathcal{AC}$ evolves independent of $\mathcal{B}$. This shows that the oscillators effectively interact even at distances greater than the correlation length of two-mode entanglement, which implies that the environment-induced interaction has long-range features.

Gathering the results for the two settings studied, they apparently show that the environment-mediated interaction induces a trade-off between the three two-mode entanglements. This feature is highly emphasized in the triangular setting, where $\mathcal{B}$ is brought closer to both $\mathcal{A}$ and $\mathcal{C}$. For identical oscillators, we observe that all possible two-mode entanglements take the same values when they form an equilateral triangle, i.e., for $r = \sqrt{3}R/2$. At smaller values for r, the entanglements $E_N(\rho_{\mathcal{AB}})$ and $E_N(\rho_{\mathcal{BC}})$ are larger than $E_N(\rho_{\mathcal{AC}})$, because $\mathcal{A}$ and $\mathcal{C}$ are further separated from each other than from $\mathcal{B}$. One of our main findings is that the presence of oscillator $\mathcal{B}$ reduces the entanglement between $\mathcal{A}$ and $\mathcal{C}$. This tendency towards separability might be enhanced by adding further oscillators. However, even though $E_N(\rho_{\mathcal{AC}})$ may be reduced or may vanish in the presence of oscillator $\mathcal{B}$, there is still the possibility of an emerging multipartite entangled such as the formation of Greenberger-Horne-Zeilinger (GHZ)-like states. This emergence of tripartite entanglement at the expense of smaller bipartite entanglement may be interpreted as a consequence of an effective three-body interaction by which all three oscillators act simultaneously via the same bath.

C. Three-mode entanglement

For the characterization of multipartite entanglement, we employ the classification scheme for tripartite Gaussian entanglement developed by Giedke *et al.* [26] and summarized in Appendix D. According to this scheme, each state falls in one of the following five classes: C1, fully inseparable states; C2, one-mode biseparable states; C3, two-mode biseparable states; C4, bound tripartite-entangled states; and C5, fully separable states. Notice that class C1 is not a strict classification but rather subsumes all so-called genuinely tripartite-entangled states [44].

Concerning tripartite entanglement, a most important question is whether an optimal arrangement for genuine tripartite entanglement exists. The results of the previous section suggest that equally spaced oscillators might be rather unfavorable for two-mode entanglement (see the inset in Fig. 3). An expectation inferred from those results (see Fig. 2) is that tripartite entanglement decreases with distance as bipartite entanglement does, i.e., it should vanish at large distances. Still it is interesting to now investigate whether three-mode entanglement is more robust against a variation of r than two-mode entanglement. Moreover, the limiting distance may be different from $R\omega_c/c$.

1. Linear arrangement

Figure 5 shows the phase diagram of the separability classes for the case in which all oscillators are coupled to a one-dimensional environment. Most importantly, it demonstrates the relative robustness of the fully inseparable states (class C1) against shifting the position of oscillator $\mathcal{B}$ and against a moderate temperature increase. Fully inseparable states are found for small temperatures and when oscillator $\mathcal{B}$ is a bit closer to $\mathcal{A}$ than to $\mathcal{C}$. This asymmetry stems from the fact that oscillator $\mathcal{C}$ is less affected by thermal fluctuations than the other two oscillators, owing to its larger frequency. In general, we expect the genuine tripartite entanglement to be rather insensitive to variations of the geometry as long as all oscillators interact strongly in the same manner through the reservoir, i.e., when oscillator $\mathcal{B}$ is roughly in the middle. Otherwise, the geometry could enhance the interaction between two particular oscillators, which may lead to a situation in which the third oscillator becomes separable. In

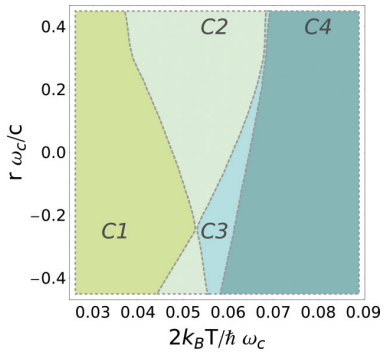

FIG. 5. (Color online) Phase diagram of the separability classes for the linear configuration as a function of temperature and position r of oscillator $\mathcal{B}$. All other parameters are as in Fig. 3.

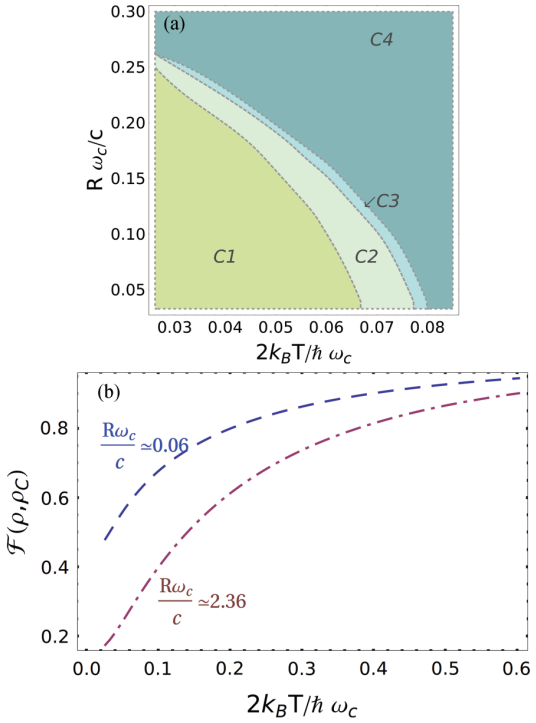

FIG. 6. (Color online) (a) Separability phase diagram for the equilateral triangular for the oscillator frequencies and coupling strengths used in Fig. 4. (b) Quantum fidelity between the stationary state and the thermal canonical state as a function of the temperature for the distances $R\omega_c/c = 0.066$ (blue dashed line) and $R\omega_c/c = 2.367$ (pink dashed-dotted line).

the phase diagram (Fig. 5), this is visible in the emergence of regions with separability class C2 when r tends towards $\pm R/2$. Thus, in contrast to the two-mode case, the equidistant placement of oscillator $\mathcal{B}$ at $r = 0$ is the optimal setting for genuine tripartite entanglement, at least in the case of equal oscillators.

2. Arrangement in an equilateral triangle

Having noticed that in the 1D case optimal tripartite entanglement is achieved in the most symmetric situation, we restrict ourselves in the 3D case to the configuration in an equilateral triangle with lateral length $R = \Delta \boldsymbol{r}^0_{\mathcal{AC}} = \Delta \boldsymbol{r}^0_{\mathcal{BC}} = \Delta \boldsymbol{r}^0_{\mathcal{AB}}$. Figure 6(a) depicts the corresponding separability phase diagram. Again we find for small R and low temperatures that the stationary state is fully inseparable (class C1). With increasing temperature, we notice a transition via the one-, two-, and three-mode biseparable classes C2, C3, and C4 to the fully separable class C5 at high temperatures $T \gtrsim \hbar\omega_c/k_B$ (the latter is beyond the plotted range). The appearance of classes C2 and C3 obviously requires some asymmetry in the setup, which stems from choosing different oscillator frequencies. In comparison to the two-mode entanglement studied in Sec. III A, however, tripartite bound entanglement (class C4) is more robust against separation and temperature effects than for two modes. Indeed, we find that it may survive up to values of $R\omega_c/c$ that clearly exceed unity. This can

be explained by the fact that the susceptibilities reflect an effective coupling of all oscillators independent of their spatial separation (cf. the discussion in Sec. II B), which enables large-distance entanglement. The latter is also in agreement with the two-mode entanglement $E_N(\rho_{\mathcal{AC}})$ discussed above: It asymptotically approaches the value found for the oscillator pair $\mathcal{AC}$ in the absence of a third oscillator (see the inset of Fig. 4) and underlines that the environment induces long-range interaction. On the other hand, the quantum fidelity (28), which shows the "sophistication" of the stationary state, reveals that the (fully separable) thermal state is reached for $k_BT \gtrsim \hbar\omega_c$ [see Fig. 6(b)], irrespective of the distances between the oscillators. Hence, only at high temperatures, decoherence dominates so that here the full separability turns out to be a decoherence phenomenon.

IV. SUMMARY AND CONCLUSIONS

We have studied the stationary entanglement of three harmonic oscillators as a generic tripartite system that becomes entangled through the interaction with a common extended environment. The oscillators are embedded in a thermal bosonic heat bath which we eliminated to obtain generalized quantum Langevin equations. Although the oscillators are not directly coupled, the contact via the heat bath provides an environment-mediated interaction which can induce bipartite and tripartite entanglement between the oscillators. The equations of motion for a 1D and 3D isotropic environment contain this interaction as a long-range coupling entering via a renormalization term and through the susceptibility, which takes the backaction into account. For both two-mode entangled and fully inseparable oscillators, the characteristic correlation length is roughly given by the ratio $R\omega_c/c$. For a 3D environment it is smaller than in the 1D case. Nevertheless, the entanglement generated by a 3D environment is more robust against thermal fluctuations.

Interestingly enough, there is a trade-off in the attainable two-mode entanglement between the different oscillator pairs, because the presence of a passive oscillator is detrimental for two-mode entanglement. This provides strong evidence that the environment-induced interaction also produces an effective many-party interaction that tends to favor multipartite correlations (here tripartite instead of bipartite), such that GHZ-like states emerge. Our numerical data suggest that the mechanism is mainly based on uncontrolled feedback which is mostly coherent at low temperatures and for moderate oscillator-environment coupling (in comparison to the fundamental frequencies). This feedback corresponds to non-Markovian memory effects and relies on the structure of the generalized spectral density, which is an oscillating decaying function of frequency for both the 1D and the 3D environment.

Our findings underline that non-Markovian effects are relevant for a deeper understanding of multipartite-entangled stationary states. This is in contrast to the behavior of subsystems coupled to independent heat baths, for which non-Markovian effects are not essential and where thermal relaxation dominates. An interesting consequence of our results in the realm of quantum information may be found in setups for quantum communication and teleportation. Considering the studied model as a simplified quantum network, our results for two-mode entanglement in the presence of a passive oscillator imply the need for sufficient microscopic control of the interaction between all constituents. Thus, an interesting task would be the prediction of the stability of such protocols under weak interaction with a common extended environment.

ACKNOWLEDGMENTS

The authors warmly thank Luis A. Correa, Robert Hussein, José P. Palao, and Antonia Ruiz for fruitful discussions. A.A.V. would like to thank A. Castro Castilla and N. García Marco for many discussions on mathematical aspects. This project was funded by the Spanish MICINN (Grants No. FIS2010-19998 and No. MAT2011-24331) and by the European Union (FEDER). A.A.V. acknowledges financial support by the Government of the Canary Islands through an ACIISI fellowship (85% cofinanced by the European Social Fund).

APPENDIX: THE SYSTEM-ENVIRONMENT MODEL

In this Appendix we derive the Langevin equation and different quantities used in the main text. We start with the Hamiltonians H_S, H_B, and H_I, Eqs. (3) and (5). We shall first neglect the counterterm (renormalization) whose contribution will be included at the end. Hence, the Hamiltonian equations of motion for p_λ and $a_{\boldsymbol{k}}$ are given by

$$\dot{p}_\lambda = -m\omega_\lambda^2 x_\lambda + \sum_k g_{\boldsymbol{k}}\left(a_{\boldsymbol{k}} e^{i\boldsymbol{k}\cdot\boldsymbol{r}_\lambda^0} + a_{\boldsymbol{k}}^\dagger e^{-i\boldsymbol{k}\cdot\boldsymbol{r}_\lambda^0}\right), \quad \text{(A1)}$$

$$\dot{a}_{\boldsymbol{k}} = -i\omega_{\boldsymbol{k}} a_{\boldsymbol{k}} + \frac{i}{\hbar}\sum_\mu g_{\boldsymbol{k}} e^{-i\boldsymbol{k}\cdot\boldsymbol{r}_\mu^0} x_\mu, \quad \text{(A2)}$$

where the latter possesses the formal solution

$$a_{\boldsymbol{k}}(t) = a_{\boldsymbol{k}}(t_0)e^{-i\omega_{\boldsymbol{k}}(t-t_0)} + \frac{i}{\hbar}\sum_\mu g_{\boldsymbol{k}} e^{-i\boldsymbol{k}\cdot\boldsymbol{r}_\mu^0}\int_{t_0}^t ds\, x_\mu(s) e^{-i\omega_{\boldsymbol{k}}(t-s)}.$$

We insert it into Eq. (A1) to obtain for the oscillators conditioned to the state of the environment the effective dynamical equation

$$\dot{p}_\lambda = -m\omega_\lambda^2 x_\lambda + F_\lambda(t) + \frac{i}{\hbar}\sum_\mu\sum_{\boldsymbol{k}} g_{\boldsymbol{k}}^2 e^{i\boldsymbol{k}\cdot(\boldsymbol{r}_\lambda^0 - \boldsymbol{r}_\mu^0)}\int_{t_0}^t ds\, x_\mu(s) e^{-i\omega_{\boldsymbol{k}}(t-s)} - \frac{i}{\hbar}\sum_\mu\sum_{\boldsymbol{k}} g_{\boldsymbol{k}}^2 e^{-i\boldsymbol{k}\cdot(\boldsymbol{r}_\lambda^0 - \boldsymbol{r}_\mu^0)}\int_{t_0}^t ds\, x_\mu(s) e^{i\omega_{\boldsymbol{k}}(t-s)}. \quad \text{(A3)}$$

This equation can be expressed in a more convenient form by introducing the fluctuating force $F_\lambda(t)$ and susceptibility $\chi_{\lambda\mu}(t)$ to read

$$\dot{p}_\lambda(t) + m\omega_\lambda^2 x_\lambda + \frac{1}{\hbar}\int_{t_0}^t d\tau \sum_\mu \chi_{\lambda\mu}(t-\tau) x_\mu(\tau) = F_\lambda(t),$$

where

$$F_\lambda(t) = \sum_{\boldsymbol{k}} g_{\boldsymbol{k}}\left[a_{\boldsymbol{k}}(t_0)e^{i[\boldsymbol{k}\cdot\boldsymbol{r}^0_\lambda-\omega_{\boldsymbol{k}}(t-t_0)]} + a^\dagger_{\boldsymbol{k}}(t_0)e^{-i[\boldsymbol{k}\cdot\boldsymbol{r}^0_\lambda-\omega_{\boldsymbol{k}}(t-t_0)]}\right],$$

$$\chi_{\lambda\mu}(t) = 2\Theta\left(t - \left|\Delta\boldsymbol{r}^0_{\lambda\mu}\right|/c\right)\sum_{\boldsymbol{k}} g^2_{\boldsymbol{k}}\sin\left(\boldsymbol{k}\cdot\Delta\boldsymbol{r}^0_{\lambda\mu} - \omega_{\boldsymbol{k}}t\right).$$

The susceptibility can be written in terms of an average over the environmental state ρ_B of the commutator of the fluctuating force, so that it becomes

$$\chi_{\lambda\mu}(t-t') = -i\Theta\left(t-t' - \left|\Delta\boldsymbol{r}^0_{\lambda\mu}\right|/c\right)\langle[F_\lambda(t), F_\mu(t')]\rangle_{\rho_B}, \tag{A4}$$

where $|\Delta\boldsymbol{r}^0_{\lambda\mu}| = |\boldsymbol{r}^0_\lambda - \boldsymbol{r}^0_\mu|$.

The environment is initially in an equilibrium state at temperature T for which $\langle a^\dagger_{\boldsymbol{k}'}a_{\boldsymbol{k}}\rangle = \delta_{\boldsymbol{k}\boldsymbol{k}'}N(\omega_{\boldsymbol{k}})$, with the bosonic thermal occupation $N(\omega_{\boldsymbol{k}}) = [\exp(-\omega_{\boldsymbol{k}}/k_BT) - 1]^{-1}$ so that the anticommutator of the fluctuating force obeys

$$\langle\{F_\lambda(t), F_\mu(t')\}\rangle_{\rho_B} = 2\sum_{\boldsymbol{k}} g^2_{\boldsymbol{k}}[2N(\omega_{\boldsymbol{k}}) + 1] \times \cos\left[\boldsymbol{k}\cdot\Delta\boldsymbol{r}^0_{\lambda\mu} - \omega_{\boldsymbol{k}}(t-t')\right]. \tag{A5}$$

In the frequency domain, this relation reads

$$\langle\{F_\lambda(\omega), F_\mu(\omega')\}\rangle_{\rho_B} = 4\pi^2\delta(\omega'+\omega)\coth\left(\frac{\hbar\omega'}{2k_BT}\right) \times \sum_{\boldsymbol{k}} g^2_{\boldsymbol{k}}[e^{ik\Delta x_{\lambda\mu}}\delta(\omega'-\omega_{\boldsymbol{k}}) - e^{-ik\Delta x_{\lambda\mu}}\delta(\omega'+\omega_{\boldsymbol{k}})], \tag{A6}$$

where we have inserted $2N(\omega_{\boldsymbol{k}}) + 1 = \coth(\hbar\omega/2K_BT)$. For a more compact notation, we introduce the spectral densities

$$J_{\lambda,\mu}(\omega) = \frac{\pi}{\hbar}\sum_{\boldsymbol{k}} g^2_{\boldsymbol{k}}\cos\left(\boldsymbol{k}\cdot\Delta\boldsymbol{r}^0_{\lambda\mu}\right)\delta\left(\omega - \omega_{\boldsymbol{k}}\right), \tag{A7}$$

with which we obtain from Eq. (A6) the quantum fluctuation-dissipation relation

$$\mathrm{Re}\,\tfrac{1}{2}\langle\{F_\lambda(\omega), F_\mu(\omega')\}\rangle = 2\pi\hbar\delta(\omega'+\omega)\Gamma_{\lambda\mu}(\omega'), \tag{A8}$$

with the imaginary part of the susceptibility

$$\Gamma_{\lambda\mu}(\omega) = -\frac{1}{\hbar}\mathrm{Im}\,\chi_{\lambda\mu}(\omega)\coth\left(\frac{\hbar\omega'}{2K_BT}\right) = J_{\lambda,\mu}(|\omega|)\coth\left(\frac{\hbar|\omega|}{2K_BT}\right), \tag{A9}$$

derived in Appendix B.

So far we have not taken into account the counterterm. In doing so, the spectral densities lead to harmonic renormalization potentials with frequencies

$$\tilde\Omega_{\lambda\lambda} = \frac{1}{\hbar}\sum_{\boldsymbol{k}}\frac{g^2_{\boldsymbol{k}}}{\omega_{\boldsymbol{k}}} = \frac{1}{\pi}\int_0^\infty\frac{J_{\lambda,\lambda}(\omega)}{\omega}d\omega,$$

$$\tilde\Omega_{\lambda\mu} = \frac{1}{\hbar}\sum_{\boldsymbol{k}}\frac{g^2_{\boldsymbol{k}}}{\omega_{\boldsymbol{k}}}\cos\left(\boldsymbol{k}\cdot\Delta\boldsymbol{r}^0_{\lambda\mu}\right) = \frac{1}{\pi}\int_0^\infty\frac{J_{\lambda,\mu}(\omega)}{\omega}d\omega. \tag{A10}$$

Owing to the linearity of the dynamical equations for x_λ and p_λ, it is straightforward to show that including the counterterm provides the Langevin equation (7).

APPENDIX B: SPECTRAL DENSITIES AND SUSCEPTIBILITIES

Irrespective of the dimension of the environment, we assume that it is isotropic and possesses the linear dispersion relation $\omega_{\boldsymbol{k}} = c|\boldsymbol{k}|$ with cutoff frequency ω_c. We model this by introducing coupling constants $g_{\boldsymbol{k}}$ that obey

$$g^2_{\boldsymbol{k}} = m\hbar\gamma\left(\omega_{\boldsymbol{k}}/\omega_c^{d-1}\right)c^dV_{\boldsymbol{k}}(d)e^{-\omega/\omega_c}, \tag{B1}$$

where d is the dimension of the environment, $V_{\boldsymbol{k}}$ is the d-dimensional $\boldsymbol{k}$-space volume per field mode, and γ is the effective coupling strength. We start from Eq. (A7) and take the continuum limit $V_{\boldsymbol{k}} \to 0$. We provide explicit expressions for the dimensions $d = 1$ and $d = 3$, while $d = 2$ is addressed mainly for highlighting the difficulties that arise in that dimension.

1. One-dimensional environment

Inserting Eq. (B1) for $d = 1$ into (A7) and (A10) yields in the continuum limit $V_{\boldsymbol{k}}(1) \to 0$ for the spectral density the closed-form form

$$J_{\lambda\mu}(\omega) = \pi m\gamma\omega e^{-\omega/\omega_c}\cos\left(\omega\left|\Delta\boldsymbol{r}^0_{\lambda\mu}\right|/c\right), \tag{B2}$$

and the potential renormalization frequencies

$$\tilde\Omega_{\lambda\lambda} = m\gamma\omega_c,$$

$$\tilde\Omega_{\lambda\mu} = \frac{m\gamma\omega_c}{1 + \left(\omega_c\left|\Delta\boldsymbol{r}^0_{\lambda\mu}\right|/c\right)^2},$$

respectively. The real part of the susceptibility $\chi_{\lambda\mu}(\omega')$ is obtained from Eq. (A9) via the Kramers-Kronig relations. Mathematically this corresponds to the Hilbert transformation [45] that can formally be expressed as

$$\mathrm{Re}\,\chi_{\lambda\mu}(\omega') = \mathcal{H}[\mathrm{Im}\,\chi_{\lambda\mu}(\omega)](\omega') := \frac{1}{\pi}P\int_{-\infty}^\infty\frac{\mathrm{Im}\,\chi_{\lambda\mu}(\omega)}{\omega-\omega'}d\omega, \tag{B3}$$

where P is the Cauchy principal value and $\mathcal{H}[f(\omega)](\omega')$ the Hilbert transform of $f(\omega)$. Hence,

$$\mathrm{Re}\,\chi_{\lambda\mu}(\omega) = -m\hbar\gamma P\int_0^\infty\omega e^{-\omega/\omega_c}\cos\left(\omega\left|\Delta\boldsymbol{r}^0_{\lambda\mu}\right|/c\right) \times\left(\frac{1}{\omega-\omega'} + \frac{1}{\omega+\omega'}\right)d\omega, \tag{B4}$$

which consists of two terms that differ by the sign of ω' and thus it is sufficient to compute

$$P\int_0^\infty\frac{\omega e^{-\omega/\omega_c}\cos\left(\omega\left|\Delta\boldsymbol{r}^0_{\lambda\mu}\right|/c\right)}{\omega-\omega'}d\omega = \omega' P\int_0^\infty\frac{e^{-\omega/\omega_c}\cos\left(\omega\left|\Delta\boldsymbol{r}^0_{\lambda\mu}\right|/c\right)}{\omega-\omega'}d\omega + \frac{\omega_c}{1+\left(\omega_c\left|\Delta\boldsymbol{r}^0_{\lambda\mu}\right|/c\right)^2},$$

where we have used $\mathcal{H}[\omega f(\omega)] = \omega\mathcal{H}(f(\omega)) + \frac{1}{\pi}\int_{-\infty}^{\infty} f(\omega)d\omega$ to arrive at

$$P\int_0^\infty \frac{e^{-(\frac{1}{\omega_c}-i|\Delta\boldsymbol{r}^0_{\lambda\mu}|/c)\omega}}{\omega-\omega'}d\omega = \begin{cases} e^{-(\frac{1}{\omega_c}-i|\Delta\boldsymbol{r}^0_{\lambda\mu}|/c)\omega'}\left\{\Gamma\left[0,-\left(\frac{1}{\omega_c}-i|\Delta\boldsymbol{r}^0_{\lambda\mu}|/c\right)\omega'\right]+i\pi\right\} & \text{if} \quad \omega'\in(0,\infty), \\ e^{-(\frac{1}{\omega_c}-i|\Delta\boldsymbol{r}^0_{\lambda\mu}|/c)\omega'}\Gamma\left[0,-\left(\frac{1}{\omega_c}-i|\Delta\boldsymbol{r}^0_{\lambda\mu}|/c\right)\omega'\right] & \text{if} \quad \omega'\in(-\infty,0), \end{cases}$$

where $\Gamma(a,z)=\int_\infty^z t^{a-1}e^{-t}dt$ denotes the incomplete gamma function. Inserting this expression into Eq. (B4), we finally obtain

$$\mathrm{Re}\,\chi_{\lambda\mu}(\omega) = -m\hbar\gamma\omega\,\mathrm{Re}\,[g(\omega)-g(-\omega)] + \pi m\hbar\,\gamma\,\omega\,\mathrm{Im}\left[\Theta(\omega)e^{-(\frac{1}{\omega_c}-i|\Delta\boldsymbol{r}^0_{\lambda\mu}|/c)\omega} - \Theta(-\omega)e^{(\frac{1}{\omega_c}-i|\Delta\boldsymbol{r}^0_{\lambda\mu}|/c)\omega}\right] - \frac{2m\hbar\gamma\omega_c}{1+\left(\omega_c|\Delta\boldsymbol{r}^0_{\lambda\mu}|/c\right)^2}, \tag{B5}$$

with $g(\omega) = e^{-(1-i\omega_c|\Delta\boldsymbol{r}^0_{\lambda\mu}|/c)\omega/\omega_c}\Gamma[0,-(1-i\omega_c|\Delta\boldsymbol{r}^0_{\lambda\mu}|/c)\omega/\omega_c]$. From this expression we find the well-known relation between the frequency shift $\Delta\omega_{\lambda\mu}$ and the real part of susceptibility [40],

$$\left(\Delta\omega_{\lambda\mu}\right)^2 = -\frac{\tilde{\Omega}_{\lambda\mu}}{m} = \frac{1}{2m\hbar}\lim_{\omega\to 0}\mathrm{Re}\,\chi_{\lambda\mu}(\omega).$$

2. Two-dimensional environment

Again, we use (B1), perform the continuum limit, and readily obtain

$$J_{\lambda\mu}(\omega) = 2\pi^2 m\gamma\frac{\omega^2}{\omega_c}e^{-\omega/\omega_c}\mathrm{J}_0\left(\omega|\Delta\boldsymbol{r}^0_{\lambda\mu}|/c\right), \tag{B6}$$

where J_0 is the zeroth-order Bessel function of the first kind. The renormalization frequencies now become

$$\tilde{\Omega}_{\lambda\lambda} = 2\pi m\gamma\omega_c,$$
$$\tilde{\Omega}_{\lambda\lambda'} = \frac{2\pi m\gamma\omega_c}{\left[1+\left(\omega_c|\Delta\boldsymbol{r}^0_{\lambda\mu}|/c\right)^2\right]^{3/2}}.$$

Accordingly, the Fourier transform of the real part of the susceptibility reads

$$\mathrm{Re}\,\chi_{\lambda\mu}(\omega') = -\frac{2\pi m\gamma\hbar}{\omega_c}P\int_0^\infty \omega^2 e^{-\omega/\omega_c}\mathrm{J}_0\left(\omega|\Delta\boldsymbol{r}^0_{\lambda\mu}|/c\right) \times\left(\frac{1}{\omega-\omega'}+\frac{1}{\omega+\omega'}\right)d\omega. \tag{B7}$$

Using the same relation of Hilbert transforms as in the previous section we can write

$$\mathcal{H}\left[\Theta(\omega)\omega^2 e^{-\omega/\omega_c}\mathrm{J}_0\left(\omega|\Delta\boldsymbol{r}^0_{\lambda\mu}|/c\right)\right](\omega') = \omega'^2\mathcal{H}\left[\Theta(\omega)e^{-\omega/\omega_c}\mathrm{J}_0\left(\omega|\Delta\boldsymbol{r}^0_{\lambda\mu}|/c\right)\right](\omega') + \frac{\omega'\omega_c}{\left[1+\left(\omega_c|\Delta\boldsymbol{r}^0_{\lambda\mu}|/c\right)^2\right]^{1/2}} + \frac{\omega_c^2}{\left[1+\left(\omega_c|\Delta\boldsymbol{r}^0_{\lambda\mu}|/c\right)^2\right]^{3/2}}. \tag{B8}$$

Here a major difficulty arises. The Hilbert transform $\mathcal{H}[\Theta(\omega)e^{-\omega/\omega_c}\mathrm{J}_0(\omega|\Delta\boldsymbol{r}^0_{\lambda\mu}|/c)](\omega')$ exists only for $R/c=1$, despite the convergence condition $0<\omega_c$. Thus, we cannot derive any closed expression for $\mathrm{Re}\,\chi(\omega)$ for all R and c. Still we obtain by using a series representation for $\mathrm{J}_0(\omega|\Delta\boldsymbol{r}^0_{\lambda\mu}|/c)$ the relation

$$\mathrm{Re}\,\chi(\omega) = \frac{2\pi m\gamma\hbar}{\omega_c}\omega^2\left[\Theta(\omega)e^{\frac{-\omega}{\omega_c}}\,\mathrm{Ei}\left(\frac{\omega}{\omega_c}\right) - \Theta(-\omega)e^{\frac{\omega}{\omega_c}}\,\mathrm{Ei}\left(\frac{-\omega}{\omega_c}\right)\right]\mathrm{J}_0\left(|\Delta\boldsymbol{r}^0_{\lambda\mu}|\omega/c\right) - 2\pi m\gamma\hbar\omega_c\sum_{l=0}^{\infty}\frac{(-1)^l}{2^{2l}}\left(\frac{|\Delta\boldsymbol{r}^0_{\lambda\mu}|\omega_c}{c}\right)^{2l} \times\sum_{k=1}^{l+1}\frac{[2(l-k)+3]!}{l!l!}\left(\frac{\omega}{\omega_c}\right)^{2(k-1)}. \tag{B9}$$

This series, however, it is not of practical use, because of its slow convergence.

3. Three-dimensional environment

Following once more the same line, we obtain the spectral densities

$$J_{\lambda\mu}(\omega) = 4\pi^2 m\gamma\frac{c}{|\Delta\boldsymbol{r}^0_{\lambda\mu}|}\left(\frac{\omega}{\omega_c}\right)^2\sin\left(\omega|\Delta\boldsymbol{r}^0_{\lambda\mu}|/c\right)e^{-\omega/\omega_c}, \tag{B10}$$

and the renormalization frequencies

$$\tilde{\Omega}_{\lambda\lambda} = 8\pi m\gamma\omega_c$$
$$\tilde{\Omega}_{\lambda\mu} = \frac{8\pi m\gamma\omega_c}{\left[1+\left(\omega_c|\Delta\boldsymbol{r}^0_{\lambda\mu}|/c\right)^2\right]^2}.$$

Now the real part of the susceptibility is given by

$$\mathrm{Re}\,\chi_{\lambda\mu}(\omega') = -\frac{4\pi m\hbar\gamma}{\omega_c^2}\left(\frac{c}{|\Delta\boldsymbol{r}^0_{\lambda\mu}|}\right)P\int_0^\infty \sin\left(\omega|\Delta\boldsymbol{r}^0_{\lambda\mu}|/c\right) \times\omega^2 e^{-\omega/\omega_c}\left(\frac{1}{\omega-\omega'}+\frac{1}{\omega+\omega'}\right)d\omega, \tag{B11}$$

where the integral can be written as

$$\begin{aligned}\frac{1}{\pi}P\int_0^\infty \frac{\omega^2\sin\left(\omega\left|\Delta\boldsymbol{r}^0_{\lambda\mu}\right|/c\right)e^{\frac{-\omega}{\omega_c}}}{\omega-\omega'}d\omega \\ = \omega'^2\mathcal{H}\left[\Theta(\omega)\sin\left(\omega\left|\Delta\boldsymbol{r}^0_{\lambda\mu}\right|/c\right)e^{\frac{-\omega}{\omega_c}}\right](\omega') \\ +\frac{\omega'}{\pi}\frac{\omega_c^2\left|\Delta\boldsymbol{r}^0_{\lambda\mu}\right|/c}{\left[1+\left(\omega_c\left|\Delta\boldsymbol{r}^0_{\lambda\mu}\right|/c\right)^2\right]} \\ +\frac{1}{\pi}\frac{2\omega_c^3\left|\Delta\boldsymbol{r}^0_{\lambda\mu}\right|/c}{\left[1+\left(\omega_c\left|\Delta\boldsymbol{r}^0_{\lambda\mu}\right|/c\right)^2\right]^2}.\end{aligned} \tag{B12}$$

After some algebra, we finally obtain for the real part of the 3D susceptibility the expression

$$\begin{aligned}\mathrm{Re}\,\chi_{\lambda\nu}(\omega) = &-\frac{4\pi m\hbar\gamma c\omega^2}{\omega_c^2\left|\Delta\boldsymbol{r}^0_{\lambda\mu}\right|}\,\mathrm{Im}\left[g(\omega)+g(-\omega)\right] \\ &-\frac{4\pi^2 m\hbar\gamma c\omega^2}{\omega_c^2\left|\Delta\boldsymbol{r}^0_{\lambda\mu}\right|}\,\mathrm{Re}\left[\Theta(\omega)e^{-(\frac{1}{\omega_c}-i\left|\Delta\boldsymbol{r}^0_{\lambda\mu}\right|/c)\omega}\right. \\ &\left.+\Theta(-\omega)e^{(\frac{1}{\omega_c}-i\left|\Delta\boldsymbol{r}^0_{\lambda\mu}\right|/c)\omega}\right] \\ &-\frac{16\pi m\hbar\gamma\omega_c}{\left[1+\left(\omega_c\left|\Delta\boldsymbol{r}^0_{\lambda\mu}\right|/c\right)^2\right]^2},\end{aligned} \tag{B13}$$

with $g(\omega)=e^{-\left(1-i\omega_c\left|\Delta\boldsymbol{r}^0_{\lambda\mu}\right|/c\right)\omega/\omega_c}\Gamma[0,-(1-i\omega_c\left|\Delta\boldsymbol{r}^0_{\lambda\mu}\right|/c)\omega/\omega_c]$ and the incomplete gamma function $\Gamma(0,x)$.

APPENDIX C: FOURIER REPRESENTATION OF EQ. (A6)

Here we give a simple proof of Eq. (A9) starting from the Fourier transform of the susceptibility

$$\begin{aligned}\chi_{\lambda\mu}(\omega) &= \int_{-\infty}^{\infty}e^{i\omega t}\chi_{\lambda\mu}(t)dt \\ &= 2\int_{\left|\Delta\boldsymbol{r}^0_{\lambda\mu}\right|/c}^{\infty}e^{i\omega t}\sum_{\boldsymbol{k}}g_{\boldsymbol{k}}^2\sin\left(\boldsymbol{k}\cdot\Delta\boldsymbol{r}^0_{\lambda\mu}-\omega_{\boldsymbol{k}}t\right)dt \\ &= -i\sum_{\boldsymbol{k}}g_{\boldsymbol{k}}^2\left[e^{i[\boldsymbol{k}\cdot\Delta\boldsymbol{r}^0_{\lambda\mu}-(\omega-\omega_{\boldsymbol{k}})\left|\Delta\boldsymbol{r}^0_{\lambda\mu}\right|/c)}\right. \\ &\quad\times\int_0^\infty e^{i(\omega-\omega_{\boldsymbol{k}})t}\,dt - e^{-i[\boldsymbol{k}\cdot\Delta\boldsymbol{r}^0_{\lambda\mu}-(\omega+\omega_{\boldsymbol{k}})\left|\Delta\boldsymbol{r}^0_{\lambda\mu}\right|/c]} \\ &\quad\left.\times\int_0^\infty e^{i(\omega+\omega_{\boldsymbol{k}})t}\,dt\right],\end{aligned}$$

where we have made the substitution $t\to t+\left|\Delta\boldsymbol{r}^0_{\lambda\mu}\right|/c$. Inserting

$$\int_0^\infty e^{i(\omega-\omega_{\boldsymbol{k}})t}\,dt = \pi\delta(\omega-\omega_{\boldsymbol{k}})+i\mathcal{H}(1)(\omega_{\boldsymbol{k}})$$

into Eq. (C1) yields

$$\begin{aligned}\chi_{\lambda\mu}(\omega) = &-i\pi\sum_{\boldsymbol{k}}g_{\boldsymbol{k}}^2\{e^{i[\boldsymbol{k}\cdot\Delta\boldsymbol{r}^0_{\lambda\mu}-(\omega-\omega_{\boldsymbol{k}})\left|\Delta\boldsymbol{r}^0_{\lambda\mu}\right|/c]} \\ &\times\delta(\omega-\omega_{\boldsymbol{k}})-e^{-i[\boldsymbol{k}\cdot\Delta\boldsymbol{r}^0_{\lambda\mu}-(\omega+\omega_{\boldsymbol{k}})\left|\Delta\boldsymbol{r}^0_{\lambda\mu}\right|/c]} \\ &\times\delta(\omega+\omega_{\boldsymbol{k}})\} \\ &+\sum_{\boldsymbol{k}}g_{\boldsymbol{k}}^2\{e^{i[\boldsymbol{k}\cdot\Delta\boldsymbol{r}^0_{\lambda\mu}-(\omega-\omega_{\boldsymbol{k}})\left|\Delta\boldsymbol{r}^0_{\lambda\mu}\right|/c]}\mathcal{H}(1)(\omega_{\boldsymbol{k}}) \\ &-e^{-i[\boldsymbol{k}\cdot\Delta\boldsymbol{r}^0_{\lambda\mu}-(\omega+\omega_{\boldsymbol{k}})\left|\Delta\boldsymbol{r}^0_{\lambda\mu}\right|/c]}\mathcal{H}(1)(\omega_{\boldsymbol{k}})\},\end{aligned}$$

where the second sum vanishes owing to $\mathcal{H}(1)(\omega_{\boldsymbol{k}})=0$ [45]. By taking the imaginary part and performing the continuum limit, we obtain Eq. (A9).

APPENDIX D: PPT CRITERION AND CLASSIFICATION OF TRIPARTITE ENTANGLEMENT

Let us consider a system composed of two parties A and B. Then a necessary and sufficient condition for the separability between $1_A\times 1_B$ (two modes), $1_A\times N_B$, and $N_A\times N_B$ bisymmetric bipartite states is the partial positive transpose (PPT) criterion [27,46]. The $N_A\times N_B$ class of systems relates to Gaussian states that are locally invariant under all permutations of modes in each of the two subsystems. Then the PPT criterion can be formulated in terms of a bisymmetric covariance matrix G as follows: A state is separable if and only if $G^{T_B}\geqslant(i\hbar/2)\sigma$ (i.e., G^{T_B} is a positive-definite matrix), where G^{T_B} is the covariance matrix of the partial transpose of G with respect to the system B, given by $G^{T_B}=:\Lambda G\Lambda$, with

$$\Lambda=\mathbb{I}_{N_A+N_B}\oplus\begin{bmatrix}\mathbb{I}_{N_A} & 0\\ 0 & -\mathbb{I}_{N_B}\end{bmatrix},$$

the N-dimensional unit matrix $\mathbb{I}_N$, and the symplectic matrix

$$\sigma=\begin{bmatrix}0 & \mathbb{I}_{N_A+N_B}\\ -\mathbb{I}_{N_A+N_B}. & 0\end{bmatrix}.$$

The PPT criterion can be readily evaluated from the symplectic eigenvalues of G^{T_B}, given by the positive square roots of the eigenvalues of $(-i/\hbar)\sigma G^{T_B}$ [36].

For a system composed of three modes, Giedke *et al.* [26] have considered the PPT criterion to provide a complete classification of the three-mode states, according their separability properties. This classification is based on the partially transposed covariance matrices $\tilde{G}^{T_\lambda}=\Lambda_\lambda G\Lambda_\lambda$, which is related to the three possible bipartitions of a three-component system, namely, $\mathcal{A}|\mathcal{BC}$, $\mathcal{AB}|\mathcal{C}$, and $\mathcal{AC}|\mathcal{B}$. Then each three-mode Gaussian state can be assigned to one of the following classes [26]:

C1: *Fully inseparable states* that are not separable under any of the three possible bipartitions. This class contains the *genuine tripartite-entangled* states [41].

C2: *One-mode biseparable states* that are separable if two of the parties are grouped together, but inseparable with respect to the other groupings.

C3: *Two-mode biseparable states* for which two of the bipartitions are separable.

C4: *Three-mode biseparable states* for which all the three bipartitions are separable, but which cannot be written as a mixture of tripartite product states. These states are also known as *tripartite bound-entangled states*.

C5: *Fully separable states* that can be written as a mixture of tripartite product states.

[1] R. Horodecki, P. Horodecki, M. Horodecki, and K. Horodecki, Rev. Mod. Phys. **81**, 865 (2009).
[2] W. H. Zurek, Rev. Mod. Phys. **75**, 715 (2003).
[3] D. Braun, Phys. Rev. Lett. **89**, 277901 (2002).
[4] M. B. Plenio and S. F. Huelga, Phys. Rev. Lett. **88**, 197901 (2002).
[5] F. Benatti, R. Floreanini, and M. Piani, Phys. Rev. Lett. **91**, 070402 (2003).
[6] F. Benatti, R. Floreanini, and U. Marzolino, Phys. Rev. A **81**, 012105 (2010).
[7] R. Doll, M. Wubs, P. Hänggi, and S. Kohler, Europhys. Lett. **76**, 547 (2006).
[8] K. Shiokawa, Phys. Rev. A **79**, 012308 (2009).
[9] A. Wolf, G. D. Chiara, E. Kajari, E. Lutz, and G. Morigi, Europhys. Lett. **95**, 60008 (2011).
[10] E. Kajari, A. Wolf, E. Lutz, and G. Morigi, Phys. Rev. A **85**, 042318 (2012).
[11] R. Doll, M. Wubs, P. Hänggi, and S. Kohler, Phys. Rev. B **76**, 045317 (2007).
[12] C. Hörhammer and H. Büttner, Phys. Rev. A **77**, 042305 (2008).
[13] T. Zell, F. Queisser, and R. Klesse, Phys. Rev. Lett. **102**, 160501 (2009).
[14] R. Vasile, P. Giorda, S. Olivares, M. G. A. Paris, and S. Maniscalco, Phys. Rev. A **82**, 012313 (2010).
[15] C. H. Fleming, N. I. Cummings, C. I. Anastopoulos, and B. L. Hu, J. Phys. A: Math. Theor. **45**, 065301 (2012).
[16] L. A. Correa, A. A. Valido, and D. Alonso, Phys. Rev. A **86**, 012110 (2012).
[17] O. S. Duarte and A. O. Caldeira, Phys. Rev. A **80**, 032110 (2009).
[18] D. M. Valente and A. O. Caldeira, Phys. Rev. A **81**, 012117 (2010).
[19] H. Krauter, C. A. Muschik, K. Jensen, W. Wasilewski, J. M. Petersen, J. I. Cirac, and E. S. Polzik, Phys. Rev. Lett. **107**, 080503 (2011).
[20] A. J. Leggett, S. Chakravarty, A. T. Dorsey, M. P. A. Fisher, A. Garg, and W. Zwerger, Rev. Mod. Phys. **59**, 1 (1987).
[21] P. Hänggi, P. Talkner, and M. Borkovec, Rev. Mod. Phys. **62**, 251 (1990).
[22] U. Weiss, *Quantum Dissipative Systems* (World Scientific, Singapore, 1999), Vol. 10.
[23] W. G. Unruh and W. H. Zurek, Phys. Rev. D **40**, 1071 (1989).
[24] H. Kohler and F. Sols, Physica A **392**, 1989 (2013).
[25] P. Hänggi and G.-L. Ingold, Chaos **15**, 026105 (2005).
[26] G. Giedke, B. Kraus, M. Lewenstein, and J. I. Cirac, Phys. Rev. A **64**, 052303 (2001).
[27] G. Adesso and F. Illuminati, J. Phys. A: Math. Theor. **40**, 7821 (2007).
[28] J.-T. Hsiang, R. Zhou, and B. L. Hu, arXiv:1306.3728.
[29] A. A. Valido, L. A. Correa, and D. Alonso, Phys. Rev. A **88**, 012309 (2013).
[30] S. Coleman and R. E. Norton, Phys. Rev. **125**, 1422 (1962).
[31] A. C. Aitken, *Determinants and Matrices* (Greenwood Press, Westport, 1983).
[32] J. Jeffers, P. Horak, S. M. Barnett, and P. M. Randmore, Phys. Rev. A **62**, 043602 (2000).
[33] J. J. Hope, G. M. Moy, M. J. Collett, and C. M. Savage, Phys. Rev. A **61**, 023603 (2000).
[34] B. M. Garraway, and B. J. Dalton, J. Phys. B: At. Mol. Opt. Phys. **39**, S767 (2006).
[35] W.-M. Zhang, P.-Y. Lo, H.-N. Xiong, M. W.-Y. Tu, and F. Nori, Phys. Rev. Lett. **109**, 170402 (2012).
[36] G. Vidal and R. F. Werner, Phys. Rev. A **65**, 032314 (2002).
[37] P. Marian and T. A. Marian, Phys. Rev. A **86**, 022340 (2012).
[38] J.-H. An and W.-M. Zhang, Phys. Rev. A **76**, 042127 (2007).
[39] M. Ludwig, K. Hammerer, and F. Marquardt, Phys. Rev. A **82**, 012333 (2010).
[40] P. S. Riseborough, P. Hanggi, and U. Weiss, Phys. Rev. A **31**, 471 (1985).
[41] F. Benatti and A. Nagy, Ann. Phys. **326**, 740 (2011).
[42] N. B. An, J. Kim, and K. Kim, Phys. Rev. A **84**, 022329 (2011).
[43] J. Anders, Phys. Rev. A **77**, 062102 (2008).
[44] C. H. Bennett, A. Grudka, M. Horodecki, P. Horodecki, and R. Horodecki, Phys. Rev. A **83**, 012312 (2011).
[45] A. Erdélyi, W. Magnus, F. Oberhettinger, and F. G. Tricomi, *Tables of Integral Transforms* (McGraw-Hill, New York, 1954), Vol. 2.
[46] A. Serafini, G. Adesso, and F. Illuminati, Phys. Rev. A **71**, 032349 (2005).

Article 3

GAUSSIAN TRIPARTITE ENTANGLEMENT OUT OF EQUILIBRIUM

Antonio A. Valido, Luis A. Correa, and Daniel Alonso

Phys. Rev. A 88, 012309 (2013)

PHYSICAL REVIEW A **88**, 012309 (2013)

Gaussian tripartite entanglement out of equilibrium

Antonio A. Valido,[1,2,*] Luis A. Correa,[1,3,†] and Daniel Alonso[1,3,‡]

[1]*Instituto Universitario de Estudios Avanzados (IUdEA), Universidad de La Laguna, La Laguna 38203, Spain*

[2]*Departamento Física Fundamental II, Universidad de La Laguna, La Laguna 38203, Spain*

[3]*Departamento Física Fundamental, Experimental, Electrónica y Sistemas, Universidad de La Laguna, La Laguna 38203, Spain*

(Received 20 May 2013; published 11 July 2013)

The stationary *multipartite* entanglement between three interacting harmonic oscillators subjected to decoherence is analyzed in the largely unexplored nonequilibrium strong dissipation regime. We compute the exact asymptotic Gaussian state of the system and elucidate its separability properties, qualitatively assessing the regions of the space of parameters in which fully inseparable states are generated. Interestingly, the sharing structure of bipartite entanglement is seen to degrade as dissipation increases even for very low temperatures, at which the system approaches its ground state. We also find that establishing stationary energy currents across the harmonic chain does not correspond with the buildup of biseparable steady states, which relates instead just to the relative intensity of thermal fluctuations.

DOI: 10.1103/PhysRevA.88.012309 PACS number(s): 03.67.Bg, 03.65.Yz, 03.67.Mn, 42.50.Lc

I. INTRODUCTION

Entangled states of continuous-variable (CV) systems have come to occupy a prominent position in quantum technologies [1] for both experimental and theoretical convenience. On the experimental side, the high degree of control in the preparation, manipulation, and measurement of Gaussian CV states [2] in a range of quantum physical supports including optical cavities, trapped ions [3], or nanomechanical devices [4], makes them ideal for the efficient implementation of quantum information protocols. In particular, entangled CV *multipartite* Gaussian states are a valuable resource for communication schemes involving many parties [5–7], whose quantum-enhanced performance has been already demonstrated in experiments [8,9].

This *outperformance* over classical protocols crucially relies on the amount and distribution of the entanglement shared by the multiple "modes," which makes the precise quantification of multipartite entanglement a matter of paramount importance. The general assessment of entanglement even in low-dimensional quantum systems remains an open and challenging problem to date [10,11] and yet tremendous progress has been made towards its characterization in the CV Gaussian multipartite scenario [12–14]. This fact, combined with the simple mathematical description that CV multimode Gaussian states enjoy, further highlights their practical convenience.

Unfortunately, entanglement is very fragile to the unavoidable decorrelating external environments and therefore, the successful implementation of quantum technologies with CVs should start with a complete understanding of noise and dissipation, so that they may be avoided or eventually engineered to protect quantum coherences. In this line, a number of recent works have extensively analyzed the dynamics and asymptotic properties of bimodal entanglement in CV Gaussian states under realistic models of noise and dissipation [15–25]. Concretely, the stationary two-mode entanglement under weak correlated and uncorrelated local noise was addressed in [17,19,20] for identical oscillators, and in [18,21] for the nonresonant case. Moreover, the problem may be solved exactly once one abandons the assumption of weak interaction between system and environment, thus making it possible to probe into the strongly non-Markovian and nonequilibrium regimes [24,25]. In contrast, much less is known about noise and dissipation in the CV Gaussian multipartite scenario [26–32] where, to our knowledge, all available results are limited by either the weak dissipation or equilibration assumptions.

The present paper aims to study multipartite stationary entanglement in the little-studied nonequilibrium strongly dissipative regime, through the extension of the exact techniques of [25]. We focus on the stationary Gaussian states that result from the contact of an interacting three-mode CV system with three local structured heat baths. A rich physical picture is gained by preparing the baths at generally different equilibrium temperatures, thus inducing steady-state energy transport. Endowed with all the versatility of an exact unconstrained stationary solution, we address the question whether robust tripartite entangled states may be generated out of equilibrium. As we shall see below, we can answer in the positive.

More precisely, we take three (generally nonresonant) modes arranged in an open chain with linear nearest-neighbor interactions and locally dissipating into uncorrelated Ohmic baths. We are then able to compute the *exact* Gaussian steady state of the system, under the sole assumption of an initially uncorrelated system and environmental degrees of freedom [33]. Our model is particularly suited for the theoretical description of tripartite CV systems in which thermal relaxation is the main source of decoherence, as it may occur, for instance, to trapped ions in a Paul trap [34] or clamped interacting nanomechanical oscillators [35,36].

Taking the exact steady state as starting point, we issue a comprehensive study of the tripartite entanglement distribution according to the classification introduced in [12]. When the three equilibrium temperatures of the reservoirs are set to the same value and identical oscillators are considered, we observe the expected competition between decoherence and interoscillator coupling in the buildup of stationary tripartite entanglement. Most interestingly, we find limiting dissipation

*aavalido@ull.es
†lacorrea@ull.es
‡dalonso@ull.es

rates above which the ground state of the interacting oscillators switches from the "weak dissipation" fully inseparable phase into a "strong dissipation" *bound entangled* phase, passing through an intermediate *two-mode biseparable* stage. As we shall see, these changes in the entanglement-sharing structure occur as a consequence of the non-negligible renormalization effects introduced by the system-bath interaction, in spite of the vanishing thermal fluctuations.

Imposing a temperature gradient across the chain proves detrimental to the formation of robust fully inseparable states unless the system is set up in an asymmetrical configuration. Nevertheless, the resulting separability structure does not seem to depend on the stationary energy currents induced across the system, but rather, with the relative intensity of thermal fluctuations on each of the modes.

Finally, we discuss how the asymptotic tripartite entanglement may be enhanced with a suitable choice of parameters leading to well-separated time scales for the thermal fluctuations and the free dynamics of the interacting modes.

This paper is organized as follows: We start by introducing the microscopic model for the system, the baths, and their dissipative interaction in Sec. II. The reduced dynamics of the oscillators is tackled via the generalized quantum Langevin equation, introduced in Sec. III A, and solved in the stationary regime in Secs. III B and III C. For a detailed derivation of the closed formula of the exact steady state, the interested reader is directed to the Appendix. We then briefly review the classification criteria for tripartite entanglement in CV Gaussian states in Sec. IV, and apply them to the steady states of our system in Sec. V: The separability properties in the case of identical equilibrium temperatures are discussed in Sec. V A, and the results on the steady-state entanglement under a temperature gradient are presented in Sec. V B. Finally, in Sec. VI, we summarize and draw our conclusions.

II. THE SYSTEM

As already mentioned, our system consists of three quantum harmonic oscillators, labeled by $\alpha \in \{\mathcal{L},\mathcal{C},\mathcal{R}\}$ after "left," "center," and "right," respectively. They have bare oscillation frequencies ω_α and equal mass m is assumed:

$$H_{S0} = \sum_\alpha \frac{p_\alpha^2}{2m} + \frac{1}{2} m\omega_\alpha^2 x_\alpha^2. \tag{1}$$

Here x_α and p_α stand for the corresponding position and momentum operators. We connect the oscillators through a generic *quadratic* interaction term of the form

$$H_{SI} = \frac{1}{2}\sum_{\alpha\beta} x_\alpha V_{\alpha\beta} x_\beta, \tag{2}$$

where $V_{\alpha\beta}$ are the entries of an Hermitian *interaction matrix* V. In particular, we shall arrange the oscillators in an open chain with nearest-neighbor interactions of strength k connecting $\mathcal{L} \leftrightarrow \mathcal{C}$ and $\mathcal{C} \leftrightarrow \mathcal{R}$, that is (see Fig. 1 below),

$$V = \begin{pmatrix} k & -k & 0 \\ -k & 2k & -k \\ 0 & -k & k \end{pmatrix}. \tag{3}$$

We address the local dissipation mechanism with the paradigmatic Caldeira-Legget model [33,37]. Therefore, three independent bosonic reservoirs are introduced, also labeled $\alpha \in \{\mathcal{L},\mathcal{C},\mathcal{R}\}$, comprised of noninteracting modes $\{q_{\alpha\mu}, p_{\alpha\mu}\}$ linearly coupled to their local oscillator $\{x_\alpha, p_\alpha\}$ with strength $g_{\alpha\mu}$:

$$H_{SB} = \sum_{\alpha\mu} \frac{p_{\alpha\mu}^2}{2m_{\alpha\mu}} + \frac{1}{2} m_{\alpha\mu}\omega_{\alpha\mu}^2 \left(q_{\alpha\mu} - \frac{g_{\alpha\mu}}{m_{\alpha\mu}\omega_{\alpha\mu}^2} x_\alpha \right)^2. \tag{4}$$

Apart from the free Hamiltonian of the reservoirs and their linear interaction with the system (i.e., the terms of the form $g_{\alpha\mu} x_\alpha q_{\alpha\mu}$), Eq. (4) also explicitly includes the *renormalization term*

$$H_R = \sum_{\alpha\mu} \frac{g_{\alpha\mu}^2}{2m_{\alpha\mu}\omega_{\alpha\mu}^2} x_\alpha^2, \tag{5}$$

which is necessary in order to compensate the distortion exerted by the system-bath coupling on H_{S0} [33]. The effects of this term only start to become relevant as the system-bath interaction grows stronger [25]. The coupling constants $g_{\alpha\mu}$ define the spectral densities

$$J_\alpha(\omega) \equiv \pi \sum_\mu \frac{g_{\alpha\mu}^2}{2m_{\alpha\mu}\omega_{\alpha\mu}} \delta(\omega - \omega_{\alpha\mu}), \tag{6}$$

which receive a phenomenological functional form suitable for a correct description of dissipation. In particular, in Sec. III C, we shall consider Ohmic spectral densities with Lorentz-Drude

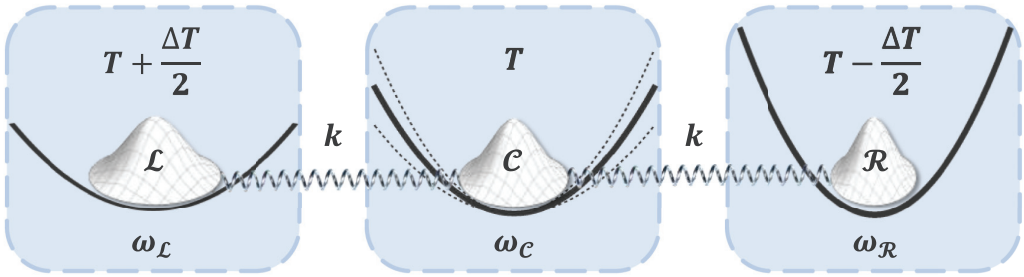

FIG. 1. (Color online) Schematic representation of our tripartite CV system comprised of nonresonant modes mechanically coupled via nearest-neighbor linear interactions of strength k. Each oscillator dissipates at a rate γ into its local bath, at temperatures $T_{\mathcal{C}} = T$ and $T_{\mathcal{L},\mathcal{R}} = T \pm \Delta T/2$, where $\Delta T \in [0,2T)$ so that a temperature gradient may be established across the system.

high-frequency cutoff

$$J_\alpha(\omega) = \frac{m\gamma_\alpha \omega}{1+\omega^2/\omega_c^2}, \tag{7}$$

where γ_α stands for the *dissipation rate*, and carries the order of magnitude of the system-bath interaction, and ω_c is the cutoff frequency, which places a lower bound in the characteristic time scale of the thermal fluctuations of the baths [38].

We initialize system and environment as $\varrho_0 = \rho_0 \otimes (\bigotimes_\alpha \tau_\alpha)$, where ρ_0 is any state of the three oscillators, $\tau_\alpha = \mathcal{Z}_\alpha^{-1} e^{-H_{B_\alpha}/k_B T_\alpha}$ is a (Gaussian) thermal equilibrium state of reservoir α at temperature T_α, and where k_B denotes the Boltzmann constant. The normalization factors are $\mathcal{Z}_\alpha \equiv \mathrm{tr}\{e^{-H_{B_\alpha}/k_B T_\alpha}\}$ and H_{B_α} stands for the free Hamiltonian of the corresponding reservoir. The linearity of the system's effective dynamics, guaranteed by the overall linear Hamiltonian and the "Gaussianity" of the baths, leads to Gaussian reduced stationary states $\rho_\infty = \mathrm{tr}_B\{\varrho_\infty\}$ [39].

Any Gaussian three-mode state is fully determined (up to local displacements) by its second-order moments, arranged in the 6×6 covariance matrix

$$\boldsymbol{\sigma} \equiv \begin{pmatrix} C_{\boldsymbol{XX}}(0) & C_{\boldsymbol{XP}}(0) \\ C_{\boldsymbol{PX}}(0) & C_{\boldsymbol{PP}}(0) \end{pmatrix}. \tag{8}$$

The 3×3 blocks $C_{\boldsymbol{AB}}(0)$ are defined as

$$C_{\boldsymbol{AB}}(t-t') \equiv \tfrac{1}{2}\langle \boldsymbol{A}(t)\boldsymbol{B}^T(t') + \boldsymbol{B}(t')\boldsymbol{A}^T(t)\rangle_{\rho_0}, \tag{9}$$

where $\boldsymbol{A},\boldsymbol{B} \in \{\boldsymbol{X},\boldsymbol{P}\}$ and $\boldsymbol{X} = \{x_\mathcal{L}, x_\mathcal{C}, x_\mathcal{R}\}^T$, $\boldsymbol{P} = \{p_\mathcal{L}, p_\mathcal{C}, p_\mathcal{R}\}^T$ are column vectors collecting position and momentum operators of the modes.

III. EXACT STATIONARY STATES

A. Generalized quantum Langevin equation

We shall now calculate the stationary matrices $C_{\boldsymbol{AB}}(0)$ and thus, the steady state of the system, by making use of the generalized quantum Langevin equation (QLE) formalism [33], which is widespreadly used in the study of quantum Brownian motion [40]. The QLE follows from the elimination of the environment in the Heisenberg equations of motion for $x_\alpha(t)$ and $p_\alpha(t)$, and may be compactly written as

$$M\ddot{\boldsymbol{X}} + \boldsymbol{\phi}\boldsymbol{X} = \boldsymbol{\eta}(t) + \frac{1}{\hbar}\int_{-\infty}^{t} d\tau\, \boldsymbol{\chi}(t-\tau)\boldsymbol{X}(\tau). \tag{10}$$

Note that this equation does not rely on any approximations and therefore, it remains valid in all regimes of parameters. We remark as well that we took the initial condition ϱ_0 at $t_0 \to -\infty$ so that for any finite t, it already describes the asymptotic properties of the system.

The 3×3 matrix M is diagonal and carries the masses of the oscillators $M_{\alpha\beta} = m\delta_{\alpha\beta}$, where $\delta_{\alpha\beta}$ stands for Kronecker delta. The effective potential is encoded in $\phi_{\alpha\beta} = m\omega_\alpha^2\delta_{\alpha\beta} + V_{\alpha\beta} + 2m\Delta\Omega_\alpha\delta_{\alpha\beta}$, where the frequency shift

$$m\Delta\Omega_\alpha \equiv \frac{1}{\pi}\int_0^\infty d\omega \frac{J_\alpha(\omega)}{\omega} \tag{11}$$

directly follows from the renormalization term of Eq. (5).

In addition to the free dynamics of the interacting oscillators, Eq. (10) also accounts for decoherence: On the one hand, the oscillators are locally driven by the stochastic quantum forces $\eta_\alpha(t)$ that enclose the effects of the thermal noise. These form the column vector $\boldsymbol{\eta}(t)$. On the other hand, the last term on the right-hand side stands for a "friction memory kernel" or "generalized susceptibility" and describes dissipation. Since the three baths are uncorrelated, the 3×3 susceptibility matrix $\boldsymbol{\chi}$ has elements

$$\chi_{\alpha\beta}(t) \equiv \delta_{\alpha\beta}\Theta(t)\frac{2\hbar}{\pi}\int_0^\infty d\omega\, J_\alpha(\omega)\sin\omega t, \tag{12}$$

where $\Theta(t)$ stands for the Heaviside step function. Thermal noise and friction are connected via the Kubo relation

$$\boldsymbol{\chi}(t-t') = -i\Theta(t-t')\langle \boldsymbol{\eta}(t)\boldsymbol{\eta}^T(t') - \boldsymbol{\eta}(t')\boldsymbol{\eta}^T(t)\rangle_B, \tag{13}$$

where $\langle A\rangle_B \equiv \mathrm{tr}\{A \bigotimes_\alpha \tau_\alpha\}$ denotes an average over the environmental degrees of freedom.

B. Formal stationary solution

Quite generically, the matrices $C_{\boldsymbol{AB}}(t)$ may be extracted from Eq. (10) by taking its Fourier transform $\tilde{f}(\omega) \equiv \int dt\, e^{i\omega t} f(t)$. One thus arrives at the linear expression

$$\tilde{\boldsymbol{X}}(\omega) = \alpha(\omega)\,\tilde{\boldsymbol{\eta}}(\omega), \tag{14}$$

where the complex matrix $\alpha(\omega)$ is defined as

$$\alpha(\omega) \equiv -\left(\omega^2 M - \phi + \frac{1}{\hbar}\tilde{\chi}(\omega)\right)^{-1}, \tag{15}$$

and the Fourier transform $\tilde{\chi}(\omega)$ of the generalized susceptibility matrix has elements such that

$$-\frac{\mathrm{Im}\,\tilde{\chi}_{\alpha\alpha}(\omega)}{\hbar} = J_\alpha(\omega)\,\Theta(\omega) - J_\alpha(-\omega)\,\Theta(-\omega). \tag{16}$$

The causality argument that renders $\chi_{\alpha\alpha}(t) = 0\ \forall t < 0$ also ensures that $\tilde{\chi}_{\alpha\alpha}(\omega)$ is analytic in the upper-half plane of complex frequencies [33]. By virtue of the Kramers-Kronig relations we then have

$$\mathrm{Re}\,\tilde{\chi}_{\alpha\alpha}(\omega) = \mathrm{P}\int_{-\infty}^{\infty}\frac{d\omega'}{\pi}\frac{\mathrm{Im}\,\tilde{\chi}_{\alpha\alpha}(\omega')}{\omega'-\omega}, \tag{17}$$

where P stands for the principal value of the integral. Let us now introduce the notation

$$\Gamma_\alpha(\omega) \equiv -\frac{\mathrm{Im}\,\tilde{\chi}_{\alpha\alpha}(\omega)}{\hbar}\coth\frac{\hbar\omega}{2k_B T_\alpha}, \tag{18}$$

for the *symmetrized power spectrum* of the quantum stochastic force $\eta_\alpha(t)$ [24,25], and the vector $\Gamma(\omega) \equiv \{\Gamma_\mathcal{L}(\omega), \Gamma_\mathcal{C}(\omega), \Gamma_\mathcal{R}(\omega)\}^T$. Then, the matrix $C_{\boldsymbol{XX}}(t)$ is written as

$$C_{\boldsymbol{XX}}(t) = \hbar\int\frac{d\omega}{2\pi}e^{-i\omega t}\alpha(\omega)\Gamma(\omega)\alpha(-\omega)^T, \tag{19}$$

while the remaining correlations are

$$C_{\boldsymbol{PP}}(t) = \hbar m^2\int\frac{d\omega}{2\pi}\omega^2 e^{-i\omega t}\alpha(\omega)\Gamma(\omega)\alpha(-\omega)^T, \tag{20}$$

and $C_{\boldsymbol{XP}}(t) = C_{\boldsymbol{PX}}(t)$,

$$C_{\boldsymbol{XP}}(t) = i\hbar m\int\frac{d\omega}{2\pi}\omega e^{-i\omega t}\alpha(\omega)\Gamma(\omega)\alpha(-\omega)^T. \tag{21}$$

Equations (15)–(21) thus formally provide the desired exact stationary states of the system for arbitrary spectral densities $J_\alpha(\omega)$.

C. Stationary solution for Ohmic baths

As already anticipated, in order to compute the steady state from Eqs. (15)–(21), we will restrict ourselves to the Ohmic spectral densities of Eq. (7) and further assume symmetric dissipation rates $\gamma_\alpha = \gamma$. In this case, $\tilde{\chi}(\omega)$ reduces to

$$\tilde{\chi}_{\alpha\beta}(\omega) = \delta_{\alpha\beta}\frac{m\hbar\gamma\omega_c^2}{i\omega - \omega_c}, \tag{22}$$

which gives $\alpha(\omega)$ and $\Gamma_\alpha(\omega)$ by immediate substitution into Eqs. (15) and (18). Note that the frequency shift of Eq. (11) is now $\Delta\Omega_\alpha = \gamma\omega_c/2$.

It is indeed possible to carry out the integration in Eqs. (19)–(21) and get closed formulas for the exact correlations by means of contour integration in the plane of complex frequencies, as in [41]. Unfortunately, little can be gained from the cumbersome expressions that result, neither from the physical, nor from the practical point of view. Their discussion is hence postponed until the Appendix, and in what follows, we shall evaluate Eqs. (19)–(21) numerically.

In the next section, we briefly review the basic tools to be employed in the characterization of the entanglement distribution in the stationary states of our system.

IV. GAUSSIAN TRIPARTITE ENTANGLEMENT

As already mentioned, the precise quantification of genuine multipartite entanglement in general mixed states still proves challenging [10,11], even in the simplest case of tripartite systems. For instance, when dealing with qubits, quantities that prove to be *bona fide* measures in the bipartite scenario, such as the concurrence [42] or the negativity [43], have to be replaced with a suitable entanglement monotone that additionally satisfies the Coffman-Kundu-Wootters (CKW) *monogamy* inequality, like the residual *tangle*, computed from the convex roof of the squared concurrence [44].

In complete analogy, a continuous-variable residual tangle, or (Gaussian) *cotangle*, was introduced in [28] that satisfies the CKW inequality for all three-mode Gaussian states. It follows from the infimum of the squared logarithmic negativity [43] taken over all possible (Gaussian) pure-state decompositions of ρ. Alternatively, a monogamous Gaussian entanglement measure may also be defined in terms of the Rényi-2 entropy [14].

As a bipartite entanglement measure, the (logarithmic) negativity exploits the positivity-of-the-partial-transpose (PPT) separability criterion [45,46] which turns out to be not only necessary, but also *sufficient* for all $1 \times n$ multimode Gaussian states [47]. Therefore, even if the (logarithmic) negativity fails to faithfully account for genuine multipartite correlations, the PPT criterion does allow for a qualitative description of the distribution of Gaussian entanglement in a three-mode CV system, according to the number of nonseparable bipartitions out of the three possible. We shall denote them as $\mathcal{L}|(\mathcal{CR})$, $\mathcal{C}|(\mathcal{LR})$, and $\mathcal{R}|(\mathcal{LC})$. This entails the following classification for tripartite Gaussian states, as introduced in [12]:

(*C1*) *Fully inseparable states*, which are not separable in any of the bipartitions.

(*C2*) *One-mode biseparable states*, which are separable only in one out of the three possible bipartitions.

(*C3*) *Two-mode biseparable states*, for which now two of the bipartitions are separable.

(*C4*) *Three-mode biseparable* or bound entangled states, which are separable under all bipartitions, but cannot be written as a mixture of product states only.

(*C5*) *Fully separable states*, which unlike those of (*C4*), *can* be written as a mixture of product states.

In order to distinguish between the PPT-equivalent classes *C4* and *C5*, we make use of the criterion for full separability of [12]. In what follows, rather than attempting to quantify genuine tripartite entanglement, we resort to the previous qualitative characterization and apply it to the exact stationary states of our system.

V. RESULTS AND DISCUSSION

Finally, we are in a position to analyze the distribution of the stationary tripartite entanglement classes in the space of parameters of the system. Even if Eqs. (15)–(21) are not underpinned by any restrictive assumptions, we shall focus on the low-temperature regime, which is optimal for the buildup of entanglement, and exploit our steady-state solution to probe into the strongly dissipative regime.

We shall also restrict to low effective interoscillator coupling strengths k, as *strong* couplings are rather unrealistic in experiments. This translates into $k/m\Omega^2 \ll 1$, where $\Omega \sim \omega_\alpha$. Indeed, by noting that $\tau_k \sim m\Omega/k$ is a characteristic time for energy transport across the system when isolated from the environment, it becomes clear that the condition $k/m\Omega^2 \ll 1$ amounts to a separation of time scales $\tau_k \gg \Omega^{-1}$ that renders transport inefficient. Consequently, the typical time scale governing the closed evolution of the whole interacting system may be approximated as $\tau_S \sim \Omega^{-1}$.

In the study of quantum Brownian motion, one usually assumes *fast* thermal fluctuations ($\tau_B \sim \hbar/k_BT \ll \tau_S, \tau_B \ll \tau_D$) as compared with the free evolution and the dissipation time $\tau_D \sim \gamma^{-1}$ [38]. On the contrary, we shall work with relatively *low* temperatures and *strong* dissipation rates ($k_BT/\hbar \lesssim \Omega$, $k_BT/\hbar \sim \gamma$) so that the system is much more insensitive to noise. In this regime, picking a cutoff frequency ω_c of the order of Ω gives rise to *nonperturbative* renormalization frequency shifts $\Delta\Omega = \gamma\omega_c/2$ that should be expected to become relevant. It is also important to note that under strong dissipation, the stationary states of the system are generally not of *thermal equilibrium* (Gibbs states) [39,41,48], even when the temperatures of the local baths coincide and no steady-state energy transport is established.

Under these conditions, the stationary tripartite entanglement is studied in absence of energy currents through the system (Sec. V A), and when the equilibrium temperatures of the baths are arranged in a gradient (Sec. V B).

A. Identical equilibrium temperatures

We shall start by taking resonant frequencies $\omega_\alpha = \Omega$ and $\Delta T = 0$ (see caption of Fig. 1). The tripartite entanglement class of the resulting stationary states is plotted in Fig. 2 as a function of the coupling strength k and the equilibrium temperatures T of the baths. Not surprisingly, the higher the temperatures, the higher the corresponding coupling k that is

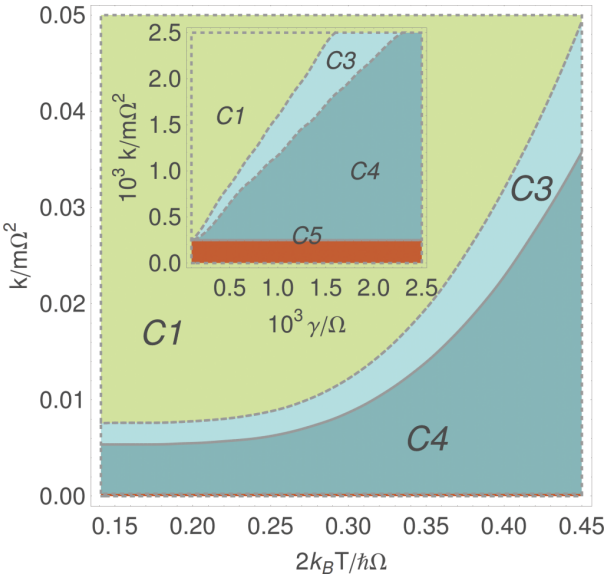

FIG. 2. (Color online) Phase diagram with Gaussian tripartite entanglement classes as a function of the interoscillator coupling strength k and the temperature of the baths $T_\alpha = T$ for $\omega_\alpha = \Omega$. The dissipation rate was fixed to $\gamma = 10^{-2}\Omega$, while the cutoff frequency is $\omega_c = 50\Omega$. For sufficiently weak coupling, the stationary state lies within the fully separable class (*C5*), which is almost imperceptible at the bottom of the plot. In the inset, the tripartite entanglement classes are shown as a function of the interaction strength k and the dissipation rate γ, at a very low temperature of just $2k_BT/\hbar\Omega = 0.05$. We observe that for any k above a temperature-dependent threshold, the ground state undergoes a transition from the fully inseparable phase, characteristic of low dissipation, to a bound entangled phase (*C4*), passing through an intermediate two-mode biseparable stage (*C3*) as the dissipation rate is increased.

required to keep the system in a fully inseparable state (*C1*). Note as well that one-mode biseparable states (*C2*) do not build up asymptotically in this configuration.

In fact, the stationary entanglement in the bipartition $\mathcal{C}|(\mathcal{LR})$ proves more resilient to noise than in either $\mathcal{L}|(\mathcal{CR})$ or $\mathcal{R}|(\mathcal{LC})$. This is obviously due to our choice of potential V in Eq. (3), which only puts mode $\mathcal{C}$ in direct interaction with the remaining two. Now, given that in this configuration the system is invariant under the exchange $\mathcal{L} \leftrightarrow \mathcal{R}$, its stationary states must be bisymmetric and, therefore, as the temperatures increase, steady-state entanglement in bipartitions $\mathcal{L}|(\mathcal{CR})$ and $\mathcal{R}|(\mathcal{LC})$ must disappear *jointly*, which entails a direct transition from *C1* to *C3*. Increasing the temperatures further, the system also becomes separable with respect to $\mathcal{C}|(\mathcal{LR})$, thus giving rise to stationary bound entangled states (*C4*). Even though class *C5* only appears for extremely low coupling in Fig. 2, at any given k there exists a temperature T above which the steady states become fully separable [49].

Most interestingly, in the inset of Fig. 2 we can see how the separability properties of the ground state (GS) of the chain depend on k and γ: For any k above a temperature-dependent threshold $k^T_{\min}$ (in the figure $k^T_{\min} \simeq 2.5 \times 10^{-3} k/m\Omega^2$), there exist dissipation rates at which the GS undergoes transitions *C1*→*C3* and *C3*→*C4*. On the contrary, for $k < k^T_{\min}$, it remains in the fully inseparable phase *C5* regardless of the dissipation strength. The sharing structure of bipartite entanglement in the GS of a harmonic chain thus depends on γ when *decohering* far from the Born-Markov regime.

This can be, at least, qualitatively understood by recalling that the system Hamiltonian $H_{S0} + H_R$ *includes* the renormalization term of Eq. (4), which amounts to a shift on the frequencies $\Omega^2 \mapsto \Omega_r^2 \equiv \Omega^2 + 2\Delta\Omega$. Hence, one may argue that the effective coupling strength $k/m\Omega_r^2$ decreases as the dissipation rate grows, thus potentially downgrading the GS to an entanglement class of higher separability.

B. Temperature gradient across the system

We now arrange the baths in a temperature gradient by allowing for $\Delta T \neq 0$ (see Fig. 1) so that stationary energy transport may be established across the harmonic chain. Let us first consider $2k_BT/\hbar\Omega = 0.35$, $\omega_{\mathcal{L},\mathcal{R}} = \Omega$, and $\omega_{\mathcal{C}} = \Omega + \delta$. This configuration is invariant with respect to the combined exchange of $\mathcal{L} \leftrightarrow \mathcal{R}$ and $\Delta T \leftrightarrow -\Delta T$ and thus, the distribution of entanglement phases must be symmetric about $\Delta T = 0$, as seen in Figs. 3(a) and 3(b).

In Fig. 3(a) we fix $k/m\Omega^2 = 0.05$ and plot the entanglement classes as a function of δ and ΔT. First, notice that one-mode biseparable stationary states (*C2*) do build up, now that the symmetry argument invoked in Sec. V A is not applicable.

One sees as well that in general, whenever $\omega_{\mathcal{C}}$ increases, the free dynamics of the central mode becomes more insensitive to noise since $k_BT/\hbar\omega_{\mathcal{C}}$ decreases. This helps to reduce the stationary *biseparability* and eventually yields fully inseparable states (*C1*). However, as illustrated in the inset, very large values of $\omega_{\mathcal{C}}$ may also cause an effective decoupling of the central mode from the rest as $k/m\omega_{\mathcal{C}}^2$ becomes smaller. In other words, *given* a fixed interaction k, fully inseparable stationary states may be generated by tuning the frequencies to a compromise between shielding the system from thermal noise and keeping the effective interaction between its modes *sufficiently strong*.

Finally, note that arranging the baths in a temperature gradient proves detrimental to the asymptotic formation of states in any of the bipartite entangled classes (*C1–C3*). This seems to occur due to the intensification of thermal noise at the hot end of the chain rather than as a consequence of the stationary energy currents established across the system. We illustrate this point further in Figs. 3(b) and 3(c), where k and ΔT are taken as the free parameters.

In Fig. 3(b) we consider resonant modes ($\delta = 0$), while in Fig. 3(c) the oscillators are set up in the asymmetrical configuration: $\omega_{\mathcal{L}} = \Omega$, $\omega_{\mathcal{C}} = 2\Omega$, and $\omega_{\mathcal{R}} = 3\Omega$. In the first case, keeping the steady state within the fully inseparable class requires stronger couplings as the temperature gradient increases in either direction. On the contrary, the asymmetric setting of Fig. 3(c) favors the formation of class *C1* steady states at *moderate* negative temperature gradients, as these provide the low-frequency mode $\mathcal{L}$ with the lowest temperature ($T - |\Delta T|$) and the high-frequency mode $\mathcal{R}$ with the highest one ($T + |\Delta T|$), which optimally shields the system from thermal noise.

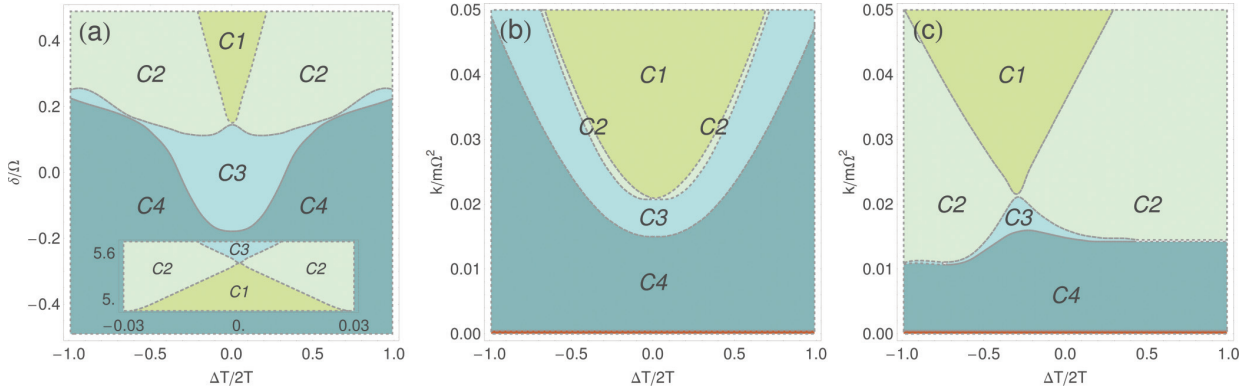

FIG. 3. (Color online) Stationary Gaussian tripartite entanglement classes versus (a) δ and ΔT for coupling strength $k/m\Omega^2 = 0.05$ and $\omega_{\mathcal{L},\mathcal{R}} = \Omega$, $\omega_{\mathcal{C}} = \Omega + \delta$; (b) k and ΔT for $\omega_\alpha = \Omega$; and (c) k and ΔT for $\omega_{\mathcal{L}} = \Omega$, $\omega_{\mathcal{C}} = 2\Omega$, and $\omega_{\mathcal{R}} = 3\Omega$ (see discussion in Sec. V B). All three figures share the same average temperature $2k_BT/\hbar\Omega = 0.35$ and the same dissipation rate γ and cutoff ω_c as in Fig. 2. In the inset of Fig. 3(a), we zoom in around $\Delta T = 0$ for large detuning δ, and observe how the fully inseparable phase (*C1*) is a *connected* region in the δ-ΔT space.

It is also noticeable how the one-mode biseparable class (*C2*) takes over bound entangled steady states (*C4*) in Fig. 3(c) as contrasted with Fig. 3(b), even though it may be seen that the magnitude of the stationary energy currents [50] is comparable in either case. This observation further suggests that the buildup of steady-state quantum correlations indeed might not share a causal relation with the efficient transport of energy at microscopic scale, as already pointed out in different contexts such as excitation transfer in biological systems [51], thermal conduction in spin chains [52] or the optimized performance of quantum refrigerators [53].

VI. CONCLUSIONS

We have addressed the qualitative classification of the bipartite entanglement distribution across three linearly coupled harmonic oscillators dissipating into independent structured baths. By making use of the quantum Langevin equation formalism, we were able to compute their exact stationary Gaussian states and then, issue a comprehensive analysis of the different entanglement classes that build up asymptotically in terms of the parameters of the system. It is important to note that this approach is not limited by the customary assumptions of equilibrium and/or weak-memoryless system-bath interactions, so that it allows one to probe into the largely unexplored nonequilibrium strong dissipation regime.

Interestingly, we saw how the ground state of the harmonic chain undergoes structural transitions between different schemes of entanglement sharing, increasing its bipartite separability as the dissipation grows stronger. This is a direct consequence of the non-negligible back action of the system-bath coupling on the system itself.

It was also noted that inducing stationary energy transport by means of a temperature gradient is generally detrimental to the formation of fully inseparable steady states due to the more intense thermal fluctuations at the hot end of the system. The resulting stationary energy currents do not seem to correlate to the asymptotic formation of biseparable states.

We finally discussed how a suitable choice of frequencies may shield the system from thermal noise while keeping the effective interoscillator coupling strong enough, so that potentially useful fully inseparable states may build up asymptotically in spite of the strong decoherence.

As was already pointed out, our model is appropriate for the theoretical description of a range of systems of interest in quantum technologies, especially arrays of interacting nanomechanical resonators. Indeed, considering typical frequencies Ω in the range of 1 MHz and masses m around 10^{-15} kg, the region of the space of parameters probed in our numerics may be achieved in present-day experiments.

One could also think of applying the powerful exact techniques illustrated here to the study of steady-state multipartite entanglement under the action of *correlated* thermal noise in a more realistic structured bath of spatial dimension greater than one. This problem is worthy of detailed study and will be considered elsewhere.

ACKNOWLEDGMENTS

The authors warmly thank A. Ruiz for reading and extensively commenting on the manuscript, and J. P. Palao, G. Adesso, D. Girolami, G. De Chiara, S. Kohler, and N. García Marco for fruitful discussions and helpful criticism. L.A.C. wants to thank N. Ramos García *in memoriam* for his unconditional support through the years. This project was funded by the Spanish MICINN (Grant No. FIS2010-19998) and the European Union (FEDER). A.A.V. and L.A.C. acknowledge the Canary Islands Government for financial support through the ACIISI fellowships (85% cofunded by European Social Fund).

APPENDIX: ANALYTICAL EXPRESSION FOR THE COVARIANCE MATRIX

As already mentioned in Sec. III C, in order to get an analytical expression for, e.g., Eq. (19), one can use the customary toolbox of complex analysis to explicitly carry out

the integration. Therefore, complete knowledge about the roots z_i of the denominator of the integrand is required. Let us start by alternatively writing $C_{XX}(0)$ as

$$\frac{[C_{XX}(0)]_{\alpha\delta}}{m\hbar\gamma\omega_c^2} = \sum_\beta \int \frac{d\omega}{2\pi} \frac{\mathrm{adj}\,[F(\omega)]_{\alpha\beta}\,\mathrm{adj}\,[F(\omega)^*]_{\beta\delta}}{|F(\omega)||F(\omega)^*|}\omega\,\coth\frac{\hbar\omega}{2k_BT_\beta}, \tag{A1}$$

where the matrix $F(\omega)$ is defined as $[F(\omega)]_{\alpha\beta} \equiv (\omega_c - i\omega)[\alpha^{-1}(\omega)]_{\alpha\beta}$. The notation $\mathrm{adj}[F(\omega)] = |F(\omega)|F(\omega)^{-1}$ stands for the *adjugate* matrix of $F(\omega)$, and the asterisk represents conjugate transposition. Note that from Eq. (22) it follows that $\alpha(-\omega)^T = \alpha(\omega)^*$.

The denominator of Eq. (A1) is a real polynomial of degree 18 comprised of the determinants $|F(\omega)|$ and $|F(\omega)^*|$, which are complex polynomials of degree nine. Provided that $F(\omega)$ is diagonalizable, $|F(\omega)|$ may be written as the product of three polynomials of degree three, and therefore, its roots can be analytically worked out, even if the resulting expressions are rather involved. When it comes to the multiplicity of those complex roots, it can be checked that they are all simple for our choice of interaction potential in Eq. (3). We shall label them so that $\{z_1,\ldots,z_9\}$ lie in the lower half plane of complex frequencies (and $\{z_{10},\ldots,z_{18}\} = \{\bar{z}_1,\ldots,\bar{z}_9\}$ are their corresponding complex conjugates).

We may now decompose the integrand of Eq. (A1) into partial fractions as

$$\frac{\mathrm{adj}[F(\omega)]_{\alpha\beta}\mathrm{adj}[F(\omega)^*]_{\beta\delta}\omega\,\coth\frac{\hbar\omega}{2k_BT_\beta}}{|F(\omega)||F(\omega)^*|} = \frac{1}{m^6}\sum_{j=1}^{9}\frac{\mathrm{adj}[F(\omega)]_{\alpha\beta}\mathrm{adj}[F(\omega)^*]_{\beta\delta}\omega\,\coth\frac{\hbar\omega}{2k_BT_\beta}}{2i\,\mathrm{Im}\,z_j\prod_{k\neq j}(z_j-z_k)\prod_{k\neq j}(z_j-\bar{z}_k)}\frac{1}{\omega-z_j} - \frac{1}{m^6}\sum_{j=1}^{9}\frac{\mathrm{adj}[F(\omega)]_{\alpha\beta}\mathrm{adj}[F(\omega)^*]_{\beta\delta}\omega\,\coth\frac{\hbar\omega}{2k_BT_\beta}}{2i\,\mathrm{Im}\,z_j\prod_{k\neq j}(\bar{z}_j-z_k)\prod_{k\neq j}(\bar{z}_j-\bar{z}_k)}\frac{1}{\omega-\bar{z}_j}, \tag{A2}$$

with $k \in \{1,\ldots,9\}$. We shall also make use of the identity

$$\coth x = \frac{1}{x} + \frac{1}{i\pi}\left[\psi\left(1+\frac{ix}{\pi}\right) - \psi\left(1-\frac{ix}{\pi}\right)\right], \tag{A3}$$

where $\psi(z)$ stands for the *digamma* or *psi function*, i.e., the logarithmic derivative of Euler's gamma function $\psi(z) \equiv d\,\ln\Gamma(z)/dz$ [54].

Combining Eq. (A3) with Eq. (A2), Eq. (A1) may be evaluated by making the analytical continuation of the integrand into the plane of complex frequencies and calculating residues. Notice that the extended function $\psi(1 \pm iz/\pi)$ has simple poles along the entire positive (negative) imaginary axis. We shall choose integration contours either in the lower or upper plane for each of the resulting terms in Eq. (A1), such that those nonanalyticities are avoided. The elements of the correlation $C_{XX}(0)$ thus result in

$$[C_{XX}(0)]_{\alpha\delta} = \frac{\hbar\gamma\omega_c^2}{m^5}\sum_\beta\sum_{j=1}^{9}\left[\frac{k_BT_\beta}{2\hbar\,\mathrm{Im}\,z_j} - \frac{2\,\mathrm{Re}\,z_j}{\pi\,\mathrm{Im}\,z_j}\mathrm{Im}\,\psi\left(1+i\frac{\hbar z_j}{2\pi k_BT_\beta}\right)\right]\mathrm{Re}\frac{\mathrm{adj}[F(z_j)]_{\alpha\beta}\mathrm{adj}[F(z_j)^*]_{\beta\delta}}{\prod_{k\neq j}(z_j-z_k)\prod_{k\neq j}(z_j-\bar{z}_k)}. \tag{A4}$$

Similarly, $C_{PP}(0)$ may be computed from Eq. (20) to yield

$$[C_{PP}(0)]_{\alpha\delta} = \frac{\hbar\gamma\omega_c^2}{m^3}\sum_\beta\sum_{j=1}^{9}\left[\frac{k_BT_\beta\mathrm{Re}\,z_j^2}{2\hbar\,\mathrm{Im}\,z_j} - \frac{2\,\mathrm{Re}\,z_j^3}{\pi\,\mathrm{Im}\,z_j}\mathrm{Im}\,\psi\left(1+i\frac{\hbar z_j}{2\pi k_BT_\beta}\right)\right]\mathrm{Re}\frac{\mathrm{adj}[F(z_j)]_{\alpha\beta}\mathrm{adj}[F(z_j)^*]_{\beta\delta}}{\prod_{k\neq j}(z_j-z_k)\prod_{k\neq j}(z_j-\bar{z}_k)}, \tag{A5}$$

and finally, Eq. (21) translates into

$$[C_{XP}(0)]_{\alpha\delta} = -\frac{\hbar\gamma\omega_c^2}{m^4}\sum_\beta\sum_{j=1}^{9}\left[\frac{k_BT_\beta\mathrm{Re}\,z_j}{2\hbar\,\mathrm{Im}\,z_j} - \frac{2\,\mathrm{Re}\,z_j^2}{\pi\,\mathrm{Im}\,z_j}\mathrm{Im}\,\psi\left(1+i\frac{\hbar z_j}{2\pi k_BT_\beta}\right)\right]\mathrm{Im}\frac{\mathrm{adj}[F(z_j)]_{\alpha\beta}\mathrm{adj}[F(z_j)^*]_{\beta\delta}}{\prod_{k\neq j}(z_j-z_k)\prod_{k\neq j}(z_j-\bar{z}_k)}, \tag{A6}$$

which provides us with the desired explicit formulas for the exact stationary Gaussian state of the system.

[1] S. L. Braunstein and P. van Loock, Rev. Mod. Phys. **77**, 513 (2005).
[2] C. Weedbrook, S. Pirandola, R. García Patrón, N. J. Cerf, T. C. Ralph, J. H. Shapiro, and S. Lloyd, Rev. Mod. Phys. **84**, 621 (2012).
[3] D. Leibfried, R. Blatt, C. Monroe, and D. Wineland, Rev. Mod. Phys. **75**, 281 (2003).
[4] K. Ekinci and M. Roukes, Rev. Sci. Instrum. **76**, 061101 (2005).
[5] P. van Loock and S. L. Braunstein, Phys. Rev. Lett. **84**, 3482 (2000).
[6] P. van Loock and S. L. Braunstein, Phys. Rev. Lett. **87**, 247901 (2001).
[7] G. Adesso, A. Serafini, and Fabrizio Illuminati, New J. Phys. **9**, 60 (2006).

[8] H. Yonezawa, T. Aoki, and A. Furusawa, Nature (London) **431**, 430 (2004).
[9] S. Koike, H. Takahashi, H. Yonezawa, N. Takei, S. L. Braunstein, T. Aoki, and A. Furusawa, Phys. Rev. Lett. **96**, 060504 (2006).
[10] R. Horodecki, P. Horodecki, M. Horodecki, and K. Horodecki, Rev. Mod. Phys. **81**, 865 (2009).
[11] C. H. Bennett, A. Grudka, M. Horodecki, P. Horodecki, and R. Horodecki, Phys. Rev. A **83**, 012312 (2011).
[12] G. Giedke, B. Kraus, M. Lewenstein, and J. I. Cirac, Phys. Rev. A **64**, 052303 (2001).
[13] G. Adesso and F. Illuminati, J. Phys. A **40**, 7821 (2007).
[14] G. Adesso, D. Girolami, and A. Serafini, Phys. Rev. Lett. **109**, 190502 (2012).
[15] J. Eisert, M. B. Plenio, S. Bose, and J. Hartley, Phys. Rev. Lett. **93**, 190402 (2004).
[16] M. Plenio, J. Hartley, and J. Eisert, New J. Phys. **6**, 36 (2004).
[17] J. P. Paz and A. J. Roncaglia, Phys. Rev. Lett. **100**, 220401 (2008).
[18] J. P. Paz and A. J. Roncaglia, Phys. Rev. A **79**, 032102 (2009).
[19] R. Vasile, S. Olivares, M. G. A. Paris, and S. Maniscalco, Phys. Rev. A **80**, 062324 (2009).
[20] R. Vasile, P. Giorda, S. Olivares, M. G. A. Paris, and S. Maniscalco, Phys. Rev. A **82**, 012313 (2010).
[21] F. Galve, G. L. Giorgi, and R. Zambrini, Phys. Rev. A **81**, 062117 (2010).
[22] F. Galve, L. A. Pachón, and D. Zueco, Phys. Rev. Lett. **105**, 180501 (2010).
[23] A. Wolf, G. De Chiara, E. Kajari, E. Lutz, and G. Morigi, Europhys. Lett. **95**, 60008 (2011).
[24] M. Ludwig, K. Hammerer, and F. Marquardt, Phys. Rev. A **82**, 012333 (2010).
[25] L. A. Correa, A. A. Valido, and D. Alonso, Phys. Rev. A **86**, 012110 (2012).
[26] M. M. Cola, M. G. A. Paris, and N. Piovella, Phys. Rev. A **70**, 043809 (2004).
[27] A. Ferraro and M. G. A. Paris, Phys. Rev. A **72**, 032312 (2005).
[28] G. Adesso, A. Serafini, and F. Illuminati, Phys. Rev. A **73**, 032345 (2006).
[29] S.-H. Xiang, B. Shao, K.-H. Song, and J. Zou, Phys. Rev. A **79**, 032333 (2009).
[30] G.-x. Li, L.-h. Sun, and Z. Ficek, J. Phys. B **43**, 135501 (2010).
[31] J. Li, T. Fogarty, C. Cormick, J. Goold, T. Busch, and M. Paternostro, Phys. Rev. A **84**, 022321 (2011).
[32] G. Manzano, F. Galve, and R. Zambrini, Phys. Rev. A **87**, 032114 (2013).
[33] U. Weiss, *Quantum Dissipative Systems*, 2nd ed., in Series in Modern Condensed Matter Physics, Vol. 10 (World Scientific, Singapore, 1999).
[34] K. Brown, C. Ospelkaus, Y. Colombe, A. Wilson, D. Leibfried, and D. Wineland, Nature (London) **471**, 196 (2011).
[35] E. Buks and M. Roukes, J. Microelectromech. Syst. **11**, 802 (2002).
[36] A. Cleland and M. Roukes, J. Appl. Phys. **92**, 2758 (2002).
[37] A. O. Caldeira and A. J. Leggett, Ann. Phys. **149**, 374 (1983).
[38] H. P. Breuer and F. Petruccione, *The Theory of Open Quantum Systems* (Oxford University Press, New York, 2012).
[39] H. Garbert, U. Weiss, and P. Talkner, Z. Phys. B **55**, 87 (1984).
[40] P. Hanggi and G.-L. Ingold, Chaos **15**, 026105 (2005).
[41] P. S. Riseborough, P. Hanggi, and U. Weiss, Phys. Rev. A **31**, 471 (1985).
[42] C. H. Bennett, D. P. DiVincenzo, J. A. Smolin, and W. K. Wootters, Phys. Rev. A **54**, 3824 (1996).
[43] G. Vidal and R. F. Werner, Phys. Rev. A **65**, 032314 (2002).
[44] V. Coffman, J. Kundu, and W. K. Wootters, Phys. Rev. A **61**, 052306 (2000).
[45] A. Peres, Phys. Rev. Lett. **77**, 1413 (1996).
[46] M. Horodecki, P. Horodecki, and R. Horodecki, Phys. Lett. A **223**, 1 (1996).
[47] R. F. Werner and M. M. Wolf, Phys. Rev. Lett. **86**, 3658 (2001).
[48] F. Haake and R. Reibold, Phys. Rev. A **32**, 2462 (1985).
[49] J. Anders, Phys. Rev. A **77**, 062102 (2008).
[50] A. Dhar and D. Roy, J. Stat. Phys. **127**, 801 (2006).
[51] M. B. Plenio and S. F. Huelga, New J. Phys. **10**, 113019 (2008).
[52] L.-A. Wu and D. Segal, Phys. Rev. A **84**, 012319 (2011).
[53] L. A. Correa, J. P. Palao, G. Adesso, and D. Alonso, Phys. Rev. E **87**, 042131 (2013).
[54] M. Abramowitz and I. A. Stegun, *Handbook of Mathematical Functions with Formulas, Graphs, and Mathematical Tables* (Dover, New York, 1972).

Article 4

QUANTUM CORRELATIONS AND ENERGY CURRENTS ACROSS FINITE HARMONIC CHAINS

Antonio A. Valido, Antonia Ruiz, and Daniel Alonso

arXiv:1503.09051 (2015)

Quantum correlations and energy currents across finite harmonic chains

Antonio A. Valido,[1,*] Antonia Ruiz,[1] and Daniel Alonso[1,†]

[1] *Instituto Universitario de Estudios Avanzados (IUdEA) and Departamento de Física, Universidad de La Laguna, La Laguna 38203 Spain*

(Dated: April 1, 2015)

We present a study that addresses both the stationary properties of the energy current and quantum correlations in a three-mode chain subjected to Ohmic and super-Ohmic dissipations. An extensive numerical analysis shows that the mean value and the fluctuations of the energy current remain insensitive to the emergence of a rich variety of quantum correlations: such as, two-mode discord and entanglement, bipartite three-mode and genuine tripartite entanglement. The discussion of the numerical results is based on the derived expressions for the stationary properties in terms of the two-time correlation functions of the oscillator operators, which carry quantum correlations. Interestingly, we show that quantum discord can be enhanced by both considering initially squeezed thermal bath states and imposing temperature gradients.

PACS numbers: 03.65.Yz, 03.67.Mn, 03.67.Bg, 42.50.Lc

Keywords: entanglement, energy current, continuous-variable, open quantum system

* aavalido@ull.es

† dalonso@ull.es

I. INTRODUCTION

Entanglement is one of the most striking phenomena in Quantum Physics. Composite systems exhibiting genuine quantum correlations defies our intuition, in the sense that they are not interpreted by classical or semiclassical means [1, 2]. Quantum correlations are at the heart of many quantum information tasks, such as quantum teleportation and quantum communication, as well as at the core of a variety of many-body physics phenomena [3]. *Quantum Thermodynamics* seeks the understanding of the emergence of thermodynamics laws from those of quantum dynamics [4, 5]. In this sense, one may wonder about the role of quantum correlations and coherence in different phenomena of interest in Quantum Thermodynamics, for instance in the thermodynamics of quantum thermal machines [4–13] or, more generally, in thermal non-equilibrium systems [14].

Quantum correlations have different fates depending on the environmental influence [15, 16]. Although entanglement is fragile with respect to thermal fluctuations and decoherence, stationary entanglement still could remain in a system subjected to dissipation [17–20]. Quantum discord [21–23] on the other hand seems more stable to environmental noise [24]. Recently, efforts have been made to study how dissipation may precisely drive the system onto preferred states, e.g. onto a genuine entangled state [25, 26], by engineering the interaction with environments [18, 27–29].

According to the non-equilibrium theory, the analysis of the (*linear*) response of many-body systems to macroscopic thermodynamic forces, such as those induced by temperature or chemical potential gradients, and to (weak) external fields provides an opportunity to test some predictions from condensed matter theory and statistical physics. As an illustration, multipartite entanglement in spin chains has been explored through precise measurements of the magnetic susceptibility [30, 31] and the heat capacity [32]. Also theoretical studies of these two magnitudes seem to provide observable signatures of entanglement in spin chains at thermal equilibrium [33, 34]. Nowadays, the energy transport through systems involving spatial continuous variables, such as chains of trapped ions, can be experimentally measured [35].

Given the increasing interest in systems under non-equilibrium thermal conditions in the quantum regime [24, 36–43], one may naturally ask whether the stationary response of a system to a temperature gradient may be influenced by the presence of pure quantum correlations, and in particular by *genuine* multipartite entanglement. The present work tries to elucidate whether the *average* properties of the stationary energy current across a harmonic chain, such the mean values and fluctuations, are sensitive to the presence of two-mode and *genuine* tripartite entanglement in the system, and more generically to quantum correlations as measured by discord. Significant

advances in the context of quantum spin networks indicate that the presence of bipartite entanglement does not play an important role on excitation transport [44], whereas a strong correlation between quantum coherence and transport efficiency can be present [45]. Although quantum correlations tend to disappear in systems subjected to a temperature gradient, it has been shown that entanglement and discord can still survive in systems under such conditions [24, 42]. Much less is known about the influence of genuine multipartite entanglement and the structure of discord on the stationary energy current in strongly dissipated harmonic chains at low temperatures. This work focuses on stationary quantum correlations in a continuous-variable system within such domain, and analyzes their possible relation to non-equilibrium conditions.

We consider an open system model composed of a linear arrange of three harmonic oscillators, each of them interacting with its own independent heat bath. We assume that the heat baths are in an initial squeezed thermal state [46]. This set-up is particularly interesting in the study of the generation of entanglement between distant modes of a quantum network [47], and also a convenient model to analyze many issues concerning the Quantum Thermodynamics of continuous variable systems [4]. We employ the open-system formalism based on the generalized Langevin equation (GLE) [48–50] to carry out an extensive numerical study of the stationary properties. We focus on the two- and three-mode entanglement and the discord in the presence of an energy current through the harmonic chain, for a large range of system parameters. We will analyze whether the average and the fluctuations of the energy current exhibit any evidence of the quantum correlations emerging under non-equilibrium thermal conditions.

The paper is organized as follows. In Section II we describe the model of the system and introduce the covariance matrix, which fully characterizes the stationary state of the system. Section III reviews the generalized Langevin equation approach considered to obtain this state. In Section IV we derive the expressions giving the average and the fluctuations of the energy current in terms of two-time correlation functions, and introduce the quatum correlations, characterized by means of the two- and three-mode entanglement and the (right) discord. The numerical results are presented in Section V, the corresponding discussion is given in Section VI, and the main conclusions are put together in Section VII.

II. MICROSCOPIC MODEL

We consider an open one-dimensional chain composed of three harmonic oscillators, see Figure 1, labeled as $\mathcal{L}$ (left), $\mathcal{C}$ (center), and $\mathcal{R}$ (right), with identical mass m, natural frequencies ω_i ($i =$

$\mathcal{L}$, $\mathcal{C}$, $\mathcal{R}$), and position and momentum operators ($\hat{x}_i$, $\hat{p}_i$). We assume bilinear interactions between first-neighbor oscillators, $\mathcal{L} \leftrightarrow \mathcal{C}$ and $\mathcal{C} \leftrightarrow \mathcal{R}$, with strength given by a single parameter k. Each ith oscillator is coupled with an independent heat bath composed of N independent harmonic oscillators, with masses $m_{i\mu}$ ($\mu = 1, \ldots, N$), frequencies $\omega_{i\mu}$ and position and momentum operators ($\hat{x}_{i\mu}$, $\hat{p}_{i\mu}$). Eventually we will consider the quasi-continuum limit $N \to \infty$. The Hamiltonian of the global system can be written as

$$\hat{H} = \sum_{i=\mathcal{L},\mathcal{C},\mathcal{R}} \left(\hat{H}_{Si} + \hat{H}_{Bi} \right) , \tag{1}$$

where

$$\hat{H}_{Si} = \frac{\hat{p}_i^2}{2m} + \frac{1}{2} m\omega_i^2 \hat{x}_i^2 + \underbrace{\sum_{j=\mathcal{L},\mathcal{C},\mathcal{R}} U_{ij} \hat{x}_i \hat{x}_j}_{\hat{H}_I} , \tag{2}$$

with

$$\boldsymbol{U} = \frac{1}{2} \begin{pmatrix} k & -k & 0 \\ -k & 2k & -k \\ 0 & -k & k \end{pmatrix} ,$$

corresponds to the isolated chain, and

$$\hat{H}_{Bi} = \sum_{\mu=1}^{N} \frac{\hat{p}_{i\mu}^2}{2m_{i\mu}} + \frac{1}{2} m_{i\mu}\omega_{i\mu}^2 \left(\hat{q}_{i\mu} - \frac{g_{i\mu}}{m_{i\mu}\omega_{i\mu}^2} \hat{x}_i \right)^2 \tag{3}$$

describes the three independent baths and their interactions with the oscillators, which are assumed bilinear with coupling constants $g_{i\mu}$. The interaction term in the microscopic model given by $\hat{H}_{Bi}$ includes the renormalization terms

$$m\Delta\Omega_i = \sum_{\mu=1}^{N} \frac{g_{i\mu}^2}{m_{i\mu}\omega_{i\mu}^2} , \tag{4}$$

which ensures that the frequency ω_i is maintained as the bare frequency of the ith oscillator [49], and the complete positivity of the total Hamiltonian (1).

In general, a system under the influence of dissipative effects will evolve in the long time limit toward a stationary state in which any trace of its initial state has been wiped out. The initial condition is only relevant in determining the transient dynamics previous to this asymptotic state. We fix the initial state at $t_0 \to -\infty$, and assume a barely chance of interaction between the system and the environment at to this point. Then it is reasonable to consider that the system and the environment are initially uncorrelated. As our analysis is based on quantum properties

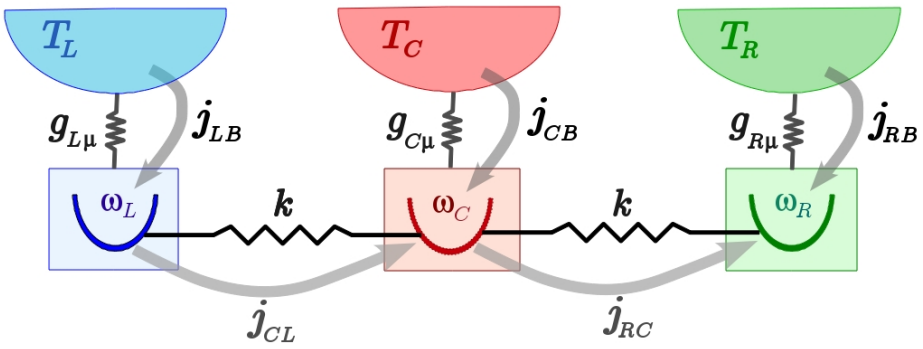

FIG. 1. (Color online) Schematic representation of the chain composed of the three oscillators coupled to independent heat baths, with temperatures $T_{\mathcal{L}}$, $T_{\mathcal{C}}$ and $T_{\mathcal{R}}$. $\hat{j}_{iB}\,(i=\mathcal{L},\,\mathcal{C},\,\mathcal{R})$ indicates the energy current from the heat bath to the ith oscillator, and $\hat{j}_{ij}$ the energy current from the jth to the ith oscillator, in the case of $T_{\mathcal{L}} > T_{\mathcal{C}} > T_{\mathcal{R}}$. k is the coupling constant between first-neighbor oscillators, and $g_{i\mu}$ the coupling constant between the ith chain oscillator and the $\mu th\,(\mu = 1,\ldots,N)$ oscillator of the bath.

in the asymptotic stationary state, without loss of generality we will assume an initial product state given by $\hat{\rho}_0 = \hat{\rho}_S \otimes (\hat{\rho}_{B\mathcal{L}} \otimes \hat{\rho}_{B\mathcal{C}} \otimes \hat{\rho}_{B\mathcal{R}})$ [42, 49], where $\hat{\rho}_S$ is the initial state of the isolated chain and $\hat{\rho}_{Bi}\,(i=\mathcal{L},\mathcal{C},\mathcal{R})$ initial Gaussian quantum states corresponding to the baths, which are not necessarily at thermal equilibrium states. Assuming that initially the baths are in squeezed thermal states with zero first-moments [51], the following averages over the initial state $\hat{\rho}_0$ are satisfied

$$\begin{aligned}
\frac{1}{2}\,\langle\{\hat{q}_{i\nu}(t_0),\hat{q}_{i\mu}(t_0)\}\rangle_{\hat{\rho}_0} &= \delta_{\nu\mu}\,\frac{\hbar}{2m_{i\mu}\omega_{i\mu}}\,[\,1+2\,N\,(\omega_{i\mu})\;+\;2\,\mathrm{Re}\,[\,M\,(\omega_{i\mu})\,]\,]\,,\\
\frac{1}{2}\,\langle\{\hat{p}_{i\nu}(t_0),\hat{p}_{i\mu}(t_0)\}\rangle_{\hat{\rho}_0} &= \delta_{\nu\mu}\,\frac{\hbar m_{i\mu}\omega_{i\mu}}{2}\,[\,1+2\,N\,(\omega_{i\mu})\;-\;2\,\mathrm{Re}\,[\,M\,(\omega_{i\mu})\,]\,]\,,\\
\frac{1}{2}\,\langle\{\hat{q}_{i\nu}(t_0),\hat{p}_{i\mu}(t_0)\}\rangle_{\hat{\rho}_0} &= \delta_{\nu\mu}\,\hbar\,\mathrm{Im}\,[\,M\,(\omega_{i\mu})\,]\,,
\end{aligned} \tag{5}$$

where $\mathrm{Re}[\,\bullet\,]$ and $\mathrm{Im}[\,\bullet\,]$ denotes the real and imaginary part of $\bullet$, and

$$\begin{aligned}
M_i(\omega_{i\mu}) &= -\cosh r_i \sinh r_i\, e^{i\theta_i}\;(\,2N_{th}\,(\omega_{i\mu})\;+\;1)\,,\\
N_i(\omega_{i\mu}) &= N_{th}\,(\omega_{i\mu})\;\left(\cosh^2 r_i + \sinh^2 r_i\right)\;+\;\sinh^2 r_i\,,
\end{aligned}$$

which satisfy the relation $|M_i(\omega_{i\mu})|^2 \leq N_i(\omega_{i\mu})(N_i(\omega_{i\mu})+1)$. We have considered the same squeeze r_i for all the oscillators of the ith bath. $\theta_i\,(-\pi < \theta_i \leq \pi)$ is a global arbitrary rotation of the bath

state $\hat{\rho}_{Bi}$, and $N_{th}(\omega_{i\mu})$ is the average occupation number of the μth oscillator in the ith bath in a thermal equilibrium state.

To induce an energy current across the chain, see Figure 1, we fix the left and right heat baths at different temperatures, $T_{\mathcal{L}} = T+\delta T$ and $T_{\mathcal{R}} = T-\delta T$ respectively, with T low enough to ensure that the system remains within the quantum regime. Then we modify the temperature of the central bath, $T_{\mathcal{C}} = T + \Delta T$, by considering different values of ΔT. This setup is particularly interesting as it makes possible to establish a quasiclassical regime in the central oscillator while maintaining the lateral oscillators in the quantum regime. Below we will show that the asymptotic stationary state derived from this manipulation of the central oscillator can exhibit a rich variety of quantum correlations, such as two-mode and bipartite three-mode and genuine tripartite entanglement.

Since the total Hamiltonian (1) is quadratic in both positions and momenta, and we have considered Gaussian initial bath states, the asymptotic stationary state, denoted by $\hat{\rho}_{\mathcal{LCR}}$, will be Gaussian for any initial state of the oscillators [52, 53]. Then, the stationary quantum properties will be determined by just the first and second moments of the positions $\hat{x}_i$ and the momenta $\hat{p}_i$. The former can be made arbitrarily close to zero by unitary local transformations that do not affect the non-local properties such as entanglement. Whereas the second moments determining all the correlation properties required in our analysis are given in terms of the covariance matrix

$$\boldsymbol{V} = \begin{bmatrix} \boldsymbol{C_{xx}}(t,t) & \boldsymbol{C_{xp}}(t,t) \\ \boldsymbol{C_{px}}(t,t) & \boldsymbol{C_{pp}}(t,t), \end{bmatrix} , \tag{6}$$

with $\hat{\boldsymbol{x}} = (\hat{x}_{\mathcal{L}}, \hat{x}_{\mathcal{C}}, \hat{x}_{\mathcal{R}})$ and $\hat{\boldsymbol{p}} = (\hat{p}_{\mathcal{L}}, \hat{p}_{\mathcal{C}}, \hat{p}_{\mathcal{R}})$, and the two-point (symmetrical) correlation functions

$$C_{ab}(t,t') \;=\; \frac{1}{2}\,\mathrm{Tr}\left(\,\hat{\rho}_0\left\{\hat{a}(t),\hat{b}(t')\right\}\right) . \tag{7}$$

The second moments of the energy currents also involve the imaginary part of the two-point correlation $\mathrm{Tr}\left[\hat{\rho}_0\,\hat{a}(t)\,\hat{b}(t')\right]$, given by

$$Y_{ab}(t,t') \;=\; \frac{1}{2}\,\mathrm{Tr}\left(\,\hat{\rho}_0\left[\hat{a}(t),\hat{b}(t')\right]\right) . \tag{8}$$

The covariance matrix of the state $\hat{\rho}_{ij}$ corresponding to the subsystem defined by the ith and jth oscillators can be obtained from (6) by just taking the elements associated with these two oscillators.

It should be emphasized that at stationary conditions the correlation functions (7) and (8) only depend on the time difference $\tau = t-t'$, and a particular initial time t is irrelevant to obtain them. This will be important in what follows, when computing these stationary correlations by using the generalized Langevin equation approach.

III. LANGEVIN APPROACH

Within the Langevin approach, the equations of motion that govern the evolution of the stationary correlations are derived from the microscopic model (1) by writing the Heisenberg equations for the oscillator positions and tracing out the degrees of freedom of the heat baths. This leads to the so-called generalized Langevin equation,

$$m\,\ddot{\hat{x}}_i + m\Omega_i^2\,\hat{x}_i + U_{ij}\,\hat{x}_j - \frac{1}{\hbar}\int_{t_0}^{t} d\tau\,\chi_i(t-\tau)\,\hat{x}_i(\tau) = \hat{F}_i(t)\,, \tag{9}$$

where we have introduced the potential

$$\Omega_i^2 \;=\; \omega_i^2 + \Delta\Omega_i = \omega_i^2 + \frac{1}{\pi m}\int_0^\infty d\omega\;\frac{J_i(\omega)}{\omega}\,, \tag{10}$$

the susceptibilities

$$\chi_i(t) \;=\; \frac{2\hbar}{\pi}\,\Theta(t)\int_0^\infty d\omega J_i(\omega)\,\sin(\omega t) \tag{11}$$

and the fluctuating forces

$$\hat{F}_i(t) \;=\; \sum_{\mu=1}^{N} g_{i\mu}\Big(\hat{x}_{i\mu}(t_0)\cos\left(\omega_{i\mu}(t-t_0)\right) + \frac{\hat{p}_{i\mu}(t_0)}{m_{i\mu}\omega_{i\mu}}\sin\left(\omega_{i\mu}(t-t_0)\right)\Big), \tag{12}$$

with $\Theta(t)$ the Heaviside step function, and the spectral density of the environment given by

$$J_i(\omega) = \frac{\pi}{2}\sum_{\mu=1}^{N}\frac{g_{i\mu}^2}{m_{i\mu}\omega_{i\mu}}\,\delta\left(\omega-\omega_{i\mu}\right)\,. \tag{13}$$

As long as the stationary solution of the generalized Langevin equation is guaranteed, one may take the limit $t_0 \to -\infty$ in Eq. (9), and then, use the Fourier transform $\tilde{x}_i(\omega) = \int dt e^{i\omega t}\hat{x}_i(t)$ to obtain the stationary solution of the position and momentum operators [19, 42, 54]. By replacing these solutions into the correlation elements (7) and averaging over the initial state $\hat{\rho}_0$, it follows

$$\begin{pmatrix} C_{x_ix_j}(t,t') \\ C_{x_ip_j}(t,t') \\ C_{p_ip_j}(t,t') \end{pmatrix} \;=\; \frac{\hbar}{2}\int\frac{d\omega}{2\pi}\int\frac{d\omega'}{2\pi}\,e^{-i(\omega t-\omega' t')}\begin{pmatrix} 1 \\ im\omega' \\ m^2\omega\omega' \end{pmatrix} G_{ij}(\omega,\omega')\,, \tag{14}$$

with

$$G_{ij}(\omega,\omega') = \sum_{l,m=\mathcal{L},\mathcal{C},\mathcal{R}}\tilde{\alpha}_{il}(\omega)\left\langle\left\{\tilde{F}_l(\omega),\tilde{F}_m(-\omega')\right\}\right\rangle_{\hat{\rho}_0}\tilde{\alpha}_{mj}(-\omega') \tag{15}$$

and

$$\tilde{\boldsymbol{\alpha}}(\omega) = (\boldsymbol{\Gamma}+\boldsymbol{U})^{-1}\,, \tag{16}$$

where $\Gamma_{ij} = \delta_{ij}\Big(- m\omega^2 + m\Omega_i^2 - \frac{1}{\hbar}\tilde{\chi}_i(\omega)\Big)$.

The two-points correlation functions $Y_{ab}(t,t')$ (8) satisfy an expression identical to (14), but replacing in $G_{ij}(\omega,\omega')$ the anticommutator of the fluctuating force by the commutator.

Expression (16) is nothing but the Fourier transform of the (matrix) Green function [51, 55] for the generalized Langevin equation (9). The real and imaginary parts of the Fourier transform $\tilde{\chi}_i(\omega)$ of the susceptibility (11) are given by (see Appendix A for further details)

$$\mathrm{Im}\,[\,\tilde{\chi}_i(\omega)\,] = \hbar\,[\,\Theta(\omega)\,J_i(\omega) - \Theta(-\omega)\,J_i(-\omega)\,]\,, \tag{17}$$

$$\mathrm{Re}\,[\,\tilde{\chi}_i(\omega)\,] = \frac{1}{\pi}\,P\int \frac{\mathrm{Im}\,[\,\tilde{\chi}_i(\omega')\,]}{\omega'-\omega}\,d\omega', \tag{18}$$

where P denotes the Cauchy principal value. The second expression is the well-known Kramers-Kronig relation [49] arising from the causal nature of the susceptibility.

In order the three-mode system can reach a stationary state, the function $\alpha_{ij}(t)$ must approach a combination of decaying exponentials in the long time limit [56]. According to a previous study of the equations of motion of the system-plus-environment complex in terms of normal modes [55], the existence of a well defined stationary solution entails that $(\tilde{\alpha}_{ij}(\omega))^{-1}$ has no any real root Ω_b corresponding to the frequency of a bound normal mode, which implies that $\mathrm{Im}\,[\,\tilde{\chi}_i(\Omega_b)\,] \neq 0$. From Eq. (17), the latter condition means that Ω_b must be contained within the domain of the bath spectral density $J_i(\omega)$ [55]. In general, the heat baths can be considered as composed of a large number of degrees of freedom with finite broad band spectrum, in which the most energetic environmental-degree is roughly determined by a cut-off frequency ω_c. This ensures that the natural frequencies of the system are well embedded in the environmental spectrum, and consequently it makes possible an irreversible energy transfer from the system to the environment, at least in a finite time much larger than the natural time scale of the system. We shall impose $\omega_c >> \sqrt{\omega_i^2 + k/m}$ $(i = \mathcal{L}, \mathcal{C}, \mathcal{R})$ in order to ensure an irreversible evolution of the three-oscillator chain toward a well defined asymptotic stationary state.

The covariance matrix of this stationary state is completely determined by the correlation functions (14) evaluated at equal time, once the correlation functions of the fluctuating forces (12) have been obtained. These correlations depend only on the initial environmental state. Below we show the relation between the fluctuating forces and the initial covariance matrix (5) of the heat baths.

A. Fluctuation-Dissipation Relation

Our choice of the initial environmental state implies the statistical independence of the fluctuating forces corresponding to different heat baths, *i.e.* $\left\langle \left\{ \hat{F}_l(t), \hat{F}_m(t') \right\} \right\rangle = 0$ for all $l \neq m$. Whereas, according to Eqs. (5), the symmetrical two-time correlation function of the fluctuating forces associated with a given lth bath is given by (see Appendix B for further details)

$$\frac{1}{2}\left\langle \left\{ \hat{F}_l(t), \hat{F}_l(t') \right\} \right\rangle_{\hat{\rho}_0} = \sum_{\mu=1}^{N} \frac{\hbar\, g_{l\mu}^2}{m_{l\mu}\,\omega_{l\mu}} \Bigg[\left(\frac{1}{2} + N_l(\omega_{l\mu}) \right) \cos\left(\omega_{l\mu}(t'-t)\right)$$

$$+\mathrm{Re}\left[\, M_l(\omega_{l\mu})\,\right] \cos\left(\omega_{l\mu}(t+t'-2t_0)\right) + \mathrm{Im}\left[\, M_l(\omega_{l\mu})\,\right] \sin\left(\omega_{l\mu}(t+t'-2t_0)\right) \Bigg] . \tag{19}$$

The average of the corresponding commutator can be expressed as

$$\frac{1}{2}\left\langle \left[\hat{F}_l(t), \hat{F}_m(t') \right] \right\rangle_{\hat{\rho}_0} = i\,\delta_{lm}\,\frac{\hbar}{2} \sum_{\mu=1}^{N} \frac{g_{l\mu}^2}{m_{l\mu}\omega_{l\mu}}\, \sin\left(\omega_{l\mu}(t'-t)\right) . \tag{20}$$

The dependence of the symmetrical two-time correlation functions on the initial time t_0 is eliminated in the case of an initial thermal equilibrium state of the lth bath, in which $M_l(\omega_{l\mu}) = 0$ and $N_l(\omega_{l\mu}) = N_{th}(\omega_{l\mu})$ for all μ values. Although in the previous section we have already fixed the time limit $t_0 \to -\infty$ in order to obtain the stationary solution, we shall maintain the notation t_0 for convenience in order to make more clear the following discussion.

As shown in Appendix B, the non-stationary terms in Eq.(19) come from the average of factors involving $a_{i\mu}^\dagger a_{i\nu}^\dagger$ and $a_{i\mu}a_{i\nu}$, with $a_{i\mu}$ ($a_{i\mu}^\dagger$) the annihilation (creation) operator of the μth mode in the ith reservoir. These terms describe non-conservative energy processes that take place in the heat bath at the initial time t_0, and therefore, they may influence the transient dynamics of the three-oscillator chain. However, they become highly oscillatory in the long time limit ($(t+t'-t_0) \to \infty$) and their contribution to the stationary properties may be disregarded [46]. When taking the quasi-continuum limit $\sum_\mu \to \int d\omega$ in the environment spectral density, only the stationary term in Eq.(19) remains. This assertion holds for an environment with a broad spectrum limited by ω_c, and a finite interaction between the reservoir modes and the system oscillators. Mathematically, the latter translates into that the spectral densities $J_l(\omega)$ are finite continuous functions, and the corresponding coupling strengths should decay at least as $1/\omega^2$ at high frequencies. Under these conditions, the long time limit of the symmetrical two-time correlation function (19) reduces to the following expression in the frequency domain (see Appendix B for details)

$$\frac{1}{2}\left\langle \left\{ \tilde{F}_l(\omega), \tilde{F}_l(\omega') \right\} \right\rangle_{\hat{\rho}_0} = 2\pi\,\delta(\omega+\omega')\,\mathrm{Im}\left[\,\chi_l(\omega)\,\right] \coth\left(\frac{\hbar\,\omega}{2\,k_B\,T_l}\right) \cosh\left(2r_l\right) . \tag{21}$$

The average of the corresponding commutator reduces to

$$\frac{1}{2}\left\langle\left[\tilde{F}_l(\omega),\tilde{F}_l(\omega')\right]\right\rangle_{\hat{\rho}_0}=2\pi\,\delta(\omega+\omega')\,\mathrm{Im}\left[\,\chi_l(\omega)\,\right]\,. \tag{22}$$

Similar results have been previously obtained within the path integral formalism [46, 57], see also [58].

We point out that an initially squeezed state of the environment makes the reduced system to *notice* an effective temperature above the temperature $T_i\,(i\in\{\mathcal{L},\mathcal{C},\mathcal{R}\})$ of the heat bath at thermal equilibrium. This effect has interesting consequences in the efficiency of thermal machines within the quantum regimen [11].

Now we can replace the autocorrelations (21) into the expressions (15), and perform the integral in the frequency ω' to obtain a closed-form expression for the two-time correlation functions $C_{ab}(t,t')$. Notice that $C_{ab}(t,t')=C_{ab}(\tau=t-t',0)$ due to the stationary condition of the fluctuating force correlation. A similar procedure is followed for the functions $Y_{ab}(t,t')$ (8).

In general, there are not analytic expressions giving the integrals involved in the correlation functions in terms of the system parameters, such as the bath temperatures, the oscillator frequencies and the coupling strengths. We will compute them by means of numerical methods.

IV. ENERGY CURRENT AND QUANTUM CORRELATIONS

The non equilibrium conditions imposed by the different bath temperatures drive an energy current through the system, see Figure 1. A discrete definition of the energy currents associated with each chain oscillator can be derived from its local energy [41, 59, 60]

$$\hat{h}_i=\frac{\hat{p}_i^2}{2m}+\frac{1}{2}m\omega_i^2\hat{x}_i^2+\hat{u}_i(\hat{\boldsymbol{x}})+\frac{1}{4}\sum_{\mu=1}^{N}m_{i\mu}\omega_{i\mu}^2\left(\frac{g_{i\mu}}{m_{i\mu}\omega_{i\mu}^2}\hat{x}_i-\hat{q}_{i\mu}\right)^2\,, \tag{23}$$

with $\hat{u}_i(\hat{\boldsymbol{x}})=(\hat{x}_i-\hat{x}_{\mathcal{C}})^2/4$ for $i=(\mathcal{L},\mathcal{R})$, and $\hat{u}_{\mathcal{C}}(\hat{\boldsymbol{x}})=[(\hat{x}_{\mathcal{C}}-\hat{x}_{\mathcal{L}})^2+(\hat{x}_{\mathcal{C}}-\hat{x}_{\mathcal{R}})^2]/4$. The time derivative of $\hat{h}_i$ leads to the discrete continuity equations

$$\frac{d\hat{h}_i}{dt}=\hat{j}_i(t)+\hat{j}_{i\mathcal{B}}(t) \tag{24}$$

with $\hat{j}_i(t)=\hat{j}_{i\,\mathcal{C}}(t)$ for $i=(\mathcal{L},\mathcal{R})$, and $\hat{j}_{\mathcal{C}}(t)=\hat{j}_{\mathcal{C}\mathcal{L}}(t)+\hat{j}_{\mathcal{C}\mathcal{R}}(t)$. The term

$$\hat{j}_{ij}(t)=-\hat{j}_{ji}(t)=\frac{k}{4m}\Big[\,\{\hat{x}_j(t),\hat{p}_j(t)\}-\{\hat{x}_i(t),\hat{p}_i(t)\}+\underbrace{\Big(\,\{\hat{x}_j(t),\hat{p}_i(t)\}-\{\hat{x}_i(t),\hat{p}_j(t)\}\,\Big)}_{\text{Correlation terms}}\Big] \tag{25}$$

can be identified as the energy current from the jth oscillator to the ith oscillator, whereas

$$\hat{j}_{i\mathcal{B}}(t) = \frac{1}{4m}\sum_{\mu=1}^{N}\Bigg(g_{i\mu}\Big(\{\hat{q}_{i\mu}(t),\hat{p}_i(t)\} - \frac{g_{i\mu}}{m_{i\mu}\omega_{i\mu}^2}\{\hat{x}_i(t),\hat{p}_i(t)\} - \frac{m}{m_{i\mu}}\{\hat{x}_i(t),\hat{p}_{i\mu}(t)\}\Big) + m\omega_{i\mu}^2\{\hat{q}_{i\mu}(t),\hat{p}_{i\mu}(t)\}\Bigg) \tag{26}$$

corresponds to the energy current from the ith heat bath into the ith oscillator. At stationary conditions the total current coming from the baths into the system becomes zero. Here we will focus on the analysis of the total current flowing from the $\mathcal{L}$- to the $\mathcal{R}$-oscillator, defined as

$$\hat{J}(t) = \hat{j}_{\mathcal{CL}}(t) + \hat{j}_{\mathcal{RC}}(t)\,. \tag{27}$$

Our study is based on the stationary properties of the total energy current, which are basically determined by its first- and second-moments, or equivalently, by its average and fluctuations. The steady state average of the total energy current

$$\left\langle \hat{J} \right\rangle = \left\langle \hat{j}_{\mathcal{RC}} \right\rangle + \left\langle \hat{j}_{\mathcal{CL}} \right\rangle \tag{28}$$

can be obtained by tracing (25) over the the stationary state and using the stationary solutions of the two-time correlation functions (14), which leads to

$$\left\langle \hat{j}_{ij} \right\rangle = \frac{k}{2m}\left[\, C_{x_jp_j}(t,t) - C_{x_ip_i}(t,t) + \big(C_{x_jp_i}(t,t) - C_{x_ip_j}(t,t)\big)\,\right] \tag{29}$$

for the local currents $\hat{j}_{\mathcal{CL}}$ and $\hat{j}_{\mathcal{RC}}$.

Since the quantum correlations shared by the oscillators, in particular entanglement, are partially encoded on the correlation terms indicated in (25), one might expect that the energy current could be sensitive to these correlations. Notice that the total current involves the correlations between the central and the side oscillators, while it does not depend on the crossed correlation function between the two side oscillators. We shall further analyze this issue in Section (VI).

A. Fluctuations of the energy current

To have a better understanding of the system behavior under non-equilibrium conditions we also study the two-time correlation functions of the energy currents (25). The fluctuations can be obtained from the symmetrical version of the classical two-time correlations, and expressed as

$$K_{j_{ij}j_{lm}}(\tau,0) = \frac{1}{2}\left\langle \Big\{ \hat{j}_{ij}(\tau)\,,\,\hat{j}_{lm}(0) \Big\} \right\rangle - \left\langle \hat{j}_{ij}(\tau) \right\rangle \left\langle \hat{j}_{lm}(0) \right\rangle . \tag{30}$$

Theoretically, the response of a system under external perturbations can be studied in terms of these correlations functions [14, 49]. Notice that we evaluate the fluctuations in the non-equilibrium stationary state, so that we might expect that Eq.(30) can elucidate some properties of stationary non-equilibrium, rather than the equilibrium quantum correlations [30]. Furthermore, it has been shown that Eq.(30) is related to the fluctuations of the stationary energy current across the chain [61].

As the stationary state obeys a Gaussian distribution, the four-time correlation terms implicit in $K_{j_{ij}j_{lm}}(t,t')$ can be decomposed into terms involving the product of two-time correlations, in the form

$$\begin{aligned}\langle\{\{\hat{x}_i(\tau),\hat{p}_j(\tau)\},\{\hat{x}_l(0),\hat{p}_m(0)\}\}\rangle &= 2\,\langle\{\hat{x}_i(\tau),\hat{p}_j(\tau)\}\rangle\,\langle\{\hat{x}_l(0),\hat{p}_m(0)\}\rangle \\ &+2\,[\langle\{\hat{x}_i(\tau),\hat{x}_l(0)\}\rangle\,\langle\{\hat{p}_j(\tau),\hat{p}_m(0)\}\rangle+\langle[\hat{x}_i(\tau),\hat{x}_l(0)]\rangle\,\langle[\hat{p}_j(\tau),\hat{p}_m(0)]\rangle\,] \\ &+2\,[\langle\{\hat{x}_i(\tau),\hat{p}_m(0)\}\rangle\,\langle\{\hat{x}_l(0),\hat{p}_j(\tau)\}\rangle-\langle[\hat{x}_i(\tau),\hat{p}_m(0)]\rangle\,\langle[\hat{x}_l(0),\hat{p}_j(\tau)]\rangle]\,. \end{aligned} \tag{31}$$

Then the current-current response function (30) can be expressed as

$$\begin{aligned}K_{j_{ij}j_{lm}}(\tau,0)=\frac{k^2}{4m^2}\sum_{\substack{\alpha,\alpha'=i,j\\ \beta,\beta'=l,m}}\Big[\,S_{\alpha,\beta}\,\Big[C_{x_\alpha x_\beta}(\tau,0)\,C_{p_{\alpha'}p_{\beta'}}(\tau,0)+Y_{x_\alpha x_\beta}(\tau,0)\,Y_{p_{\alpha'}p_{\beta'}}(\tau,0)\Big] \\ +S_{\alpha,\beta'}\Big[\,C_{x_\alpha p_\beta}(\tau,0)\,C_{x_{\beta'}p_{\alpha'}}(-\tau,0)-Y_{x_\alpha p_\beta}(\tau,0)\,Y_{x_{\beta'}p_{\alpha'}}(-\tau,0)\Big]\Big]\,,\end{aligned} \tag{32}$$

where $S_{a,b}$ is the sign of the cofactor of the element (a,b) in the 4×4 array defined by the indexes $\{i,j,l,m\}$. Finally, according to Eq.(27), the autocorrelation function of the total current flowing from the $\mathcal{L}$- to the $\mathcal{R}$-oscillator is given by

$$K_{JJ}(\tau,0)=K_{j_{\mathcal{CL}}j_{\mathcal{CL}}}(\tau,0)+K_{j_{\mathcal{CL}}j_{\mathcal{RC}}}(\tau,0)+K_{j_{\mathcal{RC}}j_{\mathcal{CL}}}(\tau,0)+K_{j_{\mathcal{RC}}j_{\mathcal{RC}}}(\tau,0)\,. \tag{33}$$

In contrast to the average energy current, the correlation function $K_{JJ}(\tau,0)$ involves crossed terms between the $\mathcal{R}$- and the $\mathcal{L}$- oscillators. In addition, while $\left\langle\hat{J}\right\rangle$ (28) is given by a linear combination of two-time correlation terms, $K_{JJ}(\tau,0)$ has a nonlinear dependence on such terms. These two aspects will be useful in the subsequent discussion. Alternatively, the behavior of $\left\langle\hat{J}\right\rangle$ and $K_{JJ}(\tau,0)$ will help us to gauge whether the average properties of the energy current are sensitive to quantum correlations, such as genuine tripartite entanglement.

B. Quantum Correlations: Discord and Entanglement

We shall analyze the two-mode quantum correlations between the ith and jth oscillators by means of the discord measure on the right [62, 63], denoted by $D^{\leftarrow}(\hat{\rho}_{ij})$. The entanglement be-

tween both modes can be quantified by the well-known logarithmic negativity $E_N(\hat{\rho}_{ij})$ [64–66]. In particular we devote special attention to the entanglement $E_N(\hat{\rho}_{\mathcal{LCR}})$ and the discord $D^{\leftarrow}(\hat{\rho}_{\mathcal{LCR}})$ between the side oscillators.

We use a recent criterion in the realm of continuous-variable systems [67] to study tripartite entanglement, which is a good estimator for κ-partite entanglement [68] in n-mode Gaussian as well as non-Gaussian states. A tripartite harmonic system may develop *bipartite* three-mode entanglement, which means that there is at least a bipartition of the three-mode system that is entangled, or *genuine tripartite* entanglement, which corresponds to the case in which all the bipartitions are entangled and the state $\hat{\rho}_{\mathcal{LCR}}$ cannot be written as a convex combination of bipartite separable states. Here, the criterion reduces to evaluate a figure of merit $\mathcal{T}_{\kappa,n}$, such as a positive value of $\mathcal{T}_{3,3}(\hat{\rho}_{\mathcal{LCR}})$ ($\mathcal{T}_{2,3}(\hat{\rho}_{\mathcal{LCR}})$) indicates that the state $\hat{\rho}_{\mathcal{LCR}}$ is genuine tripartite entangled (bipartite three-mode entangled) [67, 68].

As we are dealing with stationary Gaussian states, all the previously mentioned indicators of quantum correlations can be directly computed from the covariance matrix $\boldsymbol{V}$ given by Eq.(6). The logarithmic negativity can be expressed as [66],

$$E_N\left(\hat{\rho}_{ij}\right) = \max\{0, -\ln\left(2\nu_-\right)\}, \tag{34}$$

where ν_- stands for the lowest symplectic eigenvalue of the partial transpose covariance matrix $\boldsymbol{V}_{ij}^{T_j}$, corresponding to the reduced density matrix $\hat{\rho}_{ij}$. The (right) discord is given by [22, 23],

$$D^{\leftarrow}\left(\hat{\rho}_{ij}\right) = I(\hat{\rho}_{ij}) - \mathcal{I}^{\leftarrow}(\hat{\rho}_{ij}), \tag{35}$$

with the total correlations

$$I(\hat{\rho}_{ij}) = S(\hat{\rho}_i) + S(\hat{\rho}_j) - S(\hat{\rho}_{ij}) \tag{36}$$

and the classical correlations

$$\mathcal{I}^{\leftarrow}(\hat{\rho}_{ij}) = \max_{\Pi_l^{(j)}} \left\{ S(\hat{\rho}_{ij}) - \sum_l p_l S(\hat{\rho}_i^{(l)}) \right\}, \tag{37}$$

which are given in terms of the von Newman entropy $S(\hat{\rho})$. Closed form expressions for the quantum discord as a function of the covariance matrix $\boldsymbol{V}_{ij}$ have been derived in [62, 63]. It is important to realize that these indicators of quantum correlations involve a non-linear dependence on the density operator and the two-time correlation functions. See Appendix C for further details of the logarithmic negativity, the quantum discord and the separability criteria $\mathcal{T}_{\kappa,n}$.

V. RESULTS

We now investigate the average properties of the total current $\hat{J}$ when the three oscillators share two-mode and tripartite entanglement. In many realistic situations, e.g. quantum Brownian motion, the interaction with the environment leads to an Ohmic dissipation. In a first approach, for a nanomechanical setup, one may think that the thermal relaxation is mainly due to the coupling with the acoustic phonons of the substrate, which may lead to linear spectral density at low oscillator frequencies. However, in some cases, the dimensionality of the environment may induce super-Ohmic dissipation. Here we analyze both the Ohmic and super-Ohmic dissipations, which are characterized by the spectral densities

$$J_i^{(Oh)}(\omega) = \frac{\pi m \gamma_i}{2}\, \omega\, e^{-\omega/\omega_c}, \tag{38}$$

and

$$J_i^{(SOh)}(\omega) = \frac{\pi m \gamma_i}{2}\, \frac{\omega^2}{\omega_c}\, e^{-\omega/\omega_c}, \tag{39}$$

respectively, with γ_i the dissipative rate for the ith oscillator and ω_c the frequency cut-off of the environmental spectrum. As argued in Section III, the stationary state is reached in a time scale larger than any of the natural time scales implicit in the dynamics of the open chain; namely $\left\{\omega_c^{-1}, \gamma^{-1}, \hbar/2\pi K_B T\right\}$.

From now on we set the environmental parameters $\gamma_1 = \gamma_3 = 10^{-4}\Omega$, $\gamma_2 = 0.05\Omega$, $\omega_c = 20\Omega$, and the typical values for nanomechanical oscillators $\Omega = 1\,GHz$ and $m = 10^{-16}\,kg$. With this configuration the system begins to exhibit quantumness at temperatures in the range of mili-Kelvin. We also assume off resonance oscillators with frequencies, $\omega_{\mathcal{L}} = \Omega + 0.4\,\delta\omega$, $\omega_{\mathcal{C}} = \Omega + 0.9\,\delta\omega$, and $\omega_{\mathcal{R}} = \Omega - 0.7\,\delta\omega$, given in terms of a detuning parameter $\delta\omega$.

A. Two-mode entanglement and average energy current

We start by analyzing the behavior of two-mode entanglements and the total energy current with the temperature gradient ΔT. As figure 2) shows, the three oscillators become two-mode entangled at low temperature gradients, with this entanglement exhibiting a plateau for negative gradients. Interestingly the total current flowing through the oscillator chain presents a similar plateau. This can be related to the proximity of the central oscillator to its ground state at very low temperatures $T_{\mathcal{C}}$, which is effectively reached for $\Delta T/T \simeq -1$. A similar result for entanglement has been obtained in the study of the influence of heat transport on the two-mode

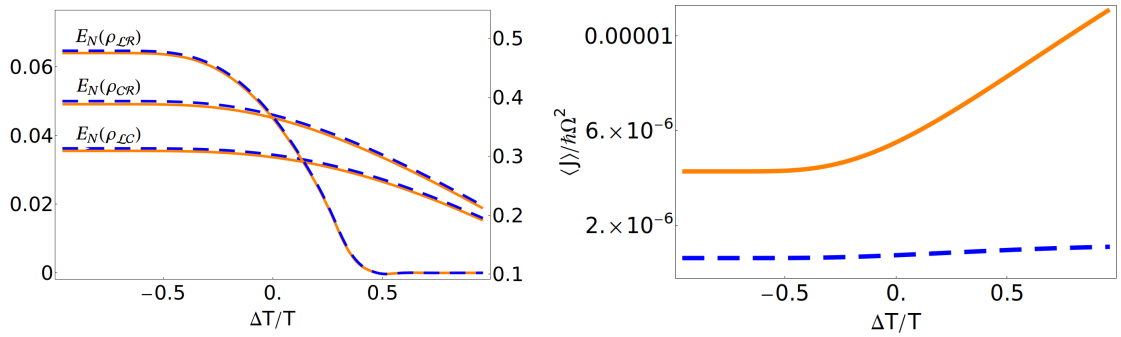

FIG. 2. (color online). Left: The two-mode $\mathcal{L}|\mathcal{R}-$ entanglement (labels on the left), and the $\mathcal{C}|\mathcal{R}-$, $\mathcal{L}|\mathcal{C}-$ entanglements (labels on the right) as a function of the temperature gradient ΔT. Right: The average of the total energy current across the chain as function of the temperature gradient. On both panels the orange solid line corresponds to Ohmic dissipation, and the blue dashed line to super-Ohmic dissipation. The temperature gradient must satisfy $\Delta T/T > -1$ to prevent the temperature of the central oscillator becomes negative. We have fixed $\delta\omega/\Omega = 0.5$, $k/m\Omega^2 = 1.8$, $\delta T/T = 0.95$ and $k_B T/\hbar\Omega \simeq 0.27$.

entanglement between oscillators that are embedded in a disordered harmonic chain connected to heat baths at both ends [69]. It has been shown that a plateau emerges when the energy spectrum is bounded from below since each site of the chain suffers an harmonic potential. As the central oscillator gets closer to the ground state for negative values of ΔT, the energy flowing across this oscillator becomes bounded as the temperature gradient decreases. In the absence of the harmonic confinement the logarithmic negativity would continue growing up to a maximum value, as the heat transport decreases [69]. Moreover, the plateau in the entanglement remains even when the average energy current across the chain becomes zero, though the temperature gradient ΔT is not zero. This occurs when $\delta T = 0$ and the left and right oscillators are identical $\Omega_{\mathcal{L}} = \Omega_{\mathcal{R}}$, and therefore $\left\langle \hat{j}_{\mathcal{CL}} \right\rangle = -\left\langle \hat{j}_{\mathcal{RC}} \right\rangle$. This last point also underlines that the appearance of entanglement is mainly attributed to proximity of the system to its ground state, rather than to the presence of an energy flow induced by non-equilibrium conditions.

The two-mode entanglement rapidly decreases for positive ΔT, while the energy current grows monotonically. This is expected as the temperature of the whole three-mode system is increased on average, which is generally harmful for entanglement. Previous results have suggested this behavior, in fact it has been shown that in a harmonic chain an increasing δT is detrimental to build up bipartite or tripartite entanglement due to the rise in the thermal noise [42]. In addition, it can be shown from (21) that an initially squeezed environmental state effectively increases the

temperature. Hence, in the present setting an initial squeezed bath state does not favor the appearance of stationary entanglement.

Moreover, one may expect that non-Markovian effects, which are more relevant for super-Ohmic dissipation, would substantially degrade the entanglement with respect to the Ohmic situation. According to figure (2), the two-mode entanglement is essentially the same for the chain suffering Ohmic or super-Ohmic dissipation; namely, $E_N(\hat{\rho}_{\mathcal{LR}})$, $E_N(\hat{\rho}_{\mathcal{RC}})$ and $E_N(\hat{\rho}_{\mathcal{CL}})$ practically coincide for both situations. This result is in contrast with the observed transient evolution of the two-mode entanglements under different environmental spectral densities, in which the super-Ohmic dissipation induces stronger disentanglement effects [70]. The coincidence of the stationary two-mode entanglements also differs from the emergence of entanglement in a situation in which the oscillators are affected by the same bath [20]. In the case of the energy current, we observe that it is strongly affected by the interaction with the heat baths, determined by the fixed spectral density.

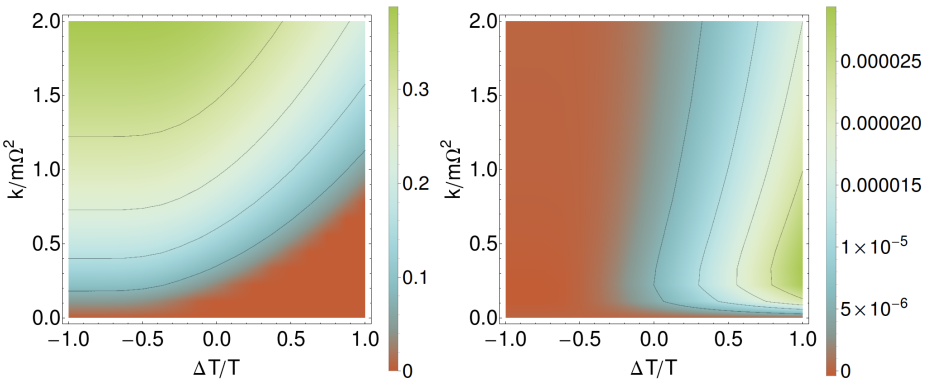

FIG. 3. (color online). The two-mode entanglement $E_N(\hat{\rho}_{\mathcal{RC}})$ (left panel) and the stationary energy current $\left\langle \hat{j}_{\mathcal{RC}} \right\rangle / \hbar\Omega^2$ (right panel) in terms of the temperature gradient ΔT and the coupling strength k under Ohmic dissipation. The system parameters are the same as figure (2).

We have performed an extensive analysis of the two-mode entanglements and the energy currents involving the central oscillator, in terms of both the temperature gradient ΔT and the coupling strength k. As figure (3) shows, a similar behavior to that illustrated in the figure (2) is reproduced for different values of k. The entanglements $E_N(\hat{\rho}_{\mathcal{RC}})$ and $E_N(\hat{\rho}_{\mathcal{LC}})$ increase for lower temperature gradients and stronger couplings. Whereas the energy currents $\left\langle \hat{j}_{\mathcal{RC}} \right\rangle$ and $\left\langle \hat{j}_{\mathcal{CL}} \right\rangle$ exhibit a relatively weak dependence on the coupling strength, and the expected increase with the temperature gradient. Also the plateau of small energy currents arising in the proximity of the ground state of the central oscillator can be clearly observed.

Hence, our results indicate that the energy currents across the system are insensitive to the emerge of two-mode entanglements between the oscillators, both under Ohmic and super-Ohmic dissipation, and irrespective of the coupling strength with the heat baths. The two-mode entanglement $E_N(\hat{\rho}_{\mathcal{LR}})$ and total energy current $\left\langle \hat{J} \right\rangle$ remain nearly unchanged provided that the central oscillator is close enough to the ground state, at temperatures between $T_{\mathcal{L}}$ and $T/2$. An increase in the temperature of this oscillator results in a deterioration of the entanglement, and an increase in the energy current.

B. Energy current correlations and three-mode entanglement

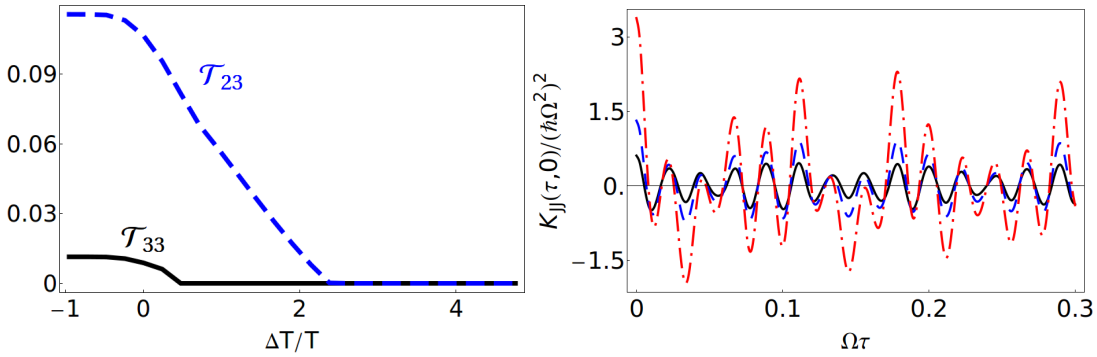

FIG. 4. (color online). Left: The criteria $\mathcal{T}_{23}$ and $\mathcal{T}_{33}$ as a function of the temperature gradient for Ohmic dissipation. Right: The time evolution of the fluctuations of the total current under Ohmic dissipation, in a system that is genuine entangled ($\Delta T/T = -0.95$) (black solid line), bipartite three-mode entangled ($\Delta T/T = 1.9$) (blue dashed line), and likely separable in the three possible bipartitions ($\Delta T/T = 4.3$) (red dot-dashed line). The remaining parameters are $k/m\Omega^2 = 2$, $\delta\omega/\Omega = 0.5$, $\delta T/T = 0.95$, and $k_B T/\hbar\Omega \simeq 0.27$.

In this section we analyze the three-mode entanglement and the energy current correlations between the left and right oscillators, which includes correlation terms involving the three oscillators, see Eq.(33). Figure (4) shows the bipartite three-mode ($\kappa = 2$) and the genuine tripartite ($\kappa = 3$) entanglements measured by the corresponding criteria $\mathcal{T}_{\kappa,3}$ [67, 68]. The results for both the Ohmic and super-Ohmic dissipations are quite similar. In the low temperature and strong coupling regime, the three-mode system exhibits genuine tripartite entanglement, though this feature rapidly disappears for positive values of ΔT, such as occurs with the two-mode entanglement. Strikingly, the system still remains bipartite three-mode entangled at relatively high temperature

gradients ($\Delta T/T \approx 2$). Hence the tripartite entanglement is more robust to temperature changes than the two-mode entanglement between the side oscillators.

Figure (4) also shows the initial time evolution of the energy current correlations for three different three-mode entanglement configurations. As expected, the fluctuations of the energy current exhibit an oscillatory behavior, which should be progressively attenuated at larger time intervals. According to a previously reported exponential time decay of the two-time correlation functions (14) in a damped harmonic oscillator at low temperature T, such oscillations should be effectively suppressed at time $\tau > \hbar/2\pi k_B T$ [56].

As evidenced by figure (4), the energy current correlations exhibit similar oscillations as the system evolves from genuine tripartite to bipartite three-mode entanglement. The most significant discrepancy between these two configurations is an increase in the oscillation amplitude, which can be attributed to the thermal fluctuations that arise with increasing the temperature gradient. Indeed, a similar oscillating behavior in the fluctuations is still observed at relatively large temperature gradients ($\Delta T/T \gtrsim 4$), when the system is expected to be separable in the three possible bipartitions.

The results we have obtained from an analysis considering an extensive set of parameters $\{T,\, k,\, \delta\omega,\, \delta T\}$ corresponding to different multipartite entanglement configurations, for both Ohmic and super-Ohmic dissipations, also indicate that the energy currents correlations across the harmonic chain are insensitive to the emerge of tripartite genuine or bipartite three-mode entanglement.

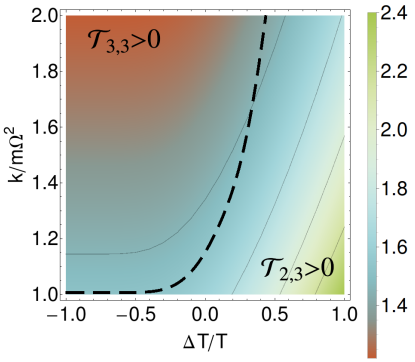

FIG. 5. (color online). Density plot of the energy current correlations $K_{JJ}(t,t)/(\hbar\Omega^2)^2$ as a function of the temperature gradient ΔT and the coupling strength k for Ohmic dissipation. A similar result is obtained for super-Ohmic dissipation. The black dashed line delimits the states in which the hierarchy $\mathcal{T}_{3,3}$ changes from positive to negative. The parameters are the same as in figure (4).

To conclude this section we focus on the energy current correlations evaluated at equal time, see figure (5), which will be useful in the subsequent discussion. Both the stationary fluctuations and the average of the energy current, see figure (3), grow with increasing the temperature gradient. But, in contrast to the average energy current, the plateau at small values of the fluctuations is observed above a given value of the coupling strength, which is larger in the case of Ohmic dissipation.

Once again, the fluctuations of the energy current are insensitive to whether the system experiences bipartite three-mode or genuine tripartite entanglement. Similar results are obtained for the current-current response involving the central and the side oscillators.

C. Quantum Discord

One might expect that a scenario similar to the one previously described for the two- and three-mode entanglement would be repeated in the presence of other non-classical correlations, such as discord. In this section we analyze a possible connection between the energy current and the quantum correlations measured by the right-discord $D^{\leftarrow}(\hat{\rho}_{\mathcal{RL}})$. Although not shown in this work, similar results are obtained from the analysis of the discord $D^{\rightarrow}(\hat{\rho}_{\mathcal{RL}})$ measured from the left . We also point out that the two-mode discord contains the contribution of the two-mode entanglement studied in previous sections.

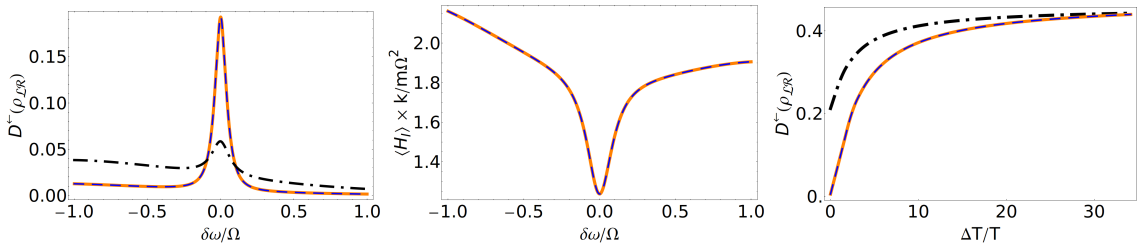

FIG. 6. (color online). Left: The right-discord as a function of the detuning $\delta\omega$, for the temperature gradients $\Delta T/T = 3.8$ and 0.95 (black dot-dashed line). Center: The averaged interaction energy $\hat{H}_I$, see Eqs. (2) and (40), in terms of $\delta\omega$. Right: The right-discord at resonance ($\delta\omega = 0$), as a function of the temperature gradient. The black dot-dashed line gives both the Ohmic and super-Ohmic dissipative discord for an initially squeezed central reservoir, with $r_{\mathcal{C}} = 1\,(r_{\mathcal{R}} = r_{\mathcal{L}} = 0)$. In the three panels the orange-solid and blue-dashed lines correspond to Ohmic and super-Ohmic dissipations respectively, and the parameters are $k/m\Omega^2 = 1.8$, $\delta T/T = 0.95$, and $k_B T/\hbar\Omega \simeq 0.53$.

We have found that discord exhibits a strong dependence on both the temperature gradient and

the frequencies of the oscillators. As shown in figure (6), its presents a sharp peak centered at the resonance condition ($\delta\omega = 0$), and with an amplitude that grows with increasing the temperature gradient. Interestingly, the discord appears strongly correlated with the mean interaction energy between the oscillators,

$$\left\langle \hat{H}_I \right\rangle = \frac{k}{2}\Big[C_{x_{\mathcal{L}}x_{\mathcal{L}}}(t,t) + 2\,C_{x_{\mathcal{C}}x_{\mathcal{C}}}(t,t) + C_{x_{\mathcal{R}}x_{\mathcal{R}}}(t,t) - 2\underbrace{\left(\,C_{x_{\mathcal{L}}x_{\mathcal{C}}}(t,t) + C_{x_{\mathcal{R}}x_{\mathcal{C}}}(t,t)\,\right)}_{\text{Correlation terms}}\Big]\,, \tag{40}$$

which has maximum strength also at resonance, see figure (6). This resonant interaction becomes stronger for higher temperature gradients, which also increase the discord. As all the negative contribution to $\left\langle \hat{H}_I \right\rangle$ comes from the crossed correlation terms, it becomes evident that the maximum interaction strength occurs when these correlations take the highest values, which also turns into the optimal conditions for discord. This result evidences an underlying connection between the interaction energy and the discord, as could be anticipated considering that the discord would be zero in the absence of interaction.

Figure (6) also shows that the discord in the resonant system begins to grow almost linearly with the temperature gradient, and then approaches a constant value at higher gradients. An initially squeezed central reservoir enhances the creation of discord, both for Ohmic and super-Ohmic dissipation. This is in agreement with the foregoing results, as the squeeze of the initial bath state effectively increases the temperature perceived by the oscillators, see Eq.(21). Then an increase of the stationary discord between the side oscillators may be induced either by initially squeezing the central reservoir or increasing its temperature. It has been shown that discord may be additionally created by local noisy operations, such as dissipation [24, 71]. Hence, it may happen that discord would be generated by an energy current induced by a temperature gradient, as this current would make each oscillator to dissipate.

Considering that the discord contains all the quantum correlations, it would be interesting to analyze whether the entanglement available in the system contributes to its increase with the temperature gradient. At this respect, since entanglement can be only created by non-local manipulations and it becomes zero at high temperature gradients, see Section (V A), we may conclude that such increase of the discord must be mainly due to local operations. The paramount role of the local manipulations in the creation of quantum correlations at resonance conditions is correlated with a maximum average interaction strength between oscillators of similar frequencies, see figure (6) and Eq. (40). Notice that the discord grows with ΔT even in the absence of an energy current between the side oscillators ($\delta T = 0$).

The plateau of maximum discord at high temperature gradients can be attributed to the very low

temperatures of the side oscillators $T_{\mathcal{L},\mathcal{R}} < \hbar\Omega/k_B$, which guarantees the "coherence" of the local manipulations. Indeed, the increase in the discord gradually disappear as the mean temperature T increases, and therefore the three-mode system approaches to a classic state. We have observed that the discord $D^{\leftarrow}(\hat{\rho}_{\mathcal{RL}})$ has almost disappeared at temperature $T \simeq 50\,\hbar\Omega/k_B$.

As expected, the two-mode discord between the central and the side oscillators is enhanced by increasing the interaction strength, see figure (7). Whereas, the trend of the central oscillator towards a classical state, by increasing its temperature through higher values of ΔT, causes a progressive deterioration of the discord. In the case of the energy currents between the central and the side oscillators, they exhibit an almost linear increase with the temperature gradient, which is barely modified by the strength of the coupling interaction. Once again, the energy currents do not seem to be related to the significant non-classical correlations shared by the oscillators.

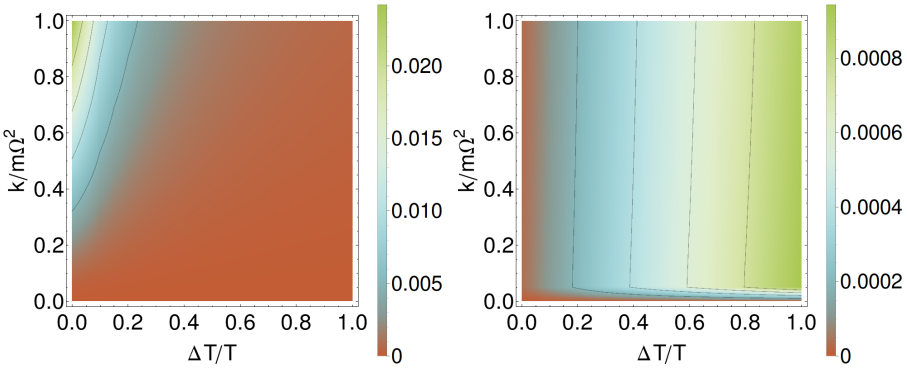

FIG. 7. (color online). The discord $D^{\leftarrow}(\hat{\rho}_{\mathcal{RC}})$ (left panel) and the energy current $\left\langle \hat{j}_{\mathcal{RC}} \right\rangle /\hbar\Omega^2$ (right panel) between the central and right oscillators in the resonant system under Ohmic dissipation. Similar results are obtained for the discord and the energy current between the $\mathcal{C}$- and $\mathcal{L}$- oscillators, both under Ohmic and super-Ohmic dissipations. The parameters are the same as figure (6).

VI. DISCUSSION

Considering that the energy current between two oscillators has an explicit dependence on crossed correlations between them, one could expect that the emerge of entanglement in the system should have detectable effects on such current. Therefore, it would be interesting to determine whether a formal connection between entanglement and the average properties of the energy current can be formally established.

The results presented in Section V A indicate that the behavior of the energy current is not

modified by the presence of two-mode entanglement. A direct comparison between the two-mode entanglement between the side oscillators $E_N(\hat{\rho}_{\mathcal{RL}})$ and the total energy current $\left\langle \hat{J} \right\rangle$ suggests an elusive correlation between them, see figure 2).

Although the most important contribution to the local currents $\left\langle \hat{j}_{ij} \right\rangle$ (29) comes from crossed correlation terms that encode part of the quantum correlations shared by the oscillators, the total current $\left\langle \hat{J} \right\rangle$ (28) does not have an explicit dependence on the correlation terms involving the $\mathcal{L}$- and $\mathcal{R}$- oscillators. Then the two-mode entanglement $E_N(\hat{\rho}_{\mathcal{RL}})$ should not necessarily affect the total current. This reasoning does not exclude, however, the possibility that the total current could be sensitive to the two-mode entanglement shared by the central and the side oscillators.

The conjecture that entanglement and energy current are intimately related would lead to the natural question whether the current $\hat{j}_{ij}$ could serve as an useful witness of the entanglement between the ith and jth oscillators. According to the theory of entanglement, an entanglement witness $\hat{W}_{\hat{O}}$ based on a (bounded) Hermitian operator $\hat{O}$ may be constructed as $\hat{W}_{\hat{O}} = \hat{O} - \inf\left\{ \langle \Psi_i | \langle \Psi_j | \hat{O} | \Psi_i \rangle | \Psi_j \rangle \right\} \hat{\mathbb{I}}$, where the last term is the infimum value of $\hat{O}$ among all the product states $|\Psi_i\rangle |\Psi_j\rangle$ [72]. For $\hat{O} = \hat{j}_{ij}$ (25) it follows

$$\hat{W}_{\hat{j}_{ij}} = \hat{j}_{ij} - \frac{k}{2m} \inf\left\{ C^{Prod}_{x_j p_j}(t,t) - C^{Prod}_{x_i p_i}(t,t) + C^{Prod}_{x_j p_i}(t,t) - C^{Prod}_{x_i p_j}(t,t) \right\} \hat{\mathbb{I}}, \tag{41}$$

where $C^{Prod}_{ab}(t,t)$ is obtained from (14) by considering the average over product states. $\hat{W}_{\hat{j}_{ij}}$ is a good candidate to unveil the two-mode entanglement $E_N(\hat{\rho}_{ij})$ provide that $\mathrm{Tr}(\hat{\rho}_{ij}\hat{W}_{\hat{j}_{ij}})$ takes a negative value for at least one entangled state. Unfortunately such a rigorous proof requires a closed form expression for $C^{Prod}_{ab}(t,t)$, which is currently out of scope as we are dealing with a system under the non-equilibrium conditions induced by two different temperature gradients. Though we cannot guarantee whether Eq.(41) constitutes a good estimator of entanglement, the results of Section V A evidence the difficulty of assessing entanglement through $\hat{W}_{\hat{j}_{ij}}$, mainly due to the apparent insensitivity of the energy current $\left\langle \hat{j}_{ij} \right\rangle$ to the two-mode entanglement $E_N(\hat{\rho}_{ij})$, see figure (3).

In addition, though the correlation terms in Eq. (25) partially carry the quantum correlations shared by the chain oscillators, they themselves do not necessarily manifest entanglement. Indeed, the so-called Peres-Hodorecki-Simon inequality [73]

$$\hat{\rho}_{ij} \text{ entangled } \implies C_{x_i x_j}(t,t) C_{p_i p_j}(t,t) - C_{x_i p_j}(t,t) C_{p_i x_j}(t,t) < 0\,, \tag{42}$$

which provides a criterion to detect the two-mode entanglement between the ith and jth oscillators, already displays a non-linear relation between entanglement and the elements of the covariance matrix.

A common feature of the entanglement measures (or entanglement monotones) is their non-linear functional dependence on the density operator [2], as occurs in the case of the logarithmic negativity [64]. In some sense, the reliable observation of entanglement relies on the ability to measure non-linear properties of the quantum state [74]. According to the expressions for the total energy current $\left\langle \hat{J} \right\rangle$ (29) and the criterion for entanglement (42), the first-moment of the energy current depends linearly on the crossed correlation terms, whereas the entanglement exhibits a non-linear dependence on such terms. Hence, the energy current between the ith and jth is not expected to manifest the emergence of two-mode entanglement.

Following the previous argument, the fluctuations of the total current (33) could manifest the emergence of entanglement, as it involves correlation terms between all the oscillators. In Section V B we focused on the tripartite entanglement, and showed that $K_{JJ}(t,t)$ seems to be insensitive to the inseparability properties of the three-mode chain. A similar conclusion was drawn from the comparison of the time evolution of the fluctuations $K_{JJ}(\tau,0)$ at different entanglement configurations of the stationary state, see figure (4). We remark that this result is not in contradiction with the previous argument based on criterion (42), as it provides a necessary, but not sufficient, condition for the existence of entanglement.

Considering that, in contrast to entanglement, almost any quantum state has a non-negative discord [75], a distinct behavior of these two quantum correlations might be expected [1]. The results of Section (V C) indicate that in the proximity of a resonance condition, a finite energy current induced by the temperature gradient ΔT may generate non-classical correlations between the left and right oscillators, even when the total energy current between them becomes zero. This behavior has been correlated with a maximum strength of the average interaction between the harmonic oscillators, see figure (6). The same results also show that the energy current is not modified by the emerge of discord, see figure (7). The average properties (mean value and fluctuations) of the energy current as a whole exhibit a 'linear' behavior ruled by the temperature gradients, irrespective of the significant two-mode quantum correlations that may be present in the system. As a measure of such correlations we have analyzed the logarithmic negativity, the tripartite entanglement, characterized by the criteria $\mathcal{T}_{2,3}$ and $\mathcal{T}_{3,3}$, and the quantum discord.

Finally, although we have focused on a specific system configuration in which each chain oscillator is connected to an independent heat bath, similar results might be expected for other arrangements, since the emergence of quantum correlations in linear harmonic chains or lattices essentially stems from the proximity of the system to the ground state. The study of the energy current and quantum correlations in systems exhibiting non-linearities deserves further attention.

VII. SUMMARY AND CONCLUDING REMARKS

We have performed an extensive analysis of the quantum correlations, and the mean value and fluctuations of the energy current across a three-oscillator linear chain at the stationary state, both under Ohmic and super-Ohmic dissipation. We have considered initially squeezed reservoir thermal states, and applied the GLE formalism to determine the correlation functions between the position and momentum operators of the chain oscillators, which completely characterize the stationary properties.

Interestingly, the results obtained for the quantum correlations are quite similar for both Ohmic and super-Ohmic dissipation. This suggests that the non-Markovian effects do not significantly modify the Markovian results for the *stationary* properties of the quantum correlations in a system of oscillators in contact with independent heat baths. Moreover, the initial squeezing of a heat bath effectively increases the temperature that the oscillator chain perceives from this bath, and eventually becomes detrimental for the build-up of stationary entanglement.

A different behavior is observed in the case of discord, which can be created by local noisy operations. These quantum correlations highly depend on both the interaction strength between the oscillators and the detuning of their natural frequencies. In particular, the two-mode discord between the side oscillators in the presence of temperature gradients is enhanced at resonance, which indicates that quantum coherence may be favored by thermal non-equilibrium conditions.

According to our results, both the average and the fluctuations of the stationary energy current across the oscillator chain are mainly determined by the two imposed temperature gradients, and do not seem to be related to the appearance of a rich variety of quantum correlations in the system, comprising two-mode discord and entanglement, bipartite three-mode and genuine tripartite entanglement. The absence of quantum correlation effects in the average energy current can be partially understood in terms of its linear dependence on the correlation terms between the oscillators. In the case of the fluctuations, the more intricate dependence on such terms makes more complex to elucidate their possible connection with quantum correlations.

Nowadays the quantum correlations under thermal non-equilibrium conditions have become a topic of great interest in the fields of quantum information, quantum thermodynamics and the theory of open quantum system. Generally the non-classical correlations, such as entanglement, exhibit a non-linear dependence on the density operator that make difficult to establish any formal connection between them and the response of the system to non-equilibrium constrains. We hope that this work may contribute to stimulate further research in this direction.

ACKNOWLEDGMENTS

The authors acknowledge fruitful discussions with L.A. Correa, J.P. Palao and B. Witt. This project was funded by the Spanish MICINN (Grant Nos. FIS2010-19998 and FIS2013-41352-P) and by the European Union (FEDER). A.A.V. acknowledges financial support by the Government of the Canary Islands through an ACIISI fellowship (85% co-financed by the European Social Fund).

Appendix A: Susceptibility

In this Appendix we derive the real and imaginary parts of the Fourier transform of the susceptibility $\chi_i(t)$ (11). Considering the spectral density (13), the imaginary part of the Fourier transform $\tilde{\chi}_i(\omega)$ can be expressed as

$$\mathrm{Im}\left[\,\tilde{\chi}_i(\omega)\,\right] = \frac{\pi\hbar}{2}\sum_{\mu=1}^{N}\frac{g_{i\mu}^2}{m_{i\mu}\omega_{i\mu}}\left[\,\delta\left(\omega-\omega_{i\mu}\right)-\delta\left(\omega+\omega_{i\mu}\right)\right] = \hbar\left[\,\Theta\left(\omega\right)J_i\left(\omega\right)-\Theta\left(-\omega\right)J_i\left(-\omega\right)\right]. \tag{A1}$$

Then the real part can be obtained from the causality of $\chi_i(t)$, according to

$$\mathrm{Re}\left[\,\tilde{\chi}_i(\omega)\,\right] = \mathcal{H}\left[\,\mathrm{Im}\left(\chi_i(\omega')\right)\,\right](\omega) \doteqdot \frac{1}{\pi}\,P\int\frac{\mathrm{Im}\left[\,\chi_i(\omega')\,\right]}{\omega'-\omega}\,d\omega', \tag{A2}$$

where $\mathcal{H}[\bullet](\omega)$ denotes the Hilbert transform of $\bullet$. Using Eq. (A1) it follows that

$$\mathrm{Re}\left[\,\chi_i(\omega)\,\right] = \mathcal{H}\left[\,\Theta(\omega')J_i(\omega')\,\right](\omega) + \mathcal{H}\left[\,\Theta(\omega')J_i(\omega')\,\right](-\omega). \tag{A3}$$

Below are given the expressions of the susceptibility for Ohmic and super-Ohmic spectral densities.

1. Ohmic case

Assuming the Ohmic spectral density (38), and considering the well-known properties of the Hilbert transform, the expression (A3) leads to

$$\begin{aligned}\mathrm{Re}\left[\,\chi_i(\omega)\,\right] &= \frac{\hbar}{2}\,\pi m\gamma_i\left[\mathcal{H}\left[\,\Theta(\omega')\,\omega' e^{-\frac{\omega'}{\omega_c}}\right](\omega) + \mathcal{H}\left[\,\Theta(\omega')\,\omega' e^{-\frac{\omega'}{\omega_c}}\right](-\omega)\right]\\ &= \frac{\hbar}{2}\,\pi m\gamma_i\,\omega\left[\mathcal{H}\left[\Theta(\omega')\,e^{-\frac{\omega'}{\omega_c}}\right](\omega) - \mathcal{H}\left[\,\Theta(\omega')\,e^{-\frac{\omega'}{\omega_c}}\right](-\omega)\right] + \hbar\,m\gamma_i\,\omega_c\\ &= \frac{\hbar}{2}\,m\gamma_i\,\omega\left[e^{-\frac{\omega}{\omega_c}}\,\Gamma(0,-\omega/\omega_c) - e^{\frac{\omega}{\omega_c}}\,\Gamma(0,\omega/\omega_c)\right] + \hbar\,m\gamma_i\,\omega_c\,,\end{aligned} \tag{A4}$$

where $\Gamma(0,x) = \int_x^\infty t^{-1}e^{-t}dt$ denotes the incomplete gamma function.

2. Super-Ohmic case

Following the same procedure as in the previous section for the super-Ohmic spectral density (39), one obtains

$$\begin{aligned}\mathrm{Re}\,[\,\chi_i(\omega)\,] &= \frac{\hbar}{2\omega_c}\,\pi m\gamma_i\left[\,\mathcal{H}\left[\,\Theta(\omega')\,(\omega')^2\,e^{-\frac{\omega'}{\omega_c}}\,\right](\omega)+\mathcal{H}\left[\,\Theta(\omega')\,(\omega')^2\,e^{-\frac{\omega'}{\omega_c}}\,\right](-\omega)\,\right]\\ &= \frac{\hbar}{2\omega_c}\,\pi m\gamma_i\,\omega^2\left[\,\mathcal{H}\left[\,\Theta(\omega')\,e^{-\frac{\omega'}{\omega_c}}\,\right](\omega)+\mathcal{H}\left[\,\Theta(\omega')\,e^{-\frac{\omega'}{\omega_c}}\,\right](-\omega)\,\right]+\hbar m\gamma_i\,\omega_c\\ &= \frac{\hbar}{2\omega c}\,m\gamma_i\,\omega^2\left[\,e^{-\frac{\omega}{\omega_c}}\,\Gamma(0,-\omega/\omega_c)+e^{\frac{\omega}{\omega_c}}\,\Gamma(0,\omega/\omega_c)\,\right]+\hbar m\gamma_i\,\omega_c\,. \end{aligned}\tag{A5}$$

Appendix B: Fluctuating Force

In this appendix we derivate the correlation function of the fluctuation forces associated with the heat baths given in Eq.(21). Considering the time dependence of these forces, it follows

$$\begin{aligned}&\frac{1}{2}\left\langle\left\{\hat{F}_i(t),\hat{F}_j(t')\right\}\right\rangle = \frac{1}{2}\sum_{\nu,\mu=1}^{N} g_{i\nu}g_{j\mu}\Bigg(\,\langle\{\hat{x}_{i\nu}(t_0),\hat{x}_{j\mu}(t_0)\}\rangle\cos(\omega_{i\nu}(t-t_0))\cos(\omega_{j\mu}(t'-t_0))\\ &+\langle\{\hat{x}_{i\nu}(t_0),\hat{p}_{j\mu}(t_0)\}\rangle\cos(\omega_{i\nu}(t-t_0))\frac{\sin(\omega_{j\mu}(t'-t_0))}{m_{j\mu}\omega_{j\mu}}\\ &+\langle\{\hat{p}_{i\nu}(t_0),\hat{x}_{j\mu}(t_0)\}\rangle\cos(\omega_{j\mu}(t'-t_0))\frac{\sin(\omega_{i\nu}(t-t_0))}{m_{i\nu}\omega_{i\nu}}\\ &+\langle\{\hat{p}_{i\nu}(t_0),\hat{p}_{j\mu}(t_0)\}\rangle\,\frac{\sin(\omega_{i\nu}(t-t_0))}{m_{i\nu}\omega_{i\nu}}\frac{\sin(\omega_{j\mu}(t'-t_0))}{m_{j\mu}\omega_{j\mu}}\Bigg)\,.\end{aligned}\tag{B1}$$

Replacing the identities (5) in Eq.(B1), and applying the Fourier transform, one obtains

$$\begin{aligned}&\frac{1}{2}\iint dt\,dt' e^{i\omega t}\,e^{i\omega' t'}\left\langle\left\{\hat{F}_i(t),\hat{F}_i(t')\right\}\right\rangle =\\ &=\sum_{\mu=1}^{N}\frac{\hbar g_{i\mu}^2}{m_{i\mu}\omega_{i\mu}}\Big(\left(\frac{1}{2}+N(\omega_{i\mu})\right)\iint dt\,dt' e^{i\omega t}\,e^{i\omega' t'}\cos(\omega_{i\mu}(t'-t))\\ &+\mathrm{Re}\,[M(\omega_{i\mu})]\iint dt\,dt' e^{i\omega t}\,e^{i\omega' t'}\cos(\omega_{i\mu}(t+t'-2t_0))\\ &+\mathrm{Im}\,[M(\omega_{i\mu})]\iint dt\,dt' e^{i\omega t}\,e^{i\omega' t'}\sin(\omega_{i\mu}(t+t'-2t_0))\Big)\,.\end{aligned}$$

To compute the previous integrals we express the trigonometric functions as complex exponentials, introduce the change of variable $t\to\tau+t'$ in the first integral, and $t\to\tau-t'$ in the second and third ones. Secondly, we use the definition of the delta function $2\pi\delta(\omega)=\int dt e^{i\omega t}$ and the identity

$1+2N_{th}(\omega_{i\mu})=\coth\left(\frac{\hbar\omega}{2k_BT_i}\right)$, which lead to

$$\frac{1}{2}\left\langle\left\{\tilde{F}_l(\omega),\tilde{F}_l(\omega')\right\}\right\rangle=2\pi\delta(\omega+\omega')\mathrm{Im}\left[\chi_l(\omega)\right]\coth\left(\frac{\hbar\omega}{2k_BT_l}\right)\cosh(2r_l)$$
$$-2\pi\hbar\delta(\omega-\omega')\coth\left(\frac{\hbar\omega}{2k_BT_l}\right)\sinh(2r_l)\mathrm{Re}\left[e^{i\theta_l}\right]\left(\int_0^\infty d\bar{\omega}\bar{J}_l(\omega-\bar{\omega})e^{2i\bar{\omega}t_0}-\int_0^\infty d\bar{\omega}\bar{J}_l(\omega+\bar{\omega})e^{-2i\bar{\omega}t_0}\right)$$
$$+2i\pi\hbar\delta(\omega-\omega')\coth\left(\frac{\hbar\omega}{2k_BT_l}\right)\sinh(2r_l)\mathrm{Im}\left[e^{i\theta_l}\right]\left(\int_0^\infty d\bar{\omega}\bar{J}_l(\omega-\bar{\omega})e^{2i\bar{\omega}t_0}+\int_0^\infty d\bar{\omega}\bar{J}_l(\omega+\bar{\omega})e^{-2i\bar{\omega}t_0}\right), \tag{B2}$$

with $J_l(\omega)=\int d\bar{\omega}\bar{J}_l(\omega-\bar{\omega})$. Before to continue, we pay attention to the four integrals having an explicit dependence on the initial time t_0. For both the Ohmic and super-Ohmic spectral densities, (38) and (39), the corresponding $\bar{J}$ decays more rapidly than $1/\bar{\omega}^2$ at high frequencies. This allows us to use the Riemann-Lebesgue Lemma which states [76]

$$\int_{-\infty}^{\infty}f(\omega)e^{i\omega t}d\omega\to 0\quad\text{as}\quad t\to\pm\infty,$$

for $f(\omega)$ an absolutely integrable function in the interval $(-\infty,\infty)$. As a consequence, only the first term in Eq.(B2) survives after taking the long-time limit $t_0\to-\infty$. The Riemann-Lebesgue Lemma has been successfully employed in the study of the properties of the stationary state for the damped harmonic oscillator [55, 58].

Appendix C: Quantum correlations

In the following we briefly describe the computation of the logarithmic negativity, quantum discord, and the separability criteria $\mathcal{T}_{\kappa,n}$.

1. Logarithmic negativity and quantum discord

The evaluation of the logarithmic negativity (34) requires the symplectic eigenvalues of the partial transpose $\boldsymbol{V}^{T_j}$. These are given by the positive square roots of the eigenvalues of $(-i/\hbar)\boldsymbol{\sigma}\boldsymbol{V}_{ij}^{T_j}$ [64], which are given in terms of the so-called symplectic matrix

$$\boldsymbol{\sigma}=\begin{bmatrix}0 & \boldsymbol{I}_2\\ -\boldsymbol{I}_2. & 0\end{bmatrix},$$

where $\boldsymbol{I}_n$ is the n-dimensional unit matrix. The corresponding partial transpose matrix is obtained from $\boldsymbol{V}_{ij}^{T_j} = \boldsymbol{\Lambda}\boldsymbol{V}_{ij}\boldsymbol{\Lambda}$, with

$$\boldsymbol{\Lambda} = \boldsymbol{I}_2 \oplus \begin{bmatrix} \boldsymbol{I}_1 & 0 \\ 0 & -\boldsymbol{I}_1 \end{bmatrix}.$$

The evaluation of the quantum discord (35) on the state $\hat{\rho}_{ij}$ involves an optimization procedure over all positive operator-valued measurements (POVMs) on the j-mode, denoted by $\Pi_l^{(j)}$. In Eq. (37), $p_l = \mathrm{Tr}_{ij}(\hat{\rho}_{ij}\Pi_l^{(j)})$ is the probability associated with the lth measurement outcome, and $\hat{\rho}_i^{(l)} = \mathrm{Tr}_j(\hat{\rho}_{ij}\Pi_l^{(j)})/p_i$ is the corresponding post-measurement reduced state of the i-mode. An explicit formula providing $D^{\leftarrow}(\hat{\rho}_{ij})$ for any input Gaussian state $\hat{\rho}_{ij}$ is given in [66]. $D^{\rightarrow}(\hat{\rho}_{ij})$ can be obtained from a similar optimization procedure on the POVMSs in the subsystem i. In general, both evaluations of discord may return different values (i.e. $D^{\leftarrow} \neq D^{\rightarrow}$).

2. Separability criteria $\mathcal{T}_{\kappa,n}$

Now we describe a hierarchy of separability criteria recently proposed to characterize from genuine multipartite to bipartite entanglement [68]. According to this proposal, the state $\hat{\rho}$ of a n-partite system is κ-partite entangled, *i.e.* there is at least a entangled subsystem composed of κ parties, provide that a given function $\tau_{\kappa,n}(\hat{\rho})$ takes a positive value.

The evaluation of the function $\tau_{\kappa,n}$ involves the selection of a set of $2n$ pure states that allows to assess multipartite entanglement. The important point is that a reliable characterization of entanglement requires an appropriate choice of such probe states. However, a priori there is no information about the 'optimal' probe states enable to unveil the entanglement encapsulated by an arbitrary density operator $\hat{\rho}$. One may circumvent this difficulty by carrying out an optimization procedure over all possible selections in order to obtain the maximum of $\tau_{\kappa,n}$, whose positive value would reveal the entanglement in the system. We denote $\mathcal{T}_{\kappa,n}$ such maximum.

In continuous-variable states a Gaussian selection of the probe states provides a readable expression of $\tau_{\kappa,n}$ [67], which can be optimized with standard procedures, and which is strong enough to detect entanglement for a broad class of Gaussian and non-Gaussian states. In the Gaussian case this expression reads [67],

$$\tau_{\kappa,n}(\hat{\rho}) = \frac{e^{-2\boldsymbol{X}^T\boldsymbol{J}_n^T\frac{1}{\boldsymbol{\Sigma}^{-1}+\boldsymbol{V}^{-1}}\boldsymbol{J}_n\boldsymbol{X}}}{\sqrt{\det(\boldsymbol{\Sigma}+\boldsymbol{V})}} - \sum_j a_j^{(\kappa,n)}\frac{e^{-\frac{1}{2}\boldsymbol{X}^T(\boldsymbol{P}_j)^T\frac{1}{\boldsymbol{\Sigma}+\boldsymbol{V}}\boldsymbol{P}_j\boldsymbol{X}}}{\sqrt{\det(\boldsymbol{\Sigma}+\boldsymbol{V})}}, \tag{C1}$$

where $a_i^{(\kappa,n)}$ are constant values [68], $\boldsymbol{X}$ is a real $2n$-vector, $\boldsymbol{J}_n$ is the standard form of the so-called symplectic matrix, and $\boldsymbol{P}_j$ and $\boldsymbol{\Sigma}$ are $2n \times 2n$ real matrices. The objects $\boldsymbol{X}$ and $\boldsymbol{\Sigma}$ denote a

compact form of the first and second moments of the probe states [67]. Hence, the detection of entanglement consists basically in optimizing Eq.(C1) over the variables $\boldsymbol{X}$ and $\boldsymbol{\Sigma}$, *i.e.*

$$\mathcal{T}_{\kappa,n}(\hat{\rho}) = \max_{\boldsymbol{X},\boldsymbol{\Sigma}} \tau_{\kappa,n}(\hat{\rho}).$$

---

[1] R. Horodecki, P. Horodecki, M. Horodecki, and K. Horodecki, Rev. Mod. Phys. **81**, 865 (2009).

[2] O. Gühne and G. Tóth, Phys. Rep. **474**, 1 (2009).

[3] V. Vedral, Nature Phys. **10**, 256 (2014).

[4] R. Kosloff, Entropy **15**, 2100 (2013).

[5] R. Kosloff and A. Levy, Annu. Rev. Phys. Chem. **65**, 365 (2014).

[6] V. Scarani, M. Ziman, P. Stelmachovic, N. Gisin, and V. Buzek, Phys. Rev. Lett. **88**, 097905 (2002).

[7] K. V. Hovhannisyan, M. Perarnau-Llobet, M. Huber, and A. Acín, Phys. Rev. Lett. **111**, 240401 (2013).

[8] O. Abah, J. Roßnagel, G. Jacob, S. Deffner, F. Schmidt-Kaler, K. Singer, and E. Lutz, Phys. Rev. Lett. **109**, 203006 (2012).

[9] R. Alicki and M. Fannes, Phys. Rev. E. **87**, 042123 (2013).

[10] L. A. Correa, J. P. Palao, G. Adesso, and D. Alonso, Phys. Rev. E **87**, 042131 (2013); *ibid.* **90**, 062124 (2014).

[11] L. A. Correa, J. P. Palao, D. Alonso, and G. Adesso, Sci. Rep. **4**, 3949(9) (2014).

[12] N. Brunner, M. Huber, N. Linden, S. Popescu, R. Silva, and P. Skrzypczyk, Phys. Rev. E **89**, 032115 (2014).

[13] R. Gallego, A. Riera, and J. Eisert, New J. Phys. **16**, 125009 (2014).

[14] J. Rammer, *Quantum field theory of non-equilibrium states* (Cambridge University Press, 2007).

[15] F. Mintert, A. R. Carvalho, M. Kuś, and A. Buchleitner, Phys. Rep. **415**, 207 (2005).

[16] L. Aolita, F. de Melo, and L. Davidovich, arXiv:1402.3713 (2014).

[17] A. Wolf, G. De Chiara, E. Kajari, E. Lutz, and G. Morigi, Europhys. Lett. **95**, 60008 (2011).

[18] H. Krauter, C. A. Muschik, K. Jensen, W. Wasilewski, J. M. Petersen, J. I. Cirac, and E. S. Polzik, Phys. Rev. Lett. **107**, 080503 (2011).

[19] M. Ludwig, K. Hammerer, and F. Marquardt, Phys. Rev. A **82**, 012333 (2010).

[20] A. A. Valido, D. Alonso, and S. Kohler, Phys. Rev. A **88**, 042303 (2013).

[21] W. Zurek, H. Ann. der Physik (Leipzig) **9**, 853 (2000).

[22] H. Ollivier and W. H. Zurek, Phys. Rev. Lett. **88**, 017901 (2001).

[23] L. Henderson and V. Vedral, J. Phys. A: Math. Gen. **34**, 6899 (2001).

[24] L.-A. Wu and D. Segal, Phys. Rev. A **84**, 012319 (2011).

[25] S. Diehl, A. Micheli, A. Kantian, B. Kraus, H. Büchler, and P. Zoller, Nature Phys. **4**, 878 (2008).

[26] B. Kraus, H.P. Büchler, S. Diehl, A. Kantian, A. Micheli, and P. Zoller, Phys. Rev. A **78**, 042307 (2008).

[27] B. Bellomo and M. Antezza, Europhys. Lett. **104**, 10006 (2013); B. Bellomo and M. Antezza, New J. Phys. **15**, 113052 (2013).

[28] G. Manzano, F. Galve, G.L. Giorgi, E. Hernández-García, and R. Zambrini, Sci. Rep. **3**, 1439 (2013); G. Manzano, F. Galve, and R. Zambrini, Phys. Rev. A **87**, 032114 (2013).

[29] S. McEndoo, P. Haikka, G. De Chiara, M. Palma, and S. Maniscalco, Eurphys. Lett. **101**, 60005 (2013)

[30] A. M. Souza, M. S. Reis, D. O. Soares-Pinto, I. S. Oliveira, and R. S. Sarthour, Phys. Rev. B **77**, 104402 (2008).

[31] D. Das, H. Singh, T. Chakraborty, R. K. Gopal, and C. Mitra, New J. Phys. **15**, 013047 (2013).

[32] H. Singh, T. Chakraborty, D. Das, H. Jeevan, Y. Tokiwa, P. Gegenwart, and C. Mitra, New J. Phys. **15**, 113001 (2013).

[33] M. Wieśniak, V. Vedral, and Č. Brukner, New J. Phys. **7**, 258 (2005).

[34] M. Wieśniak, V. Vedral, and Č. Brukner, Phys. Rev. B **78**, 064108 (2008).

[35] M. Ramm, T. Pruttivarasin, and H. Häffner, New J. Phys. **16**, 063062 (2014).

[36] N. Li, J. Ren, L. Wang, G. Zhang, P. Hänggi, and B. Li, Rev. Mod. Phys. **84**, 1045 (2012).

[37] A. Asadian, D. Manzano, M. Tiersch, and H. J. Briegel, Phys. Rev. E **87**, 012109 (2013).

[38] T. Prosen, Phys. Rev. Lett. **112**, 030603 (2014).

[39] A. Bermudez, M. Bruderer, and M. B. Plenio, Phys. Rev. Lett. **111**, 040601 (2013).

[40] N. Freitas, E. Martinez, and J. P. Paz. arXiv:1312.6644 (2013).

[41] A. Ruiz, D. Alonso, M. B. Plenio, and A. del Campo, Phys. Rev. B **89**, 214305 (2014).

[42] A. A. Valido, L. A. Correa, and D. Alonso, Phys. Rev. A **88**, 012309 (2013).

[43] B. Bellomo, R. Messina, D. Felbacq, and M. Antezza, Phys. Rev. A **87**, 012101 (2013).

[44] M. B. Plenio and S. F. Huelga, New J. Phys. **10**, 113019 (2008).

[45] B. Witt and F. Mintert, New J. Phys. **15**, 093020 (2013).

[46] B. L. Hu and A. Matacz, Phys. Rev. D **49**, 6612 (1994).

[47] T. Kuwahara, New J. Phys. **14**, 123032 (2012).

[48] P. Hänggi and G.-L. Ingold, Chaos **15**, 026105 (2005).

[49] U. Weiss, *Quantum dissipative systems*, (World Scientific, 1999).

[50] G.W. Ford, J.T. Lewis, and R.F. O'Connell, Phys. Rev. A **37**, 4419 (1988).

[51] H.-P. Breuer and F. Petruccione, *The theory of open quantum systems* (Oxford University Press, 2002).

[52] H. Grabert, U. Weiss, and P. Talkner, Z. Phys. B **55**, 87 (1984).

[53] F. Haake and R. Reibold, Phys. Rev. A **32**, 2462 (1985).

[54] G. W. Ford and R. F. O'Connell, Phys. Rev. D **64**, 105020 (2001).

[55] A. Dhar and K. Wagh, Europhys. Lett. **79**, 60003 (2007).

[56] R. Jung, G.-L. Ingold, and H. Grabert, Phys. Rev. A **32**, 2510 (1985).

[57] C. H. Fleming, B. L. Hu, and A. Roura, Phys. Rev. E **88**, 012102 (2013).

[58] D. Pagel, P. Nalbach, A. Alvermann, H. Fehske, and M. Thorwart, New J. Phys. **15**, 105008 (2013).

[59] A. Dhar, Adv. Phys, **57**, 457 (2008).

[60] S. Lepri, R. Livi, and A. Politi, Phys. Rep. **377**, 1 (2003).

[61] A. Kundu, Phys. Rev. E **82**, 031131 (2010).

[62] P. Giorda and M. G. A. Paris, Phys. Rev. Lett. **105**, 020503 (2010).

[63] G. Adesso and A. Datta, Phys. Rev. Lett. **105**, 030501 (2010).

[64] G. Vidal and R. F. Werner, Phys. Rev. A **65**, 032314 (2002).

[65] M. B. Plenio, Phys. Rev. Lett. **95**, 090503 (2005).

[66] G. Adesso and F. Illuminati, J. Phys. A: Math. Theor. **40**, 7821 (2007).

[67] A. A. Valido, F. Levi, and F. Mintert, Phys. Rev. A **90**, 052321 (2014).

[68] F. Levi and F. Mintert, Phys. Rev. Lett. **110**, 150402 (2013).

[69] C. Gaul and H. Büttner, Phys. Rev. E **76**, 011111 (2007).

[70] J.-H. An and W.-M. Zhang, Phys. Rev. A **76**, 042127 (2007).

[71] A. Streltsov, H. Kampermann, and D. Bruß, Phys. Rev. Lett. **107**, 170502 (2011).

[72] J. Sperling and W. Vogel, Phys. Rev. A **79**, 022318 (2009).

[73] R. Simon, Phys. Rev. Lett. **84**, 2726 (2000).

[74] F. Mintert, Appl. Phys. B **89**, 493 (2007).

[75] A. Ferraro, L. Aolita, D. Cavalcanti, F. M. Cucchietti, and A. Acín, Phys. Rev. A **81**, 052318 (2010).

[76] K. Chandrasekharan, *Classical Fourier Transforms* (Springer, 1989).

Appendix A

Microscopic model

In this appendix is extensively illustrated the derivation of the Hamiltonian given in Eq.(1.37) starting from the Hamiltonian that describes the minimal coupling of the system oscillators with a free bosonic field. In the subsequent derivation, we have followed a previous work of Kohler and Sols, where the authors analyse the damped harmonic oscillator model [143].

We are considering that the system oscillators are well localized around certain positions of equilibrium, and whose motion are practically confined in one direction. Then all the relevant dynamics of the λth oscillator resides on the spatial displacement, given by $\hat{x}_\lambda$, from the position equilibrium $\boldsymbol{r}_\lambda^0$. In this way, an a priori three-dimensional oscillator consists mechanically on one mode. Under these considerations, the minimal-coupling Hamiltonian of a n-mode system in contact with a free bosonic field can be cast in the form,

$$\hat{H} = \sum_{\lambda=1}^{n} \left(\frac{1}{2m} \left(\hat{p}_\lambda + \hat{A}(\boldsymbol{r}_\lambda^0) \right)^2 + \frac{m\omega_\lambda^2}{2} \hat{x}_\lambda^2 \right) + \sum_{\boldsymbol{k}} \hbar\omega_{\boldsymbol{k}} a_{\boldsymbol{k}}^\dagger a_{\boldsymbol{k}}, \tag{A.1}$$

where $\hat{A}(\boldsymbol{r}_\lambda^0)$ is refereed to as the gauge field and it is given by,

$$\hat{A}(\boldsymbol{r}_\lambda^0) = i \sum_{\boldsymbol{k}} \frac{g_{\boldsymbol{k}}}{\omega_{\boldsymbol{k}}} \left(\hat{a}_{\boldsymbol{k}} e^{i\boldsymbol{k}\cdot\boldsymbol{r}_\lambda^0} - \hat{a}_{\boldsymbol{k}}^\dagger e^{-i\boldsymbol{k}\cdot\boldsymbol{r}_\lambda^0} \right). \tag{A.2}$$

Notice that in Eq.(A.1) we have already assumed the dipole approximation. Accordingly, the Göppert-Mayer transformation is defined as

$$\hat{\mathcal{U}} = exp\left(\frac{i}{\hbar} \sum_{\lambda=1}^{n} \hat{A}(\boldsymbol{r}_\lambda^0) \hat{x}_\lambda \right). \tag{A.3}$$

Thanks to the dipole approximation the exponential in Eq.(A.3) is linear in the reservoir operators (*i.e.*, $\hat{a}_{\boldsymbol{k}}^\dagger$ and $\hat{a}_{\boldsymbol{k}}$) as well as in the coordinate operators $\hat{x}_\lambda$. This feature simplifies considerably the algebraic manipulation of the Göppert-Mayer transformation of the system-plus-reservoir operators. Using the canonical commutation rules for the latter

[160], one obtains the following transformation rules,

$$\hat{\mathcal{U}}\ \hat{x}_\lambda\ \hat{\mathcal{U}}^\dagger = \hat{x}_\lambda, \tag{A.4}$$

$$\hat{\mathcal{U}}\ \hat{p}_\lambda\ \hat{\mathcal{U}}^\dagger = \hat{p}_\lambda - \hat{A}(\boldsymbol{r}_\lambda^0), \tag{A.5}$$

$$\hat{\mathcal{U}}\ \hat{a}_{\boldsymbol{k}}\ \hat{\mathcal{U}}^\dagger = \hat{a}_{\boldsymbol{k}} - \sum_{\lambda=1}^{n} \frac{g_{\boldsymbol{k}}}{\hbar\omega_{\boldsymbol{k}}} e^{-i\boldsymbol{k}\cdot\boldsymbol{r}_\lambda^0}\hat{x}_\lambda. \tag{A.6}$$

Applied to the Hamiltonian (A.1), the above transformation rules (Eqs.(A.4)-(A.6)) return the following expression for the system-plus-reservoir Hamiltonian,

$$\begin{aligned}\hat{H} &= \sum_{\lambda=1}^{n}\Big(\frac{1}{2m}\hat{p}_\lambda^2 + \frac{m\omega_\lambda^2}{2}\hat{x}_\lambda^2\Big) + \underbrace{\sum_{\boldsymbol{k}}\hbar\omega_{\boldsymbol{k}}a_{\boldsymbol{k}}^\dagger a_{\boldsymbol{k}}}_{\hat{H}_R} - \underbrace{\sum_{\lambda=1}^{n}\hat{x}_\lambda\sum_{\boldsymbol{k}} g_{\boldsymbol{k}}\Big(\hat{a}_{\boldsymbol{k}}e^{i\boldsymbol{k}\cdot\boldsymbol{r}_\lambda^0} + \hat{a}_{\boldsymbol{k}}^\dagger e^{-i\boldsymbol{k}\cdot\boldsymbol{r}_\lambda^0}\Big)}_{\hat{H}_I} \\ &+ \underbrace{\sum_{\lambda,\mu=1}^{n}\hat{x}_\lambda\hat{x}_\mu\sum_{\boldsymbol{k}}\frac{g_{\boldsymbol{k}}^2}{\hbar\omega_{\boldsymbol{k}}}\cos(\boldsymbol{k}\cdot\Delta\boldsymbol{r}_{\lambda\mu}^0)}_{\text{Renormalization Term}},\end{aligned} \tag{A.7}$$

where we have defined the spatial separation $\Delta\boldsymbol{r}_{\lambda\mu}^0 := \boldsymbol{r}_\lambda^0 - \boldsymbol{r}_\mu^0$. Notice that to derive the renormalization term we have used the fact that $[\hat{x}_\lambda, \hat{x}_\mu] = 0$ for $\lambda, \mu = 1, \ldots, n$. Clearly, after doing the Göppert-Mayer transformation in the Hamiltonian given in Eq.(A.1), one obtains the expressions for the reservoir and system-reservoir interaction illustrated in Sec.1.3.1 (see Eq.(1.36)), whereas the last term in Eq.(A.7) corresponds to the mentioned renormalization term. Notice that this term turns into the expression (1.39) in the generalized Langevin equation.

One may proceed further in order to recover the Hamiltonian $\hat{H}_{RI}$ given in Eq.(1.37) by doing the following substitution,

$$\hat{a}_{\boldsymbol{k}} = (m_{\boldsymbol{k}}\omega_{\boldsymbol{k}}\hat{\boldsymbol{x}}_{\boldsymbol{k}} + i\hat{\boldsymbol{p}}_{\boldsymbol{k}})/\sqrt{2\hbar m_{\boldsymbol{k}}\omega_{\boldsymbol{k}}},$$

and its adjoint in Eq.(A.7). Doing so, it is immediate to obtain the following expressions for the reservoir and system-reservoir interaction Hamiltonia, respectively,

$$\hat{H}_R = \sum_{\boldsymbol{k}}\frac{1}{2m_{\boldsymbol{k}}}\hat{\boldsymbol{p}}_{\boldsymbol{k}}^2 + \frac{1}{2}m_{\boldsymbol{k}}\omega_{\boldsymbol{k}}^2\hat{\boldsymbol{x}}_{\boldsymbol{k}}^2, \tag{A.8}$$

$$\hat{H}_I = -\sum_{\boldsymbol{k}} g_{\boldsymbol{k}}\left(\frac{m_{\boldsymbol{k}}\omega_{\boldsymbol{k}}\hat{\boldsymbol{x}}_{\boldsymbol{k}}}{\sqrt{2\hbar m_{\boldsymbol{k}}\omega_{\boldsymbol{k}}}}\sum_{\lambda=1}^{n}\hat{x}_\lambda\cos(\boldsymbol{k}\cdot\boldsymbol{r}_\lambda^0) + \frac{\hat{\boldsymbol{p}}_{\boldsymbol{k}}}{\sqrt{2\hbar m_{\boldsymbol{k}}\omega_{\boldsymbol{k}}}}\sum_{\lambda=1}^{n}\hat{x}_\lambda\sin(\boldsymbol{k}\cdot\boldsymbol{r}_\lambda^0)\right). \tag{A.9}$$

Using trigonometric identities, the renormalization term can be written as follows,

$$\begin{aligned}&\sum_{\lambda,\mu=1}^{n}\hat{x}_\lambda\hat{x}_\mu\sum_{\boldsymbol{k}}\frac{g_{\boldsymbol{k}}^2}{\hbar\omega_{\boldsymbol{k}}}\cos(\boldsymbol{k}\cdot\Delta\boldsymbol{r}_{\lambda\mu}^0) = \\ &\sum_{\boldsymbol{k}}\frac{g_{\boldsymbol{k}}^2}{\hbar\omega_{\boldsymbol{k}}}\left(\left(\sum_{\lambda=1}^{n}\hat{x}_\lambda\cos(\boldsymbol{k}\cdot\boldsymbol{r}_\lambda^0)\right)^2 + \left(\sum_{\lambda=1}^{n}\hat{x}_\lambda\sin(\boldsymbol{k}\cdot\boldsymbol{r}_\lambda^0)\right)^2\right).\end{aligned} \tag{A.10}$$

Summing Eqs. (A.8), (A.9), and (A.10), and after some convenient manipulation, one obtains the Hamiltonian given in Eq.(1.37) which characterizes both the reservoir and system-reservoir interaction.

Bibliography

[1] L. Abellanas und A. Galindo: *Espacios de Hilbert (Geomertría, Operadores, Espectros)*. Eudema Universidad, (1987).

[2] A. Acín, D. Bruß, M. Lewenstein und A. Sanpera, *Phys. Rev. Lett.* **87** (2001), 040401.

[3] G. Adesso, *Phys. Rev. A* **83** (2011), 024301.

[4] G. Adesso und A. Datta, *Phys. Rev. Lett.* **105** (2010), 030501.

[5] G. Adesso, D. Girolami und A. Serafini, *Phys. Rev. Lett.* **109** (2012), 190502.

[6] G. Adesso und F. Illuminati, *Phys. Rev. A* **72** (2005), 032334.

[7] G. Adesso und F. Illuminati, *New J. Phys.* **8** (2006), 15.

[8] G. Adesso und F. Illuminati, *J. Phys. A: Math. Theor.* **40** (2007), 7821.

[9] G. Adesso, S. Ragy und A.R. Lee, *Open Syst. Inf. Dyn.* **21** (2014).

[10] G. Adesso, A. Serafini und F. Illuminati, *Phys. Rev. Lett.* **93** (2004), 220504.

[11] G. Adesso, A. Serafini und F. Illuminati, *Phys. Rev. A* **73** (2006), 032345.

[12] G.S. Agarwal, *Phys. Rev. A* **4** (1971), 739.

[13] G.S. Agarwal, *New J. Phys.* **13** (2011), 073008.

[14] G.S. Agarwal und A. Biswas, *New J. Phys.* **7** (2005), 211.

[15] M. Allegra, P. Giorda und M.G.A. Paris, *Phys. Rev. Lett.* **105** (2010), 100503.

[16] D. Alonso und I. de Vega, *Phys. Rev. Lett.* **94** (2005), 200403.

[17] D. Alonso und I. de Vega, *Phys. Rev. A* **75** (2007), 052108.

[18] A. Altland und B.D. Simons: *Condensed matter field theory*. Cambridge University Press, (2010).

[19] L. Amico, R. Fazio, A. Osterloh und V. Vedral, *Rev. Mod. Phys.* **80** (2008), 517.

[20] J. Anders, *Phys. Rev. A* **77** (2008), 062102.

[21] E. Andersson und P. Öhberg: *Quantum Information and Coherence*. Springer, (2014).

[22] A. Anisimov, W. Buchmüller, M. Drewes und S. Mendizabal, *Ann. Phys.* **324** (2009), 1234.

[23] L. Aolita, D. Cavalcanti, A. Acín, A. Salles, M. Tiersch, A. Buchleitner und F. de Melo, *Phys. Rev. A* **79** (2009), 032322.

[24] L. Aolita, R. Chaves, D. Cavalcanti, A. Acín und L. Davidovich, *Phys. Rev. Lett.* **100** (2008), 080501.

[25] L. Aolita, F. de Melo und L. Davidovich, *Rep. Prog. Phys.* **78** (2015), 042001.

[26] M. Aspelmeyer und K. Schwab, *New J. Phys.* **10** (2008), 095001.

[27] K. Audenaert, J. Eisert, M.B. Plenio und R.F. Werner, *Phys. Rev. A* **66** (2002), 042327.

[28] K. Audenaert und M. Plenio, *New J. Phys.* **8** (2006), 266.

[29] J. Audretsch: *Entangled World*. John Wiley & Sons, (2008).

[30] J.S. Bell, *Physics* **1** (1964), 195.

[31] B. Bellomo und M. Antezza, *New J. Phys.* **15** (2013), 113052.

[32] B. Bellomo, R. Lo Franco und G. Compagno, *Phys. Rev. Lett.* **99** (2007), 160502.

[33] B. Bellomo, R. Messina, D. Felbacq und M. Antezza, *Phys. Rev. A* **87** (2013), 012101.

[34] I. Bengtsson und K. Zyczkowski: *Geometry of quantum states: an introduction to quantum entanglement*. Cambridge University Press, (2006).

[35] C.H. Bennett, H.J. Bernstein, S. Popescu und B. Schumacher, *Phys. Rev. A* **53** (1996), 2046.

[36] C.H. Bennett, A. Grudka, M. Horodecki, P. Horodecki und R. Horodecki, *Phys. Rev. A* **83** (2011), 012312.

[37] C.H. Bennett und P.W. Shor, *IEEE Trans. Inf Theory* **44** (1998), 2724.

[38] I. Bloch, J. Dalibard und W. Zwerger, *Rev. Mod. Phys.* **80** (2008), 885.

[39] F.G.S.L. Brandão, *Phys. Rev. A* **72** (2005), 022310.

[40] D. Braun, *Phys. Rev. Lett.* **89** (2002), 277901.

[41] S. Braunstein und P. van Loock, *Rev. Mod. Phys.* **77** (2005), 513.

[42] G. Brawley, M. Vanner, P. Larsen, S. Schmid, A. Boisen und W. Bowen, *arXiv:1404.5746* (2014).

[43] H.P. Breuer und F. Petruccione: *The theory of open quantum systems.* Oxford University Press, (2002).

[44] A. Buchleitner, A. Carvalho und F. Mintert, *Acta Physica Polonica A Gen. Phys.* **112** (2007), 575.

[45] E. Butkov: *Mathematical physics.* Addison-Wesley, (1973).

[46] A.O. Caldeira und A.J. Leggett, *Physica A: Stat. Mech. Appl.* **121** (1983), 587.

[47] H.J. Carmichael: *An open systems approach to Quantum Optics: lectures presented at the Université Libre de Bruxelles.* Springer, (1993).

[48] H.J. Carmichael: *Statistical methods in quantum optics.* Springer-Verlag, (2002).

[49] A.R.R. Carvalho, F. Mintert und A. Buchleitner, *Phys. Rev. Lett.* **93** (2004), 230501.

[50] K. Chandrasekharan: *Classical Fourier Transforms.* Springer, (1989).

[51] J.I. Cirac, *arXiv:1205.3742* (2012).

[52] V. Coffman, J. Kundu und W.K. Wootters, *Phys. Rev. A* **61** (2000), 052306.

[53] C. Cohen-Tannoudji, J. Dupont-Roc und G. Grynberg: *Quantum Mechanics, Volumen I.* John Wiley & Sons, (1977).

[54] C. Cohen-Tannoudji, J. Dupont-Roc und G. Grynberg: *Photons and Atoms: Introduction to Quantum Electrodynamics.* John Wiley & Sons, (2001).

[55] L.A. Correa, J.P. Palao, G. Adesso und D. Alonso, *Phys. Rev. E* **87** (2013), 042131.

[56] L.A. Correa, J.P. Palao, D. Alonso und G. Adesso, *Sci. Rep.* **4** (2014).

[57] M. Cramer, A. Bernard, N. Fabbri, L. Fallani, C. Fort, S. Rosi, F. Caruso, M. Inguscio und M. Plenio, *Nat. Commun.* **4** (2013).

[58] M. Cramer, M. Plenio und H. Wunderlich, *Phys. Rev. Lett.* **106** (2011), 020401.

[59] V. D'Auria, S. Fornaro, A. Porzio, S. Solimeno, S. Olivares und M.G.A. Paris, *Phys. Rev. Lett.* **102** (2009), 020502.

[60] G. De Chiara, R. Fazio, C. Macchiavello und G. Palma, *Europhys. Lett.* **67** (2004), 714.

[61] G. De Chiara, M. Paternostro und G.M. Palma, *Phys. Rev. A* **83** (2011), 052324.

[62] T.F. Demarie, T. Linjordet, N.C. Menicucci und G.K. Brennen, *New J. Phys.* **16** (2014), 085011.

[63] A. Dhar und D. Roy, *J. Stat. Phys.* **125** (2006), 801.

[64] A. Dhar und K. Wagh, *Europhys. Lett.* **79** (2007), 60003.

[65] S. Diehl, A. Micheli, A. Kantian, B. Kraus, H. Büchler und P. Zoller, *Nat. Phys.* **4** (2008), 878.

[66] L. Diósi: *A short course in quantum information theory: an approach from theoretical physics*. Springer, (2011).

[67] T. Dittrich, P. Hänggi, G.L. Ingold, B. Kramer, G. Schön und W. Zwerger: *Quantum transport and dissipation*. Wiley-Vch, (1998).

[68] M.J. Donald, M. Horodecki und O. Rudolph, *J. Math. Phys.* **43** (2002), 4252.

[69] J.P. Dowling und G.J. Milburn, *Philosophical Transactions of the Royal Society A: Mathematical, Physical and Engineering Sciences* **361** (2003), 1655.

[70] L.M. Duan, G. Giedke, J.I. Cirac und P. Zoller, *Phys. Rev. Lett.* **84** (2000), 2722.

[71] W. Dür und J. Cirac, *Phys. Rev. A* **61** (2000), 042314.

[72] W. Dür, G. Vidal und J.I. Cirac, *Phys. Rev. A* **62** (2000), 062314.

[73] A. Einstein, B. Podolsky und N. Rosen, *Phys. Rev.* **47** (1935), 777.

[74] J. Eisert, F.G. Brandão und K.M. Audenaert, *New J. Phys.* **9** (2007), 46.

[75] J. Eisert, M. Cramer und M.B. Plenio, *Rev. Mod. Phys.* **82** (2010), 277.

[76] J. Eisert, P. Hyllus, O. Gühne und M. Curty, *Phys. Rev. A* **70** (2004), 062317.

[77] J. Eisert und M. Plenio, *Int. J. Quantum Inf.* **1** (2003), 479.

[78] J. Eisert, S. Scheel und M.B. Plenio, *Phys. Rev. Lett.* **89** (2002), 137903.

[79] A. Erdilyi, W. Magnus, F. Oberthettinger und F. Tricomi: *Tables of Integral Transforms, Vol I.* McGraw-Hill, (1954).

[80] K. Fang und S. Fan, *Phys. Rev. Lett.* **111** (2013), 203901.

[81] K. Fang, Z. Yu und S. Fan, *Nat. Photon.* **6** (2012), 782.

[82] A. Ferraro, L. Aolita, D. Cavalcanti, F.M. Cucchietti und A. Acín, *Phys. Rev. A* **81** (2010), 052318.

[83] R.P. Feynman und F. Vernon Jr, *Ann. Phys.* **24** (1963), 118.

[84] C. Fleming, A. Roura und B.L. Hu, *Ann. Phys.* **326** (2011), 1207.

[85] C. Fleming, A. Roura und B.L. Hu, *arXiv:1106.5752* (2011).

[86] G.W. Ford, M. Kac und P. Mazur, *J. Math. Phys.* **6** (1965), 504.

[87] G.W. Ford, J.T. Lewis und R.F. O'Connell, *J. Stat. Phys.* **53** (1988), 439.

[88] G.W. Ford, J.T. Lewis und R.F. O'Connell, *Phys. Rev. A* **37** (1988), 4419.

[89] G.W. Ford und R.F. O'Connell, *Phys. Rev. D* **64** (2001), 105020.

[90] R.L. Franco, B. Bellomo, S. Maniscalco und G. Compagno, *Int. J. Mod. Phys. B* **27** (2013).

[91] A. Gabriel, B.C. Hiesmayr und M. Huber, *Quantum Info. Comput.* **10** (2010), 829.

[92] A. Gabriel, M. Huber, S. Radic und B.C. Hiesmayr, *Phys. Rev. A* **83** (2011), 052318.

[93] A. Galindo und P. Pascual: *Mecánica cuántica*. Eudema Universidad, (1989).

[94] F. Galve, G.L. Giorgi und R. Zambrini, *Phys. Rev. A* **81** (2010), 062117.

[95] F. Galve, L.A. Pachón und D. Zueco, *Phys. Rev. Lett.* **105** (2010), 180501.

[96] C. Gardiner und P. Zoller: *Quantum noise: a handbook of Markovian and non-Markovian quantum stochastic methods with applications to quantum optics*. Springer-Verlag, (2001).

[97] G. Giedke und J. Ignacio Cirac, *Phys. Rev. A* **66** (2002), 032316.

[98] G. Giedke und B. Kraus, *Phys. Rev. A* **89** (2014), 012335.

[99] G. Giedke, B. Kraus, M. Lewenstein und J.I. Cirac, *Phys. Rev. Lett.* **87** (2001), 167904.

[100] G. Giedke, B. Kraus, M. Lewenstein und J.I. Cirac, *Phys. Rev. A* **64** (2001), 052303.

[101] D.T. Gillespie, *Am. J. Phys.* **64** (1996), 1246.

[102] N. Goldman, G. Juzeliūnas, P. Öhberg und I.B. Spielman, *Rep. Prog. Phys.* **77** (2014), 126401.

[103] G. Gour und N.R. Wallach, *New J. Phys.* **13** (2011), 073013.

[104] G. Gour und N.R. Wallach, *Phys. Rev. Lett.* **111** (2013), 060502.

[105] H. Grabert, *Chem. Phys.* **322** (2006), 160.

[106] H. Grabert, P. Schramm und G.L. Ingold, *Phys. Rep.* **168** (1988), 115.

[107] H. Grabert, U. Weiss und P. Talkner, *Z. Phys. B* **55** (1984), 87.

[108] S. Gröblacher, K. Hammerer, M.R. Vanner und M. Aspelmeyer, *Nature* **460** (2009), 724.

[109] S. Gröblacher, A. Trubarov, N. Prigge, M. Aspelmeyer und J. Eisert, *arXiv:1305.6942* (2013).

[110] O. Gühne und N. Lütkenhaus, *Phys. Rev. Lett.* **96** (2006), 170502.

[111] O. Gühne, M. Reimpell und R.F. Werner, *Phys. Rev. Lett.* **98** (2007), 110502.

[112] O. Gühne und G. Tóth, *Phys. Rep.* **474** (2009), 1 .

[113] O. Gühne, G. Tóth und H.J. Briegel, *New J. Phys.* **7** (2005), 229.

[114] Q. Guo, L. Huang, L.Y. Hu, X.X. Xu und H.L. Zhang, *Int. J. Theor. Phys.* **52** (2013), 2886.

[115] L. Gurvits, *J. Comput. System Sci.* **69** (2004), 448.

[116] F. Haake und R. Reibold, *Phys. Rev. A* **32** (1985), 2462.

[117] H. Häffner, W. Hänsel, C. Roos, J. Benhelm et al. , *Nature* **438** (2005), 643.

[118] P. Hänggi und G.L. Ingold, *Chaos* **15** (2005), 026105.

[119] S. Haroche, *Rev. Mod. Phys.* **85** (2013), 1083.

[120] L. Henderson und V. Vedral, *J. Phys. A: Math. Theor.* **34** (2001), 6899.

[121] T. Hiroshima, G. Adesso und F. Illuminati, *Phys. Rev. Lett.* **98** (2007), 050503.

[122] G. Hooft, *J. Stat. Phys.* **53** (1988), 323.

[123] C. Hörhammer und H. Büttner, *Phys. Rev. A* **77** (2008), 042305.

[124] R.A. Horn und C.R. Johnson: *Matrix analysis*. Cambridge university press, (2012).

[125] M. Horodecki, P. Horodecki und R. Horodecki, *Phys. Lett. A* **223** (1996), 1.

[126] M. Horodecki, P. Horodecki und R. Horodecki, *Phys. Rev. Lett.* **78** (1997), 574.

[127] M. Horodecki, P. Horodecki und R. Horodecki, *Phys. Lett. A* **283** (2001), 1.

[128] R. Horodecki und M. Horodecki, *Phys. Rev. A* **54** (1996), 1838.

[129] R. Horodecki, P. Horodecki, M. Horodecki und K. Horodecki, *Rev. Mod. Phys.* **81** (2009), 865.

[130] B.L. Hu, J.P. Paz und Y. Zhang, *Phys. Rev. D* **45** (1992), 2843.

[131] L.Y. Hu, F. Jia und Z.M. Zhang, *J. Opt. Soc. Am. B* **29** (2012), 1456.

[132] Y. Huang, *New J. Phys.* **16** (2014), 033027.

[133] M. Huber, F. Mintert, A. Gabriel und B.C. Hiesmayr, *Phys. Rev. Lett.* **104** (2010), 210501.

[134] P. Hyllus und J. Eisert, *New J. Phys.* **8** (2006), 51.

[135] A. Isar, *Phys. Scripta* **2010** (2010), 014023.

[136] A. Isar, A. Sandulescu, H. Scutaru, E. Stefanescu und W. Scheid, *Int. J. Mod Phys. E* **3** (1994), 635.

[137] R. Jung, G.L. Ingold und H. Grabert, *Phys. Rev. A* **32** (1985), 2510.

[138] B. Jungnitsch, T. Moroder und O. Gühne, *Phys. Rev. Lett.* **106** (2011), 190502.

[139] E. Kajari, A. Wolf, E. Lutz und G. Morigi, *Phys. Rev. A* **85** (2012), 042318.

[140] R. Karrlein und H. Grabert, *Phys. Rev. E* **55** (1997), 153.

[141] M.S. Kim, *J. Phys. B: At. Mol. Opt. Phys.* **41** (2008), 133001.

[142] A. Kitaev und J. Preskill, *Phys. Rev. Lett.* **96** (2006), 110404.

[143] H. Kohler und F. Sols, *Physica A: Statistical Mechanics and its Applications* **392** (2013), 1989.

[144] S. Kohler, T. Dittrich und P. Hänggi, *Phys. Rev. E* **55** (1997), 300.

[145] S. Kohler, J. Lehmann und P. Hänggi, *Phys. Rep.* **406** (2005), 379.

[146] T. Konrad, F. De Melo, M. Tiersch, C. Kasztelan, A. Aragão und A. Buchleitner, *Nat. Phys.* **4** (2007), 99.

[147] B. Kraus, H.P. Büchler, S. Diehl, A. Kantian, A. Micheli und P. Zoller, *Phys. Rev. A* **78** (2008), 042307.

[148] H. Krauter, C.A. Muschik, K. Jensen, W. Wasilewski, J.M. Petersen, J.I. Cirac und E.S. Polzik, *Phys. Rev. Lett.* **107** (2011), 080503.

[149] J. Laurat, G. Keller, J.A. Oliveira-Huguenin, C. Fabre, T. Coudreau, A. Serafini, G. Adesso und F. Illuminati, *J. Opt. B: Quantum Semiclass. Opt.* **7** (2005), S577.

[150] M. Le Bellac, F. Mortessagne und G.G. Batrouni: *Equilibrium and non-equilibrium statistical thermodynamics*. Cambridge University Press, (2004).

[151] A.J. Leggett, S. Chakravarty, A.T. Dorsey, M.P.A. Fisher, A. Garg und W. Zwerger, *Rev. Mod. Phys.* **59** (1987), 1.

[152] D. Leibfried, E. Knill, S. Seidelin, J. Britton, R.B. Blakestad, J. Chiaverini, D.B. Hume, W.M. Itano, J.D. Jost, C. Langer et al. , *Nature* **438** (2005), 639.

[153] L. Lepori, G. De Chiara und A. Sanpera, *Phys. Rev. B* **87** (2013), 235107.

[154] F. Levi und F. Mintert, *Phys. Rev. Lett.* **110** (2013), 150402.

[155] M. Lewenstein, B. Kraus, J.I. Cirac und P. Horodecki, *Phys. Rev. A* **62** (2000), 052310.

[156] D.A. Lidar, I.L. Chuang und K.B. Whaley, *Phys. Rev. Lett.* **81** (1998), 2594.

[157] P. Linz: *Analytical and numerical methods for Volterra equations*. SIAM, (1985).

[158] R. Lo Franco, B. Bellomo, E. Andersson und G. Compagno, *Phys. Rev. A* **85** (2012), 032318.

[159] P. van Loock und A. Furusawa, *Phys. Rev. A* **67** (2003), 052315.

[160] W.H. Louisell: *Quantum statistical properties of radiation*. John Wiley & Sons, (1990).

[161] M. Ludwig, K. Hammerer und F. Marquardt, *Phys. Rev. A* **82** (2010), 012333.

[162] A.I. Lvovsky und M.G. Raymer, *Rev. Mod. Phys.* **81** (2009), 299.

[163] X.S. Ma, T. Herbst, T. Scheidl, D. Wang, S. Kropatschek, W. Naylor, A. Mech, B. Wittmann, J. Kofler, E. Anisimova et al. , *Nature* **489** (2010), 269.

[164] S. Maniscalco, S. Olivares und M.G.A. Paris, *Phys. Rev. A* **75** (2007), 062119.

[165] G. Manzano, F. Galve und R. Zambrini, *Phys. Rev. A* **87** (2013), 032114.

[166] G.F. Mazenko: *Nonequilibrium statistical mechanics*. John Wiley & Sons, (2008).

[167] S. McEndoo, P. Haikka, G. De Chiara, G. Palma und S. Maniscalco, *Europhys. Lett.* **101** (2013), 60005.

[168] F. Mintert, *Appl. Physics B* **89** (2007), 493.

[169] F. Mintert und A. Buchleitner, *Phys. Rev. Lett.* **98** (2007), 140505.

[170] F. Mintert, A.R. Carvalho, M. Kuś und A. Buchleitner, *Phys. Rep.* **415** (2005), 207 .

[171] F. Mintert, B. Salwey und A. Buchleitner, *Phys. Rev. A* **86** (2012), 052330.

[172] A. Miranowicz und M. Piani, *Phys. Rev. Lett.* **97** (2006), 058901.

[173] A. Miranowicz, M. Piani, P. Horodecki und R. Horodecki, *Phys. Rev. A* **80** (2009), 052303.

[174] C. Monroe und J. Kim, *Science* **339** (2013), 1164.

[175] C. Navarrete-Benlloch, R. García-Patrón, J.H. Shapiro und N.J. Cerf, *Phys. Rev. A* **86** (2012), 012328.

[176] M. Van den Nest, *Phys. Rev. Lett.* **110** (2013), 060504.

[177] H. Nha und J. Kim, *Phys. Rev. A* **74** (2006), 012317.

[178] H. Nha, S.Y. Lee, S.W. Ji und M.S. Kim, *Phys. Rev. Lett.* **108** (2012), 030503.

[179] A.D. O'Connell, M. Hofheinz, M. Ansmann, R.C. Bialczak, M. Lenander, E. Lucero, M. Neeley, D. Sank, H. Wang, M. Weides et al. , *Nature* **464** (2010), 697.

[180] S. Olivares, *Eur. Phys. Special Topics* **203** (2012), 3.

[181] H. Ollivier und W.H. Zurek, *Phys. Rev. Lett.* **88** (2001), 017901.

[182] A. Osterloh, *Int. J. Mod. Phys. B* **27** (2013).

[183] A. Osterloh, L. Amico, G. Falci und R. Fazio, *Nature* **416** (2002), 608.

[184] M. Oszmaniec und M. Kuś, *Phys. Rev. A* **88** (2013), 052328.

[185] D. Pagel, A. Alvermann und H. Fehske, *Phys. Rev. E* **87** (2013), 012127.

[186] D. Pagel, P. Nalbach, A. Alvermann, H. Fehske und M. Thorwart, *New J. Phys.* **15** (2013), 105008.

[187] M. Paris, *Eur. Phys. Special Topics* **203** (2012), 61.

[188] J.P. Paz und A.J. Roncaglia, *Phys. Rev. Lett.* **100** (2008), 220401.

[189] J.P. Paz und A.J. Roncaglia, *Phys. Rev. A* **79** (2009), 032102.

[190] A. Perelomov: *Generalized coherent states and some of their applications.* Springer-Verlag, (1986).

[191] A. Peres: *Quantum theory: concepts and methods.* Kluwer Academic Publishers, (1995).

[192] A. Peres, *Phys. Rev. Lett.* **77** (1996), 1413.

[193] T.G. Philbin, *New J. Phys.* **14** (2012), 083043.

[194] A.C. Pipkin: *A course on integral equations.* Springer, (1991).

[195] M.B. Plenio, *Phys. Rev. Lett.* **95** (2005), 090503.

[196] M.B. Plenio, J. Eisert, J. Dreißig und M. Cramer, *Phys. Rev. Lett.* **94** (2005), 060503.

[197] M.B. Plenio, J. Hartley und J. Eisert, *New J. Phys.* **6** (2004), 36.

[198] M.B. Plenio und S.F. Huelga, *Phys. Rev. Lett.* **88** (2002), 197901.

[199] M.B. Plenio und S.F. Huelga, *New J. Phys.* **10** (2008), 113019.

[200] M.B. Plenio und S. Virmani, *Quantum Info. Comput.* **7** (2007), 1.

[201] S. Popescu, A.J. Short und A. Winter, *Nat. Phys.* **2** (2006), 754.

[202] N. Prokof'ev und P. Stamp, *Rep. Prog. Phys.* **63** (2000), 669.

[203] J. Rammer: *Quantum field theory of non-equilibrium states.* Cambridge University Press, (2007).

[204] E. Rieper, J. Anders und V. Vedral, *New J. Phys.* **12** (2010), 025017.

[205] G. Rigolin und M.C. de Oliveira, *Phys. Rev. A* **79** (2009), 030302.

[206] P.S. Riseborough, P. Hanggi und U. Weiss, *Phys. Rev. A* **31** (1985), 471.

[207] H. Risken: *The Fokker-Planck Equation. Methods of Solution and Applications.* Springer-Verlag, (1996).

[208] Á. Rivas und S.F. Huelga: *Open Quantum Systems: An Introduction.* Springer, (2011).

[209] Á. Rivas, A.D.K. Plato, S.F. Huelga und M.B. Plenio, *New J. Phys.* **12** (2010), 113032.

[210] A. Ruiz, D. Alonso, M.B. Plenio und A. del Campo, *Phys. Rev. B* **89** (2014), 214305.

[211] K. Rzazewski und W. Zakowicz, *J. Phys. A: Math. Theor.* **9** (1976), 1159.

[212] K.K. Sabapathy, J.S. Ivan und R. Simon, *Phys. Rev. Lett.* **107** (2011), 130501.

[213] A. Saboia, F. Toscano und S.P. Walborn, *Phys. Rev. A* **83** (2011), 032307.

[214] M. Schlosshauer, J. Kofler und A. Zeilinger, *Studies in History and Philosophy of Science Part B: Studies in History and Philosophy of Modern Physics* **44** (2013), 222.

[215] E. Schrödinger, *Proceedings of the Cambridge Philosophical Society* **31** (1935), 555.

[216] N. Schuch, J.I. Cirac und M.M. Wolf, *Commun. Math. Phys.* **267** (2006), 65.

[217] B. Schumacher, *Phys. Rev. A* **51** (1995), 2738.

[218] J. Schwinger, *J. Math. Phys.* **2** (1961), 407.

[219] I.R. Senitzky, *Phys. Rev.* **119** (1960), 670.

[220] A. Serafini und G. Adesso, *J. Phys. A: Math. Theor.* **40** (2007), 8041.

[221] A. Serafini, G. Adesso und F. Illuminati, *Phys. Rev. A* **71** (2005), 032349.

[222] A. Serafini, F. Illuminati, M.G.A. Paris und S. De Siena, *Phys. Rev. A* **69** (2004), 022318.

[223] A. Serafini, M. Paris, F. Illuminati und S. De Siena, *J. Opt. B: Quantum Semiclass. Opt.* **7** (2005), R19.

[224] E. Shchukin und W. Vogel, *Phys. Rev. Lett.* **95** (2005), 230502.

[225] E. Shchukin und W. Vogel, *Phys. Rev. A* **74** (2006), 030302.

[226] K. Shiokawa, *Phys. Rev. A* **79** (2009), 012308.

[227] R. Simon, *Phys. Rev. Lett.* **84** (2000), 2726.

[228] A.S. Sørensen und K. Mølmer, *Phys. Rev. Lett.* **86** (2001), 4431.

[229] J. Sperling und W. Vogel, *Phys. Rev. A* **79** (2009), 022318.

[230] J. Sperling und W. Vogel, *Phys. Rev. Lett.* **111** (2013), 110503.

[231] S. Szalay und Z. Kökényesi, *Phys. Rev. A* **86** (2012), 032341.

[232] J.C. Taylor, *J. Phys.: Condens. Matter* **19** (2007), 106223.

[233] B.M. Terhal, *Theor. Comp. Sci.* **287** (2002), 313.

[234] M. Tiersch, F. De Melo und A. Buchleitner, *J. Phys. A: Math. Theor.* **46** (2013), 085301.

[235] M. Tiersch, F. de Melo, T. Konrad und A. Buchleitner, *Quantum Inf. Process.* **8** (2009), 523.

[236] G. Tóth, *Phys. Rev. A* **71** (2005), 010301.

[237] A. Trabesinger, *Nat. Phys.* **8** (2012), 263.

[238] C. Tsallis, S. Lloyd und M. Baranger, *Phys. Rev. A* **63** (2001), 042104.

[239] R.O. Umucalilar und I. Carusotto, *Phys. Rev. A* **84** (2011), 043804.

[240] R. Vasile, P. Giorda, S. Olivares, M.G.A. Paris und S. Maniscalco, *Phys. Rev. A* **82** (2010), 012313.

[241] R. Vasile, S. Olivares, M.G.A. Paris und S. Maniscalco, *Phys. Rev. A* **80** (2009), 062324.

[242] V. Vedral, *Nat. Phys.* **10** (2014), 256.

[243] V. Vedral, M.B. Plenio, K. Jacobs und P.L. Knight, *Phys. Rev. A* **56** (1997), 4452.

[244] V. Vedral, M.B. Plenio, M.A. Rippin und P.L. Knight, *Phys. Rev. Lett.* **78** (1997), 2275.

[245] I. de Vega: *Ph.D. thesis, Relaxation properties in non-Marvonian quantum systems.* University of La Laguna, (2005).

[246] I. de Vega, *arXiv:1403.8102* (2014).

[247] G. Vidal und R.F. Werner, *Phys. Rev. A* **65** (2002), 032314.

[248] D. Vitali, S. Gigan, A. Ferreira, H.R. Böhm, P. Tombesi, A. Guerreiro, V. Vedral, A. Zeilinger und M. Aspelmeyer, *Phys. Rev. Lett.* **98** (2007), 030405.

[249] M. Walter, B. Doran, D. Gross und M. Christandl, *Science* **340** (2013), 1205.

[250] C. Weedbrook, S. Pirandola, R. García-Patrón, N.J. Cerf, T.C. Ralph, J.H. Shapiro und S. Lloyd, *Rev. Mod. Phys.* **84** (2012), 621.

[251] U. Weiss: *Quantum dissipative systems.* World Scientific, (1999).

[252] R.F. Werner, *Phys. Rev. A* **40** (1989), 4277.

[253] R.F. Werner und M.M. Wolf, *Phys. Rev. Lett.* **86** (2001), 3658.

[254] D.J. Wineland, *Rev. Mod. Phys.* **85** (2013), 1103.

[255] B. Witt und F. Mintert, *New J. Phys.* **15** (2013), 093020.

[256] A. Wolf, G. De Chiara, E. Kajari, E. Lutz und G. Morigi, *Europhys. Lett.* **95** (2011), 60008.

[257] M.M. Wolf, G. Giedke, O. Krüger, R.F. Werner und J.I. Cirac, *Phys. Rev. A* **69** (2004), 052320.

[258] S. Wolfram: *The mathematica book, fifth edition.* Wolfram Media Inc., (2003).

[259] Y.J. Xu und X.G. Meng, *Int. J. Theor. Phys.* **52** (2013), 3066.

[260] T. Yu und J. Eberly, *Science* **323** (2009), 598.

[261] T. Zell, F. Queisser und R. Klesse, *Phys. Rev. Lett.* **102** (2009), 160501.

[262] C. Zhang, S. Yu, Q. Chen und C.H. Oh, *Phys. Rev. Lett.* **111** (2013), 190501.

[263] U. Zürcher und P. Talkner, *Phys. Rev. A* **42** (1990), 3267.

[264] U. Zürcher und P. Talkner, *Phys. Rev. A* **42** (1990), 3278.

[265] W. Zurek, *Rev. Mod. Phys.* **75** (2003), 715.

[266] R. Zwanzig: *Nonequilibrium statistical mechanics.* Oxford University Press, (2001).